

**Best
Available
Copy**

AD-778 344

PACKET RADIO COMMUNICATIONS VOLUME 1

Collins Radio Company

Prepared for:

Advanced Research Projects Agency

17 April 1974

DISTRIBUTED BY:

NTIS

**National Technical Information Service
U. S. DEPARTMENT OF COMMERCE
5285 Port Royal Road, Springfield Va. 22151**



first quarterly technical report

Volume 1

Packet Radio Communications
Collins Radio Company

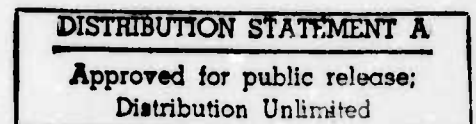
Principal Investigator:
F. H. Dickson

ARPA Order No. 2305
Program Code No. P3P10
Contractor: Collins Radio Company
Contract No. DAHC15-73-C-0192
Effective Date: 1 October 1973
Expiration Date: 31 July 1974

Sponsored by:
Advanced Research Projects Agency
Department of Defense

The views and conclusions contained in this document are those of the authors and should not be interpreted as necessarily representing the official policies, either expressed or implied, of the Advanced Research Projects Agency or the US Government.

Printed in United States of America



Collins Radio Company | Dallas, Texas

1. TECHNICAL PROBLEM

This project is one part of a larger effort directed at extending the packet switching technology to include a flexible access and distribution capability for resource sharing networks. The objectives of the Collins investigations are:

Perform research covering the application of radio frequency technology to packet switching/communications.

Participate in the overall Advanced Research Projects Agency (ARPA) Packet Communication Technology Program under the guidance of the Packet Radio Communications Working Group. In support of these overall objectives, the following specific objectives are:

- Provide one set of equipment for propagation/noise measurements.
- Identify salient characteristics of packet radio link design including bounds on rf carrier frequency, data rate, channelization, and ranges.
- Determine the modulation and detection methods for the experimental packet radio system.
- Determine the state of technology and suitability of various selected equipment components for the packet radio application.
- Recommend a terminal-to-terminal security system for the ARPA packet switch network.

2. GENERAL METHODOLOGY

The approach to the packet radio investigations has been a combination of theoretical analysis and laboratory experimental activities. The theoretical analysis has drawn on sources of information available from the literature and the experience Collins has developed in radio communication design and development. Experimental activities have been the evaluation of candidate equipment components for packet radio application. The thrust of activity has been the translation of packet radio concepts into equipment requirements. Specific activities have included development of computer analysis program tools to aid in the signal processing design for the experimental packet radio system and investigation of radio link characteristics based on hypothesized and empirically obtained channel information. The question of security has been addressed by consideration of the various threats to the security of a packet switch network that may be expected and the strengths and weaknesses of the network to these threats. The report on this work is found in other documents.

summary

3. TECHNICAL RESULTS

Results reported in this document are the completion of the development and introduction into the measurement system of the propagation/noise measurement equipment and identification of essential radio link parameters for the experimental system. The developed propagation/noise measurement equipment consists of a transmitter and receiver. The transmitter generates and transmits a code spread biphase modulation at dual frequencies of 430 MHz and 1370 MHz with output power of 10 watts and 6 watts, respectively. The receiver has dual fixed-frequency front ends, a common if channel, and utilizes surface wave devices for signal correlation. Two omnidirectional type antennas (one with gain of 2 dBi at 430 MHz and 9 dBi at 1370 MHz, and another with gain of 2 dBi at both frequencies) were provided. A complete design data package and description of equipment is included in volume 2 of this report. The following radio link parameters have been identified for the experimental system:

- Frequency bounds of 1 GHz to 2 GHz with target band of 1710 MHz to 1850 MHz
- Dual data rates of 420 kb/s for repeater-to-repeater links and 100 kb/s for terminal-to-repeater links
- One common channel with spread spectrum differentially coherent minimum shift keying modulation
- Antennas with vertical directivity and omnidirectional coverage in azimuth plane (9-dBi gain)
- Expected ranges for terminal-to-repeater links in urban environment of the order of 2 miles.

In defining the experimental system, other related accomplishments that have been made are the following:

- Microprocessor investigation and selection for the experimental system
- Operational computer design aids for signal processing analysis and design.

4. PLAN FOR NEXT QUARTER ACTIVITIES

The activities for the next quarter are the translation of system design parameters into an equipment design plan. This will include the specific design of equipments for the experimental packet radio system. This experimental system will consist of three network elements that can be cast as network terminals or repeaters, and represents the first phase of development of a packet radio network. The issue of the frequency allocation of the experimental system will also be addressed. The results of this effort will be a frequency allocation plan.

	Page
Summary	i
Section 1 Packet Radio — Radio Link Considerations	1-1
1.1 Introduction	1-1
1.2 Radio Propagation and Relations to System Design	1-1
1.2.1 Antenna and Space Loss Relationships	1-1
1.2.2 Propagation in a Real Environment	1-4
1.2.3 Transmission Within and Through Buildings	1-11
1.3 Spread Spectrum Techniques	1-17
1.3.1 Pseudorandom Sequences	1-19
1.3.2 Alternates to Pseudorandom Sequences	1-23
1.3.3 Issues	1-24
1.4 Packet Radio System Power Budget	1-24
1.4.1 Assumed System Parameters	1-24
1.4.2 The Power Budget Equation	1-25
1.4.3 Transmission Loss	1-27
1.4.4 Required Signal-to-Noise Ratio	1-27
1.4.5 Repeater Spacing	1-27
1.4.6 Dynamic Range	1-29
1.4.7 Conclusions	1-30
Section 2 Modulation and Detection	2-1
2.1 Evaluation of Modulation Methods	2-1
2.1.1 Time and Code Discrimination of Spread Spectrum	2-1
2.1.2 Modulation Waveform Types	2-3
2.2 Synchronization for Packet Radio Systems	2-27
2.2.1 General Concept of Bit Synchronization	2-29
2.2.2 Synchronization Preambles	2-35
2.3 Analysis Tools for Signal Processing	2-54
2.3.1 Description of CODCOR and COREL	2-54
2.3.2 Selection of the 127-Chip Length Code	2-55
2.3.3 Description of the Computer Program AUTCOR ..	2-55
2.3.4 Filtering Effect on Correlators Performance	2-60
Appendix 2A Crystal Oscillator Stability	
Appendix 2B Probability of Detection for Coherent Combining of Bits	

table of contents (cont)

	Page
Section 3 Equipment Considerations	3-1
3.1 Introduction	3-1
3.2 Surface Acoustic Wave Devices	3-1
3.2.1 Theory of Surface Acoustic Wave Devices, Signal Processing Techniques	3-1
3.2.2 Design and Operation of Coded Surface Acoustic Wave Devices	3-6
3.2.3 Surface Acoustic Wave Device Characteristics ..	3-7
3.2.4 Test Results	3-11
3.2.5 State of Technology in SAWD	3-16
3.2.6 Performance Limitations	3-18
3.2.7 SAWD Technology Summary	3-19
3.2.8 Summary of Definitions	3-19
3.3 Evaluation of Antenna for Packet Radio	3-20
3.3.1 Terminal Antenna	3-21
3.3.2 Repeater Antenna	3-27
3.4 RF Sources for Packet Radio	3-27
3.4.1 Introduction	3-27
3.4.2 General Considerations in RF Source Design and Economics	3-28
3.4.3 Characteristics of Available RF Sources	3-28
3.4.5 Summary	3-31
3.5 Microprocessor Evaluation for Packet Radio	3-31
3.5.1 Evaluation Factors	3-32
Section 4 Propagation/Noise Measurement Equipment	4-1
4.1 Introduction and Overview Summary	4-1
4.2 Technical Description	4-3
4.2.1 Elements of the Test Set	4-3
4.2.2 Transmitter Characteristics	4-3
4.2.3 Receiver Characteristics	4-9
4.2.4 Specification Summary	4-13
Appendix 4A Design Details	
Appendix 4B Alignment	
Appendix 4C Performance Data	

Unclassified

Security Classification

AD-778344

DOCUMENT CONTROL DATA - R & D

(Security classification of title, body of abstract and indexing annotation must be entered when the overall report is classified)

1. ORIGINATING ACTIVITY (Corporate author) Collins Radio Company	2a. REPORT SECURITY CLASSIFICATION Unclassified
	2b. GROUP None

3. REPORT TITLE
FIRST QUARTERLY TECHNICAL REPORT,
FOR THE PROJECT "PACKET RADIO COMMUNICATIONS"

4. DESCRIPTIVE NOTES (Type of report and inclusive dates)
First Quarterly Technical Report

5. AUTHOR(S) (First name, middle initial, last name)
Collins Radio Company

6. REPORT DATE 17 April 1974	7a. TOTAL NO. OF PAGES 308	7b. NO. OF REFS 86
---------------------------------	-------------------------------	-----------------------

8a. CONTRACT OR GRANT NO. DAHC15-73-C-0192 b. PROJECT NO. c. d.	9a. ORIGINATOR'S REPORT NUMBER(S) 523-0699742-001C3L
	9b. OTHER REPORT NO(S) (Any other numbers that may be assigned this report)

10. DISTRIBUTION STATEMENT
Distribution of this document is unlimited.

11. SUPPLEMENTARY NOTES Report consists of two volumes	12. SPONSORING MILITARY ACTIVITY Advanced Research Projects Agency, Department of Defense
---	---

13. ABSTRACT

Four major areas of activities in support of packet radio communications are reported in this document. These are: 1) evaluation and selection of radio link parameters for experimental packet radio system, 2) evaluation and selection of modulation and synchronization methods for experimental system, 3) equipment components analysis, 4) propagation/noise measurement equipment design data. Radio link parameter selection includes frequency range, data rates, antenna type, and expected ranges. Modulation and synchronization evaluation is based on both performance and implementation. Component evaluation consists of technological assessment in surface acoustic wave devices, RF sources, antennas, and micro-processors for packet radio application. A brief technical description and detailed design package including schematics and photographs of the propagation/noise measurement equipment are also reported.

Reproduced by
NATIONAL TECHNICAL
INFORMATION SERVICE
U S Department of Commerce
Springfield VA 22151

14

KEY WORDS	LINK A		LINK B		LINK C	
	ROLE	WT	ROLE	WT	ROLE	WT
Packet radio communications, propagation, surface acoustic wave devices, microprocessors, spread spectrum, data communications, modulation, detection, synchronization.						

ia

list of illustrations

Figure	Page
1-1	Free-Space Loss Relationships for 400-MHz and 8-GHz Bands 1-4
1-2	Estimated Fade Margin Distributions - UHF Curves (450 to 1000 MHz) 1-7
1-3	Median Field Strength, Urban Environment 1-9
1-4	Plot of Maximum Distance Between Terminals 1-10
1-5	Street Level Signal Defraction 1-12
1-6	Attenuation in Tunnels and Buildings Between Half-Wave Dipoles and Between Transmission Line and Half-Wave Dipole at 160 MHz 1-16
1-7	Relative Attenuation Between 200-Ohm Balanced Transmission Line and Half-Wave Dipole Antenna at 160 MHz 1-17
1-8	Transmission Loss Versus Distance 1-26
1-9	P_e versus E_b/N_0 for Differential Coherent (MSK)... 1-28
1-10	Hypothesized Repeater Spacing 1-29
2-1	Time Discrimination 2-2
2-2	Crosscorrelation Function Between Codes No. 1 and No. 2 2-4
2-3	DPSK Modulator No. 1 2-6
2-4	DPSK Modulator No. 2 2-6
2-5	Differentially Coherent PSK Demodulator 2-8
2-6	Effect of Timing Offsets to Maximum Likelihood Decoding 2-9
2-7	E_b/N_0 Performance Loss Due to Timing Offsets 2-10
2-8	Window Peak Sample and Store Detector 2-11
2-9	DC Quadriphase Modulator 2-12
2-10	MSK Signaling 2-13
2-11	Coherent MSK Modulator No. 1 2-14
2-12	Coherent MSK Modulator No. 2 2-14
2-13	Coherent MSK Demodulator 2-16
2-14	Differentially Coherent MSK Modulator 2-17
2-15	Differentially Coherent (DC) MSK Demodulator (10- μ s SAWD) 2-18
2-16	Differentially Coherent (DC) MSK Demodulator (20- μ s SAWD) 2-19
2-17	Effect of Timing Offsets for Sampling Detection of MSK Signaling 2-20
2-18	Pseudo-Orthogonal (PO) MSK Modulator No. 1 2-21
2-19	PO MSK Modulator No. 2 2-21
2-20	PO MSK Demodulator 2-23
2-21	8'ARY MSK Modulator 2-24
2-22	8'ARY MSK Demodulator 2-25

list of illustrations (cont)

Figure	Page
2-23 Performance Comparison of Different Modulation Approaches	2-26
2-24 Relative Spectral Density for MSK, Quadriphase PSK and Biphase PSK	2-28
2-25 System with No Spread Spectrum	2-32
2-26 Signal Separation on the Basis of Time of Arrival	2-32
2-27 Framing for Zero Epoch Error	2-34
2-28 Probability of Preamble Detection (Coherent Combining of Bits)	2-37
2-29 Noncoherent Combining of Bits	2-38
2-30 13-Bit Barker Code Followed by 13-Bit Barker Complemented	2-40
2-31 Autocorrelation of 7-Bit Barker Sequence Where Each Bit Consists of 127 Chips of a Maximum Length Sequence at 100 kb/s Rate	2-41
2-32 7-Bit Barker Preamble and Bit Sync Detector Coherent Combining Detection	2-42
2-33 7-Bit Barker Preamble and Bit Sync Detector Differentially Coherent Combining Detection	2-44
2-34 Repeat Preamble with End of Preamble Detector ...	2-46
2-35 Autocorrelation of Seven 1's where Each Bit Consists of 127 Chips of a Maximum Length Sequence at 100 kb/s	2-47
2-36 13-Bit Barker, Barker Preamble and Bit Sync Detector (Noncoherent Detection)	2-48
2-37 Digital Implementation of Preamble Filter	2-49
2-38 Digital/Analog Implementation of Preamble Filter	2-49
2-39 Autocorrelation Output at Point for 1's and 13-Bit Barker Followed by 13-Bit Inverter Barker	2-50
2-40 Functional Diagram of Bit Sync Loop	2-51
2-41 Binary Shift Register Generator	2-57
2-42 AUTOCOR Computer Program Structure	2-59
2-43 Autocorrelation Property of 7, 3, 2, 1 Tap Code ...	2-61
2-44 Matched Filter Response of a 127-Chip Coded Filtered Signal	2-62
3-1 Timing Diagram for Binary Spread Spectrum System	3-2
3-2 Principles of the SAWD Matched Filter for Phase-Coded Waveforms	3-5
3-3 Tap Phase-Coding Techniques	3-5
3-4 Tapped Delay Line Finger Placement	3-6

list of illustrations (cont)

Figure		Page
3-5	Minimum Achievable Insertion Loss for Two Transducers on Various Substrates	3-9
3-6	Loss in Processing Gain Versus Frequency Error...	3-10
3-7	SAWD Test Setup	3-12
3-8	Test Result A.....	3-13
3-9	Test Result B	3-13
3-10	Test Result C	3-13
3-11	Test Result D	3-13
3-12	Test Result E	3-13
3-13	Test Result F	3-13
3-14	Test Result G	3-14
3-15	Current Fabrication Capabilities for Coded Devices	3-17
3-16	Quarter-Wave Monopole	3-21
3-17	Half-Wave Dipole	3-22
3-18	Pictorial Representation of Linear, Elliptical, and Circular Polarization	3-24
3-19	Tri-Dipole Loop Antenna	3-25
3-20	Conical Spiral	3-25
3-21	Diagonal Dipoles	3-26
3-22	Slot-Fed Bicone	3-26
4-1	Transmit System Block Diagram	4-4
4-2	Transmitter.....	4-5
4-3	Transmitter Control	4-6
4-4	Burst Mode Control	4-7
4-5	High-Gain Antenna	4-8
4-6	Receiver System Block Diagram	4-10
4-7	Receiver System Front Panel	4-11
4-8	Low-Gain Antenna Construction	4-12

list of tables

Table		Page
1-1	Frequency Bands	1-5
1-2	Calculations for 453 to 1920 MHz	1-10
2-1	Modulation Approach Comparison	2-5
2-2	Hoffman's Analysis for Transient Response	2-52
2-3	Preamble Approach Parameters	2-53
2-4	7, 3, 2, 1 Tap Code and Its Autocorrelation	2-56
2-5	Mean and Variance of the 18 Maximal Length Codes	2-58
3-1	Worst-Case Frequency Errors	3-10
3-2	Test Results	3-14
3-3	SAWD Performance	3-16
3-4	Typical Lithography Limitations	3-19
3-5	SAWD State-of-the-Art Technology	3-20
3-6	List of Available Microprocessor Sets	3-32
3-7	MOS Random Access Memories	3-35
3-8	MOS Programmable Read Only Memories	3-36
3-9	CPU Parameters Used in Evaluation	3-36
3-10	RAM Parameters Used in Evaluation	3-38
3-11	Comparison of Microprocessor Sets.....	3-39

1.1 INTRODUCTION

It is envisioned that the packet radio techniques under investigation can provide an effective and efficient technique for communication in a wide variety of environments and for a wide variety of applications. It is therefore desirable that the systems being investigated provide for portable operation of equipment and allow the building of systems of substantial extent in an environment that is not conducive to care in siting of equipment and that does not allow time for propagation surveys. In this regard, packet radio systems have much in common with mobile radio systems. Prior work by others in this field has been very helpful in this investigation. The need for portability and the restraints on siting will influence the choice of frequency, power output requirements, antenna design, repeater distribution, and compatibility with other systems that may share the same radio spectrum. Results of investigations into these subjects are summarized in this report.

1.2 RADIO PROPAGATION AND RELATIONS TO SYSTEM DESIGN

Antennas for packet radio systems must provide essentially omnidirectional coverage in the azimuth plane. Fixed stations may employ antennas with moderate vertical directivity since it is permissible to assume some care in siting and installation of fixed stations. Such installations will typically be repeaters or stations.

The criteria stated above implies relatively simple antennas, such as vertical dipoles. Vertical polarization is assumed primarily because it results in a more convenient antenna configuration. At frequencies that are acceptable for packet radio, either vertical or horizontal polarization offers essentially the same propagation performance. The relationships between frequency, antenna size, and free-space loss are reviewed briefly in the following paragraph.

1.2.1 Antenna and Space Loss Relationships

It is convenient to relate all antennas to a theoretical omnidirectional antenna. For transmitters, this antenna radiates the energy equally in all directions; therefore, assuming no I^2R losses in the antenna, the power density at distance d from the radiator in the resulting radiated field is:

$$P_D = \frac{P_T}{4\pi d^2}$$

where

P_D = Power density in watts per unit area

P_T = Transmitter power

d = Distance from source.

packet radio — radio link considerations

It is convenient to consider the receive antenna as having a capture area when placed in the transmitted field. The capture area of the theoretical isotropic antenna is:

$$A_i = \frac{\lambda^2}{4\pi}$$

where

A_i = Effective area of isotropic antenna

λ = Wavelength.

From the above equation one can derive the free-space loss between isotropic antennas as:

$$\alpha = \frac{(4\pi)^2 d^2 f^2}{c^2}$$

where

α = Space loss

d = Distance between antennas

f = Frequency

c = Velocity of light.

This equation reduces to the familiar one of:

$$\alpha = 36.6 + \log f + 20 \log d \text{ in dB}$$

where

α = Space log between isotropic antennas in dB

f = Frequency in MHz

d = Distance in miles.

It is important to emphasize at this point that the isotropic receive antenna has a capture area that is a function of the square of the wavelength or inverse square of the frequency. Since, by definition, free-space loss is the loss between isotropic transmit and receive antennas, space loss increases as the square of the frequency.

For applications allowing use of directive antenna (i.e., point-to-point circuits), it is equally proper to relate path loss to a constant antenna aperture. If antenna aperture is held constant for both transmit and receive antenna, then the path loss decreases as the square of the frequency. This of course results because the receiving antenna capture area remains constant while the transmitting antenna beamwidth becomes smaller with increasing frequency, resulting in greater power density at the receiving location.

It will therefore be noted from the above relationships that the ratio of path loss between fixed-aperture antennas and omnidirectional antennas changes as the fourth power of the frequency.

The above points are reviewed because they have an important impact on the choice of operating frequency for packet radio systems independent of other considerations of multipath, noise level, etc. If the frequency band selection is to be based on free-space propagation conditions alone, then the rules for selection may be simply stated as follows.

- a. For systems employing omnidirectional antennas at each end of the link, the operating frequency should be chosen as low as possible consistent with adequate available bandwidth and reasonable antenna size for portable systems.
- b. For systems employing directional antennas at each end of the link, the frequency should be chosen as high as possible consistent with economic microwave devices and low attenuation due to rainfall. (This indicates that the choice of frequency for directive systems is limited primarily by rain and, hence, may operate at frequencies to at least 10 GHz.)
- c. If the system employs directive antennas at terminal points and omnidirectional antennas at the repeaters, then the selection of frequency is not an important consideration from free-space propagation considerations.

These space loss relationships are illustrated for 400-MHz and 8-GHz bands in figure 1-1.

Transmit power requirements are compared for 400-MHz and 8-GHz systems with omnidirectional and fixed antenna aperture with a 4-foot diameter paraboloid for the following assumed system parameters for all examples:

Receiver noise figure = 6 dB

Data rate = 10^5 bits/second

Receiver bandwidth = 2×10^5

Required signal-to-noise = 20 dB (Note: This provides 6- to 8-dB margin.)

From above:

Noise level = $-174 + 53 + 6 = -115$ dBm

Required receive power = $-115 + 20 = -95$ dBm

It is assumed that the experimental system is to operate in a band assigned to government services. Several candidate bands are listed in table 1-1 with the effective area of the isotropic antenna for each band.

packet radio — radio link considerations

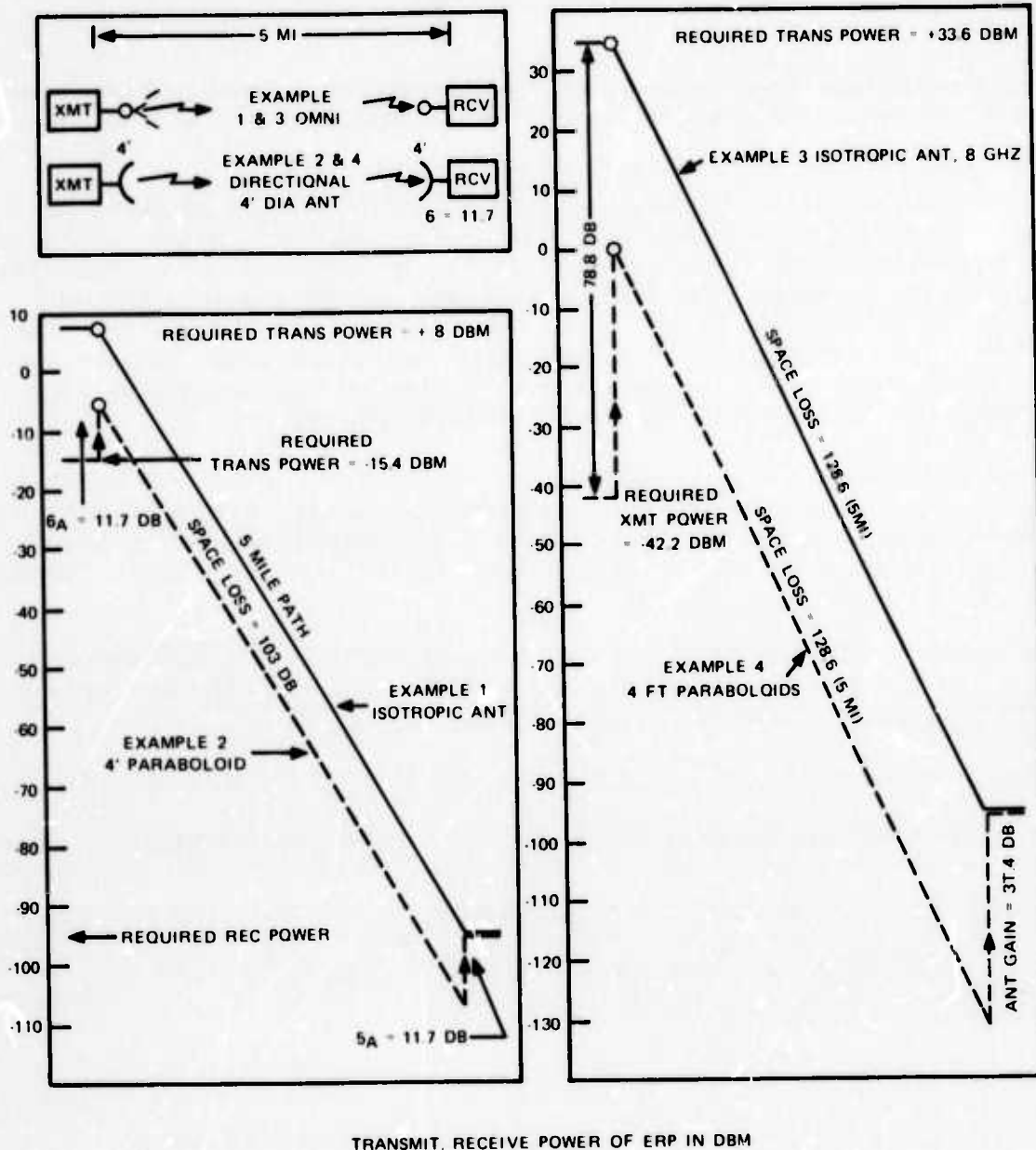


Figure 1-1. Free-Space Loss Relationships for 400-MHz and 8-GHz Bands.

1.2.2 Propagation in a Real Environment

Propagation between two isotropic antennas in free space was reviewed in paragraph 1.2.1. It was pointed out that the frequency dependence of the propagation is due to the decreasing size of our isotropic receiving antenna as frequency is increased. In a practical environment, other factors influence the performance to be obtained. Of particular importance is the multipath characteristics in an urban environment. In this regard, packet radio systems are similar to mobile radio services, although they are likely more sensitive to multipath due to its effect on error rate. Some of the path design considerations are summarized in the following paragraph.

Table -1. Frequency Bands.

FREQUENCY (MHz)	WAVELENGTH* λ (FEET)	WAVELENGTH* λ (INCHES)	AREA OF ISOTROPIC ANTENNA (SQUARE FEET)	GAIN IN DB ABOVE ISOTROPIC OF 1 SQ FT EFFECTIVE APERTURE
406-420	2.4	28.6	0.46	3.36
1700-1850	0.55	6.1	2.4×10^{-2}	16.2
2200-2300	0.44	5.2	1.54×10^{-2}	18.1
4400-5000	0.21	2.5	3.34×10^{-3}	24.75
7125-8500	0.125	1.5	1.24×10^{-3}	29.06
13200-16000	0.067	0.8	3.88×10^{-4}	34.1

*All wavelengths, areas, and gain are for midband frequency of band listed.

1.2.2.1 Line-of-Sight Paths

It is common to refer to the radio horizon of line-of-sight (LOS) as calculated geometrically with the tower heights on a curved earth of 4/3 the true earth radius. This LOS distance can be calculated by:

$$d = \sqrt{2(h_t + h_r)} \text{ miles}$$

where h_t and h_r are the transmitting and receiving antenna heights above the average terrain, measured in feet. However, during propagation anomalies, the effective earth radius may reduce to 2/3 true earth radius and this is often used for worst case system design.

With this conservative estimation, the 30-meter antennas might be as far apart as 16.8 miles unless there is a compelling reason for closer spacing due to multipath, path loss, etc.

1.2.2.2 Path Clearance

In addition to establishing a shorter LOS in the interest of increasing reliability, the path of the optical ray must clear large obstacles on all sides of the array by at least 0.6 of the Fresnel zone radius.

$$R_f = 550 \frac{\sqrt{d_1(d - d_1)}}{d f}$$

packet radio — radio link considerations

where

d = Path length in kilometers (km)

d_1 = Distance along path to measurement point (km)

f = Frequency in MHz.

For example, if the path was to go close by a hillside 10 km from one terminal on a 15-km path length and the frequency was 1000 MHz, then the geometric center of the path must clear the mountain by at least 31.7 meters if we are to achieve near free-space propagation performance.

1.2.2.3 Path Loss

The loss between unobstructed isotropic antennas in free space is defined in paragraph 1.2.1; however, in a real environment where propagation is influenced by multipath and obstructions, one must consider the statistical nature of propagation between randomly selected points. This has been done by CCIR for uhf frequencies suitable for mobile services. Curves derived from the CCIR¹ are plotted in figure 1-2. These curves define propagation reliability in percent as a function of fade margin for various functional line-of-sight paths.

1.2.2.4 Multipath and Its Relation to Antenna Gain

There is considerable evidence from the operation of point-to-point microwave systems to indicate that well designed point-to-point paths employing directional antennas present no data rate limitations at any rate likely to be used for packet radio systems. However, one cannot be assured that this experience is valid for systems employing wide beam or omnidirectional antennas. Such systems will suffer additional degradation due to discrete reflections in the immediate vicinity of one terminal, transverse reflections from objects in the antenna field at greater range, and finally background scatter or generally incoherent scattering from objects spread out on an asymmetric topography. Investigations to date indicate the following relative to the influence of multipath on packet radio system design.

- a. For fixed-location terminals, multipath effects are carrier frequency independent, but are signaling rate dependent.
- b. Multipath in the immediate vicinity of terminals can often be mitigated against in a fading sense by moving the antenna a half-wavelength or so, but probably not for a wide sector of coverage angles.
- c. Even though the close-in multipath is mitigated against from a signal level point of view, the existence of the multipath will still limit the maximum signaling rate that can be used.
- d. Insofar as modem performance is concerned, the irreducible error rate (beyond which no increase in signal level will improve performance) does not require strictly equal amplitude interferors but there can be a spread of 10 to 20 dB in amplitude over which the influence of a weaker reflection can be important.
- e. The significance of multipath becomes less as the antenna gain is increased.

¹See the Bibliography at the end of this section for footnote references.

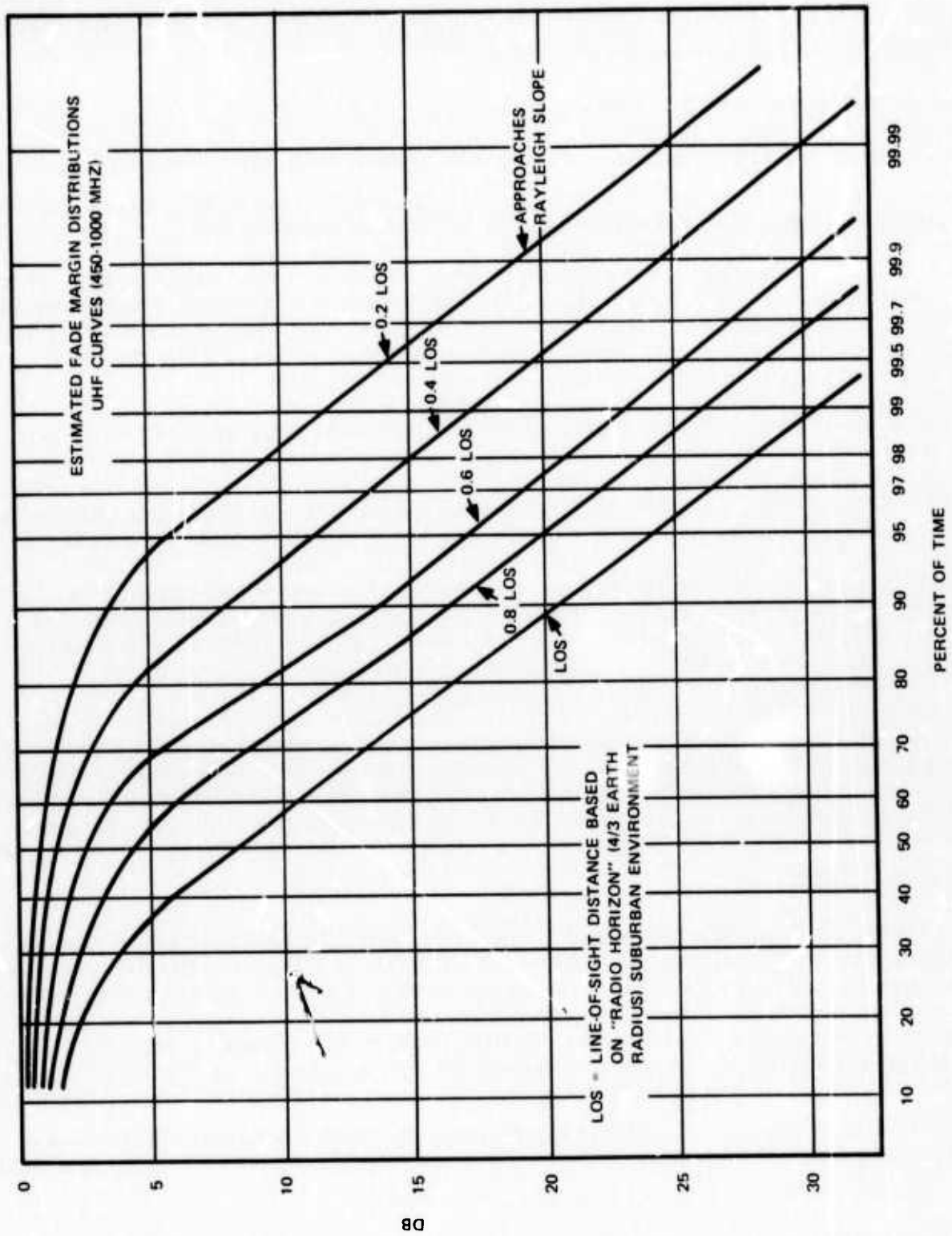


Figure 1-2. Estimated Fade Margin Distributions — UHF Curves (450 to 1000 MHz).

packet radio — radio link considerations

In semirural areas, transverse multipath levels of several tenths of a microsecond delay are to be expected. For long suburban paths (of the order of 10 miles or so), $1 \mu\text{s}$ or $2 \mu\text{s}$ can be expected. In urban areas, short paths (1 to 3 miles) will exhibit 1 to $2 \mu\text{s}$ on an average; and for longer paths, 5 to $7 \mu\text{s}$ are not uncommon.^{1, 2}

1.2.2.5 Urban Terminal to Repeater

In general, the worst propagation conditions will be seen in an urban environment. Extensive measurements have been made by Okumura⁴ and his associates and their work is used here exclusively for estimating the performance of terminal to repeater links.

Figure 1-3 shows median field strengths for three frequencies. The receiver antenna height was 3 meters and the transmit antenna height was 30 meters. The transmitter power was 1 kW from a dipole (1kW erp). Using these curves with proper adjustments for difference in transmit power and the other specified system parameters, we can calculate some maximum ranges for three frequencies in the urban environment.

Assuming a 1-W hand-held transmitter with a dipole antenna at the user end of the link, an 8-element vertical collinear array 30 meters high at the repeater receiver (11 dB>isotropic, and an operating frequency of 453 MHz, the maximum range based on median field strength is computed as 3 kilometers or 5 miles. Similar calculations are also performed for 922 and 1920 MHz, resulting in ranges of 3.4 and 2.2 miles, respectively. (See table 1-2 and figure 1-4.)

It can be seen from this that the range is inversely proportional to the square root of the ratio of frequencies; however, the number of repeaters required to blanket an area is inversely proportional to the square of the ratio of the range. Therefore, if we cut the frequency in half, we cut the number of repeaters in half.

If the terminal is in an automobile, it will experience a spread of the spectrum of the signal in the city due to doppler. If it were in a simple deterministic field, it would experience merely a shift of frequency by $(2 v/\lambda)$ Hz, where v is the velocity of the vehicle relative to the direction of wave propagation. In the city, however, the vehicle is driving through a myriad of reflections of the wave arriving from all directions. Consequently, the power spectrum of a stable signal will be spread so that the -10-dB points are at $(\pm 2s/\lambda)$ Hz, where s is the speed of the vehicle.⁵

W.R. Young, Jr.² measured echoes at various frequencies in New York City. These echoes are a reflection-multipath problem and are not a function of frequency. His data shows a 50-percent probability of a 2-ns echo, a 45-percent chance of a 3-ns echo and a 30-percent chance of a 5-ns echo. All these echoes are within 12 dB of the strongest pulse. There appear to be echoes on every trace shown within 10 dB of the strongest pulse, the only variability is when it will come. There is even a 2-percent chance of a strong echo at 10-ns delay. To allow for strong 10-ns echoes, the maximum signaling rate would be less than 50 kilobits. Mesenberg⁶ explores the realm of irreducible bit error rates in his article. Assuming a 20-dB signal-to-noise ratio and a 6-dB echo, the bit error rate would be on the order of 3×10^{-3} for noncoherent fsk signaling.

Multipath fading is always present in the city with depths of fades being greater than 20 dB. Since these nulls exist in the standing wave field, a stationary user can move his radio a few feet to avoid the nulls; a mobile user will have to suffer. The nulls are spaced approximately at half wavelength intervals; therefore, the fade rate in a moving vehicle is proportional to the frequency.

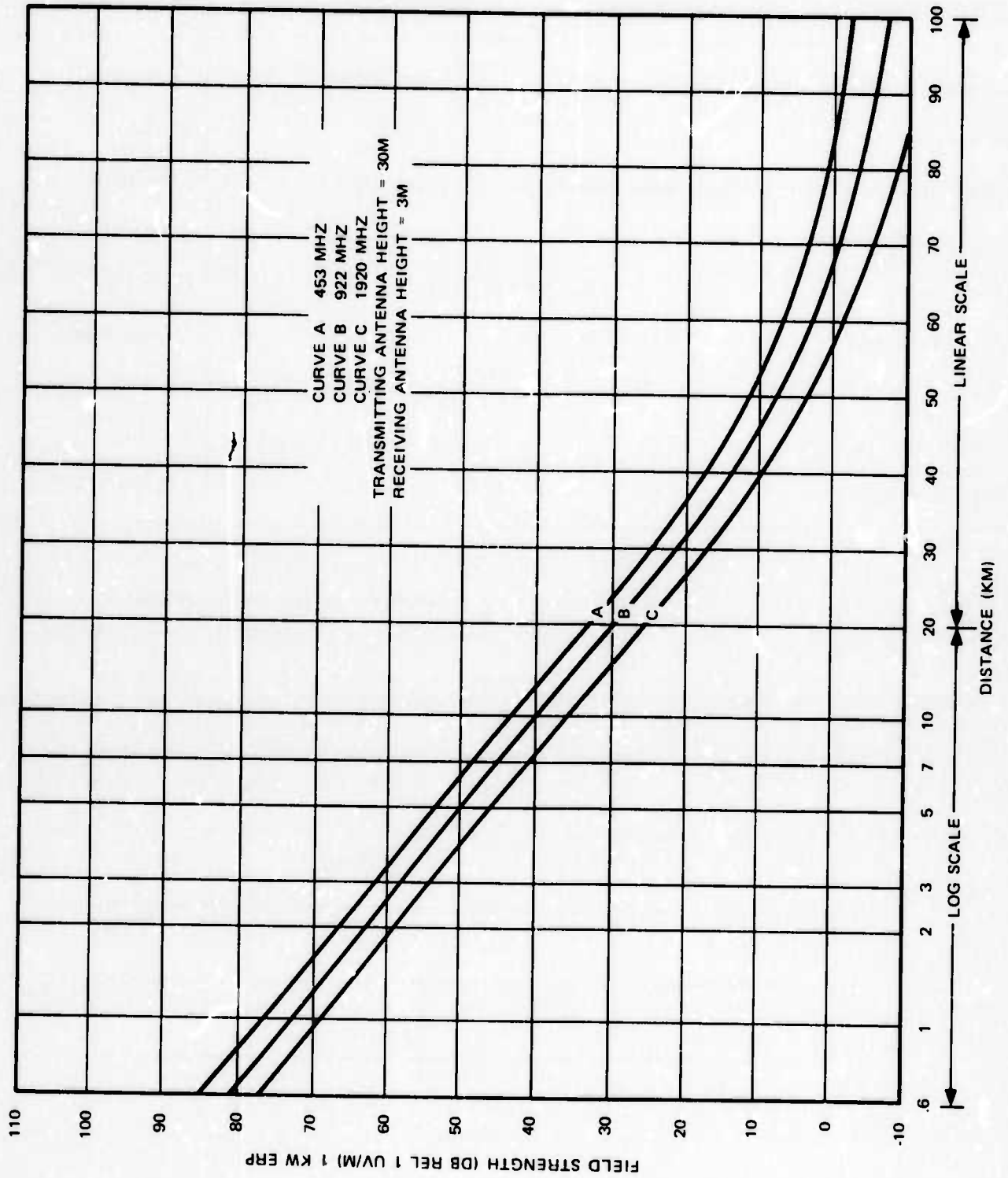
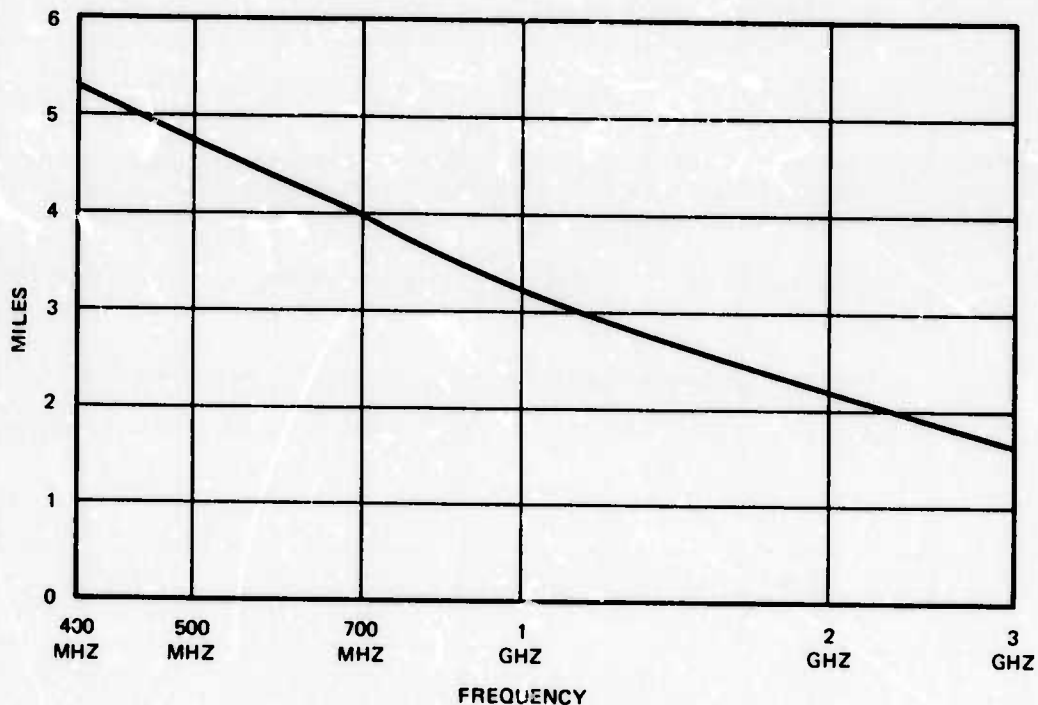


Figure 1-3. Median Field Strength, Urban Environment.

Table 1-2. Calculations for 453 to 1920 MHz.

FREQUENCY	453 MHz	922 MHz	1920 MHz
Required received power	-133.2 dBW	-134 dBW	-138 dBW
Receive antenna gain	11 dB	11 dB	11 dB
Equivalent isotrope power	-144.2 dBW	-145 dBW	-149 dBW
Equivalent isotrope power	3.8×10^{-15}	3.16×10^{-15} W	1.26×10^{-15}
Field power density	1.09×10^{-13} W/m ²	3.75×10^{-13} W/m ²	6.5×10^{-13} W/m ²
Field strength	6.4 μV/m	11.9 μV/m	15.6 μV/m
Field strength +30 dB	46 dBμ	51.5 dBμ	53.9 dBμ
Maximum distance	8 km	5.5 km	3.5 km
Maximum distance	5 mi	3.4 mi	2.2 mi



(Repeater assumes 1-watt peak power terminal at low height to a repeater having an 11-dBi gain antenna at 30-meter height.)

Figure 1-4. Plot of Maximum Distance Between Terminals.

1.2.2.6 Suburban Terminal-to-Repeater

Referring to Okumura's curves in figure 1-3, the field strength in a suburban area is taken from the urban curve for the frequency and distance, and then a correction factor is added for frequency correction. This correction factor is 8.5 dB at 500 MHz and increases at 2 dB per octave up through 3 GHz, the limit of their measurements. The effect of the frequency correction curve is to remove the frequency dependence, and essentially causes the correlated field strengths to agree with those shown in the CCIR Rec. 370-1. Here again, the user antenna is quite low compared to that of the repeater.

Echoes and doppler spreads appear quite frequently in suburban areas as they did in the city. Buildings are more likely to be uniform in size and spacing in the suburbs, which makes the echoes easier to explain but no easier to avoid.

Considering the very local diffraction effects in a city among tall buildings, it is informative to determine the path loss (excluding multipath) around sharp corners. In figure 1-5 a block geometry is defined as perhaps representing a typical situation in a large city. The figure shows a transmitter located at street level in the middle of the block and then successive locations of a receiver. Frequencies of 30, 300, and 3000 MHz are chosen, and simple knife edge diffraction around the corners is assumed. The added loss per bend is 20 dB at 30 MHz, 30 dB at 300 MHz, and 40 dB at 3000 MHz. It is doubtful if more than two bends could be tolerated. If the antenna were located at rooftop level, one bend would be involved in getting to the street. It is easy to see where the added 30 dB or more of loss in an urban environment comes from. Obviously, the lower the frequency, the better in such an environment.

1.2.2.7 Open Area Terminal-to-Repeater

Again, referring to Okumura's curves in figure 1-3, he provides another frequency correction factor for smooth terrain to values taken from the curves of figure 1-3. Hence, the correction factor is 21.5 to 26.5 dB at 500 MHz, depending on how smooth the terrain is, and increases at 3 dB per octave. Very smooth terrain gets the higher factor, where the lower factor is for gently rolling hills of 20 meters knoll to valley. A sample calculation might prove interesting. Again, choosing 1920 MHz and using 23.5 for our 500-MHz correction factor, we have a correction factor at 1920 MHz of 29.33 dB. This would provide a median range of 16 miles in open areas compared to the 2.2 miles covered in the city.

1.2.2.8 Conclusions

The limiting case for the terminal-to-repeater link is the urban location. The range will be short (generally less than 3 miles). With omnidirectional antennas at both ends, multipath will limit the signaling rate as well as range. If propagation were the only consideration, frequency should be as low as possible. The number of repeaters necessary to blanket an area is roughly proportional to frequency, other parameters remaining constant. Suburban repeater-to-repeater links are similarly limited without the problem of location variability and restricted range.

1.2.3 Transmission Within and Through Buildings

Several articles have appeared in the literature which address the approach of radiating into buildings. At least two more are in process, one by the Federal Communications Commission (FCC) and another by the British Post Office. These data must be used with some caution for packet radio system design, since most testing has been relative to voice or low data rate transmission systems that are relatively tolerant to signal distortions resulting from multipath. The multipath or signal dispersion problem is expected to be far more critical for packet radio systems operating at data rates in the range of 100 kilobits/second (kb/s).

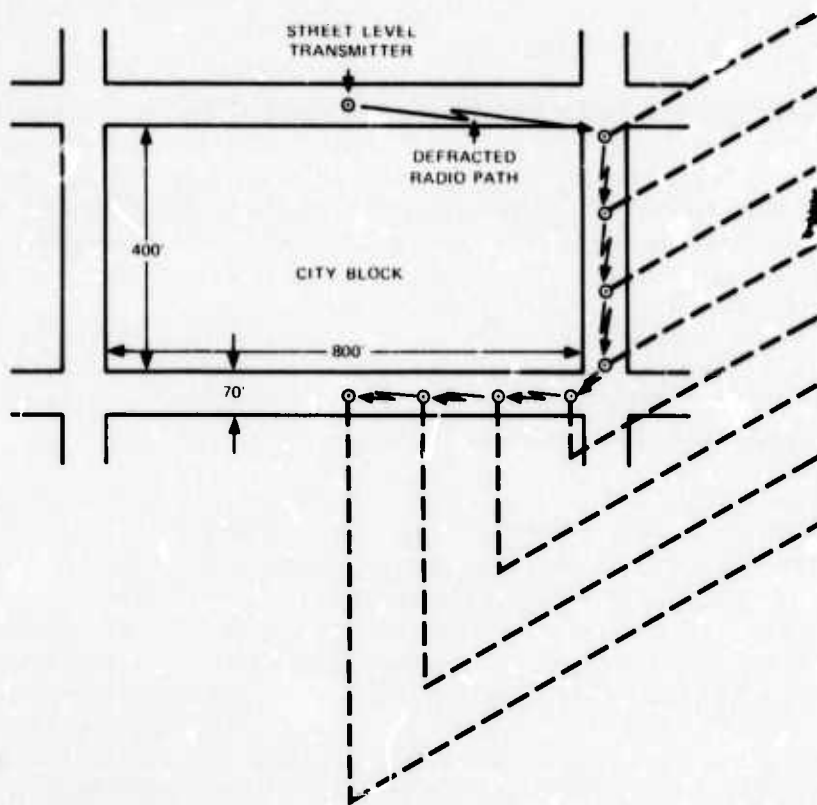


Figure 1-5. Street Level Signal Defraction.

1.2.3.1 Radiation into Buildings

Radio waves suffer little loss at vhf frequencies since they pass through dielectric type walls such as wood, glass, or drywall construction. Some loss data is shown below for conducting walls ('semi-conducting' might be a more accurate term) at a frequency of 160 MHz.

ATTENUATION AT 160 MHz²

<u>Wall Material</u>	<u>Transmission Loss</u>
8-inch concrete block	5-8 dB
6-inch solid concrete without steel reinforcing	10-15 dB
Suspended metal ceiling	15-20 dB
Solid metal walls	20-40 dB
Right-angle bends in hallways	15-20 dB

Statistical building penetration measurements have been made at 35 MHz, 150 MHz, 450 MHz, and 910 MHz.^{7,8,9} In general, these measurements were made by illuminating a building from a sufficient distance such that the field strength is uniform outside the building along one wall. Measurements were then made inside the building in interior rooms, not in rooms on the illuminated side of the building. Of course, within a room, many standing waves

exist. Maximums occur at intervals of approximately one-half wavelength in all three planes, interspersed with nulls in the field. The maximums tend to be quite steady in amplitude, but the minimums vary in level due to people moving around in the building or even in adjacent rooms and hallways.

Results of these measurements were stated as excess loss, or the loss accrued due to penetration of the building is as follows.

BUILDING PENETRATION BY RADIATION, 35 MHz to 910 MHz

1% of measurements, excess loss < 7 dB

50% of measurements, excess loss < 29 dB

99% of measurements, excess loss < 35 dB

These measurements are valid for floors above ground. Signals measured in first-level basements are 18 to 30 dB below ground floor signal levels.

Variation of excess loss with frequency is inconclusive from the data. The 900-MHz measurements were markedly better than 450-MHz signals in some rooms, but were worse in others. Rice⁷ stated that 150 MHz was slightly better than 35 MHz, however, schefer⁸ was not able to corroborate Rice's findings.

Radio waves apparently enter buildings by two mechanisms. At low frequencies, the radiation penetrates the dielectric type walls. At higher frequencies where the windows are larger than one-half wavelength, the radiation comes in through the windows. These statements are intuitive and one might be led to believe that somewhere between good wall penetration at 35 MHz and good window penetration at microwave frequencies, there might be a frequency in between that would display statistically poorer results than the ends of the spectrum under discussion. Some of the writers of these articles agreed at a conference in Boulder⁹ that one frequency is not significantly better, worse, or even different from another from a statistical viewpoint.

If a distant transmitter does not deliver a sufficient signal into a particular building, a possible solution is to locate a repeater on a nearby building to provide a stronger illumination. This technique was applied to a 30-story hotel building;⁸ the repeater was on a 9-story building nearby. It is reported to have worked well, even into the basement and in the elevators.

1.2.3.2 Signal Conduction into Buildings

Conducting signals into buildings would probably furnish stronger, more reliable signals at the cost of physically wiring the building itself for this special purpose. Of course, this presupposes that a two-way repeater is situated on top of the building. It must receive the signal from outside and send it inside the building; it must also receive the signal off the wire from inside the building and transmit it outside the building. For the conductors themselves, one must consider the use of existing wiring, telephone wiring or power wiring. If these are not suitable, a balanced transmission line might be used as suggested by Farmer, et al.⁸

The repeater must receive some special attention. It might receive and retransmit rf if the in-building distribution wiring is capable of carrying the rf. On the other hand, the repeater

packet radio — radio link considerations

might be required to receive an rf signal, down-convert to a carrier signal, and vice versa. If the repeater sends and receives rf, it will probably be simply an amplifier.

If the wiring will not handle the rf, then the repeater must receive an rf signal and down-convert to a low frequency carrier for transmission into the building. An additional box would then be required at the terminal to translate back up to rf so the terminal could receive the data. Alternatively, the terminal might have a carrier frequency input-output mode for such operation. Only a patch cord to connect the terminal to the building wiring would then be required.

1.2.3.3 Telephone Lines

If a suitable terminal device is available, the telephone lines are quite capable of carrying a high data rate at carrier frequencies. It should be pointed out that FCC Tariff No. 260 makes provisions for connecting company-owned in-plant terminals and wiring to the telephone industry's outside-plant transmission and switching network. To avoid the problem of telephone industry requirements, the discussion which follows assumes that the in-plant telephone system is privately owned and that it meets the telephone industry requirements at the interface between private terminals and the telephone industry's transmission and switching equipment.

Telephone lines inside a building consist of twisted pairs of No. 20 to No. 26 wire. These are bundled into cables and passed through conduits to terminal blocks and switchboards. The Bell System uses such lines for its T-1 carrier system at data rates of 1.544 mbits/s.

This digital signal is transmitted over twisted pairs with regenerative repeaters located typically every 6000 feet. The distance is determined primarily by the frequency response of the line; that is, the attenuation and group delay as a function of frequency. Lines used are toll grade cable; hence, distance between repeaters is considerably greater than would be possible with in-building wiring where cable of 20 to 26 wires is typical. In-building distances, however, would certainly be less than 6000 feet. Signal levels should be held to the range of 0 dBm to -10 dBm. Higher levels increase the risk of crosstalk onto other lines that might not be filtered before they leave the premises. The maximum signal levels at the telephone company interface located on the premises is shown below. The packet radio signals must be filtered out before they reach that interface.

MAXIMUM APPLIED SIGNAL LEVELS TO 600-OHM¹⁰ VOICE PRIVATE LINES

300 to 3000 Hz *	-29 dBm 3 second average (measurement methods prescribed by Bell System)
3995 to 4005 Hz	-47 dBm
4000 Hz to 10000 Hz	-32 dBm
10000 Hz to 25000 Hz	-40 dBm
25000 Hz to 40000 Hz	-52 dBm
40000 Hz up	-66 dBm

*Note that 2600 Hz must be blocked by user equipment. At no time shall energy appear solely between 2450 and 2750 Hz. When power is applied in that band, it shall not exceed the power currently present in the 800- to 2450-Hz band.

The telephone distribution wiring inside a building is a poor vehicle at rf frequencies because it is small and nonuniform as a transmission line causing high loss, as much as 2 dB/ft at 3 GHz.

1.2.3.4 Power Wiring

Another vehicle that might be considered for conductive in-building distribution of packet radio signals is the power wiring. Measurements were made on a sample of typical commercial power wiring. It was 40 feet long, 3/4-inch thin wall conduit with three No. 10 wires pulled through. The wires were individually insulated with polyvinylchloride insulation. Two of the three wires were grounded to the conduit; the third was the conductor in an unbalanced configuration. The impedance of the line was nominally 55 ohms with a vswr of 1.5 to one over a frequency range from 400 MHz to 4 GHz. Of course, the line is nonuniform so that the impedance changes with frequency. A good reason for the line having such a low vswr is that it is so lossy. Loss measurements are shown below.

POWER LINE ATTENUATION AT MICROWAVE FREQUENCIES

<u>Frequency (GHz)</u>	<u>Attenuation (dB/100 ft)</u>
0.4	62.5
1.0	80
2.0	100
3.0	115

By comparison, RG-8/U coaxial cable has 16 dB/100 ft attenuation at 3 GHz, RG-58/U has 37.5 dB/100 ft, and commercial TV 300-ohm flat twin lead has 7.6 dB/100 feet at 3 GHz. Obviously, the power wiring is quite lossy at microwave frequencies; however, it is universally installed in buildings and can be used with very simple couplers between any ordinary outlet and a packet radio on one end and an outlet and the roof-mounted receiver on the other end. Although we are working with a transmitter and receiver with a combined transmission loss of 100 dB, one can radiate signals inside a typical building with less loss provided he does not have to penetrate metal walls.

The power wiring can handle low frequency carrier signals, probably with less loss than the telephone lines discussed previously; however, the noise generated by ac appliances can be both quite high and quite variable. It would be necessary to conduct an extensive measurement program on the power distribution wiring before attempting to design a data system that used it for transmission.

1.2.3.5 Special Wiring

Buildings and tunnels have been successfully wired to distribute radio signals using balanced transmission line as the conductor. Balanced open wire transmission line such as TV twin lead is not a perfect transmission line in that it does radiate some of the signal it carries, i. e., it leaks. The power lost to leakage is considerably less than the I^2R loss, so it is considered a good transmission line. We can use this leakage to our advantage. A roof-mounted repeater might receive a signal from the outside world, amplify it, and send it into a many-branched twin lead transmission line, each branch being terminated at the far end. The twin lead is installed near the ceilings of the hallways of the building, in the ceilings if they are of sheetrock or acoustical tile construction. These lines radiate a small signal along their length that is quite steady and strong enough for a packet radio terminal to receive on its regular antenna.

packet radio — radio link considerations

The curves of figures 1-6 and 1-7 are taken from Farmer, et al⁸ and were measured at 160 MHz; however, the radiation from a particular line increases with the square of the frequency. An increase in the leakage of the line is desirable in our peculiar use of the line. This can be achieved by twisting the line tightly, on the order 1/4 twist per line spacing as measured along the line. Figure 1-7 shows a 30-dB increase in radiation achieved by twisting the line.

1.2.3.6 Wired Television Systems (CATV)

Wired television systems are found in many areas and increasingly are being considered as a shared broadband transmission facility for other types of services. Such systems appear to offer a viable technique for distribution of digital packets within a building or in an urban area where radio transmission is poor. This technique is being investigated by others and, hence, was not investigated as part of the radio transmission investigations.

1.2.3.7 Conclusions

Every building will require some analysis to determine which technique is required to deliver a usable signal to a terminal inside. If the building has windows and is relatively close to a system repeater, no special techniques will be required. At greater distances, a simple repeater with directional antennas focused on specific buildings will deliver the signals to interior users by radiation. Buildings that are effectively shielded must have a simple, dedicated repeater to receive a signal and pipe it into the building over conductors of one type or another. Of the three conductor types considered here, the twin lead system appears to be the most attractive since the line is cheap and it requires no increased complexity of the terminal circuitry over that required for out-of-doors use.

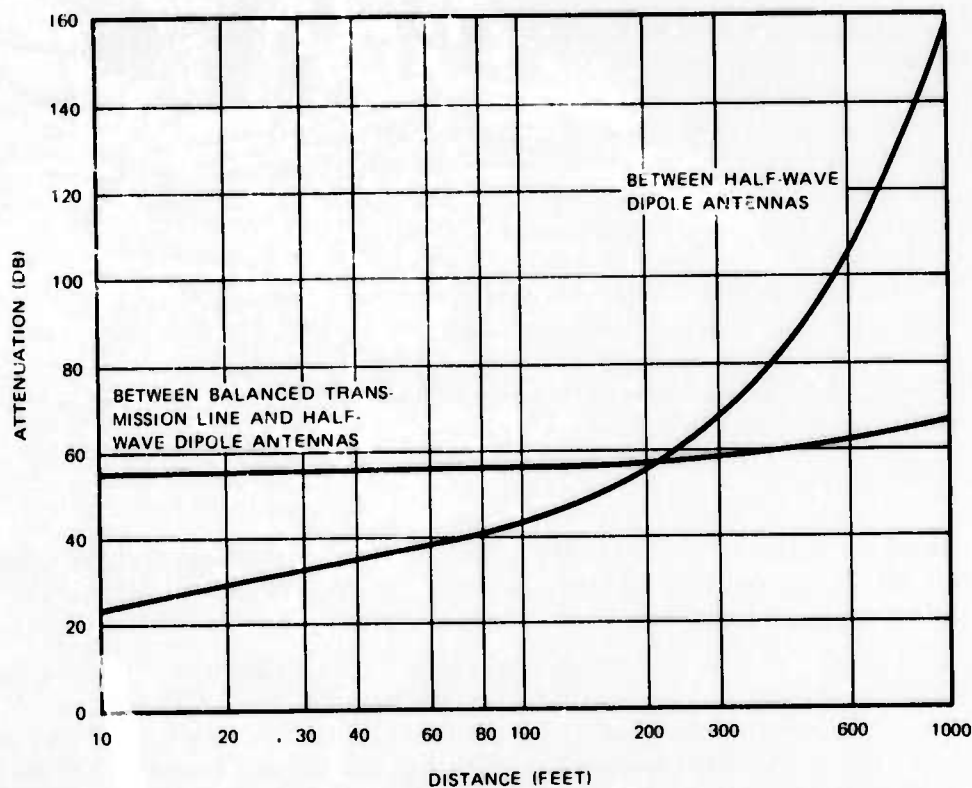


Figure 1-6. Attenuation in Tunnels and Buildings Between Half-Wave Dipoles and Between Transmission Line and Half-Wave Dipole at 160 MHz.

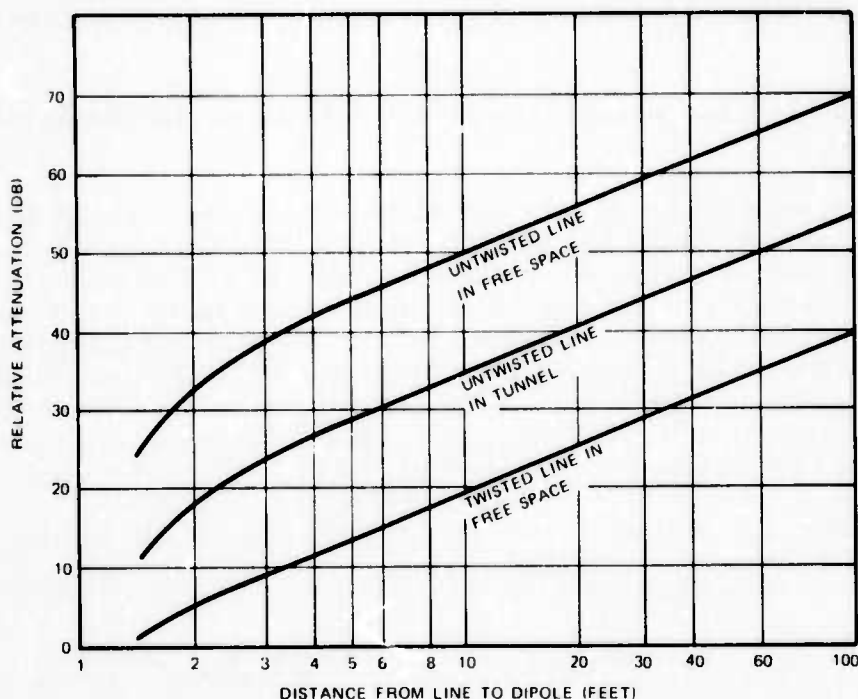


Figure 1-7. Relative Attenuation Between 200-Ohm Balanced Transmission Line and Half-Wave Dipole Antenna at 160 MHz.

1.3 SPREAD SPECTRUM TECHNIQUES

Spread spectrum techniques offer potential for solving some of the problems in the application of the packet radio systems. Of particular interest is the potential for more efficient use of the spectrum that might result from a more even distribution of energy over the frequency spectrum of interest and separation of channels by correlation techniques. In networks as complex as envisioned for packet radio, it is desired that complex synchronization systems be avoided and that the traffic flow control be sufficiently intelligent to negate the effects of random contention for a channel. Spread spectrum techniques may aid in solving the contention problem by separation of signals by time of arrival or by use of different codes.

The use of spread spectrum techniques is becoming increasingly attractive because of the drastic reduction in hardware complexity now being made possible by recent advances in device technology. Of particular interest is the Surface Acoustic Wave Device (SAWD). This device has been applied in the propagation test system described in detail in volume 2 of this report.

The following briefly summarizes the techniques employed in the generation of spread signals and lists issues requiring further investigation.

The basic concepts underlying all spread spectrum techniques are those that are embodied in communication theory with respect to matched filters and correlation detection. That is, when the receiver has exact knowledge of the possible waveforms that it will be receiving, the receiver can be configured to select the desired set of waveforms and exclude the other waveforms that appear simultaneously at the receiver input. The degree of selection and exclusion depends upon two factors.

packet radio — radio link considerations

- a. The degree to which the receiver appears as a perfect matched filter to the desired waveforms
- b. The degree to which the desired waveforms and the undesired waveforms are orthogonal (uncorrelated).

In general, perfect-match filtering cannot be achieved because of the effects of distortion by the transmission medium. Similarly, perfect orthogonality cannot be achieved because of timing errors. Further, it can be shown that the number of orthogonal waveform/codes that can be employed is directly proportional to the transmission bandwidth. In general, the larger the transmission bandwidth, the greater the ability to reject interfering signals. The validity of the last statement is dependent upon the linearity of the transmission medium. For example, it can be shown that for a radio transmission path subject to multipath, there is an optimum spread spectrum bandwidth for each link and the use of excess bandwidths can result in reduction of signal quality.

If the interfering signal is noncorrelated with the desired signal, the output signal-to-noise ratio is given by the following expression:

$$\text{SNR}_o = \frac{S}{S_i + N} \left(\frac{W}{b}\right)$$

where

S = Desired signal strength

S_i = Interfering signal strength in the transmission bandwidth, W

N = Noise level in the transmission bandwidth, W

b = Information bandwidth.

Most spread spectrum techniques employ digital modulation techniques with chip rates that are an order of magnitude or greater than the basic message data rate. From the above formula it is seen that if $W = 10b$, $S/N = 10$, and $S_i = S$, and that $\text{SNR}_o = 9$, compared to a value of 100 in the absence of no interference or to a value of 0.9 in the presence of interference without spread spectrum techniques.

One of the detection approaches commonly employed is to crosscorrelate the received signal with a stored replica of the desired spreading waveform/code and then process the product through integrate-and-dump filters. The crosscorrelation process will despread the desired signal; that is, it will coherently collapse the spread signal in a bandwidth, W, into the original message signal in a bandwidth, b. Any interfering signal simply becomes respread and, if the interfering signal is uncorrelated, simply appears as an increase in the background noise level. The integrate-and-dump filter simply provides an output that is used to decide whether or not the output of the crosscorrelation is a desired signal or not.

The decision process involves a minimum time delay on the order of $T = 1/b$ second, assuming that the optimum integration time is employed; that is, the maximum output of the integrate-and-dump filter reaches its maximum output for a correlation signal at the T seconds following the arrival of a packet.

The implications of the use of greater bandwidths for spread spectrum techniques can be summarized as follows:

Advantages of Greater Bandwidth

1. Greater ability to reject interference
2. Greater number of orthogonal waveform/codes

Disadvantages of Greater Bandwidth

1. Wasted capacity of transmission medium
2. Greater costs in equipment complexity

1.3.1 Pseudorandom Sequences

At the heart of most spread spectrum systems is a pseudorandom sequence generator. There are several reasons why this is so. For the application of interest for packet radio systems, the primary reason is their simplicity of generating orthogonal codes, their flexibility, and their positive reproducibility for reference/correlation purposes at the receiver.

Feedback shift register generators are available that can be quickly modified by appropriate switching to provide entirely different (i.e., uncorrelated) sets of pseudorandom waveforms. Moreover, any number of units can be produced to accurately and positively generate identical sequences so that multiple-user applications can be implemented. Further, such pseudorandom sequences can have desirable randomness properties. The so-called maximal-length sequences have an autocorrelation function which has a tall central peak in the vicinity of zero shift, but which is very small for time shifts greater than the width of one digit. Also, the crosscorrelation function for two different maximal-length sequences of the same length approaches zero for all time shifts. Pseudonoise generated in this fashion has an advantageous property over truly random noise in its ability to be exactly reproduced at remote locations.

The type of binary code or pseudorandom sequence under consideration in this section is that usually produced by a feedback shift register generator or a tapped delay line. A simple shift register consists of several (say, n) 2-state active devices (commonly referred to as flip-flops) connected in a cascade arrangement. The binary state of each stage of the register represents a binary digit or bit (0 or 1), and the "state" of the entire shift register at any instant is characterized by the n -bit binary number formed by the n digits stored in the register.

A shift register transfers the binary state (i.e., the binary digit stored in each stage) to the next succeeding stage whenever a shift pulse occurs. Such shift pulses are normally produced by a "clock" that is essentially a highly stable oscillator or frequency generator. When the shift pulses are regularly spaced, as from a clock, each particular digit will propagate at a uniform rate down the shift register, much as a pulse flows down a delay line.

We are interested here not in simple shift registers, but in feedback shift register generators (FSRG). An FSRG is formed, in general, by taking an output from each of the n stages of the register and combining these outputs in a connection matrix and feeding the resultant output back to the input of the register. Thus, binary digits flowing out of the FSRG at the clock frequency are some function of the n preceding digits that were stored in the register. The code or pseudorandom sequence generated by an FSRG is a specific function of the interconnections between the stages of the register. Particular codes are selected by choosing certain stages for feedback, and by the feedback logic used in the connection matrix.

packet radio — radio link considerations

The key to a pseudorandom sequence usually refers to the choice of stages for inputs to the connection matrix, whereas the class of codes (i.e., either linear or nonlinear) produced by the FSRG is determined by the type of operations performed in the connection matrix. The key may also refer to the binary coefficients, $a_i = (0 \text{ or } 1)$, in a transportation

$F(a_1, b_1, a_2, b_2 \dots a_n, b_n)$, perhaps nonlinear, performed on the outputs of the n stages of the FSRG to form a new output sequence. Linear logic results in linear codes and higher order operations produce nonlinear codes.

The operation of an FSRG also may be visualized as a sequence of binary states, each of which is characterized by the n -bit (-digit) binary number stored in the register. The sequence of binary numbers formed in the register is a specific function of the initial state conditions of the register and of the feedback logic. Thus, given an n -bit number in the register, the FSRG produces a new deterministic n -bit number when triggered by a shift pulse. Consequently, such a generator is periodic since the deterministic process will eventually reestablish the initial state conditions in the register; i.e., the original binary number will be re-formed, and the sequence proceeds to repeat itself at that point. The length of the sequence or code is the number of digits in one period. Since the total number of n -bit binary numbers (including the all zero number) that can be formed from n binary digits is 2^n and the binary code produced by the generator is a specified function of the n -bits in the register, the maximum length of such a code is $2^n - 1$ digits and the maximum period is $2^n - 1 / f_c$ seconds, where f_c is the clock frequency. If the period of the code is long enough, the code has the appearance of randomness over any subsection of the period, despite the deterministic method of generation, and it is termed a pseudorandom sequence.

The most general code produced by an FSRG is composed of binary digits, b_i , either 0 or 1, determined mathematically by a modulo-2 recursion relation of the form:

$$b_i = \sum_{\text{mod-2}} c_0 + c_j b_{i-j} + c_{jk} b_{i-j} b_{i-k} + c_{jkl} b_{i-j} b_{i-k} b_{i-l} \dots \quad (1)$$

where b_{i-j} is the j^{th} binary digit in the register preceding b_i .

The c -s are binary coefficients, either 0 or 1, that describe the operations performed in the connection matrix. The notation of equation (1) indicates that the summation is extended over all possible single terms, pairs, triples, etc, of the n digits preceding b_i . Also, the summation is performed by modulo-2 or mod-2 addition, defined by the rules $1 + 1 = 0 + 0 = 0$ and $1 + 0 = 0 + 1 = 1$. A modulo-2 addition device simply compares two inputs and generates a binary symbol 1 if the inputs are dissimilar and a 0 if they are alike. The total number, N_c , of possible coefficients in equation (1) is the total number of combinations of n things taken none, one, two, . . . up to n at a time, or:

$$N_c = \sum_{k=0}^n \frac{n!}{k!(n-k)!} = (1+1)^n = 2^n \quad (2)$$

Thus, the total number of possible coefficients is equal to the maximum possible number of code digits in one period of the code. Since the 2^n coefficients may be chosen arbitrarily, it appears that an FSRG implementing equation (1) can produce an arbitrary code. However,

in general, a given set of feedback connections produces sequences of periods less than 2^n digits, since repetition commences at any point where an n -digit binary number is repeated in the register. The complete set of distinct periodic codes produced by any particular set of feedback connections will total $2^n - 1$ (all zero condition excluded), the different codes being generated with different initial state conditions in the register.

The simplest type of feedback connection that may be used is one retaining only the linear terms in equation (1). The appropriate formula is a special case of the general form as follows:

$$b_i = c_0 + \sum_{j=1}^n c_j b_{i-j} \quad (3)$$

where all digits are binary, either 0 or 1, and the addition is modulo-2.

Whenever the digits of a sequence are generated by some linear (modulo-2 sum) combination of the n preceding digits, the sequence is termed linear. Linear codes are of considerable importance because they can display correlation properties and spectral distributions approaching the ideal for use in producing spread spectrum signals. For the linear case of the binary, coefficients (c_j) are represented by open or closed switches in the feedback network. A closed switch causes the corresponding coefficient in equation (3) to have the value unit, whereas an open switch assigns the value zero to the coefficient.

This simple form of an FSRG is only one method of generating a linear sequence. Other more complicated methods exist. Compound FSRG's or combinations of more than one simple FSRG can also be used to produce linear sequences. Examples of these are the multiple-return generator consisting of several feedback loops around more than one simple FSRG or several simple FSRG's acting independently in a cascade arrangement, one serving as the input for the next, or connected in a "beat" or parallel fashion so that their outputs add modulo-2. However, it can be shown that the sequences from these compound generators can be generated by a simple FSRG of equal or fewer total stages. Also, although we emphasized the use of flip-flop shift registers, tapped delay lines can also be used to drive the feedback logic. In any case, the sequence generated by any of these generators will be linear if modulo-2 addition is the only logic operation employed. Two types of linear generators will be discussed. Generators which, because of a particular feedback logic, produce only cyclic permutations of one sequence no matter what the initial register contents (so long as they were not all zero) are called maximal generators. Generators that produce more than one sequence for a particular logic are called nonmaximal.

The mathematical theory of linear sequences and generators has been thoroughly studied and expounded upon by several groups to the extent that we feel it unnecessary to provide proof here. However, we will distinguish between maximal and nonmaximal generators. Determination of whether a specific FSRG is maximal or nonmaximal need not be a complicated task since tables exist listing all maximals with 19 or fewer stages.

1.3.1.1 Properties of Maximal Generators and Maximal-Length Sequences

The following outlines the properties of maximal generators and maximal-length sequences.

- a. A maximal generator of n stages produces a maximal-length sequence of length $L = 2^n - 1$ digits. The period of such a code is L/f_c second, where f_c is the clock frequency.

packet radio — radio link considerations

For example, if $n = 32$ and $f_c = 10$ kHz, the period of the sequence is almost 5 days.

- b. The number of distinct maximal-length sequences for any n is $\phi(2^n - 1)/n$, where $\phi(x)$ (the Euler phi-function) is the number of integers less than x which are prime to x . This number is roughly L/n .
- c. The autocorrelation function of a maximal-length sequence is periodic with a tall triangular peak of height (L) and base the width of two digits reoccurring at multiples of the period L/f_c , and otherwise has the value -1 . Since the peak value $(L = 2^n - 1)$, the excellent approximation for large n , the height of the peak relative to the subsidiary off-peak autocorrelation (the pedestal) doubles per each stage of the register.
- d. The power density spectrum of the maximal-length sequence (i.e., the Fourier transform of the autocorrelation function) contains harmonic lines (impulses) at multiples of f_c/L with an envelope given by $(\sin \pi f/f_c)^2 / (\pi f/f_c)^2$, which is determined solely by the triangular peaks of the autocorrelation function. Note that the bandwidth of the spectrum is proportional to the clock frequency, f_c .
- e. The crosscorrelation properties between maximal-length sequences from differently connected generators with equal number of stages has been studied experimentally. It has been experimentally demonstrated that the cross-correlation of two different maximal-length sequences of the same length is negligible. Similarly, it has been experimentally determined that the crosscorrelation function for any time shift has roughly a Gaussian distribution of amplitudes about (i.e., perpendicular to and centered on) the time axis with an average absolute value proportional to $1/\sqrt{L}$.

The above correlation and spectral properties are obtained for averages over a full period of the sequence; but for long sequences, such averaging may be impractical and short-time averages would be more appropriate. Unfortunately, not a great deal is known about the short-time properties of these sequences.

1.3.1.2 Properties of Nonmaximal Generators and Their Sequences

The following outlines the properties of nonmaximal generators and their sequences.

- a. The longest possible nonmaximal-length sequence (less than $2^n - 1$ digits) is produced by the initial state conditions of all 0's stored in the register, except a single one in either the first or last stage. All other initial conditions produce shorter length sequences.
- b. Ignoring the trivial sequence of all 0's, the sum of the lengths of all the different nonmaximal-length sequences is $2^n - 1$ digits.
- c. The autocorrelation and crosscorrelation characteristics of certain nonmaximal codes have been shown to be excellent. For the longest sequences, the height of the central autocorrelation peak relative to the highest subsidiary peak doubles for every stage of a generator constructed with the minimum number of stages required to generate the sequence.
- d. The autocorrelations and power spectra can be obtained by determining the equivalent compound or beat-type generator which consists of a combination of only maximal generators.

Since nonmaximal-length sequences can be generated by a combination of maximal generators, an appropriate choice of the maximal sequences used in these configurations can produce a nonmaximal sequence that has a length nearly equal to the maximal sequence length that could have been generated with the same number of total stages. That is, two generators of n_1 and n_2 stages used in combination have properties that are nearly as good as a generator $n_1 + n_2$ stages with a maximal length $2^{n_1+n_2} - 1$ digits. For example, consider a 36-stage generator. In order to set up a maximal 36-stage FSRG, a knowledge of which feedback connections yield maximal generators is required, and as was mentioned before, only maximal generators of 19 or less stages have been tabulated. Thus, since one does not know how to connect up a 36-stage maximal generator, one must be satisfied with a nonmaximal-length sequence generated by the combination of two maximal generators of perhaps 19 and 17 stages. Since the periods of the two component maximal-length sequences ($L_1 = 2^{19} - 1$ and $L_2 = 2^{17} - 1$) are relatively prime (no common factors), the longest period of a nonmaximal-length sequence is $L_1 + L_2$. This length differs by less than 0.001 percent from $L = 2^{36} - 1$, the period that would have been obtained with a maximal generator of 36 stages. The long-time average secondary autocorrelation peaks are down from the central peak by a factor approximately 10^{-5} , as compared to about 10^{-11} for the maximal-length sequence. Although nonmaximal sequences are not so amenable to general analysis, they may be very close to being equally good theoretically and possibly better from a practical viewpoint than maximal sequences. This points up the fact that nonmaximal sequences are not to be considered unimportant.

1.3.2 Alternates to Pseudorandom Sequences

There are a number of other spreading techniques that could be considered other than the use of digital pseudorandom sequences. For example, conventional frequency modulation is a spread spectrum technique that provides rejection of interference at the expense of greater bandwidths.

Although the randomness aspects of pseudorandom sequences were not particularly emphasized in the preceding paragraph, this is a desired characteristic for military and secure communication links. Properly employed, the transmitted energy tends to be distributed, on the average, evenly over the transmission band.

Conceptually, one could achieve this randomness for spreading the transmitted energy evenly over the transmission bands by other means. For example, the energy could be spread by simply modulating the white Gaussian noise. The difficulty is in reproducing the noise waveform at the receive terminal for despreading. Also, one could achieve the same effect by employing a finite length of white noise, retaining only the zero crossings and matching this to a series of Walsh functions. This could easily be reproduced at the receive terminal for despreading with the key being the set of coefficients that specifies the required Walsh functions.

For the packet message network, randomness to the degree often sought for military and secure links may not be as desirable. An excellent alternative could be to use single Walsh functions as the spreading code/waveform. Walsh functions are orthogonal and are easily generated/processed by digital techniques. These and related functions are being employed in a number of communication applications such as for compressed digital voice transmission, multiplexing, etc.¹²

packet radio — radio link considerations

1.3.3 Issues

If spread spectrum techniques are to be applied to packet radio systems in a viable manner, there remains a number of issues to be resolved which require further investigation. These include at least the following:

- a. Is the packet radio system to share the frequency spectrum with other services with quite different characteristics? If so, what are the characteristics of these systems and what constraints, if any, can be placed on the siting of the different types of systems (i.e., what is the requirement for isolation between systems?)
- b. Can spread spectrum techniques provide an adequate means of allowing multiple terminals to communicate simultaneously with a repeater using time of arrival or code isolation?
- c. Can spread spectrum provide a technique of transmitting low rate control, bookkeeping, diagnostic information, synchronization, etc., independent of the normal traffic (i.e., by spreading at a power level 20 to 25 dB below the packet signal)?
- d. Can spread spectrum be implemented within the economic objectives for wide deployment of a packet radio network?

The above issues require further investigation. The question of coexistence or shared usage of a common spectrum by packet radio and other systems is a particularly difficult problem because of the potential operation of packet radio systems as portable digital communication systems with no control over the spatial isolation of the systems that are to share the same radio spectrum.

1.4 PACKET RADIO SYSTEM POWER BUDGET

The following presents a power budget and defines a repeater configuration that reflects the best estimate of system parameters at this point in the program. A transmit power level is assumed based on what is believed reasonable with current devices, considering both the need for battery powering and reasonable terminal and repeater costs. The repeater and terminal spacings are then determined based on measured propagation data. A spread spectrum system is assumed, although this does not influence the propagation range relationships in a noninterfering environment. The dynamic range requirements of the receiving equipment are also estimated.

1.4.1 Assumed System Parameters

The following assumptions are made about system parameters for the power budget calculations.

- a. Carrier frequency range is 1700 MHz to 1850 MHz.*

*The relatively high operating frequency assumed is based on spectrum availability considerations and is not necessarily optimum from a propagation point of view. Selection is tentative for purpose of example, and final choice will be influenced by the results of propagation and noise measurements.

- b. Channel Characteristics. Path loss is corrected according to Okumura, et.al.⁴ for repeater-to-terminal links where the repeater antenna is assumed to be at 45m height and the terminal antenna at 3m. Free-space loss is assumed between repeaters with both antennas at the 45m height. Nonadditive white Gaussian noise is assumed.
- c. Data rate is 100 kb/s for repeater-to-terminal links, and 500 kb/s for repeater-to-repeater links.
- d. The modulation is differential coherent minimum shift keying (dcmsk). For this modulation method, the ratio of hertz per bit is approximately 1.5.
- e. Code spread of 100 for terminal-to-repeater links and 20 for repeater-to-repeater links.
- f. Noise figure of receiver is 9 dB.
- g. Antenna gain above isotropic is 0 dB for the terminal and 5 dB for the repeater.
- h. The transmitter power amplifier output is 10 watts.
- i. The required probability of a bit error is less than 1×10^{-5} .

1.4.2 The Power Budget Equation

The basic relationship for determining the carrier-to-noise power relation (C/N) is given in the following equation:

$$C/N \text{ (in dB)} = \text{erp} - \text{path loss} + G_{ra} - 10 \log KT_o B - NF$$

where

erp = Effective radiated power in dBm

G_{ra} = Receive antenna gain

KT_o = Noise spectral density

B = Occupied bandwidth

NP = Noise figure of receiver in dB.

The occupied bandwidth for the assumed system parameters is:

$$B = (\text{spread factor}) \times (\text{data rate}) \times (\text{Hz/bit factor}) = 15 \text{ MHz}$$

for repeater-to-repeater and repeater-to-terminal links.

The relationship between signal-to-noise and bit error performance for dcmsk is given in figure 1-8. It should be noted that signal-to-noise is expressed in E_b/N_o , where E_b is the energy per bit. Hence, one must convert C/N to E_b/N_o . This can be accomplished by multiplying C/N by τ (the bit interval) and E_b/N_o by $1/B$ to yield:

$$\frac{C \cdot \tau}{N} = \frac{E_b}{N_o \cdot B}$$

packet radio — radio link considerations

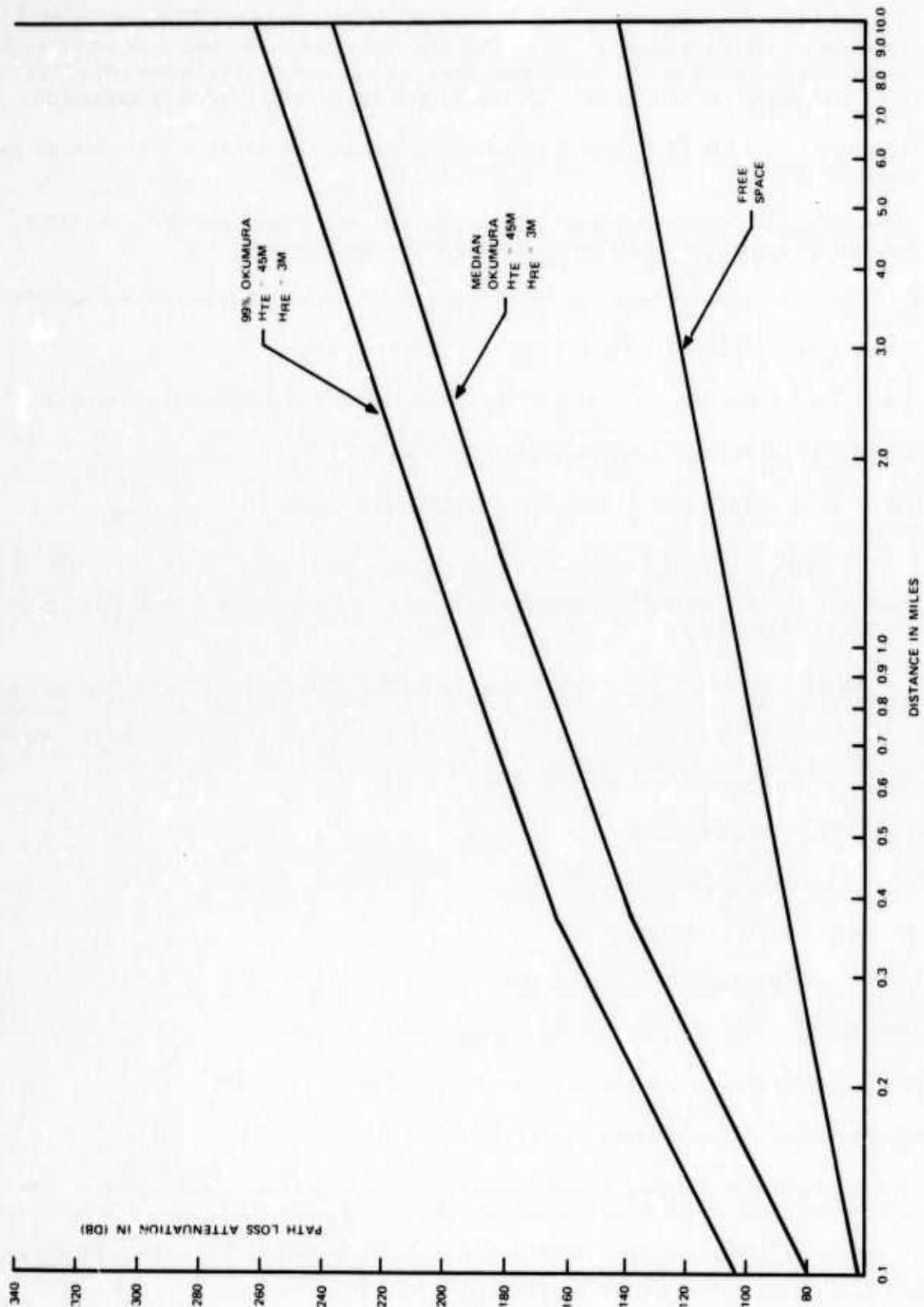


Figure 1-8. Transmission Loss Versus Distance.

so that

$$E_b/N_o = C/N \cdot B$$

The factor τB can be viewed as the product of the processing gain and the Hz/bit factor. The noise power (N) also has this factor, and therefore, E_b/N_o is independent of the code spread and Hz/bit. The relationship for E_b/N_o is then:

$$E_b/N_o = \text{erp} - \text{path loss} + G_{ra} - 10 \log KT_o B^1 - NF$$

or where other system parameters are specified, the maximum allowed path loss is:

$$\text{path loss}_{\text{max}} = \text{erp} - E_b/N_o + G_{ra} - 10 \log KT_o B^1 - NF$$

where $B^1 =$ data rate, and erp and $10 \log KT_o B$ are in dBm.

1.4.3 Transmission Loss

The free-space loss equation must be altered for the poor siting of repeater-to-terminal links. Okumura provides statistical data for a mobile radio environment that approximates the conditions expected for packet radio systems. For the assumed antenna heights, the median path loss, per Okumura, at 1 mile is approximately 34 dB greater than the free-space loss. Transmission loss, Okumura corrected, varies with distance at approximately 40 dB/decade, compared with free-space loss of 20 dB/decade. Figure 1-9 shows the transmission loss for free space versus distance, the median Okumura loss, and the 99-percent Okumura loss. The 99-percent line provides insight into the variance of Okumura statistics and is interpreted to be the value for which the probability of the loss at any time, being less than or equal to this value, is 0.99.

1.4.4 Required Signal-to-Noise Ratio

The minimum E_b/N_o for P_o of 10^{-5} or less can be obtained from figure 1-8. For demsk, E_b/N_o must be greater than or equal to 10.4 dB.

1.4.5 Repeater Spacing

The statistics of propagation derived from measurements are based on a reasonably well sited repeater (i.e., 45m antenna height) and a poorly sited terminal (i.e., 3m antenna height randomly located). Therefore, the repeater spacing will be determined by the characteristics of the terminal-to-repeater link and not the repeater-to-repeater link if communications to all repeaters is to be achieved with a high degree of probability.

For the system parameters assumed, the maximum allowable path loss is calculated as 153.6 dB from the equation. From Okumura's data plotted in figure 1-10 and a specified 99-percent probability of communication, this indicates that the maximum distance between the terminal and repeater should not exceed about 1.4 miles. The received power for $E_b/N_o = 10.4$, and the assumed system parameters is -104.6 dBm.

In many cases, the propagation loss between repeaters will approach free space values due to the close spacing dictated by the repeater-to-terminal links and the moderate elevation of repeater antennas. For example, at 10 miles or the spacing of seven in-line repeaters, the

packet radio — radio link considerations

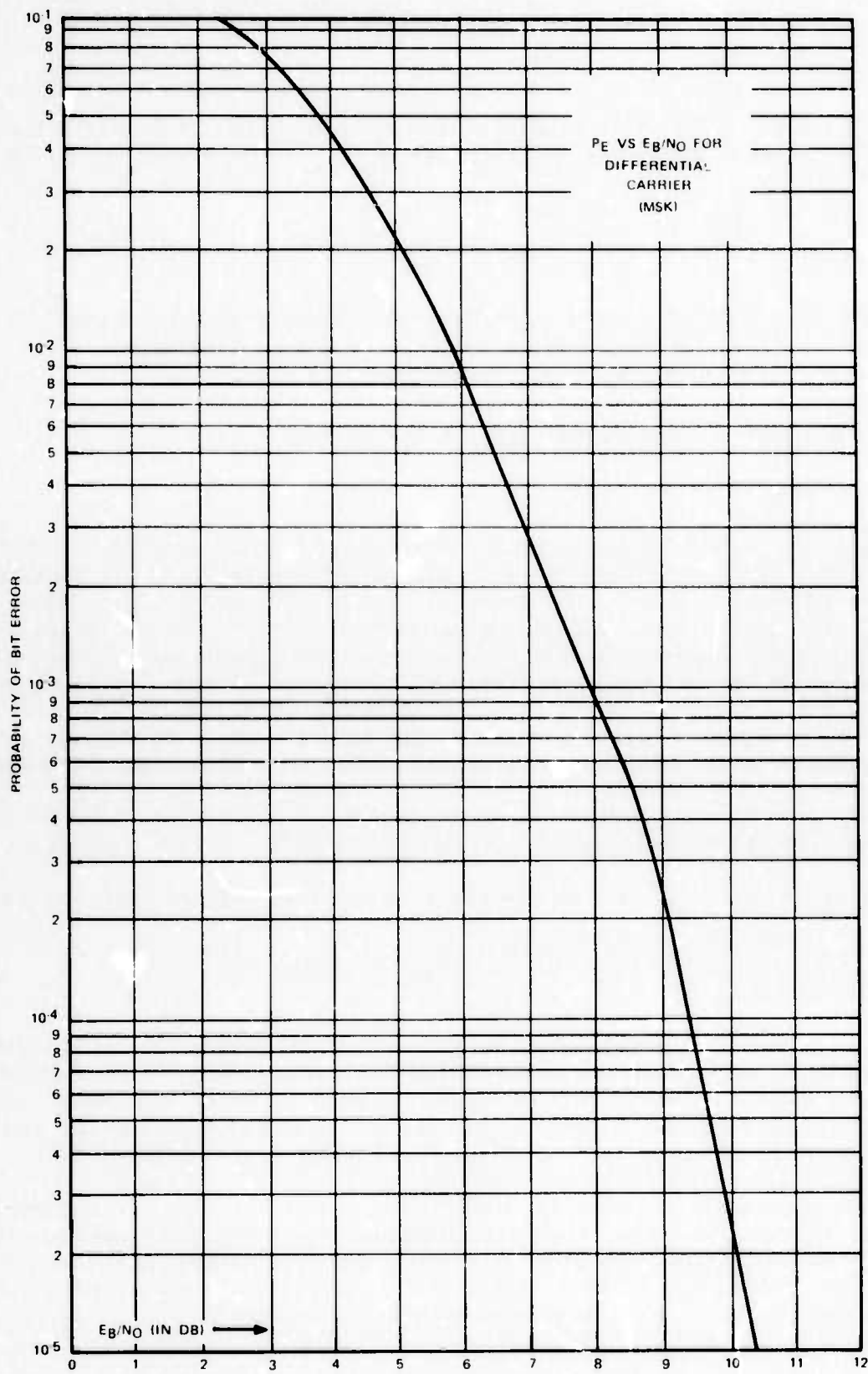


Figure 1-9. P_e versus E_b/N_0 for Differential Coherent (MSK).

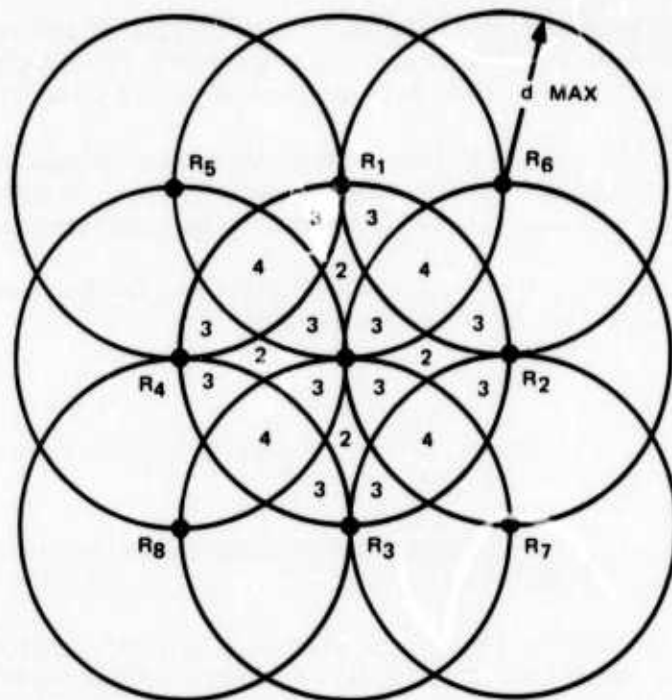


Figure 1-10. Hypothesized Repeater Spacing.

free-space loss is about 121.6 dB and the resulting E_b/N_0 is about 42 dB. The wide variation in path loss and, hence, receive power indicates that consideration should be given to adaptive power control to ensure that the power radiated to communicate with a particular terminal or repeater is not many times greater than that required to provide reliable communication. This is desirable to minimize interference to other systems that may share the same frequency.

The large variability in the communications ranges (between terminals to repeaters and repeater to repeater) is also of considerable importance in planning a routing algorithm; since in many instances, it will be possible to hop over several repeaters in a path to a station, resulting in less transmission delay and more efficient use of the network.

1.4.6 Dynamic Range

The repeaters must communicate with terminals that may be very close (possibly even under its antenna) out to the limit of its range. Also, terminals must be designed so that they may be operated within a few feet of each other while communicating with a distant repeater. Though there is no need for terminal-to-terminal communication in such an environment, the terminal must recover rapidly from blockage by such transmission so that they may receive the following transmissions from a repeater.

packet radio — radio link considerations

A reasonable minimum communication distance between terminal and repeater may be equivalent * to 1/8 mile of free space. This results in a maximum received power level of -34 dBm and a dynamic range from minimum to maximum signal of about 70 dB.

Therefore, the terminals and repeaters should be designed to operate over a dynamic range of at least 70 dB and the terminals should recover rapidly from signal blockages from nearby sources that may be received at a level 85 dB above the minimum usable signal.

Although these dynamic ranges are not particularly unusual, the fast response time required by the packet radio system is an important consideration.

1.4.7 Conclusions

The following conclusions can be drawn from this analysis based on the assumed system parameters.

- a. The maximum spacing between repeater and terminal is in the order of 1 mile for 99-percent communication reliability.
- b. The close repeater spacing dictated by the terminal-to-repeater link will result in a repeater-to-repeater range that extends over several repeater spacings. This is an important consideration in considering routing and interference.
- c. The overall dynamic range of signal levels is independent of repeater spacing, is dependent only on minimum distance between terminals, and increases 6 dB each time the minimum distance is halved.
- d. One solution to the large variation between repeater signal levels and terminal signal levels would be to normalize the repeater signal level through power control.

*Distance is specified as equivalent free space since the repeater antenna will have directivity toward the horizon. This not only increases the power level at a distance where needed, but also reduces the power level for close in terminals below the main beam. Hence, with proper repeater antenna design the 1/8-mile criteria may be adequate even for terminal directly below the repeater antenna.

BIBLIOGRAPHY

1. CCIR Rec. 370-1. Oslo, Vol. II, 1966, p 24.
2. W. R. Young, "Echoes in Transmission at 450 Megacycles from Land to Car Radio Units," Proceedings of the IRE, March 1959, pp 255-258.
3. D. C. Cox, "Delay Doppler Characteristics of Multipath at 910 MHz in a Suburban Mobile Radio Environment." IEEE Trans on Antennas and Propagation, September 1972.
4. Terry Cory, private correspondence.
5. W. C. Jakes, Jr., "Comparisons of Mobile Radio Transmission at UHF and X-Band," IEEE Trans. on Vehicular Technology, VT-16, October 1967, pp 10-14.
6. M. Mesenbergs, "Binary Error Probability Due to an Adaptable Fading Model," IEEE Trans. on Communications Systems, March 1964, pp 64-73.
7. L. P. Rice, "Radio Transmissions into Buildings at 35 and 150 MHz," BSIJ, January 1959, pp 197-210.
8. R. A. Farmer, and H. H. Shepherd, Guided Radiation — The Key to Tunnel Talking," IEEE Trans. on Vehicular Communications, March 1965, pp 93-102.
9. Joshua Schefer, "Propagation Statistics of 900-MHz and 450-MHz Signals Inside Buildings," Microwave Mobile Radio Symposium, Boulder, Colorado.
10. "Data Communications Using the Switched Telecommunications Network," Bell Syst Technical Reference, Pub 41005, May 1971, p 21.
11. Peter Bocker, "Data Transmission Over Telephone Circuits," NTZ, Heft 5, 1969, pp 297-303.
12. R. B. Lackey, "The Wonderful World of Walsh Functions," ICC 1972, paper 38-1, June 1972.
13. Yoshihisa Okumura, Eiji Ohmori, Tomihiko Kawano, and Kanehara Fukuda, "Field Strength and Its Variability in VHF and UHF Land Mobile Radio Service," Review of the Electrical Communication Laboratory, Volume 16, September-October 1968, pp 825-873.

The selection of the modulation methods and subsequent detection is vital to the overall performance of packet radio communications. In an effort to identify and select a viable modulation and detection method, analysis of previously developed techniques has been evaluated along with the development and innovation of new approaches to the question of modulation and detection. The work in this area can be divided into three basic subareas. These are the evaluation of modulation methods, the evaluation of synchronization methods, and the development of analysis tools for signal processing.

2.1 EVALUATION OF MODULATION METHODS

Modulation techniques have been evaluated based on an ensemble of several performance criteria. These criteria are bit error performance versus signal-to-noise ratios; bandwidth utilization; timing requirements; and equipment complexity, size, and cost. The analysis is restricted to code spread spectrum waveform modulation as described in paragraph 1.2.1. Signal processing via spread spectrum has the potential to provide time discrimination for overlapping signals. An explanation of this property of spread spectrum is first presented and is followed by the analysis of several modulation types subject to the above criteria.

2.1.1 Time and Code Discrimination of Spread Spectrum

The short duration impulses corresponding to the correlation peaks used for data detection make it possible to significantly reduce the interference caused by overlapping packets. This is illustrated in figure 2-1. Biphase chip modulation is assumed in this discussion.

The figure illustrates a case of two overlapping packet signals as seen at the matched filter output. The receiver time base has been set for detection of packet 1 data so that the autocorrelation peaks resulting from packet 2 are ignored by the receiver timing, as shown in the figure.

Packet 2 data does result in an interfering chip noise having an rms value of E_2/N , where N is the number of chips used to encode the bit.

NOTE

High level interference or several lower level interferors can result in packet 1 bit errors, even though the autocorrelation functions of the multiple signals do not overlap in time.

If a select group of codes are used, it may be possible to reduce the packet interference time from $2T_c$ to 0. One class of codes to consider is the maximal length codes identified by:

$$\phi \frac{(2^k - 1)}{k}$$

where $\phi(x)$ is the Euler phi-function.

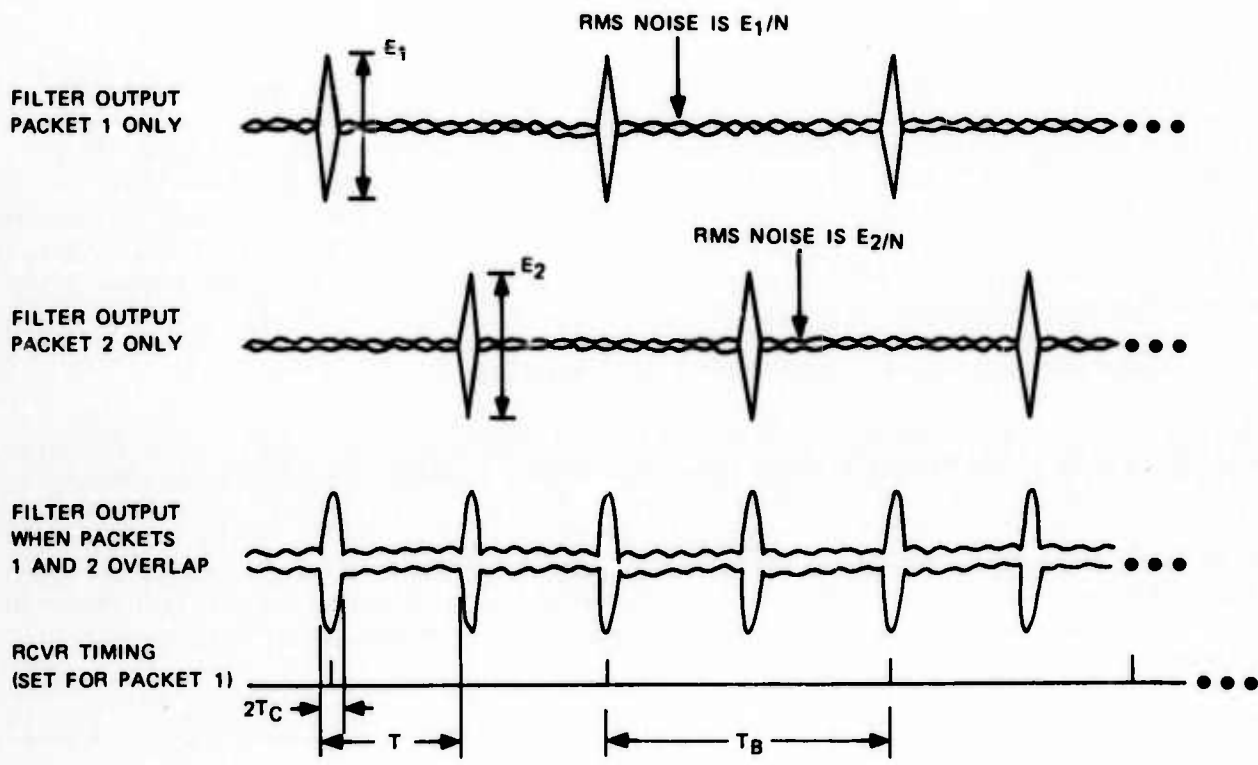


Figure 2-1. Time Discrimination.

The crosscorrelation function for two of these codes, 31 chips in length, is shown in figure 2-2. The figure illustrates the caution which must be used when attempting to apply code discrimination in a random access network. The rms interference level between two overlapping packets has been increased to $6.5 (E_2/\sqrt{N})$ versus (E_2/N) for packets having the same code. The relative crosscorrelation interference can be reduced by using longer length codes.

It is felt that the time discrimination provided by spread spectrum can significantly reduce the self-interference in the packet radio network. Transmission strategies can be developed for random packets having the same codes that enable detection of the first arriving packet, provided the start of a second packet is not received during the short interval $2T_c$. It may also be reasonable to consider equipping the repeater with multiple gating functions so that overlapping packets, having the same code, could be processed concurrently when favorable multipath conditions exist.

It should be pointed out that the use of large spread factors for minimizing the interference time, $2T_c$, increases receiver complexity and bandwidth utilization.

2.1.2 Modulation Waveform Types

Several basic pseudonoise spread spectrum modulation approaches are considered as potential candidates for rf transmission over packet radio. A comparison of these different modulation approaches is summarized in table 2-1. The modulation approaches considered are differentially coherent biphase psk, differentially coherent quadri-phase psk, coherent msk, differentially coherent (dc) msk, and noncoherent (nc) 8' ary msk signaling. The psk and msk refer to chip modulation, and coherency refers to bit modulation.

Each of these approaches will be examined with respect to their implementation and performance. Each approach considered is flexible in that the processing gain can be increased by using a larger number of chips per bit. Also, frequency hopping can be readily superimposed upon the pseudonoise spread spectrum baseline concept.

Each approach is also shown implemented at both the modulator and demodulator with surface acoustic wave devices (SAWD). The advantages and potential of these devices appear very great, particularly with respect to considerations of fast acquisition, low power, and size requirements. These factors are especially important for the hand-held packet radio transceiver.

2.1.2.1 Differentially Coherent Biphase FSK Modulator/Demodulator

The differentially coherent biphase psk modulation approach was discussed in the Packet Radio Temporary Note No. 33. The modulator differentially encodes the data. Each time a logic 1 bit is to be transmitted, the bit sequence is inverted; however, each time a logic 0 bit is to be transmitted, the code sequence remains the same. One implementation of the modulator is shown in figure 2-3. For the baseline system, spread factors of 100 are assumed; therefore, a data bit 1 transmits a sequence of 100 phase modulated chips with each chip either 0 or 180 degrees. The data sequence from the source may be represented by the following sequence:

1 0 1 1 0 1 0 0 . . .

After differentially encoding the data, the sequence becomes:

1 1 0 1 1 0 0 0 1 . . .

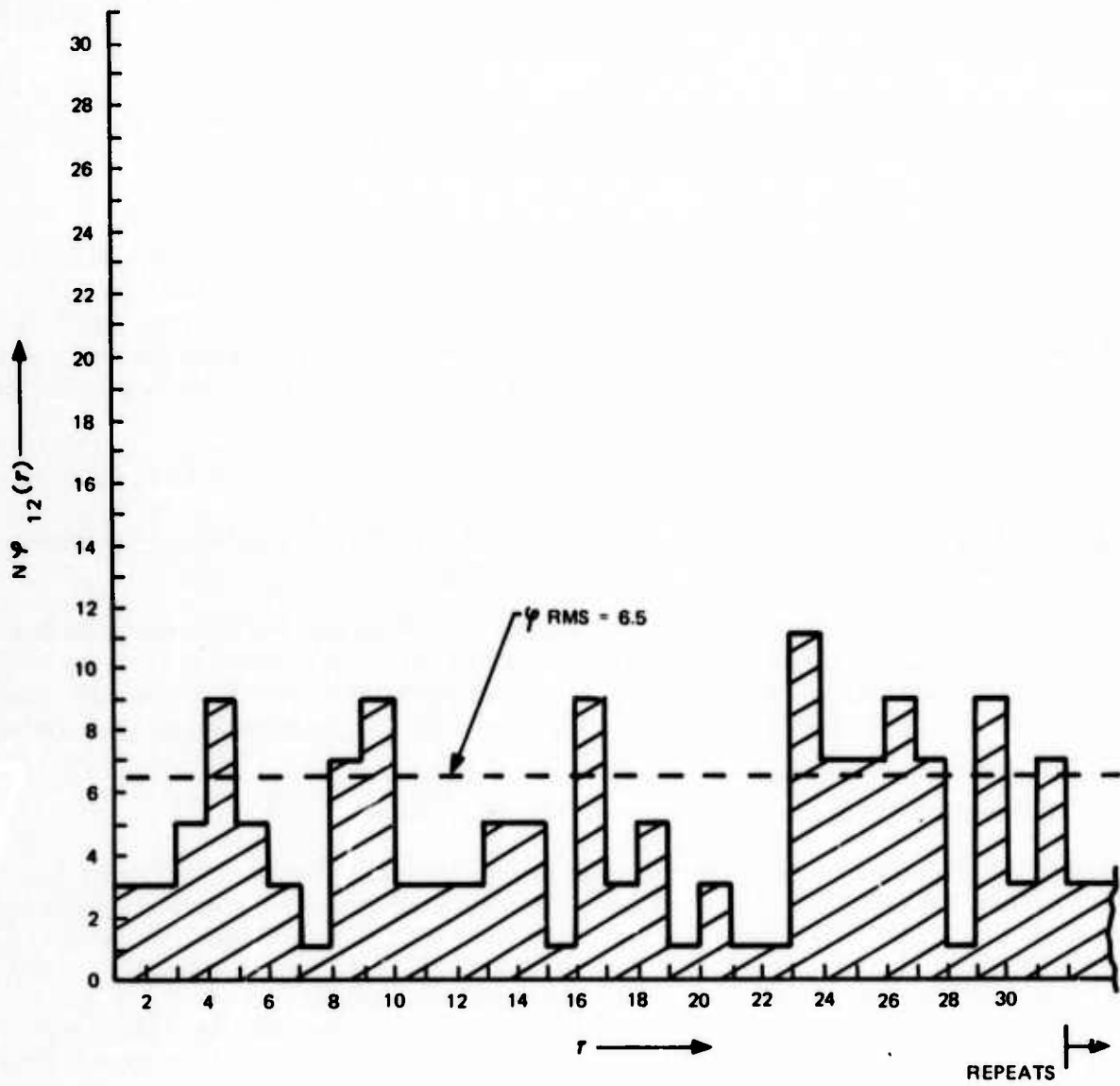


Figure 2-2. Crosscorrelation Function Between Codes No. 1 and No. 2.

Table 2-1. Modulation Approach Comparison.

TRADEOFF PARAMETERS MODULATION TYPE	PERFORMANCE BER vs E_b/N_0 at 10^{-5} BER	BANDWIDTH UTILIZATION	TIMING REQUIREMENTS (BIT SYNC)	SAWD LIMITATIONS	EQUIPMENT COMPLEXITY	ESTIMATED COST	EQUIPMENT SIZE
Differentially coherent biphase psk	3	3	3	2	1	1	1
Differentially coherent quadri-phase psk	3	2	2	3	2	2	2
Coherent msk	2	1	5	1	4	3	4
Differentially coherent msk	3	1	1	2	1	1	1
Pseudo-orthogonal msk	4	1	1	2	3	3	3
8'ary msk	1	1	2	4	5	4	5

Evaluation Scale: 1 — Most desirable
to
5 — Least desirable

The impulse generator drives the 100 tap SAWD with either a positive or negative impulse. The output of the SAWD at the point where the taps are summed is:

$$s(t) = \sum_{i=1}^{100} d_{101-i} \cos(\omega_0 t + \phi) \{u[t - (i-1)T_c] - u[t - iT_c]\}$$

where d_i is ± 1 , depending upon the sign of the chip, and T_c is the chip duration.

An alternate dpsk modulator is shown in figure 2-4. The chip sequence for a data bit is exclusive-ored with the differentially encoded data bit. The impulses are generated on a chip basis, yielding a phase-modulated carrier at the SAWD output. A positive impulse may correspond to a 0-degree phase shift, and a negative impulse corresponds to a 180-degree phase shift.

modulation and detection

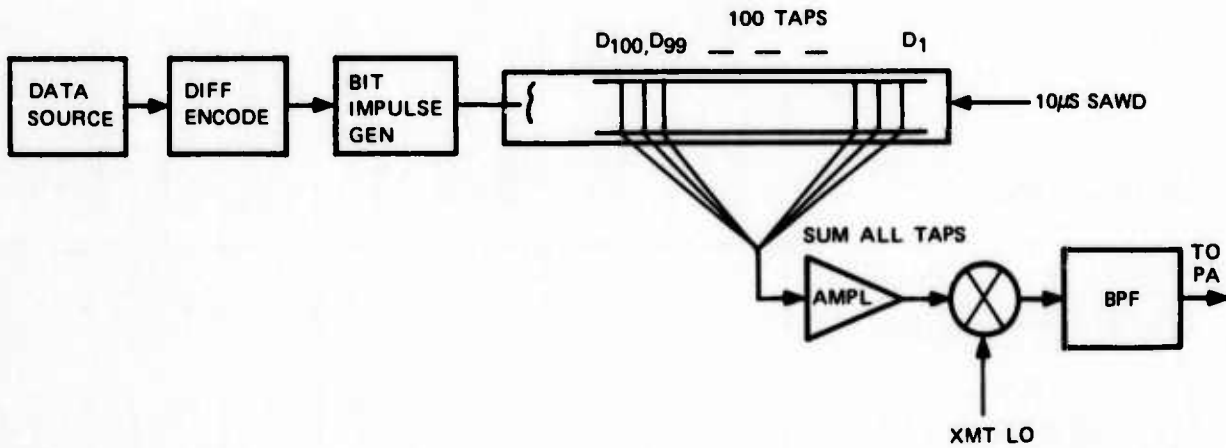


Figure 2-3. DPSK Modulator No. 1.

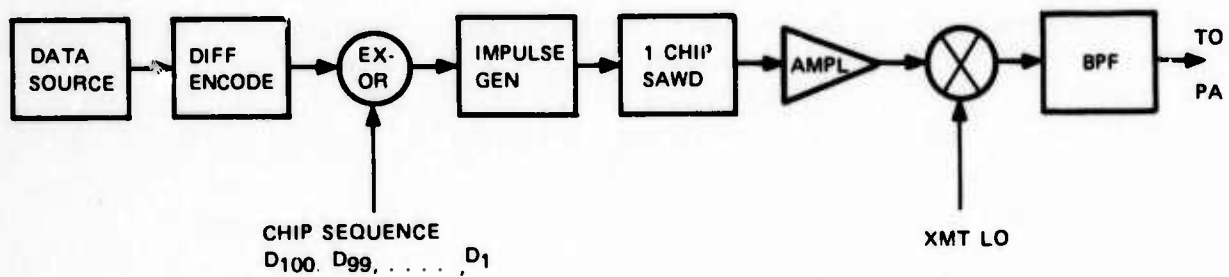


Figure 2-4. DPSK Modulator No. 2.

One of the shortcomings of biphase psk modulation is its spectral density response which, as shown in figure 2-24, rolls off as $1/f^2$ or 20 dB per decade.

The dpsk demodulator is shown in figure 2-5. It is a matched filter at the if. As shown, a single SAWD is matched to the chip sequence, and the same chip sequence delayed one data bit time. The outputs of the taps are summed both for the present received bit and the previously received bit. This summing operation takes place right in the SAWD. The sum and difference is obtained from the two outputs. These are envelope detected, compared, and the output is sampled. The sample time is established by the preamble detector and the sampling occurs at the peak of the baseband pulse. The sign of the sampled signal determines whether the data bit is a 1 or a 0.

Maximum likelihood detection assumes ideal bit timing and ideal sampling of the correlation waveform peak. Ideal timing is never achieved for bit timing. For non-ideal bit timing, figure 2-6 shows the result of loss of signal envelope detection versus timing error. Figure 2-7 shows the loss of signal/noise (E_b/N_0) as a function of number of chips per bit with timing error τ as a parameter for T_B of 10 μ s (100-kB/s data rate).

Hence, for $N = 100$ and 10-ns bit timing error for 100 kB/s data, a 1-dB loss of E_b/N_0 is incurred. Note that 10 ns out of 10- μ s bit period is 0.36 degree of timing accuracy and requires a 100-MHz clock if a counter is allowed to free run from a master clock. A 1.0-degree error (28 ns) results in 3-dB loss. Thus, bit timing requirements are quite important for spread spectrum maximum likelihood detection.

An alternate method of data detection is achieved by sampling the SAWD matched filter output by a timing window that is $2T_C$ ($T_C =$ chip interval) wide, storing the peak value during the timing window, and making a bit decision at the end of the timing window. This method greatly alleviates the bit timing problems that the maximum likelihood detection requires since, ideally, bit timing of only T_C accuracy is required (100 ns for $N = 100$).

It is estimated that this form of detection degrades performance by 0.5 dB (for a $2T_C$ window case) from the ideal timing. A $2T_C$ window is suggested for two reasons. One is that a $2T_C$ window is easy to generate. The second is that, intuitively, a window equal in width to the correlation peak width would result in best performance.

Thus, for much easier timing requirements, a 0.5-dB performance penalty results. Hence, performance of dpsk with $P_e = 10^{-5}$ requires $E_b/N_0 = 10.9$ dB rather than 10.4 dB. A suggested method of implementing the detector is shown in figure 2-8.

2.1.2.2 Differentially Coherent Quadrature PSK Modulator/Demodulator

Quadrature modulation has certain advantages over biphase modulation. One is that the timing requirements are less severe since the symbols are twice as long as the chips. Another is that the bandwidth requirements are less, as shown in figure 2-24.

An implementation of the modulator is shown in figure 2-9. The demodulator for quadrature psk is similar to that shown in figure 2-5 for biphase demodulation. An orthogonal channel is required that is phase shifted 90 degrees from the other channel. This can be achieved by a 90-degree phase shift of the two SAWD outputs (A and B). These 90-degree phase shifted outputs are input to a hybrid, and the sum and difference of the outputs are envelope detected and compared in the same manner as the other channel.

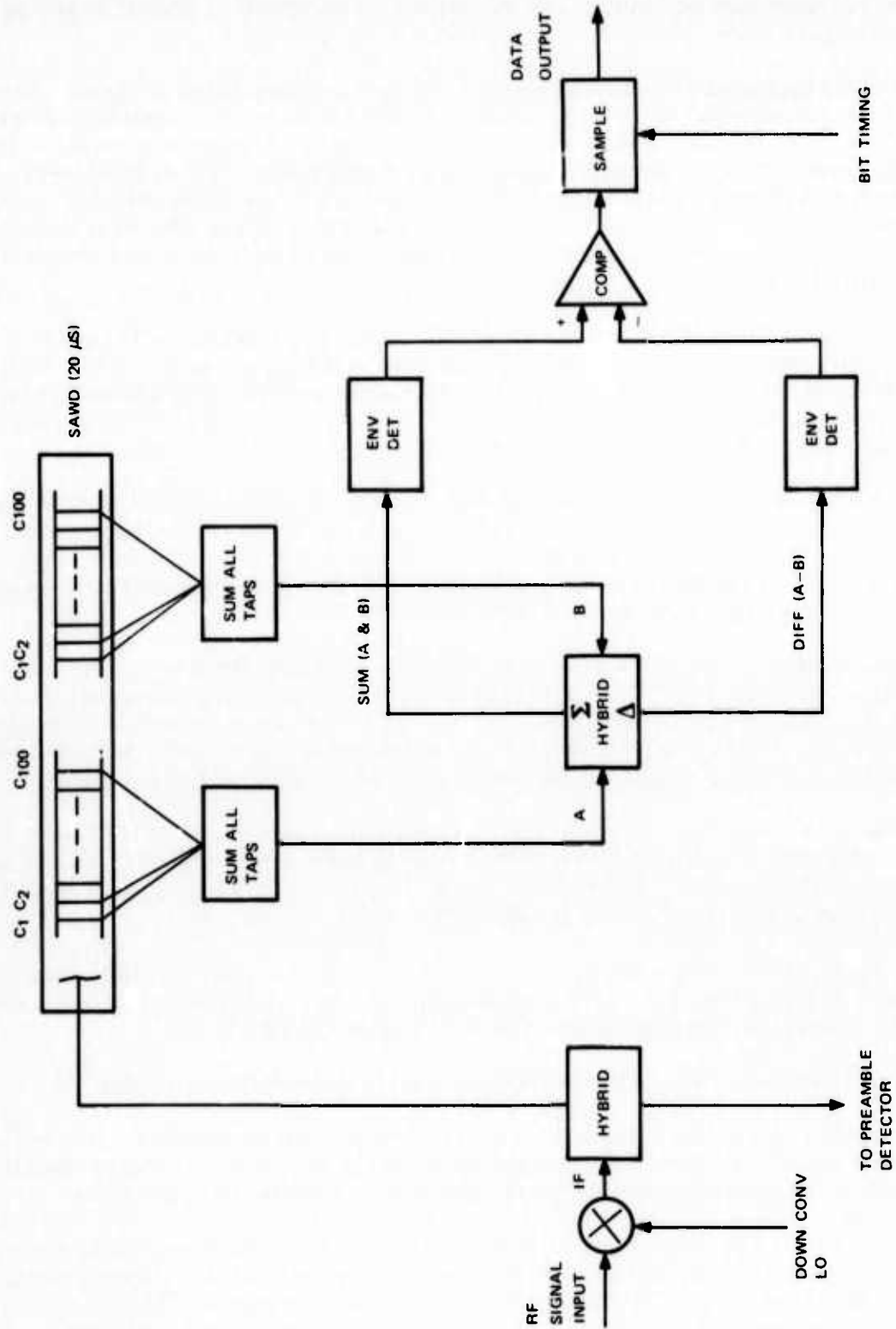


Figure 2-5. Differentially Coherent PSK Demodulator.

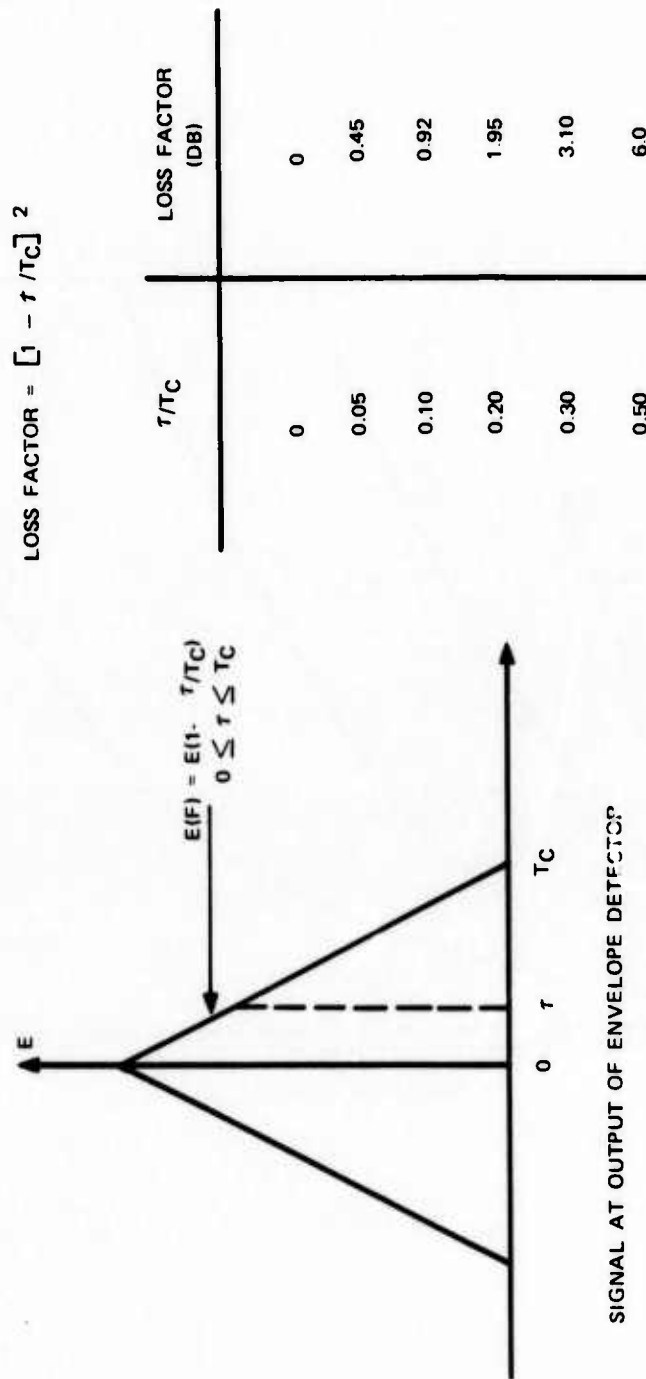


Figure 2-6. Effect of Timing Offsets to Maximum Likelihood Decoding.

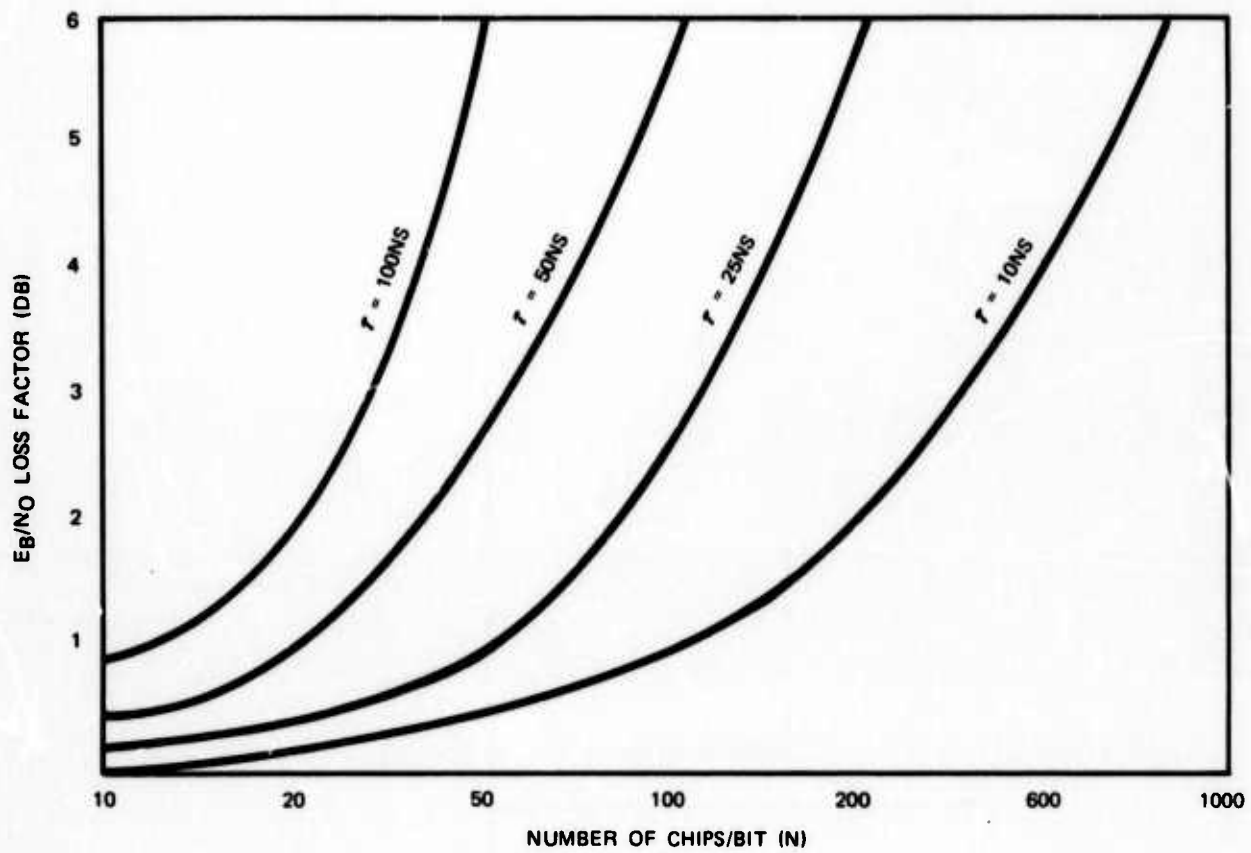


Figure 2-7. E_b/N_0 Performance Loss Due to Timing Offsets (τ).

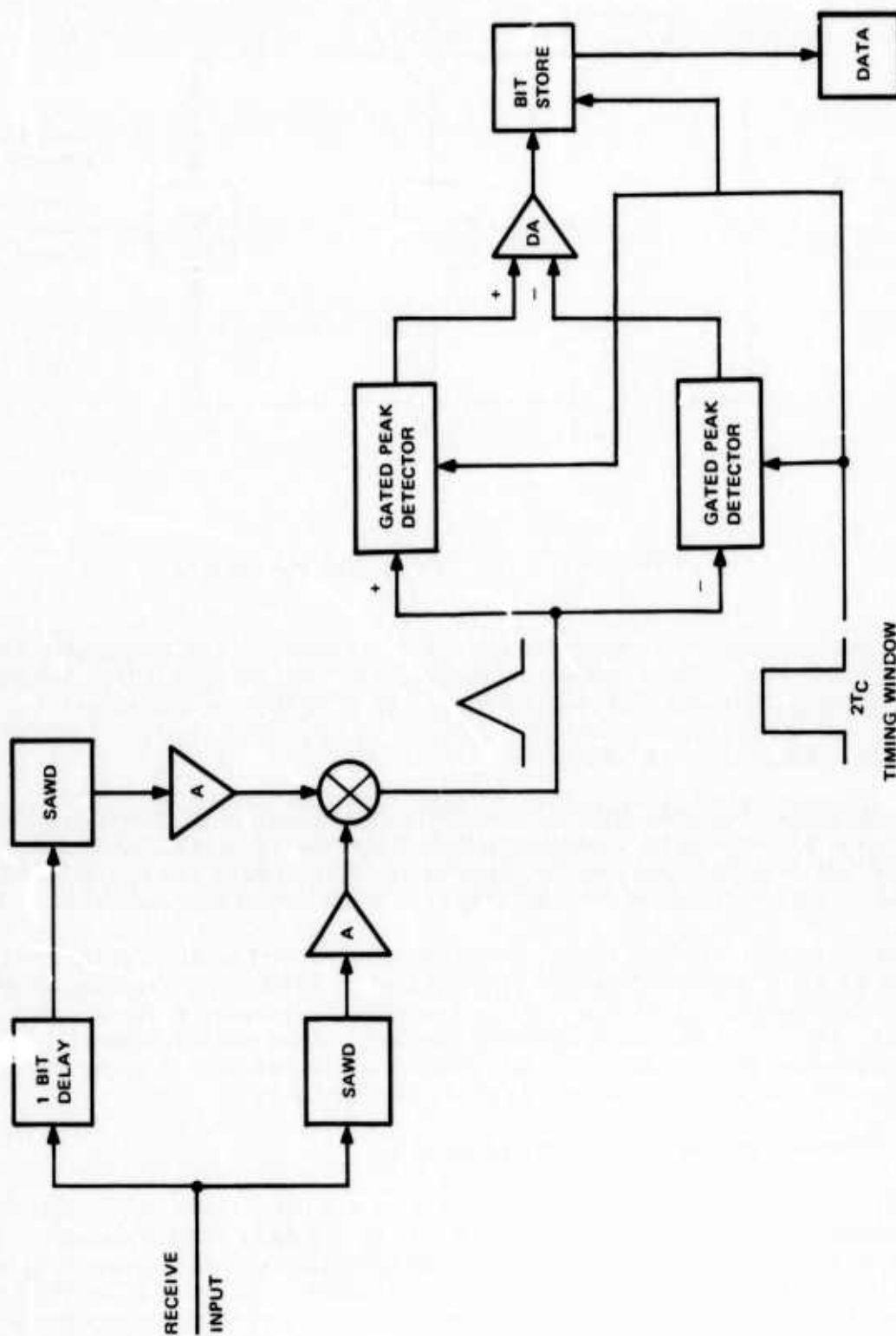


Figure 2-8. Window Peak Sample and Store Detector.

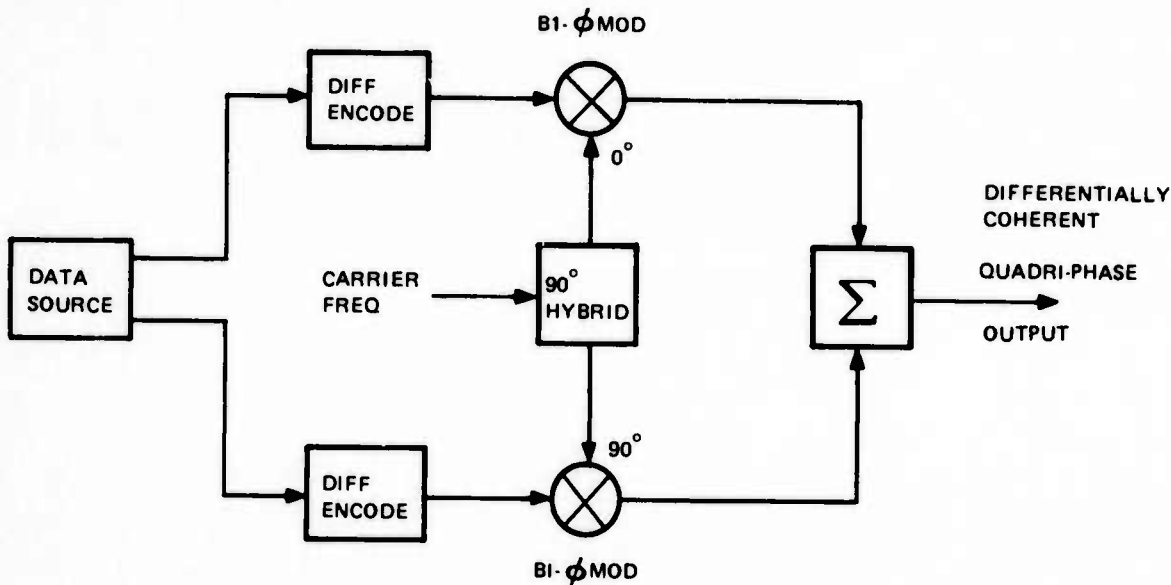


Figure 2-9. DC Quadriphase Modulator.

Maximum likelihood detection and gated peak store detection criteria discussed for biphase apply for quadriphase, except symbol intervals ($T_c/2$) must be used in the applicable equations and curves. Note that there are two chips per symbol for quadriphase.

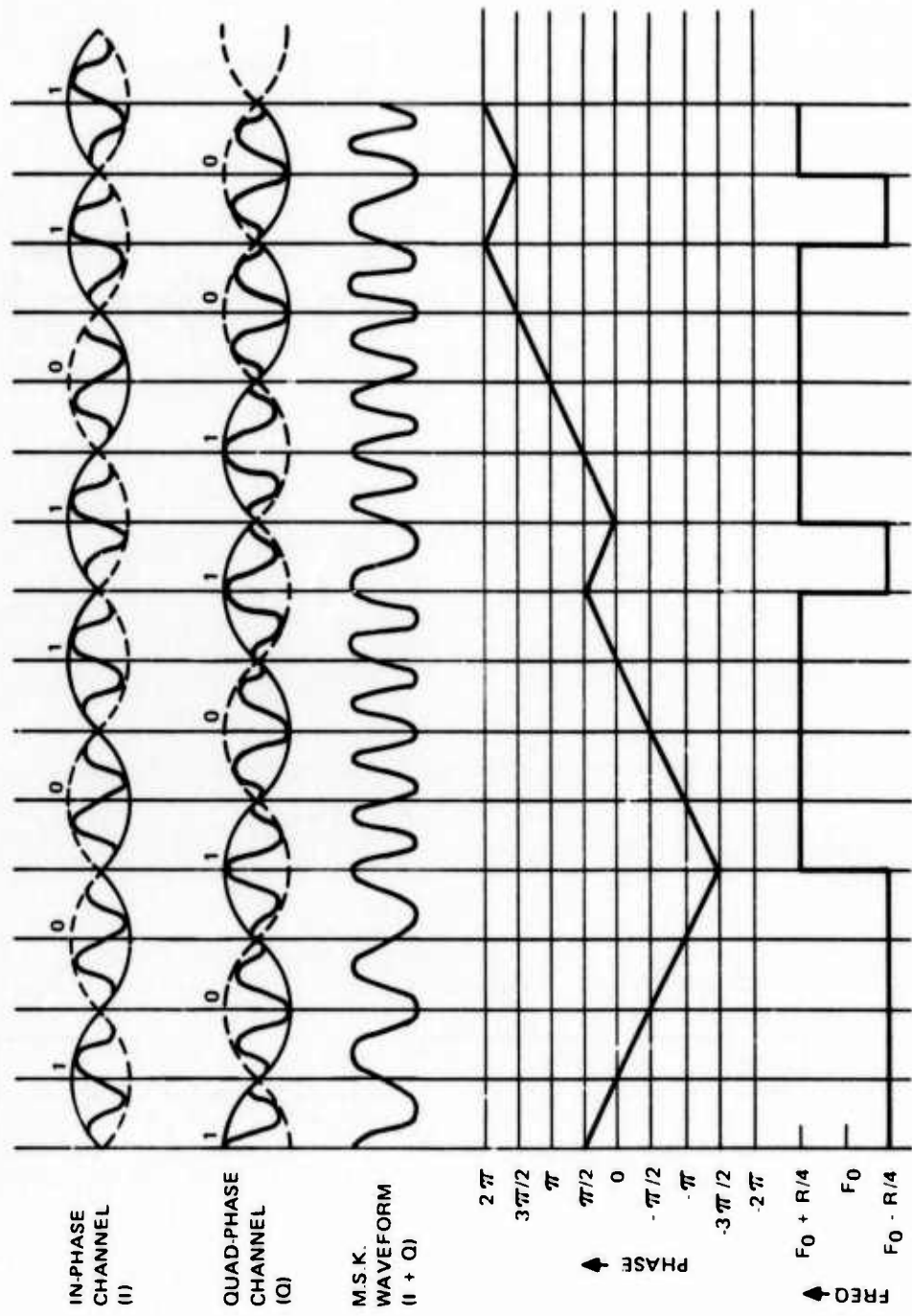
2.1.2.3 MSK Modulation/Demodulation

An alternate approach to psk signaling is sometimes referred to as minimum shift keying (msk). It is a two-orthogonal channel amplitude weighting psk modulation scheme. The in-phase and quadrature phase carrier channels are staggered by one chip and shaped with orthogonal cosine weightings of two chip length. This is illustrated in figure 2-10.

To achieve a constant envelope signal, the quadrature channel is added to the in-phase channel as shown in the msk waveform diagram. Also shown is the resultant phase and frequency for the example chip stream. Phase transitions can occur at the null points of each subchannel. This property results in phase continuity of the msk waveform. This property produces increased attenuation of the higher signaling frequencies. Its spectral density rolls off as $1/f^4$, or 40 dB per decade as shown in figure 2-24.

2.1.2.4 Coherent MSK Modulator/Demodulator

Several approaches to msk modulation/demodulation are being considered. The first of these approaches is termed coherent msk. A data bit 1 consists of a sequence of 100 chips, and a data bit 0 consists of the same sequence with inverted signs. Figures 2-11 and 2-12 illustrate two implementation techniques for the modulator. In figure 2-11, the data source determines the sign of the impulse driving the SAWD. The input transducer has a cosine pulse weighting and has a duration of two chip periods. The SAWD has 100 taps, each tap corresponding to one of the chips. The even taps are summed for one msk subchannel and



NORMALIZED FOR:
 $F_0 = 1\text{HZ}$
 $T_C = 1\text{ SECOND}$
 CHIP RATE, $R = \frac{1}{2}\text{HZ}$

Figure 2-10. MSK Signaling.

modulation and detection

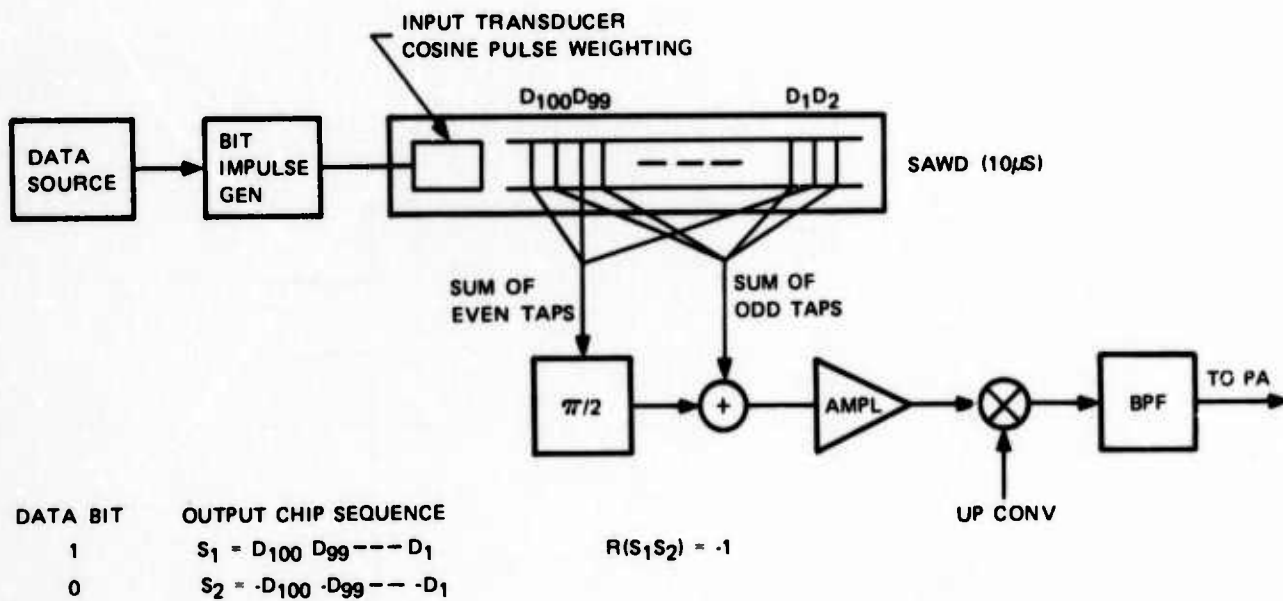


Figure 2-11. Coherent MSK Modulator No. 1.

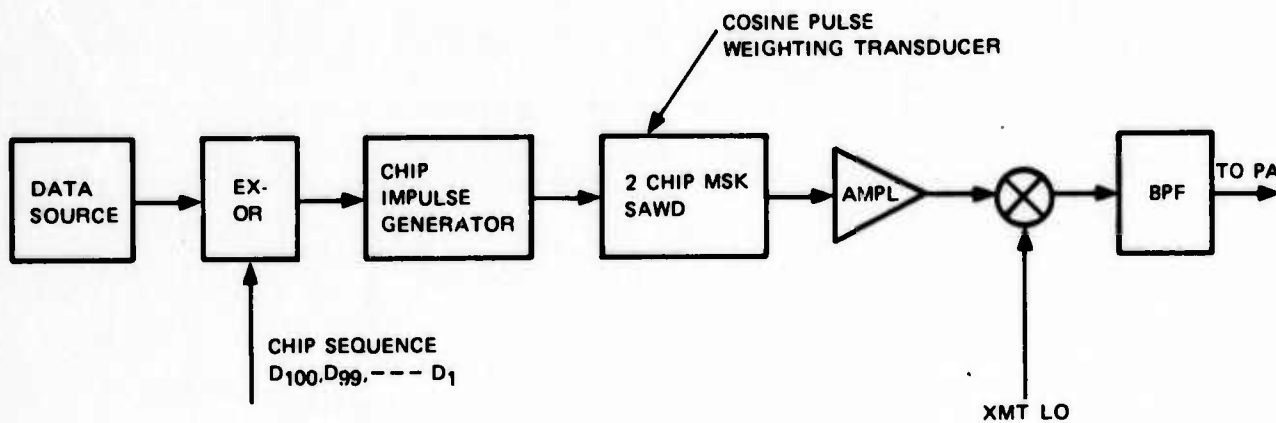


Figure 2-12. Coherent MSK Modulator No. 2.

its output is phase-shifted 90 degrees. The odd taps are summed for the other subchannel. The two outputs are then added together yielding the msk signal. The signal can be represented mathematically as follows:

$$s(t) = \sqrt{2P} \left\{ \cos(\omega_0 t + \phi) \sum_{k=0}^{49} d_{2k+1} \text{cosp} \left[\frac{\pi}{2T} (t-2kT) \right] \right. \\ \left. + \sin(\omega_0 t + \phi) \sum_{k=0}^{49} d_{2k+2} \text{sinp} \left[\frac{\pi}{2T} (t-2kT) \right] \right\}$$

where cosine pulse (cosp) is defined by:

$$\text{cosp} \frac{\pi t}{2T} = \cos \frac{\pi t}{2T} [\mu(t+T) - u(t-T)]$$

and sine pulse (sinp) is defined by:

$$\text{sinp} \frac{\pi t}{2T} = \sin \frac{\pi t}{2T} [u(t) - u(t-2T)]$$

and the chip interval is given by T.

The if. output is then up-converted and amplified for transmission. The summing of the odd and even taps is accomplished in the SAWD. It may be feasible to also do the phase shifting in the SAWD; however, further investigation in this area is required.

An alternate approach to the modulator is shown in figure 2-12. The SAWD is impulsed at the chip rate. The sign of the impulse determined by the exclusive output of the SAWD generates a cosine weighted pulse that exists for two chip periods. The impulse sign determines carrier phase in the cosine pulse.

The demodulator is shown in figure 2-13. The demodulation process is coherent. The matched filter demodulator is identical to the modulator discussed above (figure 2-11), except that the tap sequence is reversed. The summing of the two SAWD output results in an amplitude-modulated carrier that is the correlation function. This if. signal must be sampled at exactly the right time because the phase of the if. carrier contains the information. Hence, near coherence is required that can be achieved by use of a phase-lock loop that encloses the surface wave detector.

In a half-duplex application, it is possible to share the SAWD between the transmitter and receiver (compare figures 2-11 and 2-12). The complexity of the switches must be compared to the complexity of a SAWD.

2.1.2.5 Differentially Coherent MSK (DC-MSK) Modulator/Demodulator

To alleviate the severe timing requirements of the coherent msk demodulator, an alternate approach is considered. With this approach, the data is differentially coded prior to being modulated, as was discussed in paragraph 2.1.2.1. A data bit from the source is differentially encoded with the previously encoded data bit. The remaining part of the modulator (figure 2-14) is identical to the modulator discussed above for the coherent msk approach. The modulator can also be constructed using the two chip SAWD, as shown in figure 2-12. The only additional requirement is the differential encoding of the data source output.

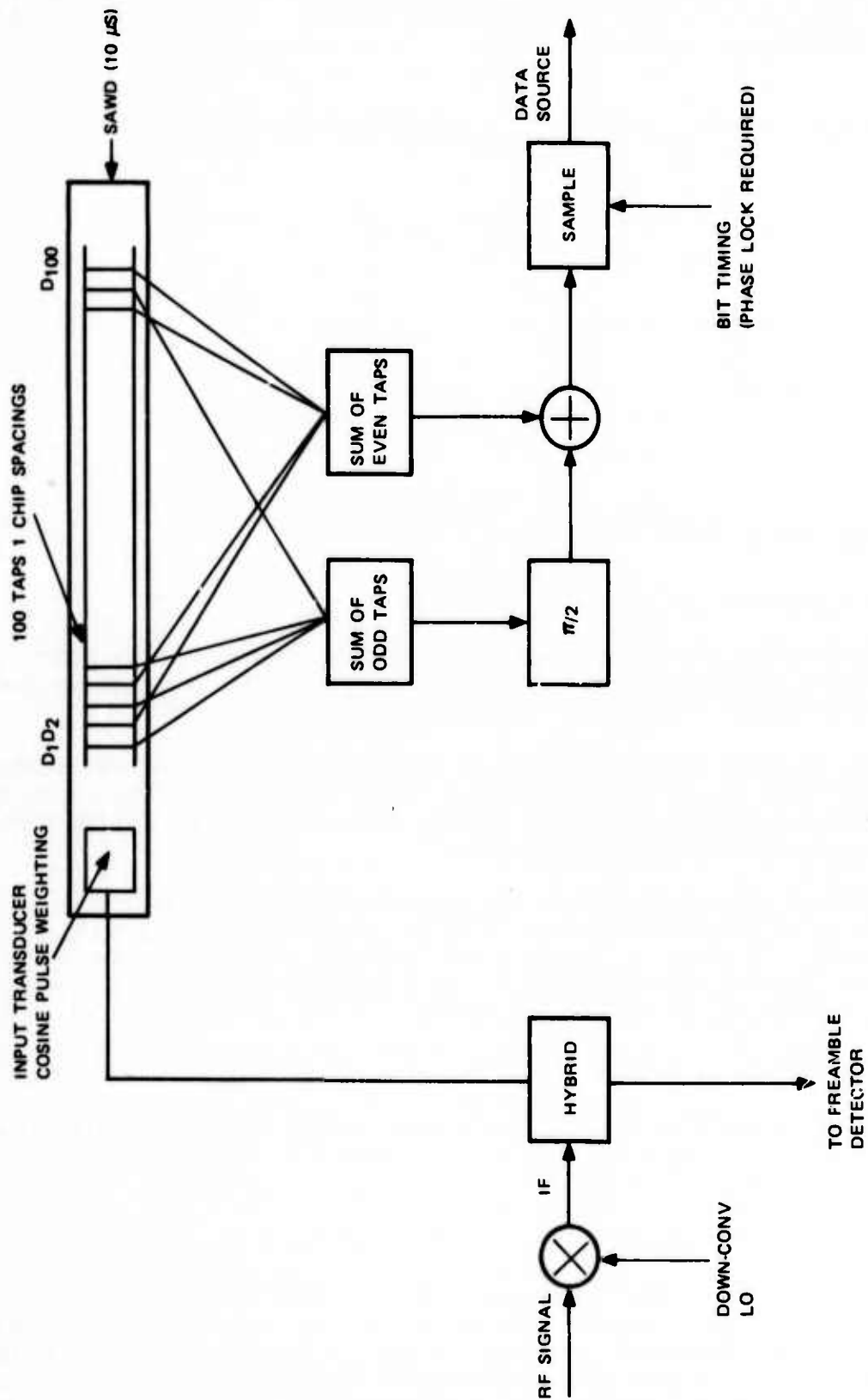


Figure 2-13. Coherent MSK Demodulator.

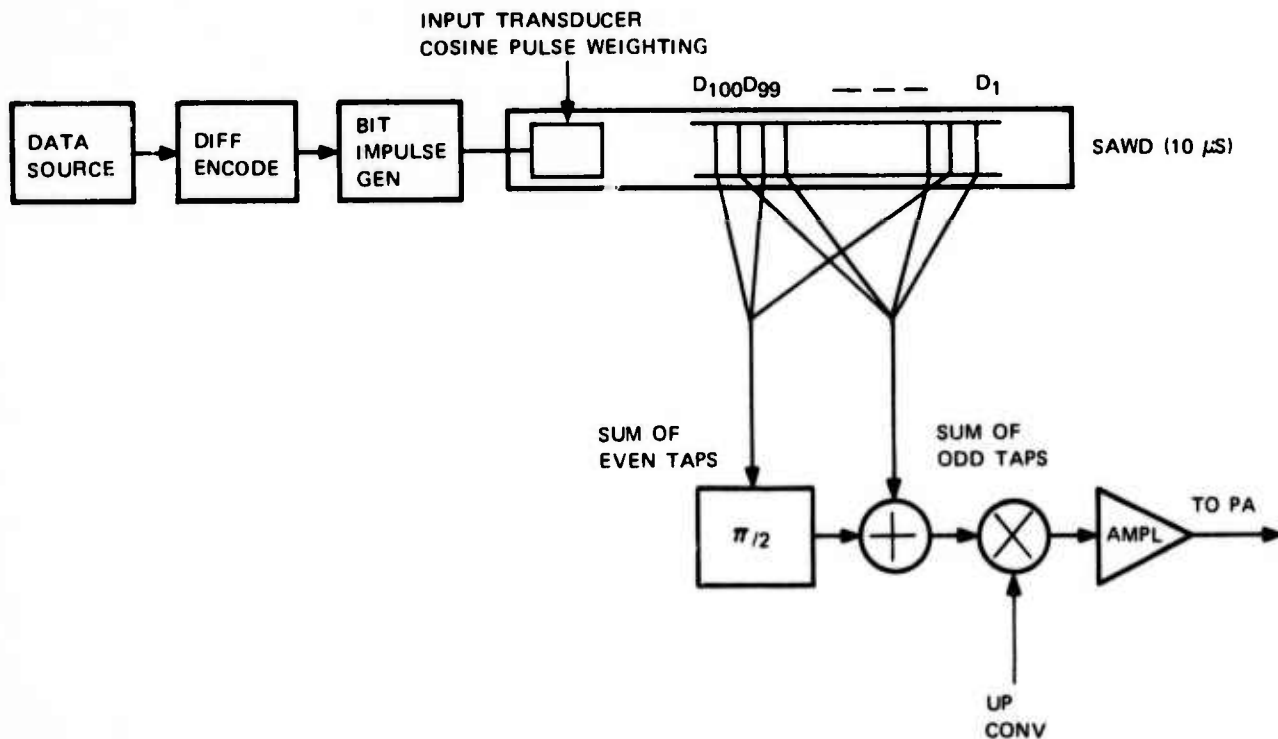


Figure 2-14. Differentially Coherent MSK Modulator.

A differentially coherent msk demodulator is shown in figure 2-15. Two SAWD's are shown. One is a 10- μ s (1 bit) msk demodulator, and the other is a 10- μ s delay. The demodulator coherently detects the present data bit and delays the previously detected bit for one bit interval. These two outputs are then multiplied coherently and low-pass filtered, yielding a baseband output whose sign determines the data bit. The bit timing derived from the preamble is used to sample the mixer output and recover the data. A second dc msk demodulator is shown in figure 2-16. The concept is the same as the dpsk demodulator shown in figure 2-5. The advantage is the elimination of the phase-coherent mixer.

The two types of detection discussed for dpsk signaling are also applicable for msk signaling. The effect of timing errors upon the loss of signal energy is shown in figure 2-17. For msk signals, the correlation function is not triangular as it is for psk signals, but is a smooth function as shown in figure 2-17. For small timing offsets, the loss factor is less than it is for 4-phase psk signaling. For timing errors in excess of 1/4 of a chip, the loss factor is less for 4-phase psk signaling. With 2-phase psk signaling, any and all timing offsets will be worse than 4-phase psk or msk.

2.1.2.6 Pseudo-Orthogonal MSK (PO-MSK) Modulator/Demodulator

Another msk modulation approach is illustrated in figures 2-18 and 2-19. To modulate the pseudo-orthogonal signals requires the selection of one of two chip sequences. These chip sequences have approximately zero crosscorrelation. In figure 2-18, data bit 1 selects (for example) the upper SAWD for the generation of the msk signal, and the data bit 0 selects the lower SAWD. In figure 2-19, the data bit selects the chip sequence that controls the impulse generator driving the msk SAWD.

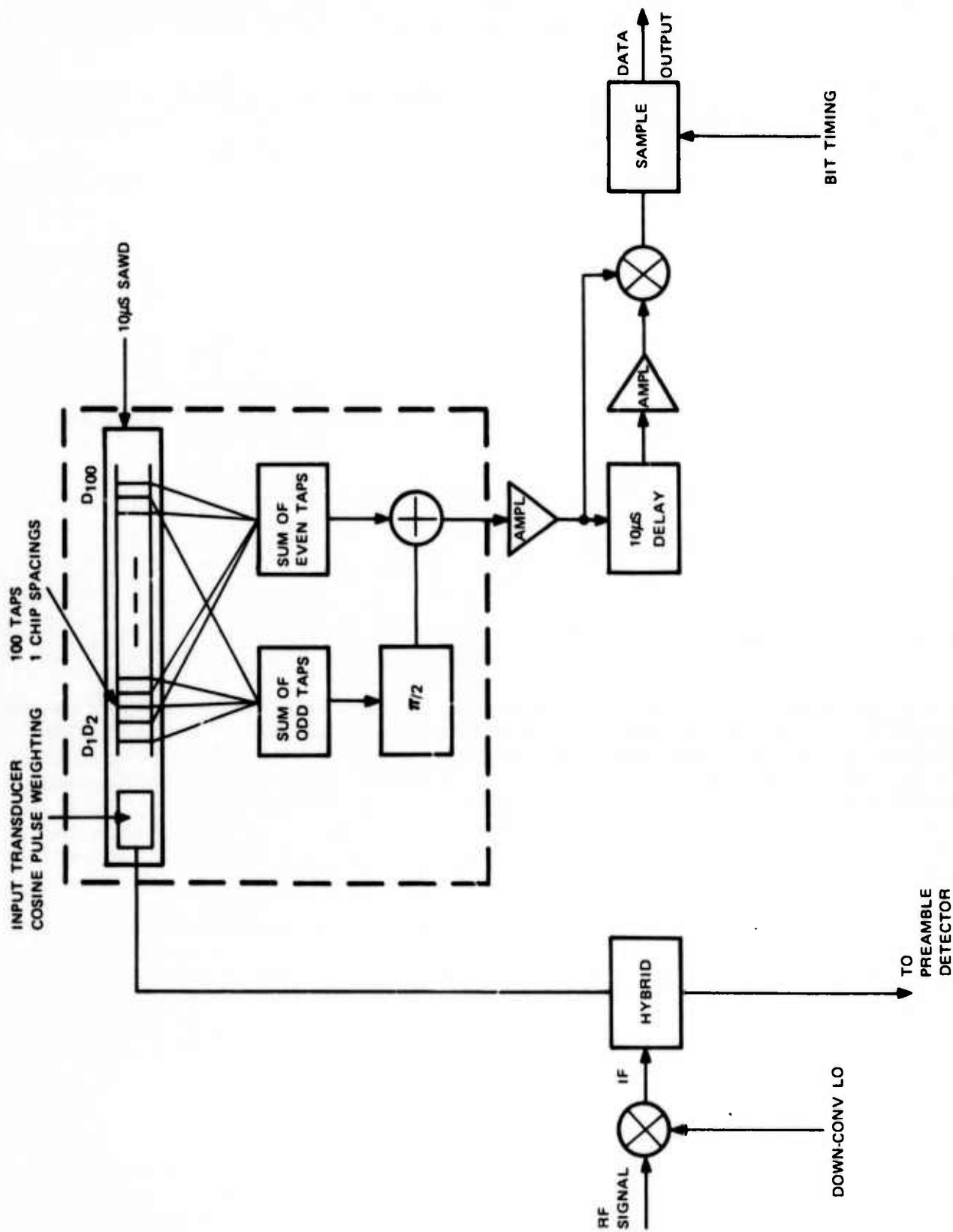


Figure 2-15. Differentially Coherent (DC) MSK Demodulator (10-µs SAWD).

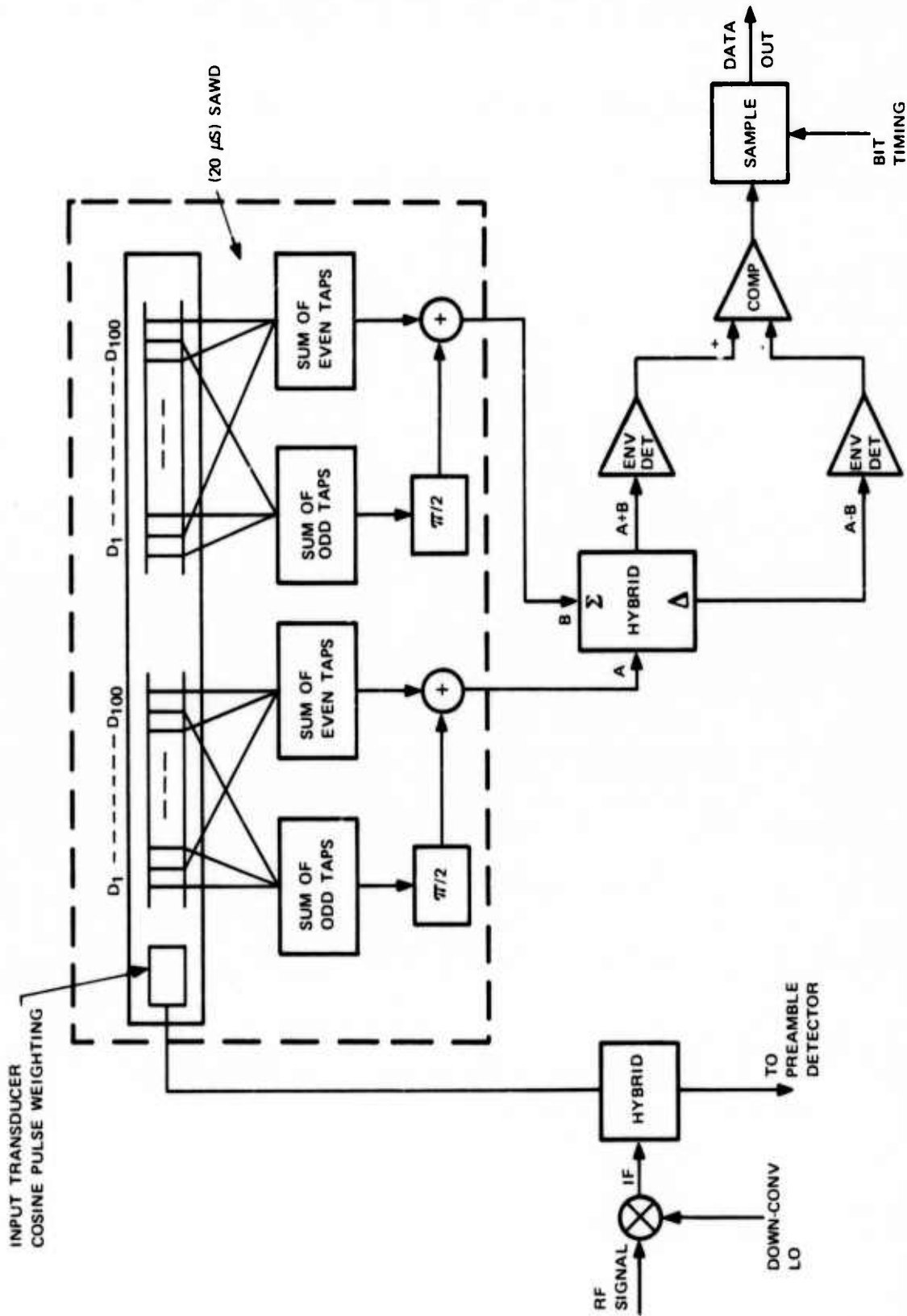
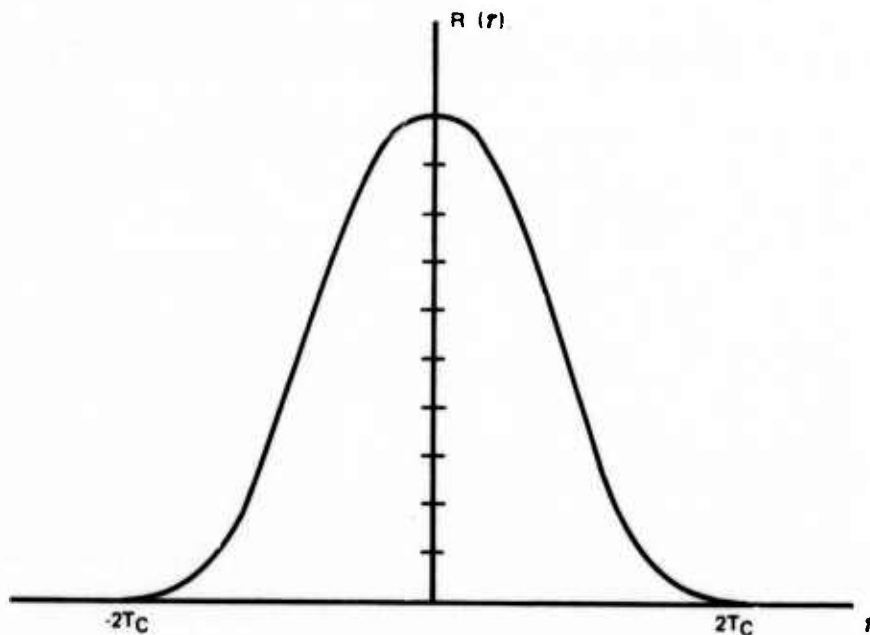


Figure 2-16. Differentially Coherent (DC) MSK Demodulator (20- μ s SAWD).

modulation and detection

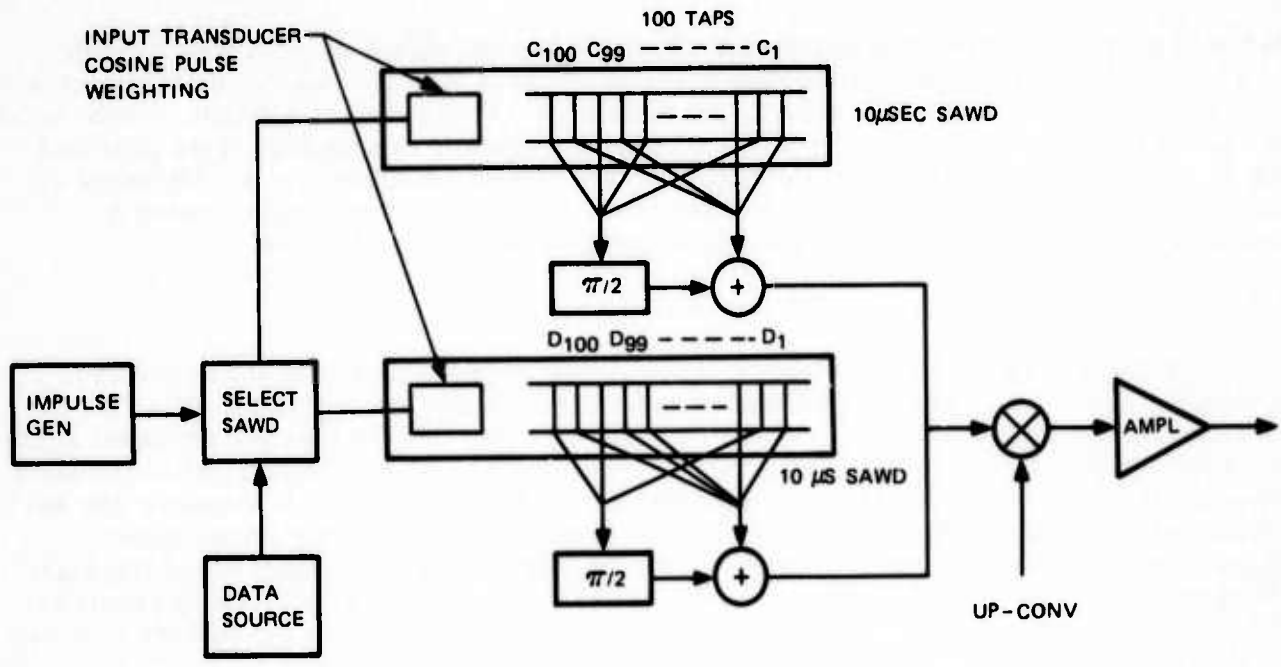
$$R(\tau) = \text{COSP} \frac{\pi \tau}{2T_C} \cdot \text{COSP} \frac{\pi \tau}{2T_C}$$



SIGNAL AT OUTPUT OF MSK DETECTOR

$\tau/2T_C$	LOSS FACTOR (DB)
0	0 IDEAL BIT TIMING
0.05	0.104
0.10	0.41
0.20	1.58
0.30	3.49
0.40	6.23
0.50	9.95

Figure 2-17. Effect of Timing Offsets for Sampling Detection of MSK Signaling.



DATA BIT	OUTPUT CHIP SEQUENCE
1	$S_1 = C_{100} C_{99} \dots C_1$
0	$S_2 = D_{100} D_{99} \dots D_1$

$R(S_1 S_2) \approx 0$

Figure 2-18. Pseudo-Orthogonal (PO) MSK Modulator No. 1.

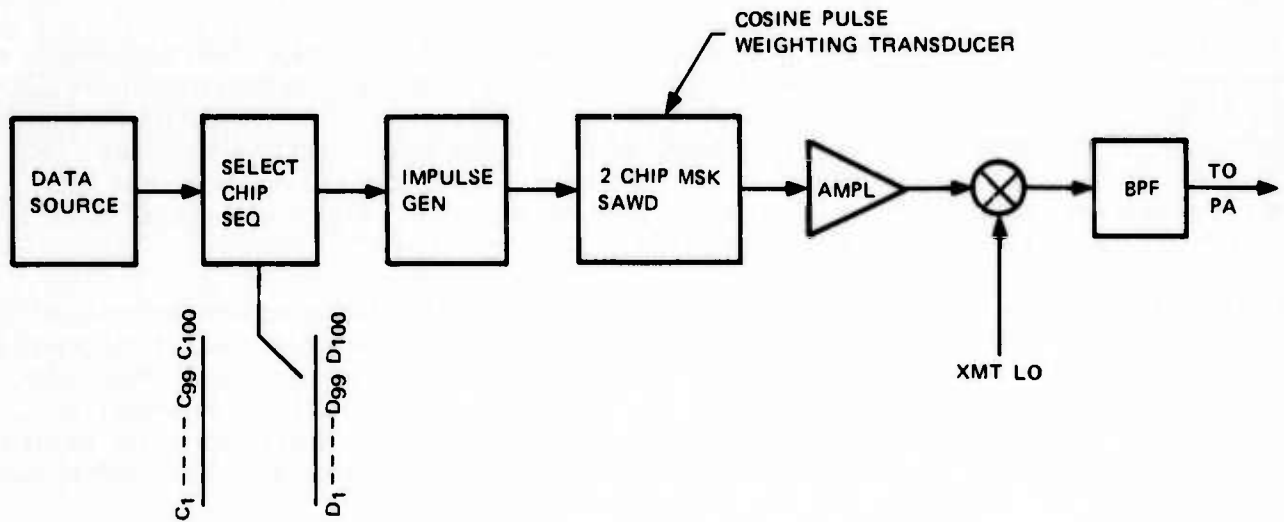


Figure 2-19. Pseudo-Orthogonal (PO) MSK Modulator No. 2.

modulation and detection

At the demodulator illustrated in figure 2-20, the incoming signal is correlated by both SAWD's, each containing one of the chip sequences. Each SAWD is an msk detector for a bit. One SAWD is matched to a data 1, the other SAWD is matched to a data 0. Each output is envelope detected and the output with the largest amplitude is selected. This approach requires two SAWD's, each of $10 \mu\text{s}$ in length. The timing requirements are the same as those for the differentially coherent msk demodulator. In this type of data detection, maximum likelihood detection and gated peak store detection may be used.

2.1.2.7 8'ARY MSK Modulator/Demodulator

Another signaling approach that yields a performance improvement over the approaches discussed above at low bit error probabilities is shown in figures 2-21 and 2-22. The modulator utilizes eight SAWD's. Each SAWD has 300 taps and the taps are arranged such that they correspond to the 300 chips for each code symbol. The crosscorrelation between the eight 300-chip sequences is approximately zero; however, each code sequence has an autocorrelation function that has a large peak four chips wide, and very low sidelobes. Three data bits from the source comprise a symbol and are used to select one of the eight chip sequences. For the chip rate in the channel to be 10 megachips per second requires 300 chips per symbol. Again, there is an input transducer for each of the SAWD's that has a cosine pulse weighting.

At the demodulator, the if. signal is power split between eight SAWD's, each of which is matched to one of the 300-chip sequences. Again, each is a matched filter for one of the eight possible 3-bit data sequences. The output of each filter is envelope-detected, and every symbol time, the largest output is selected. The most likely bits are the three bits associated with the largest output. The timing requirements for this approach are more stringent than dc msk, since for 300 chips, the same correlation peak occurs. Two of the drawbacks are the number of SAWD's required and the lengths of the SAWD's ($30 \mu\text{s}$). This can be alleviated in the modulator by using programmable SAWD's. The modulator could be implemented by using a programmable digital code generator driving a chip SAWD msk generator.

2.1.2.8 Performance Comparison

A probability of bit error performance comparison between the six modulation/demodulation approaches discussed above is shown in figure 2-23. The chip rates in the channel are all the same. The comparison is made on the basis of probability of bit error (BER) versus the energy per bit to noise spectral density required to achieve a given error probability. For bit error probabilities in excess of 7×10^{-5} , coherent psk or msk is superior. For bit error probabilities less than 7×10^{-5} , 8'ary msk is superior. It requires 0.4 dB less energy per bit than coherent msk at 10^{-5} BER.

Differentially coherent psk and differentially coherent msk have identical theoretical performance. At 10^{-5} BER, their performance is 1 dB less than coherent msk and 1.4 dB poorer than 8'ary msk. Pseudo-orthogonal (PO) msk gives the poorest performance. Basically, this is because the correlation between the chip sequences is not positive N or negative N, but is either positive N or nearly zero. Hence, the signal detector space geometric separation between signals is not as great with the result of poorer performance. The performance of PO msk is 3 dB worse than coherent dmsk as shown in the figure.

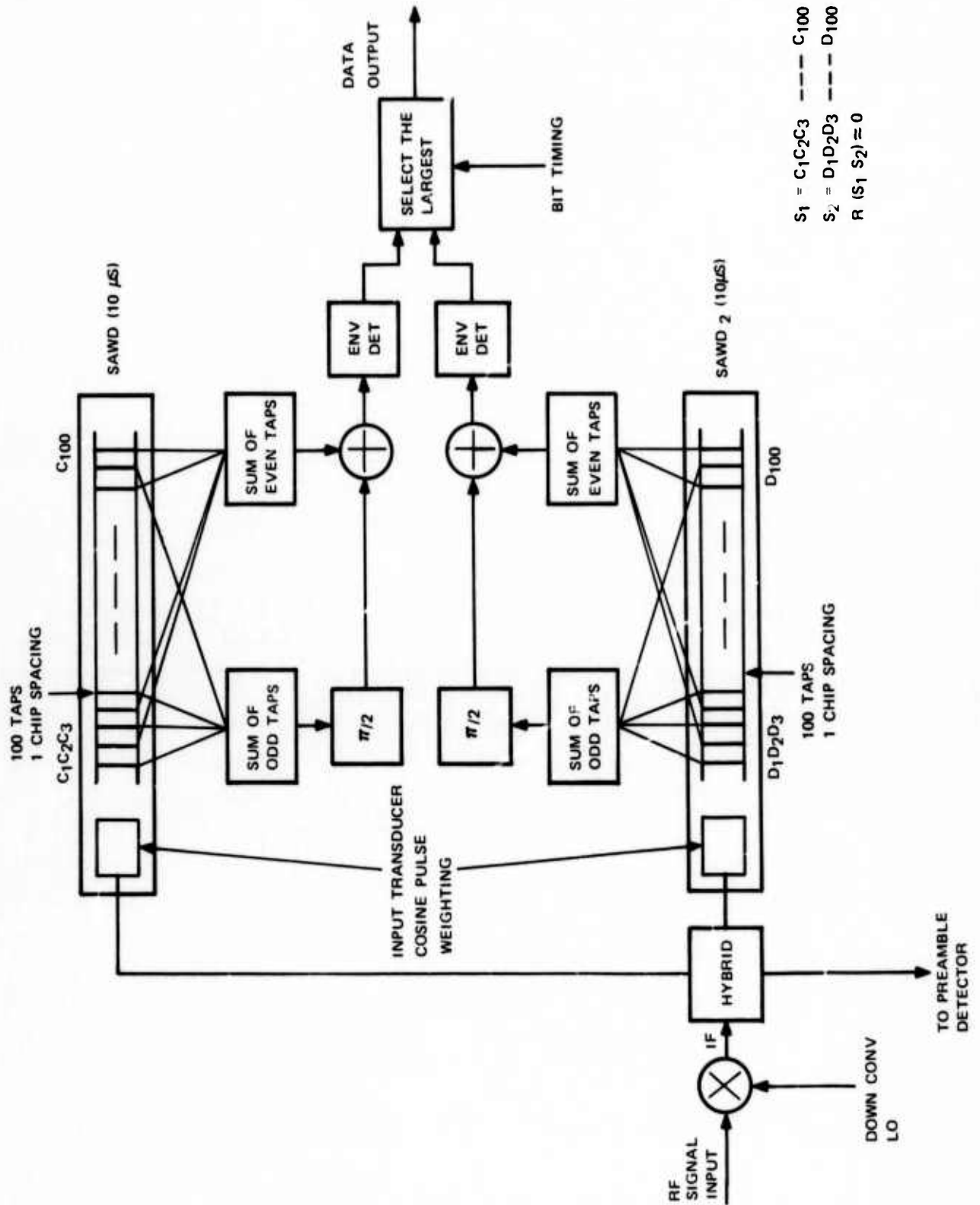


Figure 2-20. PO MSK Demodulator.

modulation and detection

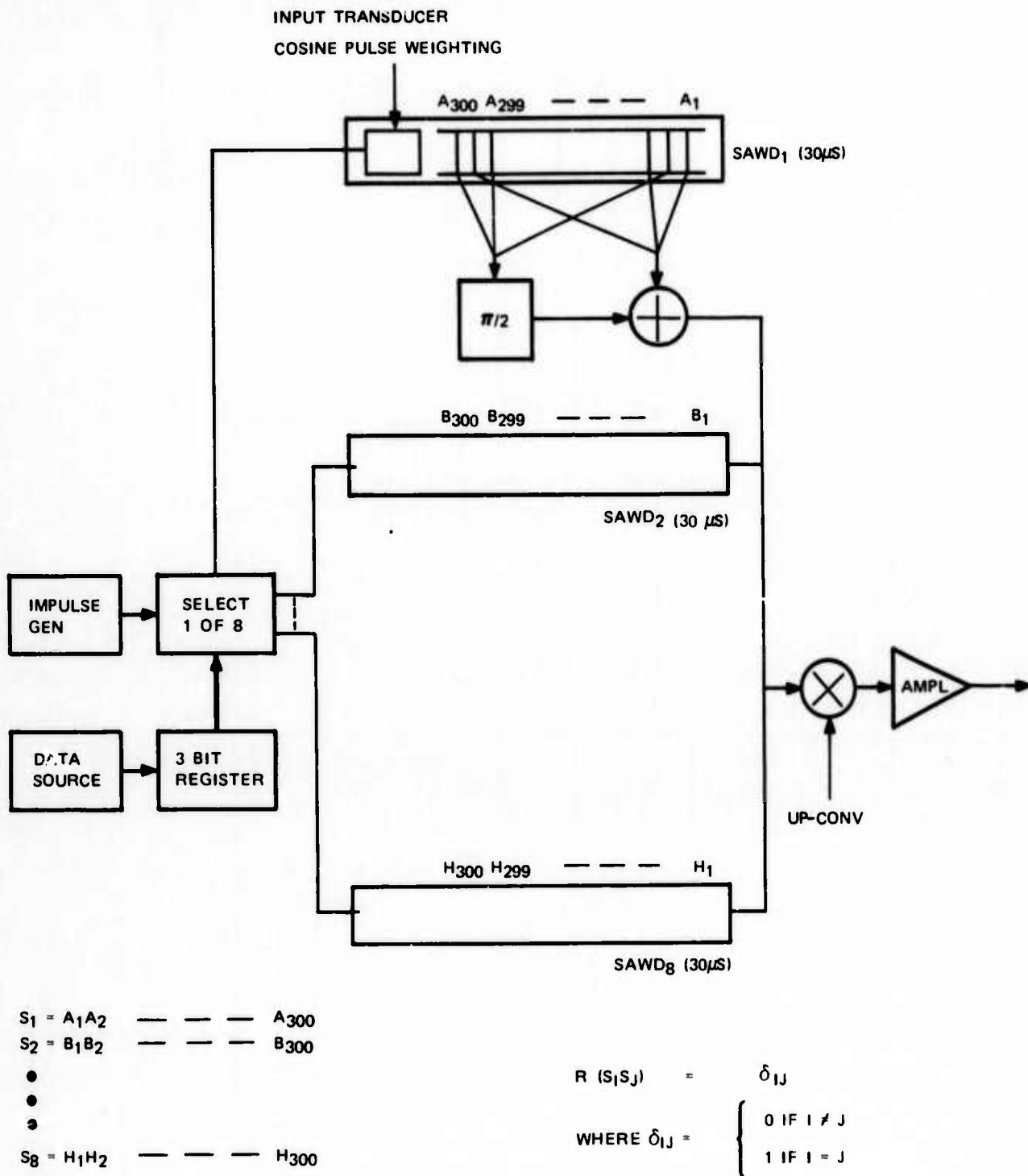


Figure 2-21. 8-ARY MSK Modulator.

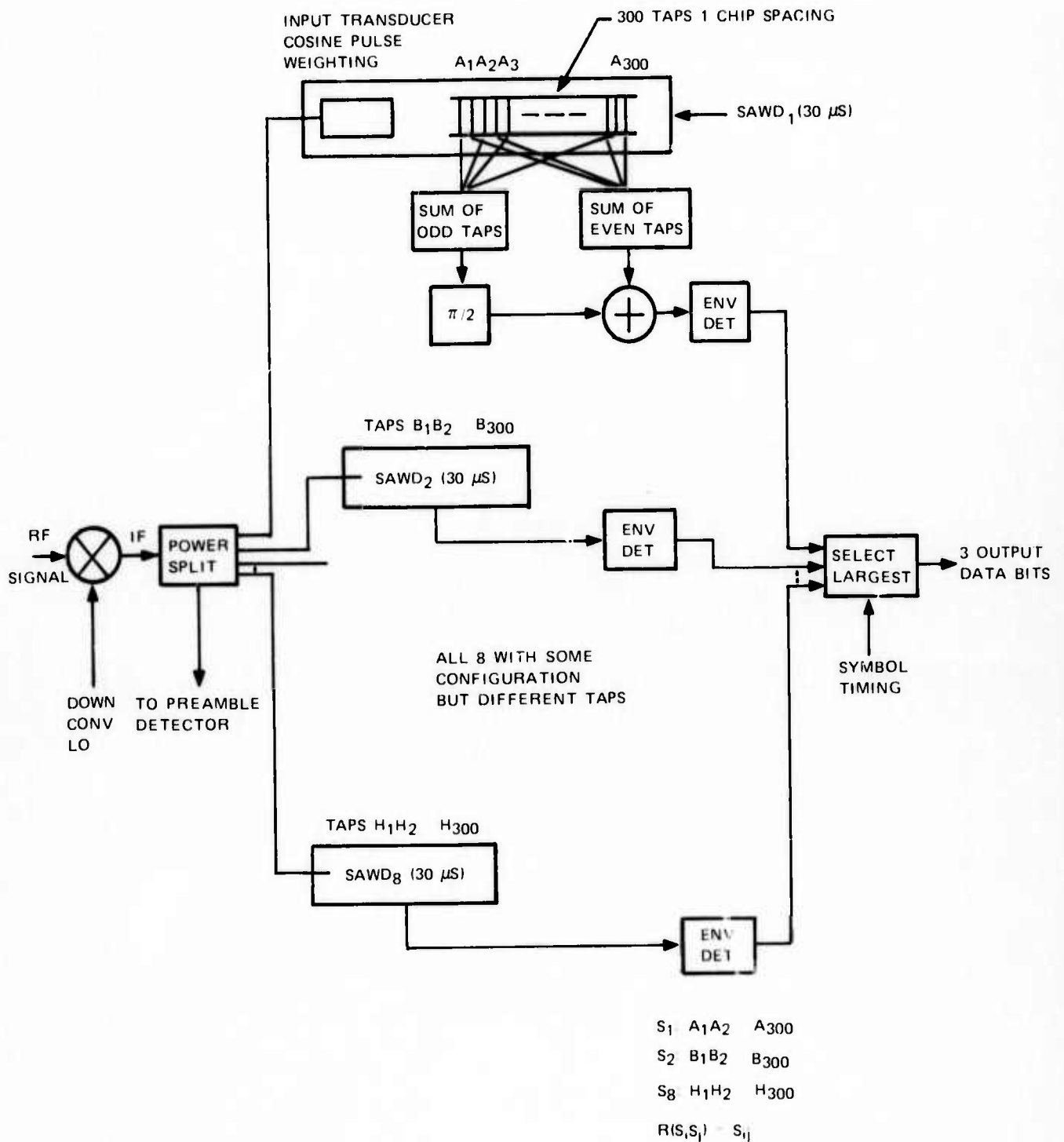


Figure 2-22. 8-ARY MSK Demodulator.

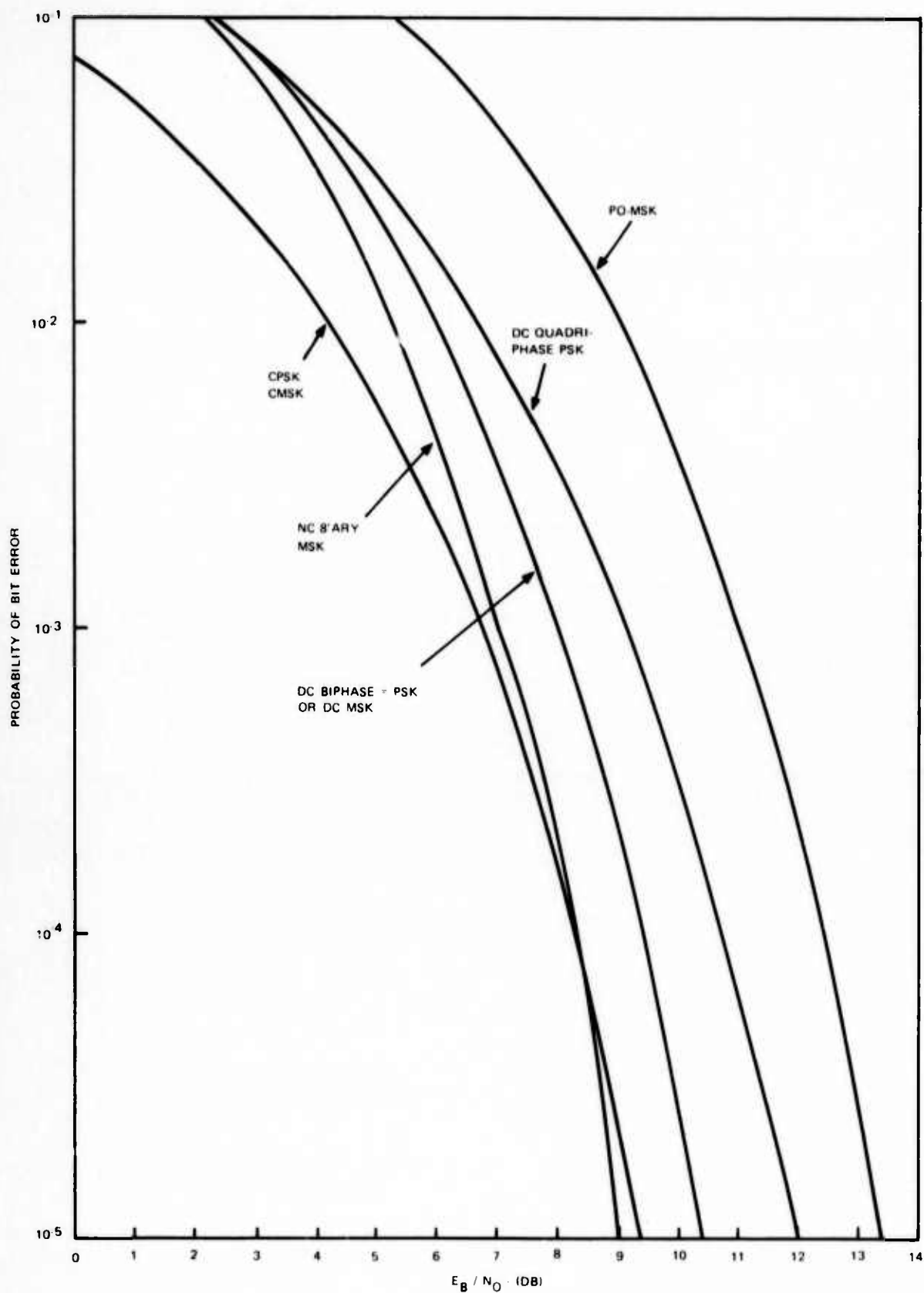


Figure 2-23. Performance Comparison of Different Modulation Approaches.

2.1.2.9 Tradeoff Parameters

Table 2-1 contains some parameters that are important for deciding which modulation or signaling waveform approach is most desirable for the ARPA packet radio network. The six modulation approaches are compared on the basis of performance. The best performance is denoted by 1 and the poorest performance is denoted by 5. These are qualitative indicators only.

The bandwidth utilization of the different modulation methods was also previously discussed. The basic difference is between the psk and msk power spectrum for an equal chip rate. (See figure 2-24.) Msk has much lower out-of-band spectral energy and, hence, is superior where spectral containment is important. The psk power spectrum rolls off at 20 dB per decade; whereas, the msk spectrum rolls off at 40 dB per decade. Quadriphase psk requires half the bandwidth of biphase psk.

The timing requirements refer to the demands upon timing accuracy. Differentially coherent msk and pseudo-orthogonal msk have the least stringent timing requirements for small timing errors. 8'ary msk is more difficult because the slope of the correlation function per bit interval is greater. Qpsk is superior for large timing errors. Biphase psk is inferior for all timing errors. Coherent msk requires the most accurate timing because one must sample the if. carrier in order to sense the sign of the data bit. To adequately recover the data from the coherent msk modulated signal will require a phase-lock loop.

The hardware limitations refer specifically to the device requirements relative to state-of-the-art technologies. For example, 10- μ s SAWD's are relatively easy to make; whereas, 20- μ s SAWD's are a little more difficult and 30- μ s SAWD's require some extra development work. On this basis, coherent msk is considered to have the fewest SAWD hardware limitations, and 8'ary msk would have the most.

The judgments on the last three tradeoff parameters are more subjective and require more extensive investigation. The evaluation is based on first-pass engineering judgment.

The conclusions one might draw from such a tradeoff is that coherent msk and differentially coherent msk are the leading contenders. Coherent msk has the problem of very accurate timing requirements since one must track the phase of the carrier for adequate detection. DC msk circumvents this phase-locking difficulty by coherently detecting two successive bit intervals; however, the price one pays is a slight performance degradation (\approx 1 dB). In actual practice, there probably will be 0.5-dB degradation due to phase tracking errors and jitter with coherent msk.

2.2 SYNCHRONIZATION FOR PACKET RADIO SYSTEMS

In the design of packet radio systems, we are concerned with at least the three following types of synchronization.

- a. Carrier synchronization (coherent systems only)
- b. Bit synchronization
- c. Packet synchronization (i. e., control of packet transmission times to minimize interference).

If a differentially coherent detection or noncoherent detection scheme is used, carrier synchronization is not required, and will not be discussed. This discussion addresses

modulation and detection

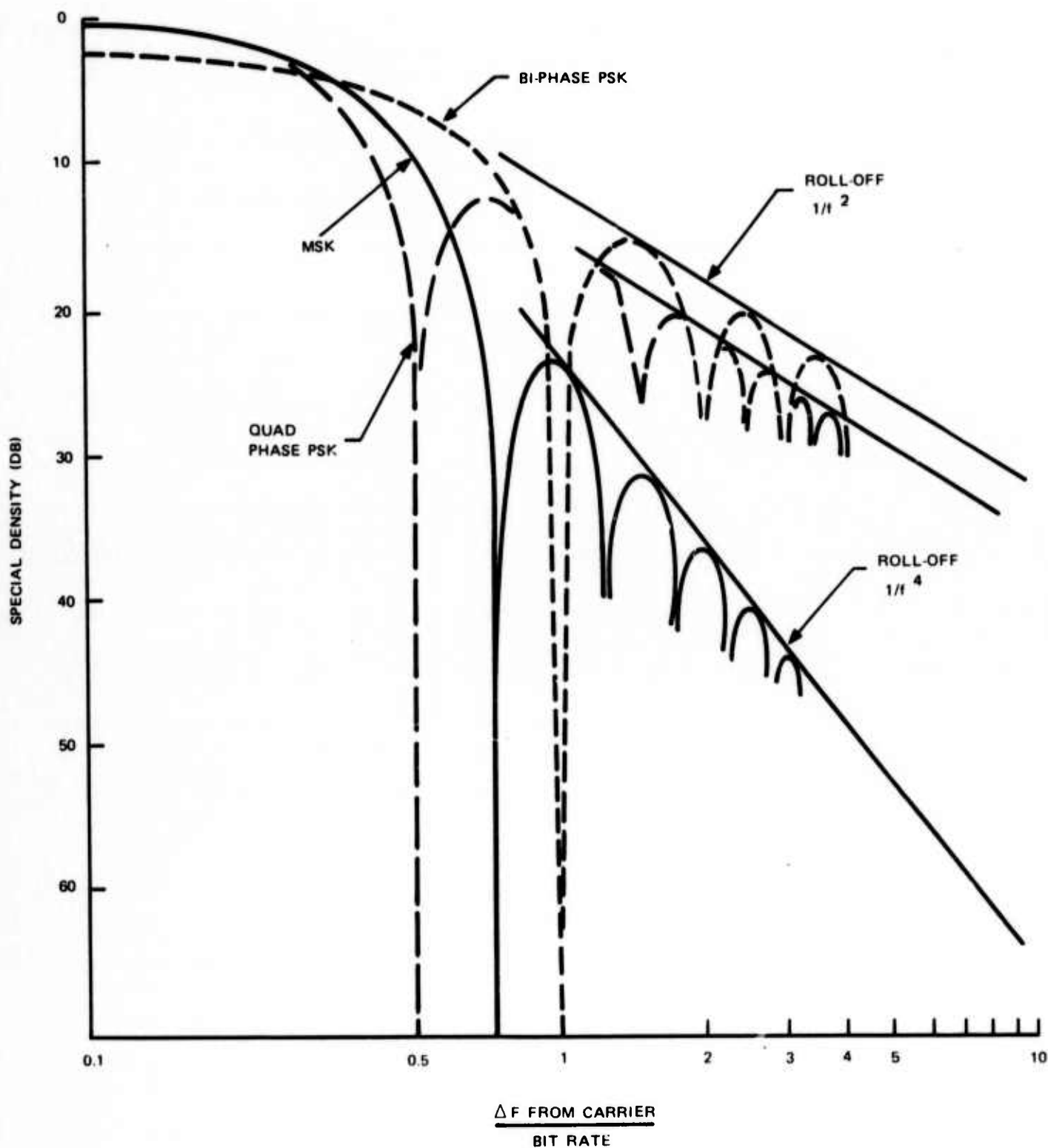


Figure 2-24. Relative Spectral Density for MSK, Quairiphase PSK and Biphase PSK.

the subject of bit synchronization; but to make the presentation more understandable, it has been related to a general terminal model, and some important design and implementation problems are briefly discussed.

This discussion suggests that there is no merit considering bit synchronization beyond the period of one packet, although there is some merit in considering synchronization of terminals and repeaters that may contribute interference during the period of one packet. Although this may sound somewhat inconsistent, it is shown that this objective can be met with proper frequency control and that the requirements here are quite reasonable, at least for the systems with no spread or a system with moderate spread. Such coordination of synchronization between stations is of more value for the system using spread spectrum techniques. In the concept outlined below, each packet is considered as a separate transaction and may originate from a different terminal or repeater and have a different time reference. Therefore, if adequate frequency stability is provided, the problem of synchronization is one of accurately defining time. One method of accomplishing this is suggested below.

Considerable emphasis has been given to the subject of bit synchronization by designers of large networks, and solutions generally evolve into the following general categories.

- a. Mutual synchronization of the total network by an averaging process
- b. Synchronization to a common master
- c. Use of bit stuffing techniques to remove clock frequency difference between users.

It is important to recognize that these solutions are dictated by the time division multiplexer required to separate the various users. The packet radio is not faced with such problems since each packet defines, by means of its address, the proper receive port on the multiplexer. It is, therefore, concluded that there is no merit in considering wide distribution of bit synchronization in the usual sense if there exists little slip in the timing over the interval of one packet. This can be achieved with proper attention to oscillator precision; and it is shown that the requirements are quite reasonable to achieve, at least for systems with no spread or with moderate spread factors. It is also shown that the stability requirements are a function of packet length and are not a function of data rate. If there is sufficient traffic density through a repeater of either real or artificial nature, it may be desirable to maintain terminals in the region of a particular repeater in continuous synchronization with the repeater to simplify the oscillator design requirements for the low cost terminal.

2.2.1 General Concept of Bit Synchronization

Consider a network of repeaters and terminals with maximum spacing of 10 miles. If the system is operated at a data rate of 100 kb/s with biphase modulation, the symbol period is 10 μ s and the clock rate is 100 kHz. Transmission time for the 10-mile path is approximately 54 μ s; hence, the beginning of the message is received about 5.4-bit periods, or almost 2000 degrees of clock phase after the start of transmission. For detection purposes, however, we need only be concerned with clock phase over a range of 350 degrees. If we wished to synchronize such a network, a time or phase reference could be established for each terminal and repeater that is referred to some control point, such as a station. Each terminal and repeater would then be required to predict the required phase at time of arrival at the repeater to which the message is addressed, and to adjust the transmit phase accordingly. Such a technique is used for time slotting of messages in TDMA satellite relay systems where the central time reference is at the satellite; however, the complexity of controlling synchronization among a number of stations in the packet radio system quickly convinces one

modulation and detection

that this would not be a satisfactory technique for maintaining bit synchronization, although a similar technique still may be considered as a method of message slotting.

The alternate and obvious approach is to synchronize independently to each packet. This was probably the first assumption, but the fixed time reference concept was summarized above to emphasize that continuous network synchronization is complex and probably of little value for packet radio systems.

For packet radio, the problem can be reduced to one of time reference (epoch) determination for each packet. If we can design all clocks to run at sufficiently constant rates independent of external control, then epoch determination from a transmitted preamble is adequate for synchronization (i.e., all that is needed is to set our clock at the beginning of each packet). For this system, our day is 10 μ s long, and no transaction extends beyond 1000 days on our calendar. We are only concerned with the time of day a particular transaction started. For convenience we reset our clocks to midnight at the beginning of the transaction, and let it run at a predetermined rate from that point.

The following is a summary of characteristics of suggested system:

- a. All stations are bit synchronous in the concept that during the period of one packet the slip rate is a small fraction of a bit once the epoch is established (i.e., all clocks have accurate rate but are arbitrary in phase).
- b. Epoch is established by a preamble, and once established, timing is not corrected during the packet transmission.
- c. Epoch is reestablished for each packet transmission.
- d. Transmit clocks at both terminals and repeaters are phase independent of receive clocks, although derived from the same time base. (This allows synchronization of terminals to a particular repeater should this prove desirable.)

The approach outlined above resolves down to one of accurately resolving a time reference (phase) during a defined preamble and accurately maintaining frequency once phase is set. No phase correction is made once phase is established. The argument for this approach is summarized below:

- a. Timing must be accurately established by the beginning of the header if header is to be accurately decoded. There is little merit in further correction (by use of phase-lock loops) if slip-rate requirements are reasonable.
- b. Preamble may be designed for optimum bit synchronization acquisition, while it is desirable that no restrictions be placed on the message or header content (i.e., may contain all 0's if we so desire). In a practical system, phase of bit recovery is influenced by bit pattern.
- c. The system allows use of the same master clock for outgoing or incoming information.
- d. Master clock may be of high precision since it is not required that it be adjusted in frequency as part of an analog or digital phase-lock loop. Phase adjustment is made using techniques that do not influence clock long-term frequency stability.

2.2.1.1 Oscillator Stability Requirements for System with No Spread

Figure 2-25 represents a system with no spread spectrum. Assuming the following tolerances on timing:

Accuracy of estimating of epoch = 12 degrees of clock phase (0.33 μ s for 10 kb/s system)

Maximum slip in clock phase over 1000-bit packet = 6 degrees of clock phase

The above values seem reasonable although they have not been evaluated in terms of loss in error threshold.

If the maximum packet length, including header, is 1000 bits, then oscillator accuracy to meet 6-degree slip is:

$$\text{Clock Accuracy} = \pm \frac{1}{1000} \times \frac{6}{360} = \pm 1.66 \times 10^{-5}$$

Since both transmit and receive clocks are involved in this tolerance, the accuracy of each clock must be twice the above value, or about eight parts per million. If $n = 100$, then the clock can be set to the nearest 1/100 of clock cycle, or 3.6 degrees (this can be improved by a factor of 2 by using both positive and negative transitions of the clock cycle). This, then, leaves about 8-degree error in determining the epoch. The ability to meet this requirement is related to preamble length, signal-to-noise, and signal dispersion due to reflections; however, it appears that if signal-to-noise is adequate to achieve a bit error rate of 10^{-5} (packet error rate of 10^{-2}), it should be possible to achieve desired synchronization accuracy with a relatively short preamble. False alarm rates under no signal conditions may be a more important consideration. The system must operate with a wide dynamic range of signals; hence, the epoch detector must be able to operate in a Gaussian noise environment with a low probability of false alarm. It appears that use of a surface acoustical wave device as a correlator may effectively establish the epoch. The advantage here is that the SAWD is an effective if. frequency correlator and does not require prior establishment of carrier or clock reference in order to function. Its use does, however, place some restrictions on frequency stability of the system.

2.2.1.2 Oscillator Stability Requirements for Spread Spectrum Systems

The use of spread spectrum and time slotting is being investigated as a means of sorting multipath and interference signals on the basis of time of arrival. With spread spectrum systems, accurate establishment of epoch and good bit sync stability is an important consideration, particularly if this technique is used to separate signals on the basis of time of arrival.

Consider the model outlined in figure 2-26. The data symbol for zero is a PRN sequence (PRN_1), and the symbol for one is an orthogonal sequence (PRN_2). It is convenient, though not necessary, to make $\text{PRN}_2 = \overline{\text{PRN}_1}$, and use differential detection. This allows use of only one code for the surface wave lines to be used in the receiver. If the sequence is 32 bits long, the bit rate = R_b and biphase modulation is used, then period of sequence $1 = 1/R_b$. (The chip rate is $32 R_b$ and chip period is $T_b/32$.)

The correlation peak for PRN sequence is two chips wide at the base; therefore, if we can accurately define epoch, then we can sample the signal through a time gate of width no longer than $T_b/16$. By this technique all interference occurring outside this frame may be

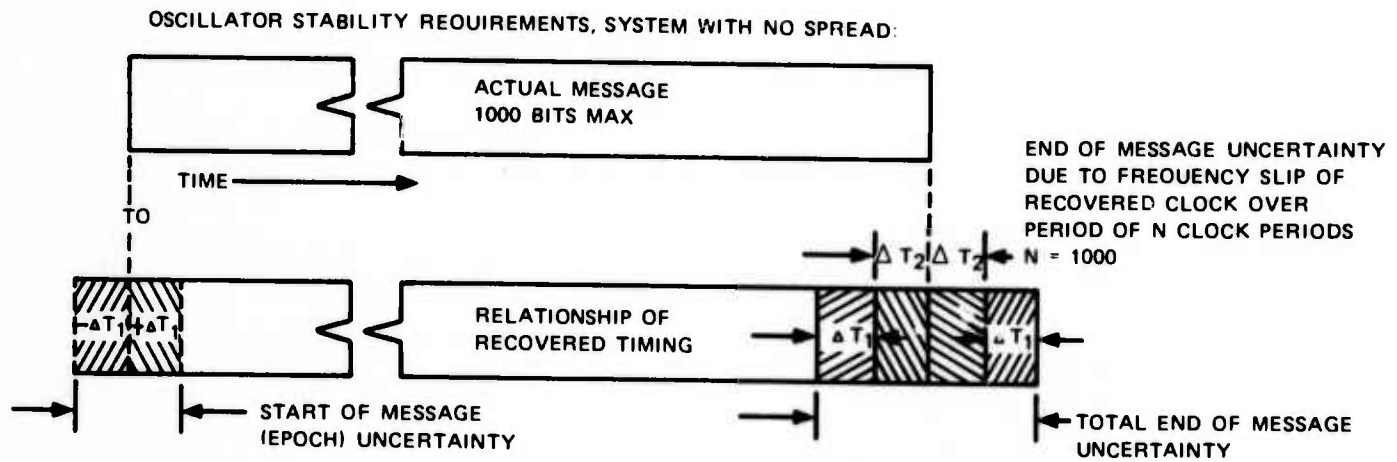


Figure 2-25. System with No Spread Spectrum.

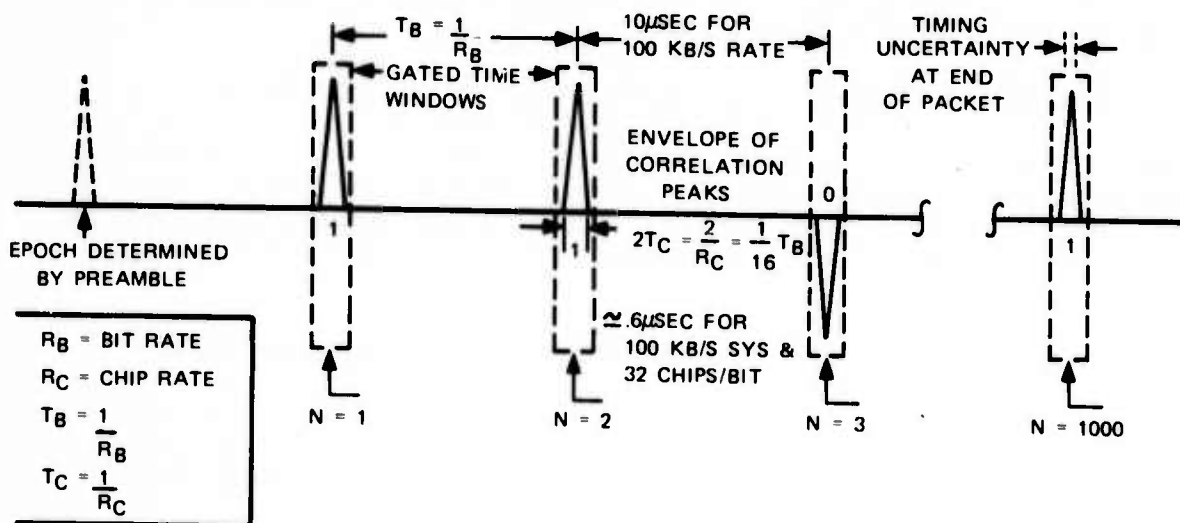


Figure 2-26. Signal Separation on the Basis of Time of Arrival.

disregarded. Therefore, if other stations transmit at random, the probability of a given interferer falling on the desired slot is $1/16 \approx 0.06$. However, this probability exists only if an interfering signal is exactly in synchronization. If two clocks slip by one cycle over packet length of 1000 bits (i.e., one transmits 1000 bits in a period and the other transmits 999 or 1001), then there is a probability of 1.0 that at least 1-bit interference will occur if both start transmitting at about the same time. However, 10^{-3} clock stability is very poor.

NOTE

The signal need not necessarily be time gated if the detection is accomplished by sampling the value at precise time intervals, since time selection is accomplished by the sampling process. However, the signal may also be selected by a time gate of some defined width and the value of the signal within the gate integrated over the period of the gate by integrate and dump techniques. The second approach may allow poorer clock stability and epoch determination. Also, multipath characteristics are almost certain to affect the optimum choice of detection technique, and the need for further evaluation is clearly indicated.

For this model, it would seem reasonable to allow a gate position drift of $1/4$ of a chip interval. This, then, results in a total gate width of $2-1/2$ chips plus any further allowance that may be required for error in defining the epoch. For this model, the framing of the first and last pulse of the packet is shown for zero epoch error. (See figure 2-27.)

For this example, the clock time is allowed to drift $1/4$ chip period, or $1/32 \times 1/4 = 1/128 T_b$ where T_b is bit period. Since two clock oscillators are involved, the accuracy should be no worse than $1/2 \times 1/128 \times 1/1000 \approx 4 \times 10^{-6}$. This is only twice the stability calculated for the nonspread system. No allowance has been made for epoch error; but for the spread system, this is expected to be small if multipath is not severe. Also, some of the skirts of the correlation peak may be clipped without significantly affecting the total energy under the correlation envelope. In fact, in transmitting through a reflective or dispersive medium, there may be some advantage in narrowing the window through which the correlation peak is sampled.

It will be noted from this discussion that required stability is a function of packet length and a function of chips per bit, but is not a function of bit rate.

2.2.1.3 Oscillator Requirements

The stability and aging characteristics of crystal oscillators vary at least two orders of magnitude with differences in the cut of crystals and choice of oscillator circuit. However, stabilities in order of a few ppm can be obtained with a well-designed temperature-compensated oscillator, and better stability is possible if precision ovens are employed. (See appendix 2A.)

It therefore appears that adequate stability can be obtained with carefully temperature-compensated crystal oscillators if only moderate spread factors are used. Further, the tolerance that may be allowed for the clock frequency of the hand-held terminal may be essentially doubled by placing much tighter requirements on the repeater. Such an approach is not unreasonable since temperature-stabilized crystals may be used at the repeater without paying a significant price in terms of power consumption. Such an approach is not attractive for the terminal, since the terminal may be operated intermittently. Crystal oven warmup times are not practical for a unit that is operated intermittently.

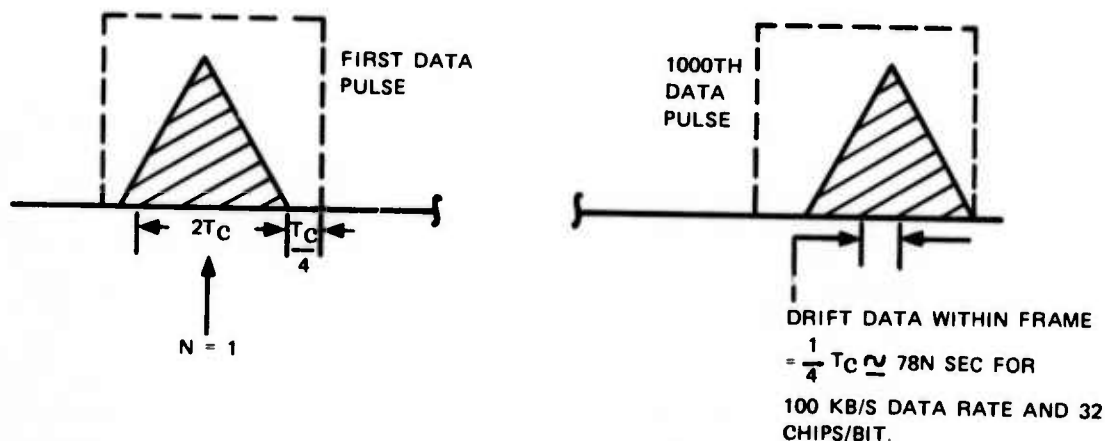


Figure 2-27. Framing for Zero Epoch Error.

If precision temperature-controlled oscillators are used at each repeater, it may be more economical to synchronize each terminal clock to a repeater if sufficient traffic through the repeater is ensured to allow reliable synchronization. The terminal need not transmit to the same terminal from which it receives synchronization, although there appears to be some merit to synchronizing the terminal to the strongest repeater and then transmitting its traffic to that repeater. If the terminal cannot lock to a repeater, then there is no merit in transmitting; hence, such an approach leads to confidence that the system is working prior to an attempt to transmit. Such an approach would require rather slow clock loops since it must hold with little slip over at least its transmit period of 1000 bits. This implies clock bandwidth well below 100 Hz for the 100-kb/s system, or some form of sample and hold technique. Since the frequency errors to be corrected result from temperature and aging, it appears that once the required correction was determined, it could be held for long periods. Such a time gated afc system with long hold periods merits further investigation if adequate stability cannot be achieved by simpler techniques.

2.2.1.4 Doppler

For the simplified timing model described above, the timing accuracy required over a packet period was about 40 ns for the system with X32 spread, and about 80 ns for the nonspread system.

NOTE

These values were for reasonable, though somewhat arbitrary, system models; hence, little significance should be given to the ratios of the above two numbers for the two quite different models.

Doppler is a time expansion or compression phenomenon; hence, the maximum relative velocity allowed is that which results in a 40-ns time expansion or compression during a packet in time of 0.01 second (1000-bit packet at 100 kb/s assumed):

$$V_{\max} = c \frac{\Delta t_2}{T_p} = \frac{1.86 \times 10^5 \times 40 \times 10^{-9}}{10^{-2}} \approx 0.74 \text{ mile/s} \approx 2680 \text{ miles/hr}$$

where

c = Velocity of light

t_2 = Allowed timing error at end of packet

T_p = Time duration of packet (0.01 second assumed, i.e., 1000-bit packet at 100 kb/s).

It is therefore concluded that doppler will not present a significant timing problem for packet radio systems even if operated from jet aircraft.

For systems using spread techniques, the doppler frequency error may be a more important consideration. See paragraph 2.1 for the relationship between bit time (T_b) and allowed frequency error if surface wave devices are used to decode the data symbols.

2.2.2 Synchronization Preambles

There are several approaches to the packet synchronization problem that can be utilized. These approaches are discussed in varying degrees of depth; from the discussion, the recommended approach is selected.

Several assumptions are made in the evaluation of the candidate preamble schemes. Some of these assumptions are:

- a. The modulation will be minimum shift keying (msk).
- b. Code spread spectrum pulsewidth of $T_C = T_B/N$, where N is the number of chips per bit, while allowing the radiated power to be constant.
- c. Minimum data rate of the order of 100 kb/s.
- d. Bit error probability of 10^{-5} .
- e. The processing gain will be in the vicinity of 10 to 20 dB.

Each of the approaches considered assumes that a bit is spread into 127 chips which make up a 127-chip maximum length sequence. Four preamble approaches are considered and compared. These approaches fall into two classifications: (1) Barker codes and (2) repeat codes.

2.2.2.1 Preamble Specifications

To begin a discussion of preamble detection, one must establish some preamble specifications. If we assume that a packet consists of 1000 bits of data maximum, then a bit error probability of 10^{-5} results in a packet error rate of 10^{-2} without error detection and correction. Since error detection with automatic request for retransmission will be used rather than error correction, it would be undesirable for the packet error probability or

retransmission probability to exceed 10^{-2} . The preamble should have a detection probability at least as good and probably better than the packet detection probability. Therefore, the design goal for the probability of preamble detection will be 99.9 percent.

A frequently used relationship between false alarm probability and average time between false alarms is given by:

$$P_{FA} = \frac{1}{T_{FA} B}$$

where

P_{FA} = False alarm probability

T_{FA} = Average time between false alarms

B = Information bandwidth = 100 kHz.

Assuming that a packet consists of 1000 bits, a packet duration is 10 ms. If we assume one false alarm for every 1000 packet times (i.e., every 10 seconds), then $P_{FA} = 10^{-6}$. This will be the false alarm probability design goal.

For differentially coherent psk on msk modulation, a 10.4-dB signal-to-noise ratio (E_b/N_0) is required to achieve a bit error rate (BER) of 10^{-5} . For this probability of bit error, 1 percent of the 1000-bit packets will be in error; however, a reasonable approach is to assume a 50-percent probability of packet error in order to come up with the worst case preamble design. The 1000-bit packet has a 50-percent probability of error for a BER = 7×10^{-4} corresponding to $E_b/N_0 = 8.2$ dB. A 200-bit packet has a 50-percent chance of being correctly received for BER = 4×10^{-3} , which corresponds to 6.5 dB. Since the preamble length is the same for either packet size, the design goal will be to provide a preamble having a 99.9-percent probability of detection in the worst case E_b/N_0 environment of 6.5 dB. This margin can also be applied to some system degradations such as timing errors, frequency offset, doppler, and sidelobes.

2.2.2.2 Preamble Analysis

- a. Coherent Combining. The required preamble length and E_b/N_0 to achieve the probability of detection of 0.999 and probability of false alarm of 10^{-6} is a function of the detection technique. Coherent combining of the preamble yields the best results. The probability of missing the preamble versus the signal-to-noise ratio for a bit is plotted in figure 2-28 with the number of bits in the preamble as a parameter. Also, the false preamble probability is 10^{-6} . The results show that 8 bits are required to achieve the design goals. The analysis deriving these results is given in appendix 2B.

The coherent combining of the bits at the output of the SAWD is difficult. The combining accuracy is a function of the if. frequency and must be less than 1 ns. The delay can be achieved with a surface wave device matched to the msk SAWD.

- b. Noncoherent Combining. If the preamble bits are combined noncoherently, additional bits are required to achieve the same design goals. This is demonstrated with figure 2-29 where the number of preamble bits required for a missed preamble probability of 10^{-3} is plotted versus the signal-to-noise ratio. The curves are shown for two values of probability of false alarm 10^{-3} and 10^{-6} . To achieve the design goals stated above

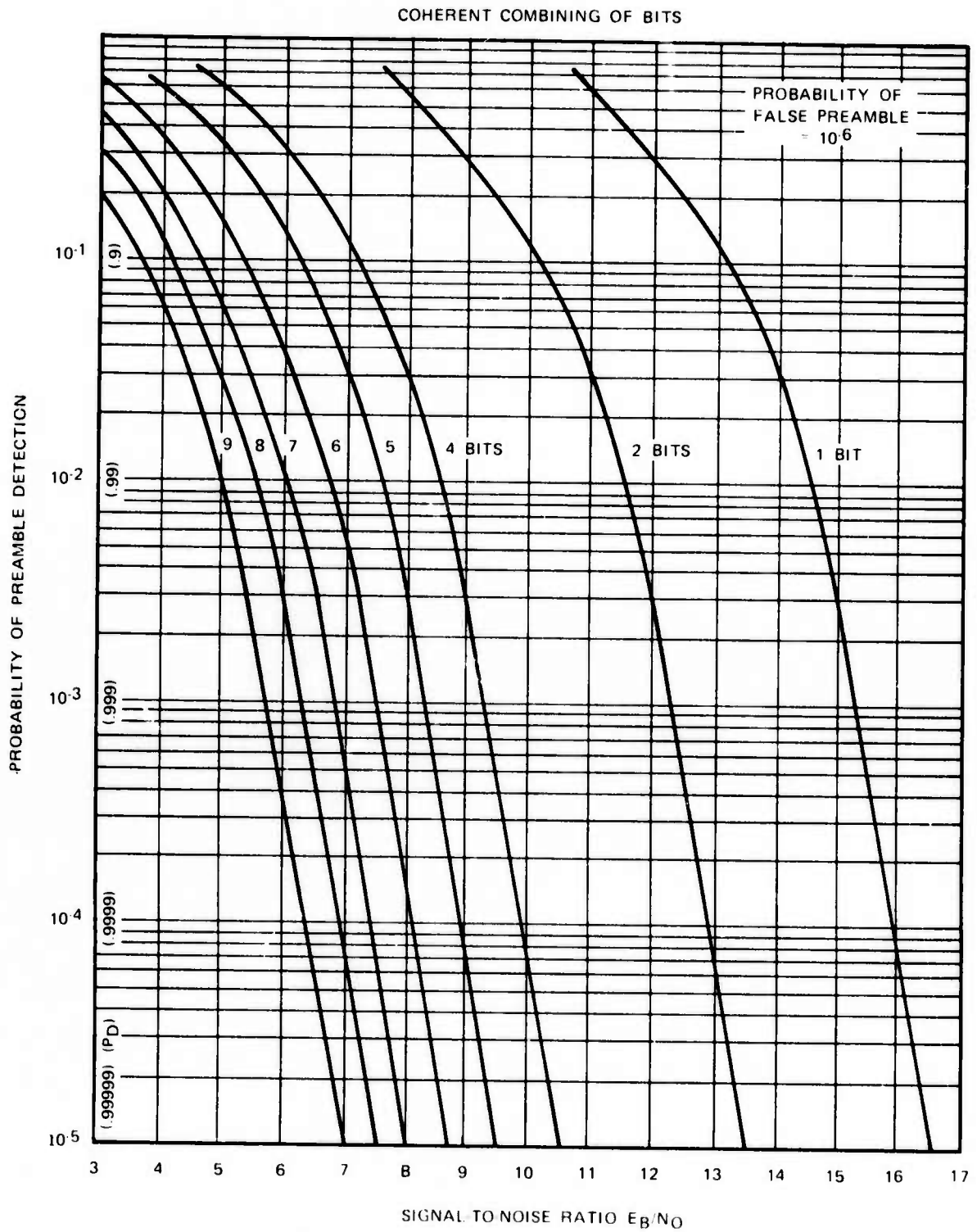


Figure 2-28. Probability of Preamble Detection (Coherent Combining of Bits).

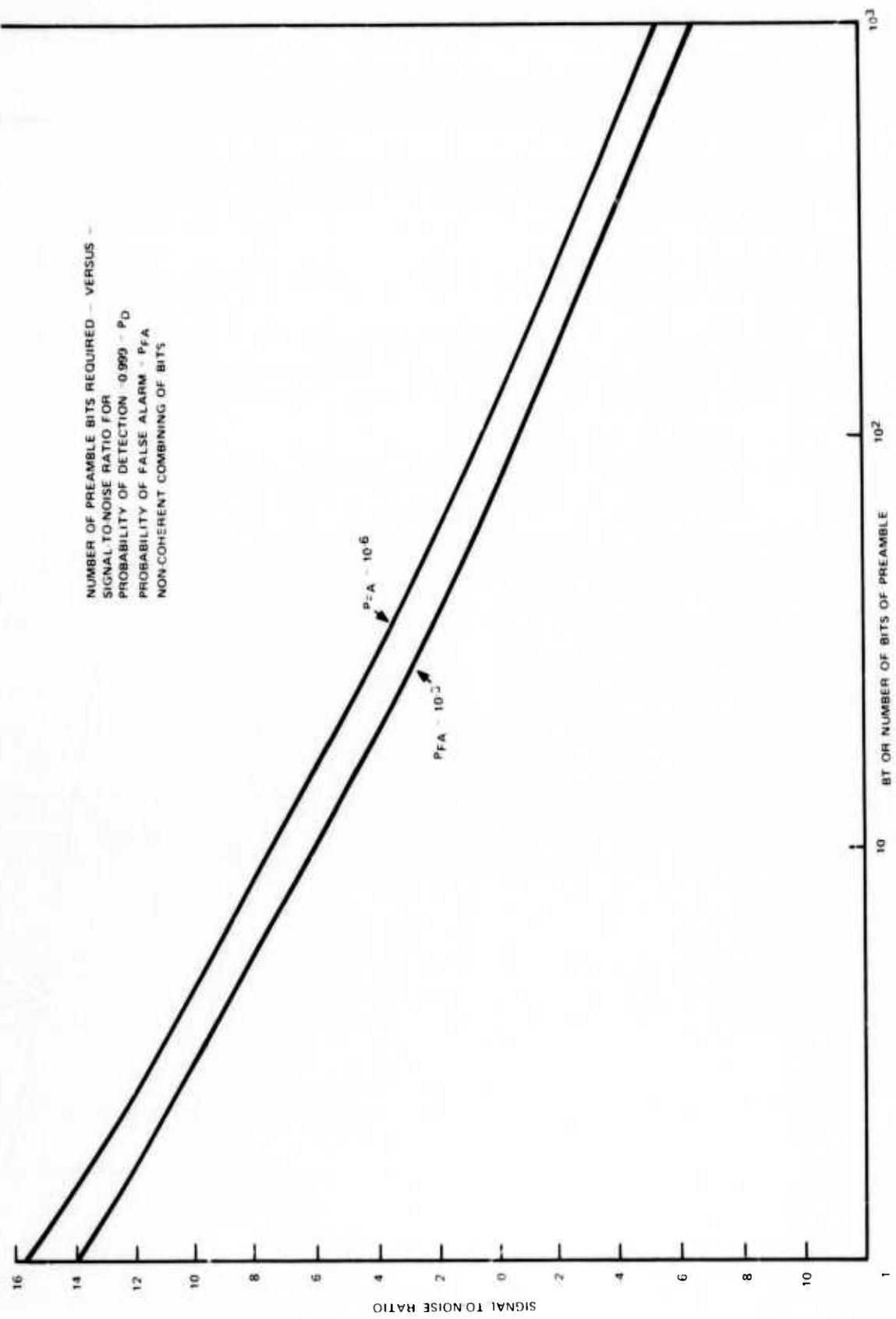


Figure 2-29. Noncoherent Combining of Bits.

requires a minimum of 13 bits of preamble. The derivation of these curves is given in appendix 2B. In order for the analysis to be tractable, some simplifying assumptions were made. For low values of BT, the results are a few tenths of a dB pessimistic.

- c. Post Detection. A detection decision is made on each bit for the third approach. To exceed the threshold for detecting, the preamble requires that M out of N bits are received correctly. In one case considered, a Barker code is used to achieve both bit timing and the sync preamble. The 13-bit Barker code is followed by another 13-bit Barker code where each bit of the second code is reversed in sign. For 26 bits of preamble, 21 or more must agree with the stored reference at the receiver to achieve the design goals. The results are plotted in figure 2-30. The derivation of these curves is given in appendix 2B.

2.2.2.3 Preamble Approaches

Four different preamble approaches are discussed in this section. Some of the advantages and disadvantages of each approach will be given. There are many variations and implementation approaches that can be suggested. In the interest of getting at the underlying principles, just a few of the possibilities are shown.

For each of the preamble approaches considered, each bit consists of 126 or 127 chips, the exact number depending upon the code used to select the chips. The basic preamble principles hold independent of the number of assumed chips per bit.

- a. Barker Preamble with Coherent Detection (Coherent Combining). One of the classic approaches is the use of the Barker sequences for preamble detection. This family of sequences is characterized by:

$$R(k) = \begin{cases} N & \text{for } k = 0 \\ \pm 1, 0 & \text{for } k = 1, 2, \dots, N \end{cases}$$

where $R(k)$ is the autocorrelation function and N is the number of bits comprising the sequence. The size of the family is restricted since there are no more than nine known Barker sequences. The Barker code coming closest to satisfying the requirements stated above is of length $N = 7$. The next largest Barker sequence is of length $N = 11$. For $N = 7$, its sequence is given by:

+++-+--

This sequence gives a ratio of 16.9 dB between the peak and the sidelobes. A plot of the autocorrelation of the Barker sequence illustrating this is given in figure 2-31. Each bit of the Barker sequence consists of 127 chips from a 127-chip maximum length shift register. If the Barker bit is positive, the 127-chip sequence is transmitted. If the Barker bit is negative, each chip of the 127-chip sequence is inverted. A possible preamble detector implementation is shown in figure 2-32. Each SAWD is matched to one bit of the Barker code. The first SAWD has the cosine pulse interdigital transducer, in addition to the 127 taps corresponding to the 127 chips. Details on possible SAWD implementations of msk detectors are discussed in paragraph 2.1. The outputs of the seven SAWD's are summed coherently, amplified, and compared to a threshold. A level sensing circuit establishes the input signal level and normalizes the output of the video amplifier so that a fixed threshold V_T can be used. When this threshold is exceeded, the presence of the preamble is indicated. A pulse is triggered at the time the threshold V_T is first exceeded. The pulse is terminated when the signal falls below the threshold. The center of this pulse is then estimated, which establishes

modulation and detection

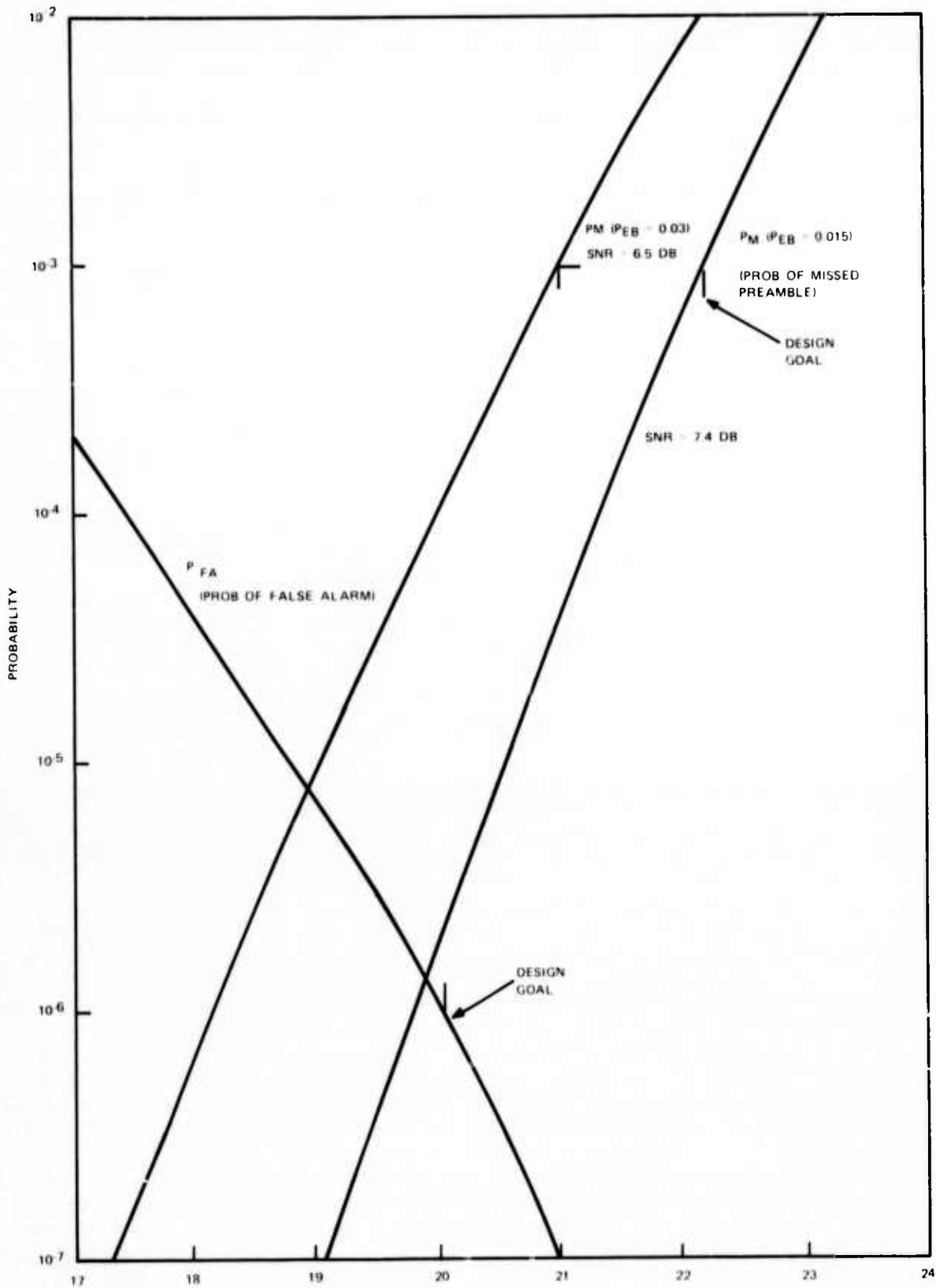


Figure 2-30. 13-Bit Barker Code Followed by 13-Bit Barker Complemented.

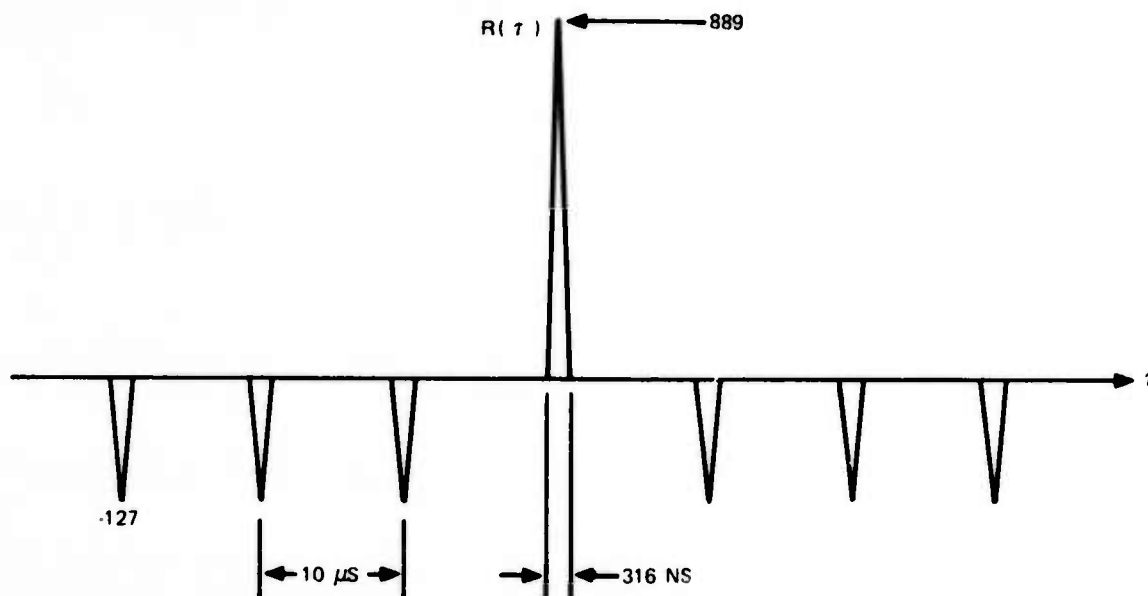


Figure 2-31. Autocorrelation of 7-Bit Barker Sequence Where Each Bit Consists of 127 Chips of a Maximum Length Sequence at 100-kb/s Rate.

the bit timing for the remainder of the packet. The preamble accomplishes two functions: (1) it establishes bit timing, and (2) it indicates the start of the message. A discussion of the accuracy to which the bit timing can be estimated was provided earlier. The following expression was derived for the time of arrival variance for a practical center pulse estimator:

$$\sigma_T^2 = \frac{\gamma^2}{2(2 E/N_0)}$$

where E/N_0 is the signal-to-noise ratio, and γ is the chip duration. For $\gamma = 79$ ns and $E_b/N_0 = 6.5$ dB, $\sigma_T = 18.6$ ns.

From the autocorrelation function of the preamble (figure 2-31), it can be seen that multipath that is delayed by 100 ns relative to the received signal will be rejected. Since coherent msk detection is used in this example, there is a 180-degree phase ambiguity of the chips and bits. Therefore, the received crosscorrelation pulse at the output of the SAWD will be either positive or negative. This presents no problem as long as we are not detecting data, since the output of the envelope detector is always positive.

As noted above, the peak-to-sidelobe ratio is 16.9 dB (7:1). The sidelobes, in effect, add to noise, thereby reducing the effective signal-to-noise ratio by 1/7 (1.34 dB).

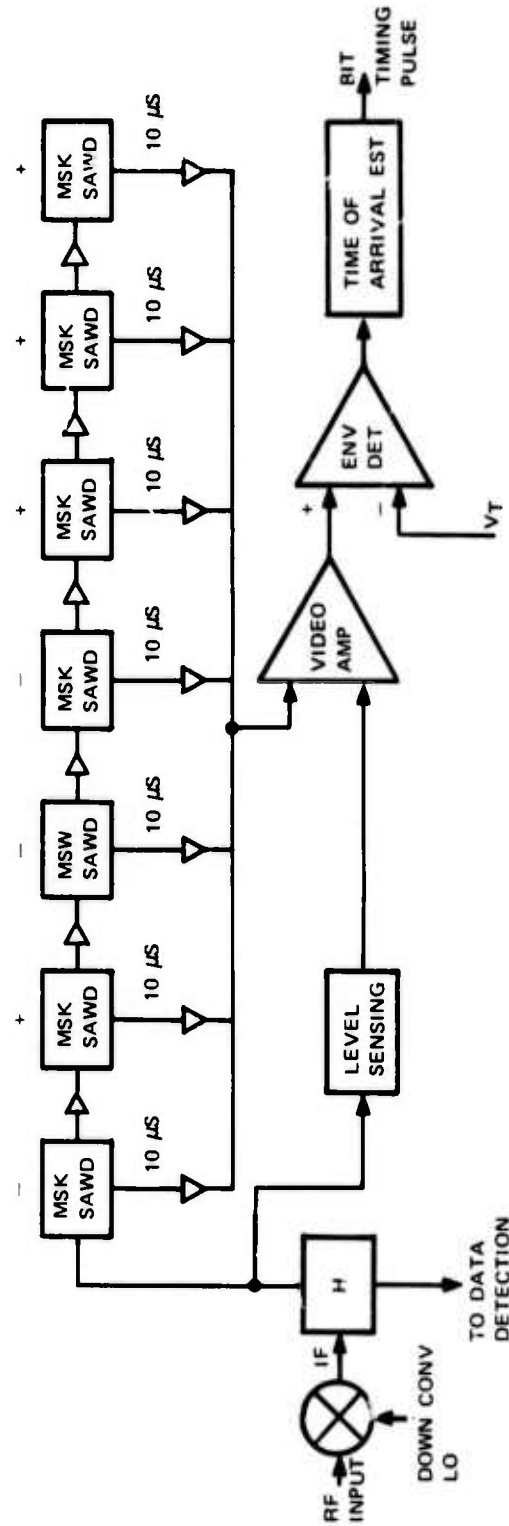


Figure 2-32. 7-bit Barker Preamble and Bit Sync Detector Coherent Combining Detection.

One practical shortcoming is in the implementation of this approach as it requires seven 10- μ s SAWD's in cascade, each of which has from 10 to 30 dB insertion loss. Longer SAWD's can be used with more taps on each SAWD. The practical limitation with today's technology is about 40 μ s.

With the use of the 7-bit Barker code described above, the design goals are missed only by 0.5 dB (the design goal required 8 bits); however, the next shortest Barker code is 11 bits long.

Another disadvantage is that the effects of doppler shift, and frequency errors are cumulative through the entire preamble. Thus, the coherent technique is much more sensitive to such offsets than a noncoherent combining technique.

One feature of this technique is that the first two SAWD's could be used for detecting differentially coded msk data signals. Also, the derivation of bit timing and the end of preamble or start of message indication do not have to be derived separately.

- b. Barker Preamble with Differentially Coherent Detection (Coherent Combining). Another Barker preamble approach is shown in figure 2-33. This approach requires only two SAWD's while yielding performance close to that of the optimum approach previously discussed. Differential msk modulation and detection are employed. The details of the modulation technique are more completely discussed in the paragraph on modulation approaches.

The msk SAWD's are 1-bit time long or 10 μ s. In essence, they are filters matched to the spread signal on a bit basis; they remove the pseudonoise spreading. A baseband preamble is obtained at the output of the comparator. Although a second analog matched filter matched to the 7-bit Barker sequence would be optimal, a close approximation can be obtained by limiting the baseband signal, as shown, and sampling at a high rate relative to the bit rate. Ten samples per chip would be realistic. This 8890 (10 x 127 x 7) length sequence of samples is then correlated in a digital matched filter with the stored sequence. It may be possible to implement this operation with a high-speed ROM. The summer consists of counting the pairs of bits that are alike. When the digital counter exceeds a predetermined threshold value, the preamble presence is established. Bit timing can also be derived in a manner similar to that discussed above.

The advantage of this approach is the reduction in the number of SAWD's. Another advantage is that, since the bits are encoded differentially, the bit detection circuitry can be used to detect subsequent message data bits without the need for separate data detection circuitry.

A disadvantage is that there is some loss of performance. A detailed analysis of the degradations due to the single bit quantization has not been done; but based on experience, it is estimated that this degradation may be in the vicinity of 1 to 2 dB, depending upon the number of samples per bit. Added to this is the 1.34-dB degradation due to sidelobes. An additional 2 dB of performance can be gained by extending the Barker preamble to 11 bits.

Another disadvantage is the rate of sampling required in order to adequately capture the correlation peaks and achieve a good estimate of bit timing. Also, the digital filter of 8890 samples operating at 100 MHz is quite complex, hardware-wise, to implement.

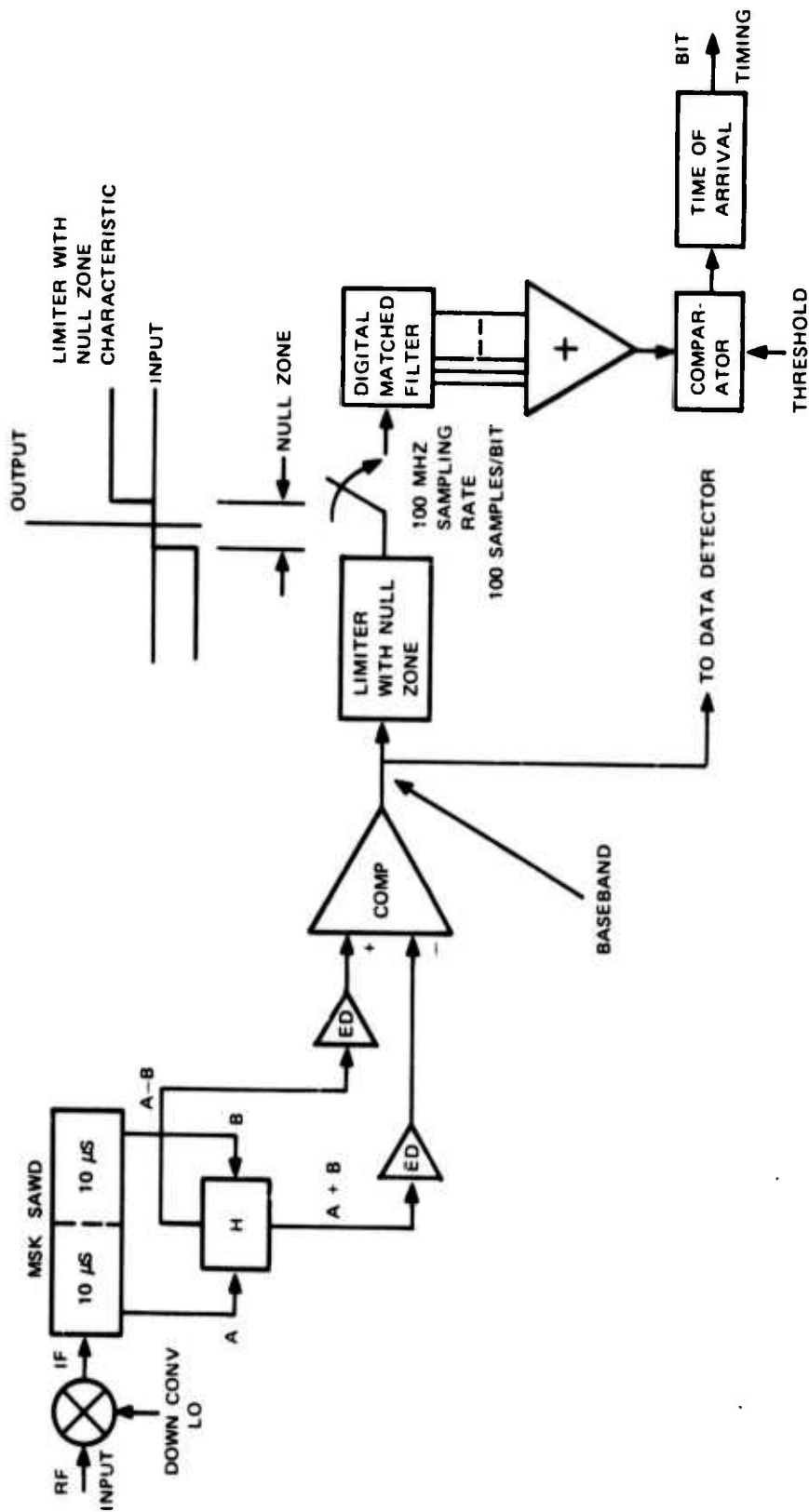


Figure 2-33. 7-Bit Barker Preamble and Bit Sync Detector Differentially Coherent Combining Detection.

- e. Repeat Preamble with End of Preamble Detector (Coherent Combining). The third candidate technique is shown in figure 2-34. The preamble, consisting of n chips from a maximum length sequence, is repeated seven times. The msk SAWD detects one bit at a time. The SAWD is matched to the n chip sequence. The output of each detected bit is coherently added to the previous outputs of detected bits. At point A in the figure, the envelope of $R(\tau)$ builds up in time as shown in figure 2-35. A pulse is triggered at the time V_T is first exceeded. The pulse is terminated when the signal falls below the threshold. The center of this pulse is then estimated, which becomes the bit timing pulse for the remainder of the packet.

The second part of the preamble is the 4-bit Barker sequence. Its purpose is to establish the end of the preamble and the beginning of the message. Each bit of the Barker code consists of n chips from a maximum length PN sequence. A logic 1 takes the sequence as is, and a logic 0 inverts the sequence. A 40- μ s SAWD may be used to match to the Barker sequence. An alternative is to use four 10- μ s SAWD's similar to that shown in figure 2-32. A threshold V_{T2} is used to indicate the presence or absence of the code at the sample time. If the output exceeds the threshold V_{T2} at sample time, then the end of preamble is indicated and data detection commences.

This approach is relatively straightforward. It requires a few extra preamble bits because the detection process is divided into two parts.

- d. M Out of N Preamble Detector (Postdetection Combining). An M out of N preamble detector, where N is the number of bits in the preamble and M is the number of bits that must match to detect the preamble, is shown in figure 2-36. The preamble length N is 26 bits. The preamble consists of a 13-bit Barker code followed by an inverted 13-bit Barker code. The Barker code and its inverse is given by:

```
++++-+-+--+ Barker
-----+-+--+ Barker
```

The msk detection process can be implemented as shown using a SAWD. The details of this implementation approach are discussed in the paragraph on modulation waveform.

In this preamble technique, the bit integration occurs after the bit decisions are made. At the detector output (point A of figure 2-36), the waveforms are correlation pulses of 4-chip duration (316 ns) occurring at the bit rate (10- μ s intervals). The pulses are either positive or negative. A positive pulse exceeding the threshold yields an output pulse from the upper comparator (C). This pulse is asynchronously into the register. An initial estimate of bit timing is also derived from this pulse that is used to clock the register at subsequent bit intervals. If the pulse at the next bit sampling interval is positive and exceeds the threshold, it is shifted into the register. If the pulse is negative, an output is obtained from the lower comparator. At the bit sampling interval, this pulse is shifted into the register as a logic 0. The matched filter consists of a shift register and taps with each tap weighted by either a 1 or a 0 in accord with the Barker code.

One digital implementation approach is shown in figure 2-37. The two sums compute the number of matches and mismatches between the incoming data and the locally stored code sequences. The difference between the two outputs is compared against a threshold. When the threshold is exceeded, an end of preamble (EOP) is obtained. If the register contains all 0's and the 26-bit Barker, Barker code is received, the difference between the two summers of the digital matched filter (point P on figure 2-37)

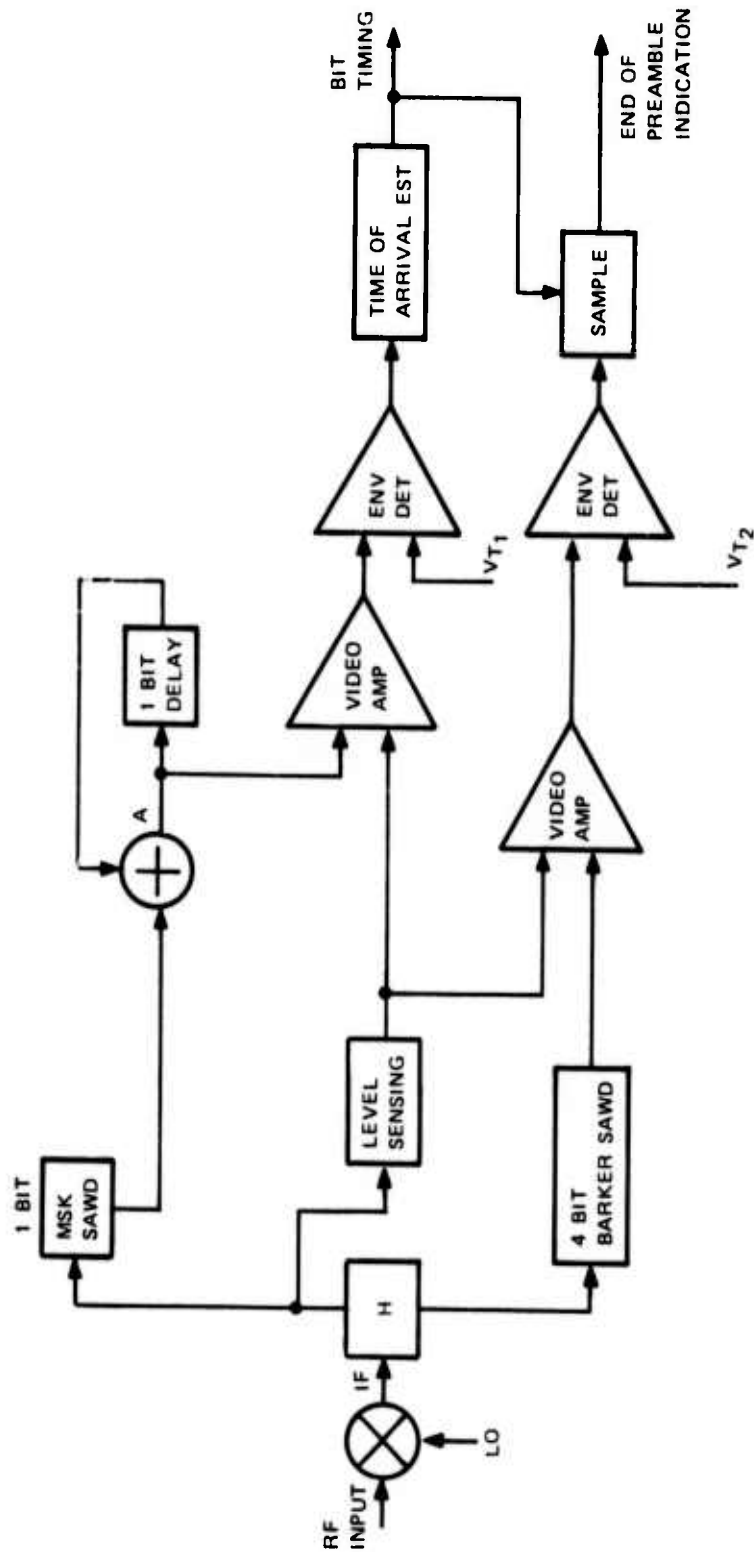


Figure 2-34. Repeat Preamble with End of Preamble Detector.

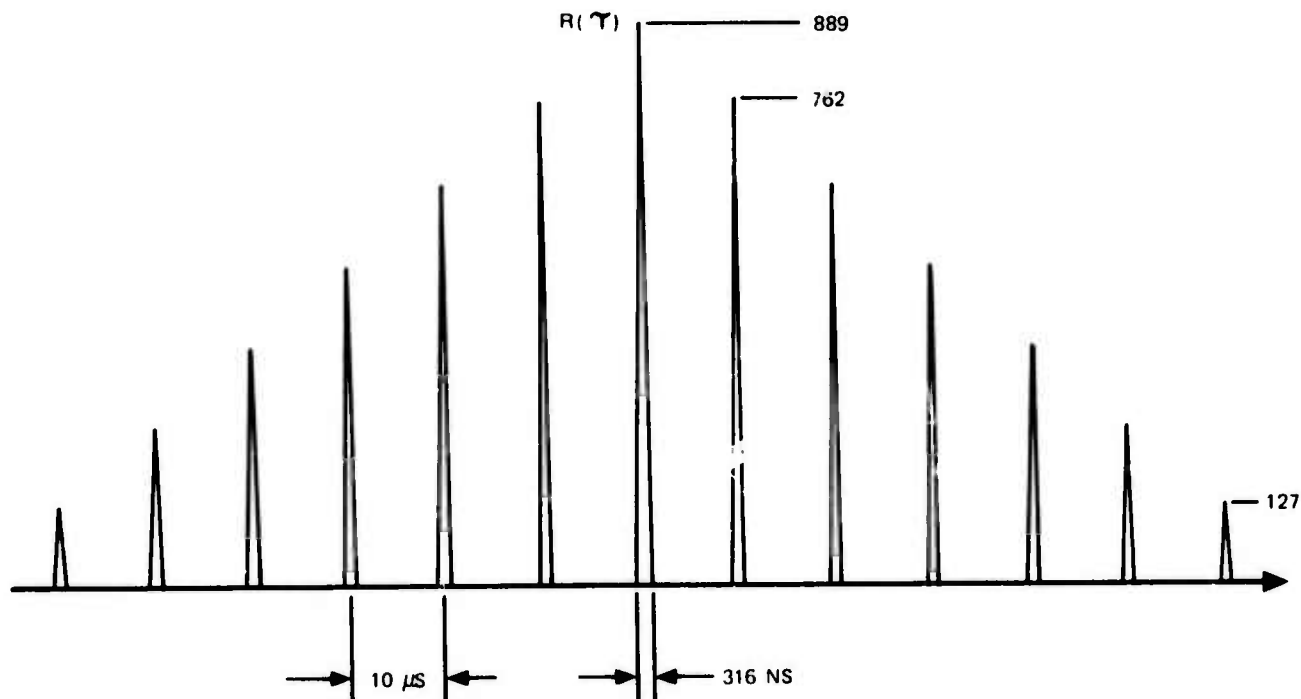


Figure 2-35. Autocorrelation of Seven 1's where Each Bit Consists of 127 Chips of a Maximum Length Sequence at 100 kb/s.

follows the correlation function shown in figure 2-39. The correlations are separated by the bit interval. Without any errors, the output is always negative or zero until the preamble lines up exactly in the register. At this time, the output is 26 units. An analog implementation of this matched filter is shown in figure 2-40.

The expected performance obtained with this preamble approach is calculated in appendix 2B. The results are plotted in figure 2-30. The probability of a false alarm and the probability of a false preamble are plotted as a function of the threshold. In this analysis two thresholds are involved. The first one is used for the detection of the bits and the second for the detection of the preamble. The probability of a false alarm is not a function of the signal-to-noise ratio. The probability of a missed preamble is a function of the signal-to-noise ratio and is plotted for an SNR of 7.4 dB and 6.5 dB. If the preamble is set to 21, the probability of a false alarm is 10^{-7} and the probability of a missed preamble is 10^{-3} for a 6.5-dB SNR. This meets our design objectives.

One of the disadvantages of this approach is the length of the required preamble when compared with the approaches discussed previously.

An advantage is the relatively simple implementation requirement. The basic speed of the detector is at the bit rate, with the exception of a counter in the center of pulse estimator which will operate from five to ten times the chip rate. The basic SAWD detector is used for detecting both the preamble bits and the subsequent data bits. The bit timing sampling pulse is derived simultaneously with the receipt of the preamble. A

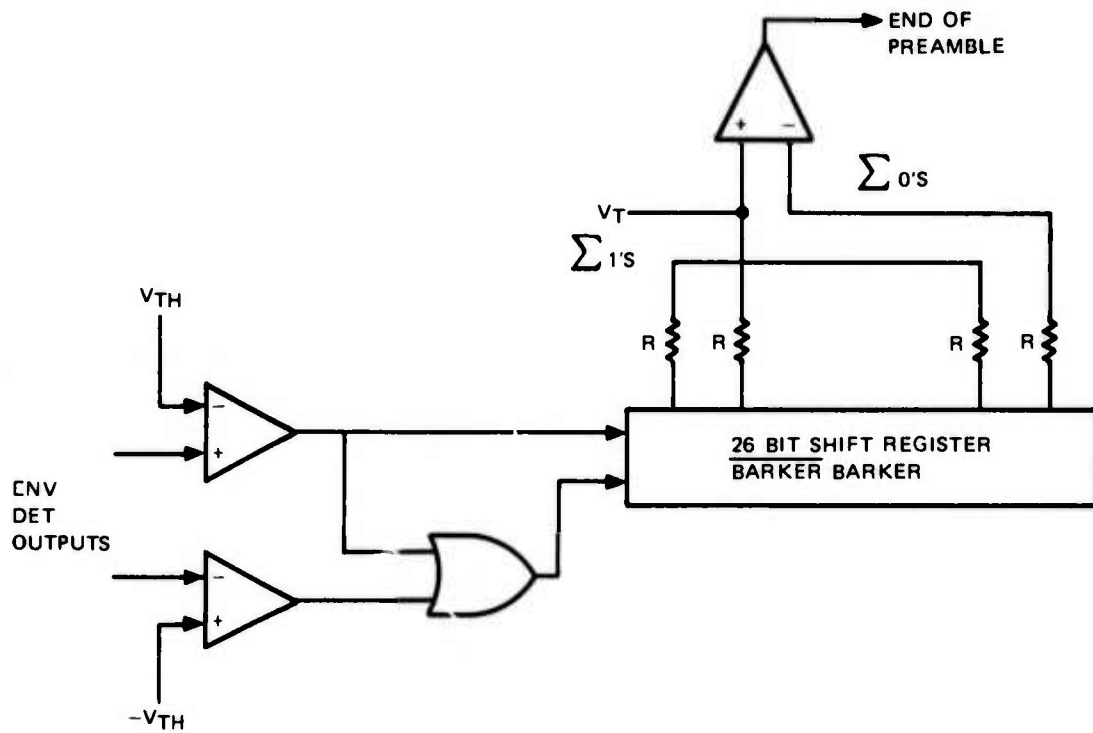


Figure 2-37. Digital Implementation of Preamble Filter.

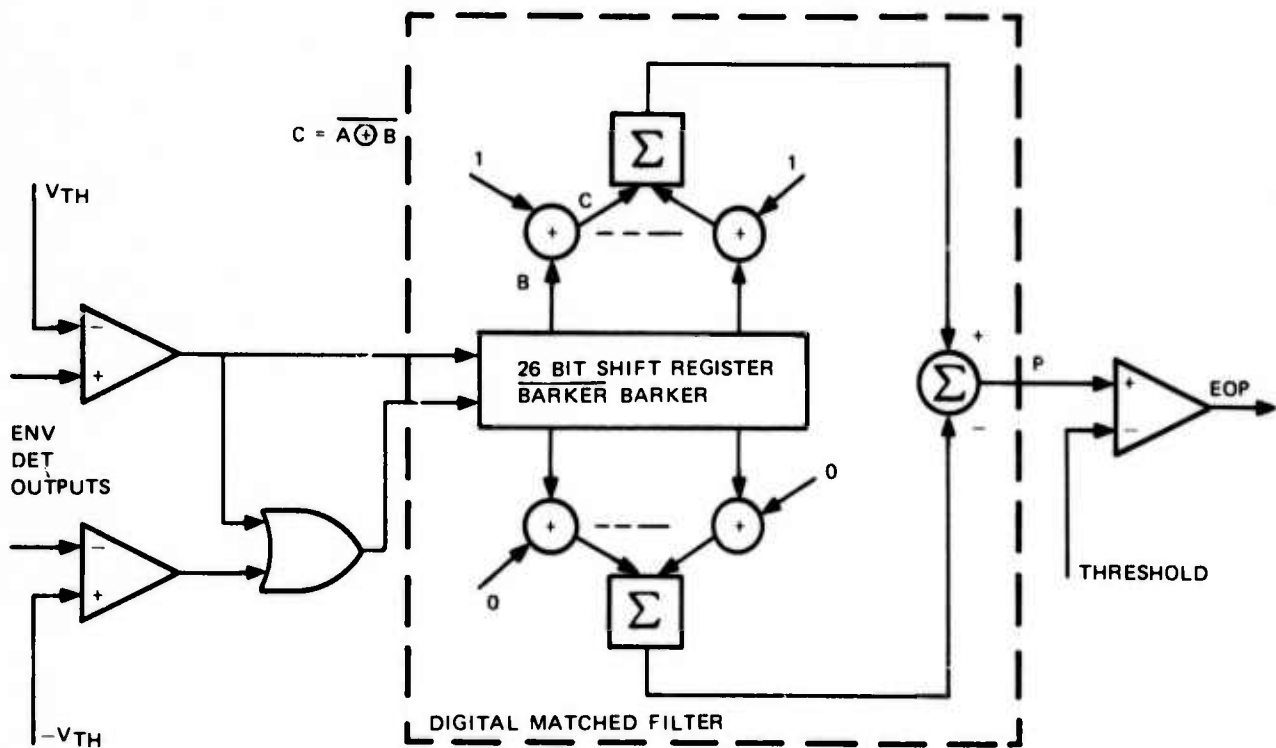


Figure 2-38. Digital/Analog Implementation of Preamble Filter.

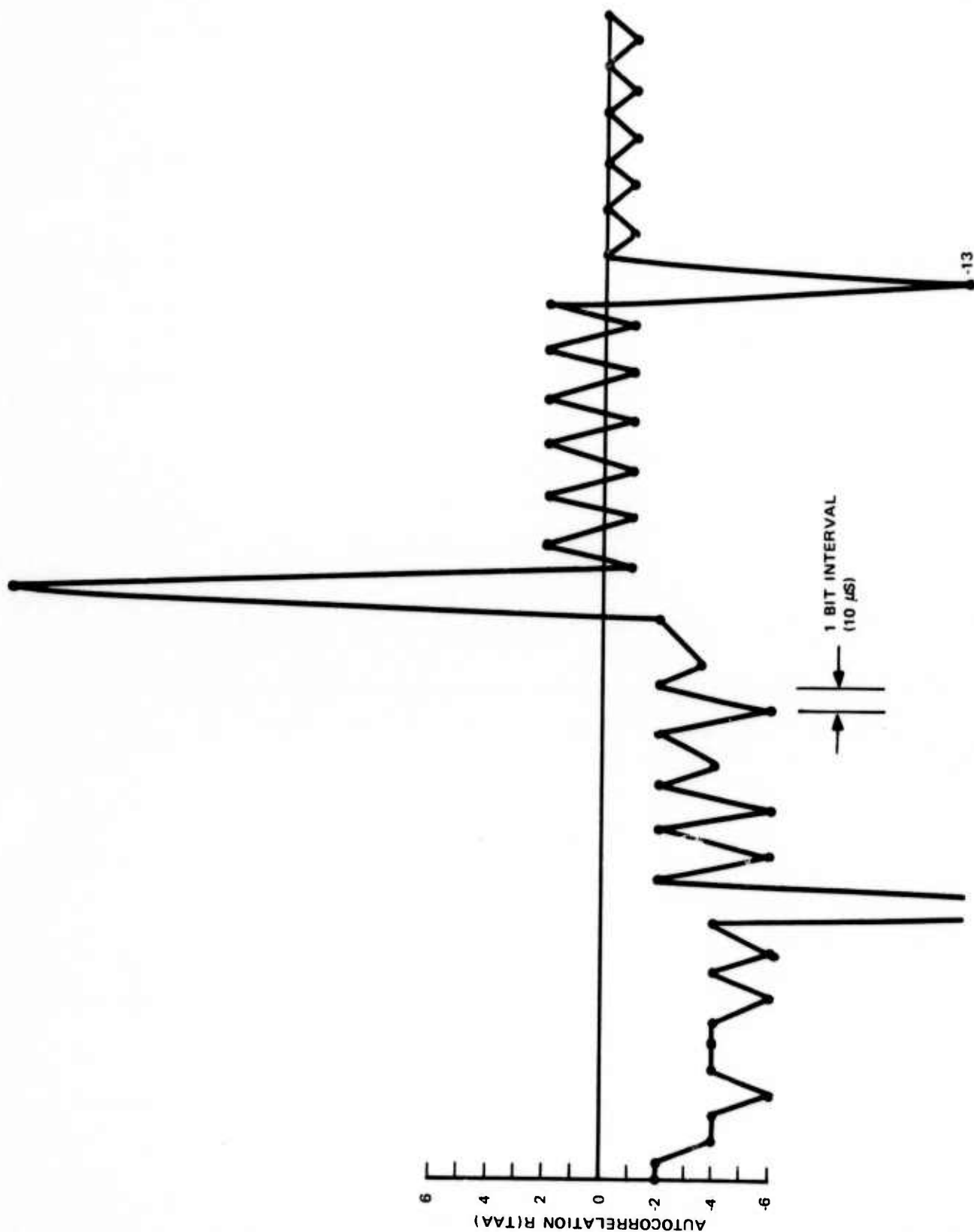


Figure 2-39. Autocorrelation Output at Point for 1's and 13-Bit Barker Followed by 13-Bit Inverter Barker.

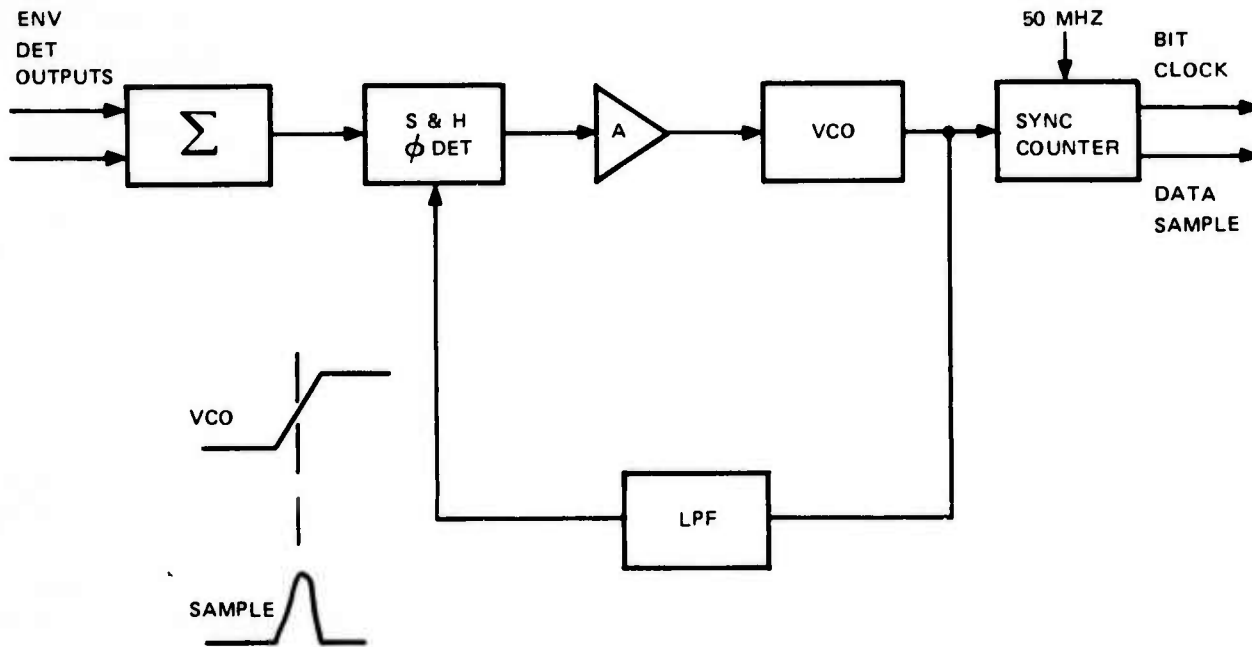


Figure 2-40. Functional Diagram of Bit Sync Loop.

continuously improved bit timing estimate during the preamble enables a continuous improvement in the performance of the detected preamble bits.

- e. **Alternate Bit Timing Recovery Approach.** Another way of acquiring bit synchronization that can be applied to any of the above preamble approaches is by using a conventional analog phase-lock loop. A VCO is phase-locked to the incoming envelope-detected correlation peaks that occur at the bit rate. The correlation pulses sample the phase of the local 100-kHz reference and hold the sample value. This sample value is filtered and the output is the control voltage for the VCO. After the VCO is locked to the correlation peaks, its timing is transferred to a counter derived from a stable clock. A method of implementing this technique is shown in figure 2-40.

For this phase-lock loop, Hoffman's* analysis for transient response is shown in table 2-2. A loop bandwidth (ω_n) of $2\pi 16$ kHz is assumed for a phase-lock loop with 100-kHz reference frequency. This assumes agc has been set and no noise is present.

For noise, no analysis is available to calculate transient time. For signal-to-noise 10 dB, doubling the number of bits required seems appropriate, i.e., up to 22 bits might be required. AGC is assumed before phase locking. Of course, the phase-locking acquisition can occur before agc is finally settled out.

*F. M. Gardner, Phase-Lock Techniques, p. 34.

Table 2-2. Hoffman's Analysis for Transient Response.

PHASE ERROR	FREQUENCY LOCK TIME ($\omega_n t$)	PHASE TRANSIENT TIME $\Delta = \omega_n t, \zeta = 1$ ($\omega_n t$) ⁿ	TOTAL ($\omega_n t$)	BITS REQUIRED, NO NOISE $\omega_n = 2\pi 16 \text{ kHz}$
10 ns \rightarrow 0.36°	2	8.5	10.5	11
28 ns \rightarrow 1°	2	7	9	9
100 ns \rightarrow 3.6°	2	5.5	7.5	8

For ideal sampling with timing offset for maximum likelihood detection, 10 ns of phase error corresponds to 0.4-dB degradation point; and 100 ns corresponds to $2T_C$ windows peak and store detection worst case where 0.5-dB degradation is seen. A 10-ns phase error requirement also places a stringent requirement on dc phase drift of the phase detector and counter circuits used. Strobing a counter with 10-ns increments requires clocks and counters operating in excess of 100 MHz.

Requirements on timing of 10 ns are possible, but difficult, either with phase locking or with SAWD's matched for preamble timing and detection. Therefore, if this approach is to be used, the window detecting method should be used.

2.2.2.4 Comparison of Preamble Approaches

Table 2-3 contains parameters that are important for deciding which preamble approach is most desirable for the ARPA packet radio network. The four preamble approaches are compared on the basis of performance and equipment complexity. Based on the probability design goals, the length of the preamble is different for each approach operating in the same signal-to-noise environment. The best performance is denoted by 1 and the poorest performance by 4. One should be cautioned that there may be other system factors that were not considered in this paper that may influence the selection of the length of the preamble.

Several approaches are possible for deriving bit timing. One approach uses a bit timing loop as previously discussed. Another uses a time-of-arrival estimator. The objective is to estimate the time of occurrence of the correlation peak. Potentially, the bit timing loop yields superior tracking performance. Both techniques can be applied to any of the preamble approaches discussed above; however, the longer preambles have the advantage of yielding more accurate bit timing estimates. On the basis of these arguments, the M out of N preamble technique can yield the best bit timing accuracy at the end of the preamble.

Multipath rejection is related to the width of the autocorrelation pulse and the sidelobe energy. Since the autocorrelation pulse width is identical in all approaches, only the sidelobes are of concern in this analysis. The sidelobe energy is greatest for the repeat preamble technique. The peak-to-sidelobe ratio is larger for the M out of N preamble detector than it is for the two coherent 7-bit Barker preamble approaches. Therefore, the multipath rejection is greater for the M out of N technique.

2.3 ANALYSIS TOOLS FOR SIGNAL PROCESSING

Several computer programs have been developed as analysis tools in the areas of signal design and processing. The general emphasis in developing these programs has been toward spread spectrum techniques, although some of the results may also be valid in the performance of the unspread waveforms.

Code selection is an important subject in the area of signal design. Although several different types of codes have been considered and their properties investigated, the maximal length codes are relatively simple to generate. Some of the maximal length codes up to 63-chip length can be found in the literature. However, anticipating a need to generate longer length codes, a program (CODCOR) has been developed to generate all possible lengths of maximal length codes. Another program (COREL) has been developed to study the autocorrelation and the crosscorrelation properties of the codes. COREL is a general program and not limited to correlating only the maximal length codes.

Another program (AUTCOR) has been developed to aid the signal processing analysis. This program utilizes a fast Fourier transform subroutine. Through the use of this program, a deterministic signal can be correlated in an analog manner with the impulse response of a matched filter, thus providing a tool to determine a matched filter response to deterministic inputs. The program, with reasonable manipulations, is valuable in analyzing the performance of both spread and unspread systems when the signal is subjected to some deterministic interference and also is corrupted by bandpass amplitude and phase distortions through filters, antenna resonances, echos from mismatched transmission lines, etc.

2.3.1 Description of CODCOR and COREL (Refer to appendix 2C for listing.)

The main program, CODCOR, generates any desired length maximal length code. The code is printed out based on the following inputs:

- a. Total number of shift register stages (7-stage shift register generator generates a $2^7 - 1 = 127$ -chip length code).
- b. Total number of taps (feedback shift registers) and their sequence numbers.
- c. Initial 1 or 0 setting of each register stage (influences the code starting point of a specific sequence).

The subroutine, COREL, computes the correlation between $CP(M)$ and $C(N)$, where $CP(M)$ consists of M number of 1's and 0's corresponding to the signal, and $C(N)$ consists of N number of 1's and 0's corresponding to the code.* The program is written for $M = 2N$, so that $CP(M)$ may consist of a specific code sequence following or preceding another code sequence (or the same code sequence for autocorrelation). The resultant correlation of $CP(M)$ with $C(N)$, denoted by $KR(J)$, consisting of $J = (M + N)$ number of integers is printed out.

The application of the above programs will become clear by means of an example, presented in the following sections, for selecting the 127-chip length code.

*It is assumed that 1's and 0's of the signal and 1's and 0's of the correlator represent identical waveforms.

2.3.2 Selection of the 127-Chip Length Code

For a 127-chip length code, irreducible polynomials are needed of degree 7. The irreducible polynomials of degree 7 are the following (in octal form):

211; 217; 235; 367, 277, 325, 203; 313; 345.

Each digit in the above octal formulation represents three binary digits. The binary digits, then, are the coefficients of the polynomials, with the high-order coefficients at the left. For example, 211's binary equivalent is 010001001, and the corresponding polynomial is $X^7 + X^3 + 1$. The reciprocal polynomial, $1 + X^4 + X^7$, is also irreducible. Hence, the feedback shift register taps are either 3, 7 or 4, 7. All of the other tap combinations appear in table 2-4. As an example, the binary shift register generator to generate a maximal length sequence corresponding to the polynomial $X^7 + X^4 + 1$ is shown in figure 2-41. An example of $X^7 + X^3 + X^2 + 1$ is also shown.

Based on the 18 possible tap combinations, 18 different 127-chip maximal length codes can be generated using the program described above. One of these codes corresponding to feedback taps 7, 3, 2, 1 along with its autocorrelation is listed in table 2-4. It will be noticed that the autocorrelation has three distinct sections: the first section corresponds to the correlation as a result of the coded signal propagating across the decoder with nothing preceding the coded signal; the second section represents the autocorrelation of the second coded bit preceded by the similarly coded first bit; and the third section is, of course, a mirror image of the first section when nothing follows the second bit. The program computes the mean and variance of the absolute value of correlation integers comprising each of the three sections of correlated output.

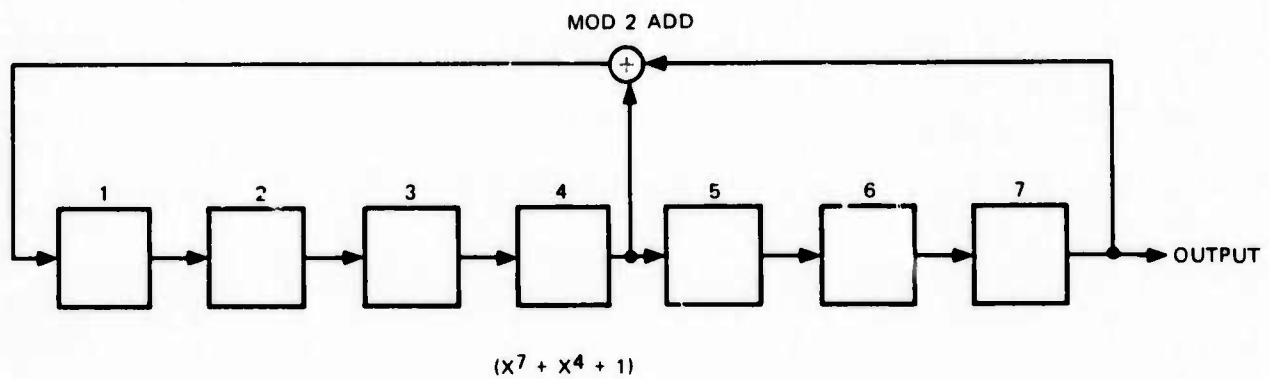
In order to optimize the peak-to-sidelobe level, table 2-5 summarizes the mean and variance of the sidelobes as applicable to the specific starting point of each code sequence (with all initial shift register settings of 1 in each case). As a result, the code generated by 7, 3, 2, 1 taps has the best minimum mean and variance combination. This is the code that has been implemented on the test set surface acoustic wave device.

2.3.3 Description of the Computer Program AUTCOR (Refer to appendix 2C for listing.)

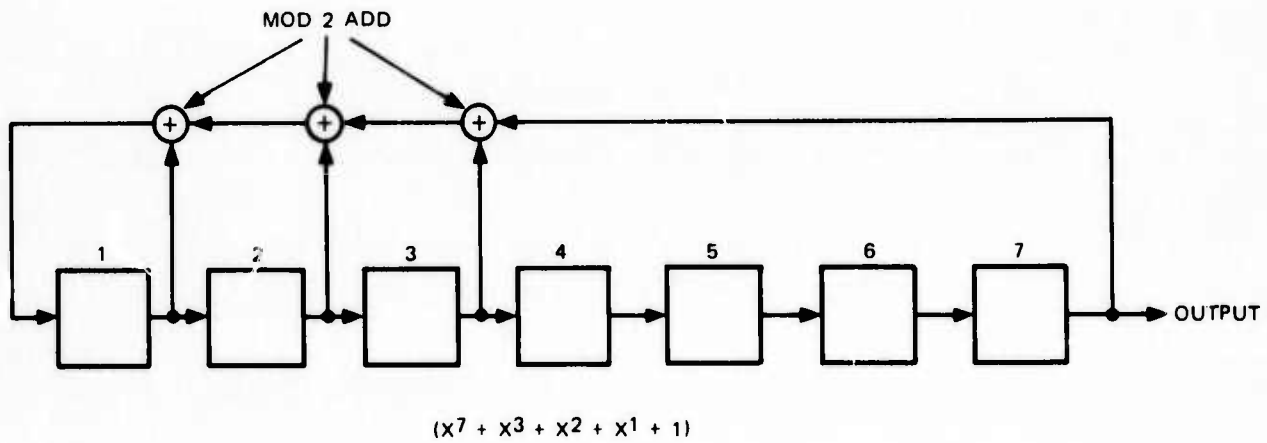
The present structure of the computer program AUTCOR is best understood by referring to figure 2-42. The biphase modulated input signal is formulated based on reading a specific length code sequence (up to 127 chips length). This sequence forms the basis of the impulse response of the matched filter, as well as the basis of the 2-bit long (both bits identical) input signal. The program is normalized for a carrier frequency of 7 Hz and a chip rate of 1 Hz. This allows seven carrier cycles (of sinewaves) for each chip interval, and may be altered if desired.

As shown in figure 2-42, the input signal may be filtered or added with a disturbance before correlating it with the matched SAWD. The various combinations of the available options are obvious from the figure. The label "channel filters" refers to any filter(s) encountered by the input signal at the transmit or the receive (or both) ends. In the present structure of the program, the channel filters consist of a normalized 2.55 Hz wide* 2-pole Chebyshev transmit filter, and a normalized 2.55 Hz wide, 3-pole Chebyshev receive filter. An additional filter shown in the figure is a normalized 2.5 Hz wide, 3-pole Butterworth filter. These filters can, of course, be changed by defining a new transfer function. Only the low-pass equivalent transfer functions of the filters need to be defined, as the program automatically converts to the normalized bandpass transfer function.

*3-dB bandwidth.



A SHIFT REGISTER GENERATOR FOR A
127 MAXIMUM LENGTH SEQUENCE (TAPS: 7, 4)



A SHIFT REGISTER GENERATOR FOR A
127 MAXIMUM LENGTH SEQUENCE (TAPS: 7, 3, 2, 1)

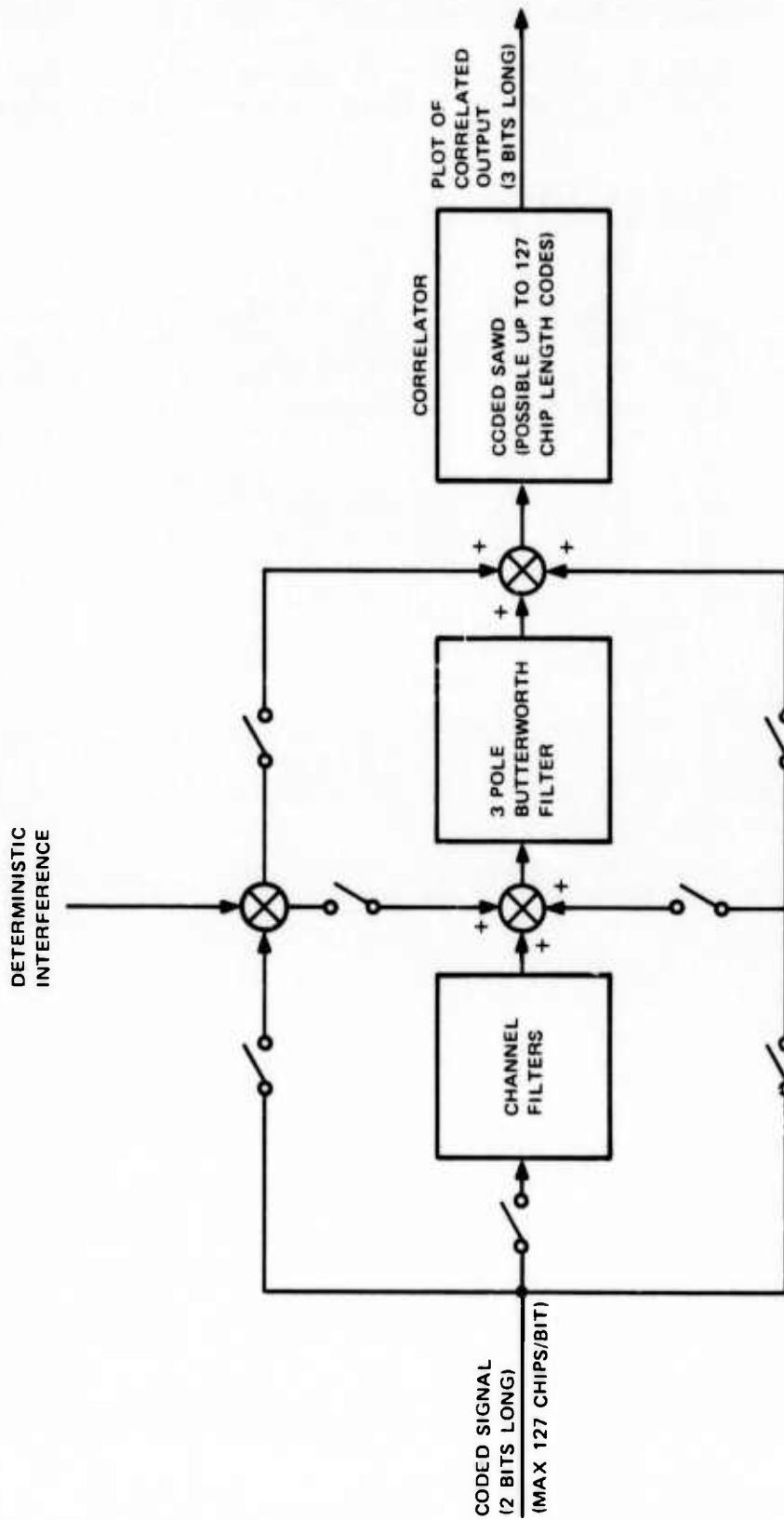
NOTE: CODE STARTING SEQUENCE DEPENDS ON INITIAL STATES OF SHIFT REGISTERS

Figure 2-41. Binary Shift Register Generator.

Table 2-5. Mean and Variance of the 18 Maximal Length Codes.

TAPS	MEAN	VAR
7, 3	4.01	8.47
7, 4	3.69	9.61
7, 3, 2, 1	3.33	4.93
7, 6, 5, 4	3.74	7.38
7, 4, 3, 2	4.25	7.90
7, 5, 4, 3	3.67	5.28
7, 6, 5, 4, 2, 1	4.02	7.17
7, 6, 5, 3, 2, 1	3.66	7.59
7, 5, 4, 3, 2, 1	3.71	8.26
7, 6, 5, 4, 3, 2	3.52	8.33
7, 6, 4, 2	3.40	8.59
7, 5, 3, 1	3.74	8.40
7, 1	3.75	4.98
7, 6	3.17	10.28
7, 6, 3, 1	4.13	9.50
7, 6, 4, 1	3.79	9.88
7, 6, 5, 2	3.66	7.53
7, 5, 2, 1	3.58	8.96

The program automatically chooses the required number of samples for the FFT subroutine based on the code length and the carrier frequency. The processing time to compute one Fourier transform, or the inverse Fourier transform, based on a certain number of samples N is directly proportional to $N \log_2 N$. In order to conserve the overall processing time, as well as the main core storage of a typical modern computer, each bit period of the correlating signals is divided into four sections, each section is sequentially correlated with its appropriate counterparts, and the sectionalized results are finally summed using what is usually referred to as the overlap-add technique. The program results into CALCOMP plots of the correlated output in the form of a continuous waveform.



NOTE: THE PROGRAM IS NORMALIZED FOR A CARRIER FREQUENCY OF 7 HZ AND CHIP RATE OF 1 HZ. PROGRAM REQUIRES ONLY THE LOW-PASS TRANSFER FUNCTION OF FILTERS WHICH IS AUTOMATICALLY CONVERTED TO THE NORMALIZED BANDPASS TRANSFER FUNCTION.

Figure 2-42. AUTOCOR Computer Program Structure.

modulation and detection

2.3.4 Filtering Effect on Correlators Performance

Figure 2-43 shows the autocorrelation property of the 7, 3, 2, 1 tap code (127-chip length) without any filtering. The signal with the same code is then processed through the following filters in cascade:

- (i) 2-pole Chebyshev 2.05 Hz wide filter
- (ii) 3-pole Chebyshev 2.55 Hz wide filter
- (iii) 3-pole Butterworth 2.5 Hz wide filter

Figure 2-44 depicts the impact of filtering on the matched filter response. The autocorrelation peak-to-maximum-sidelobe ratio reduces from 127 to 3 (24 dB) to that of 78 to 8 (19 dB). This indicates that the transmit and receive filtering in the test system may be reducing the processing gain of the spread signal matched filter.

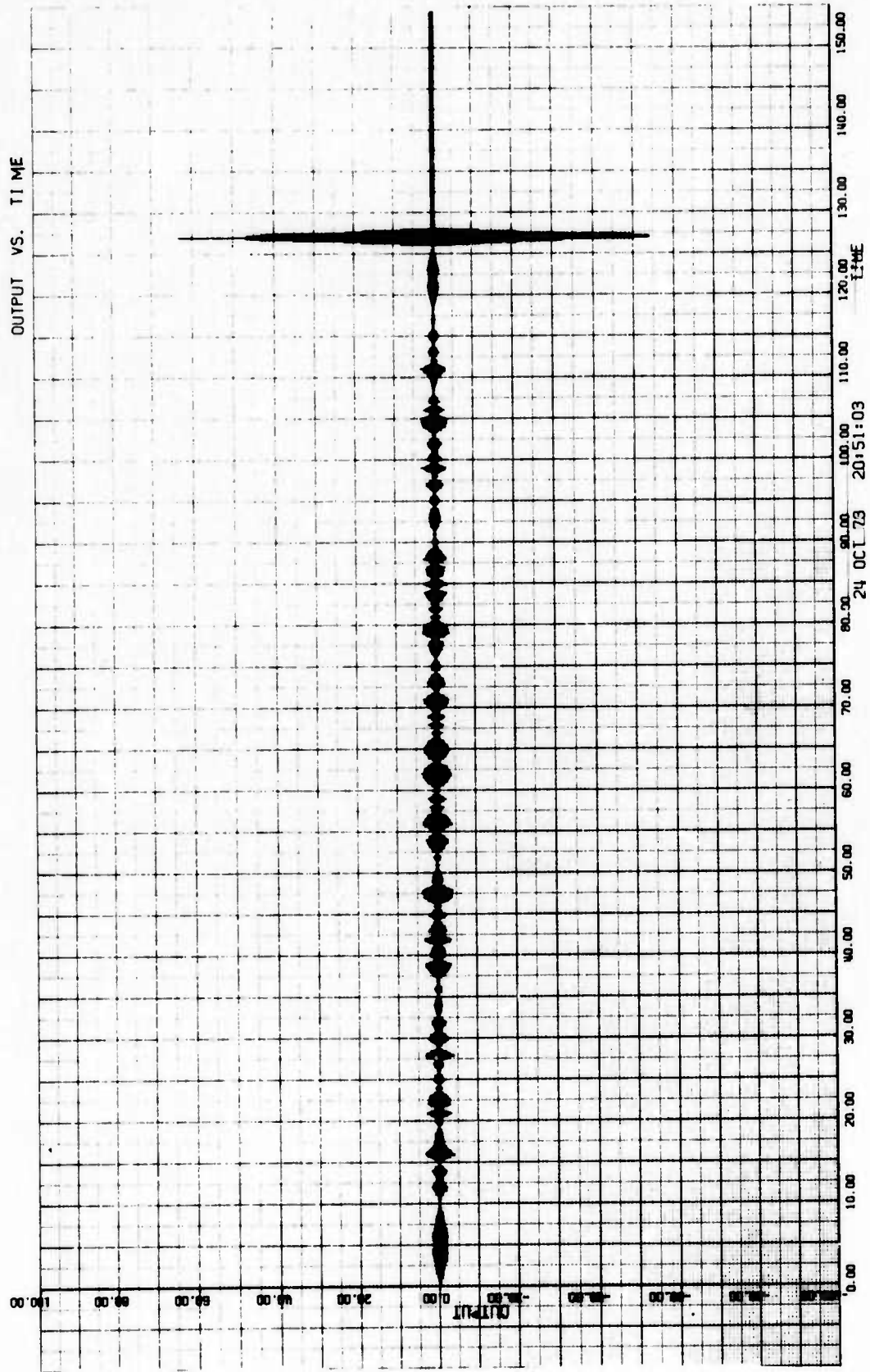


Figure 2-43. Autocorrelation Property of 7, 3, 2, 1 Tap Code.

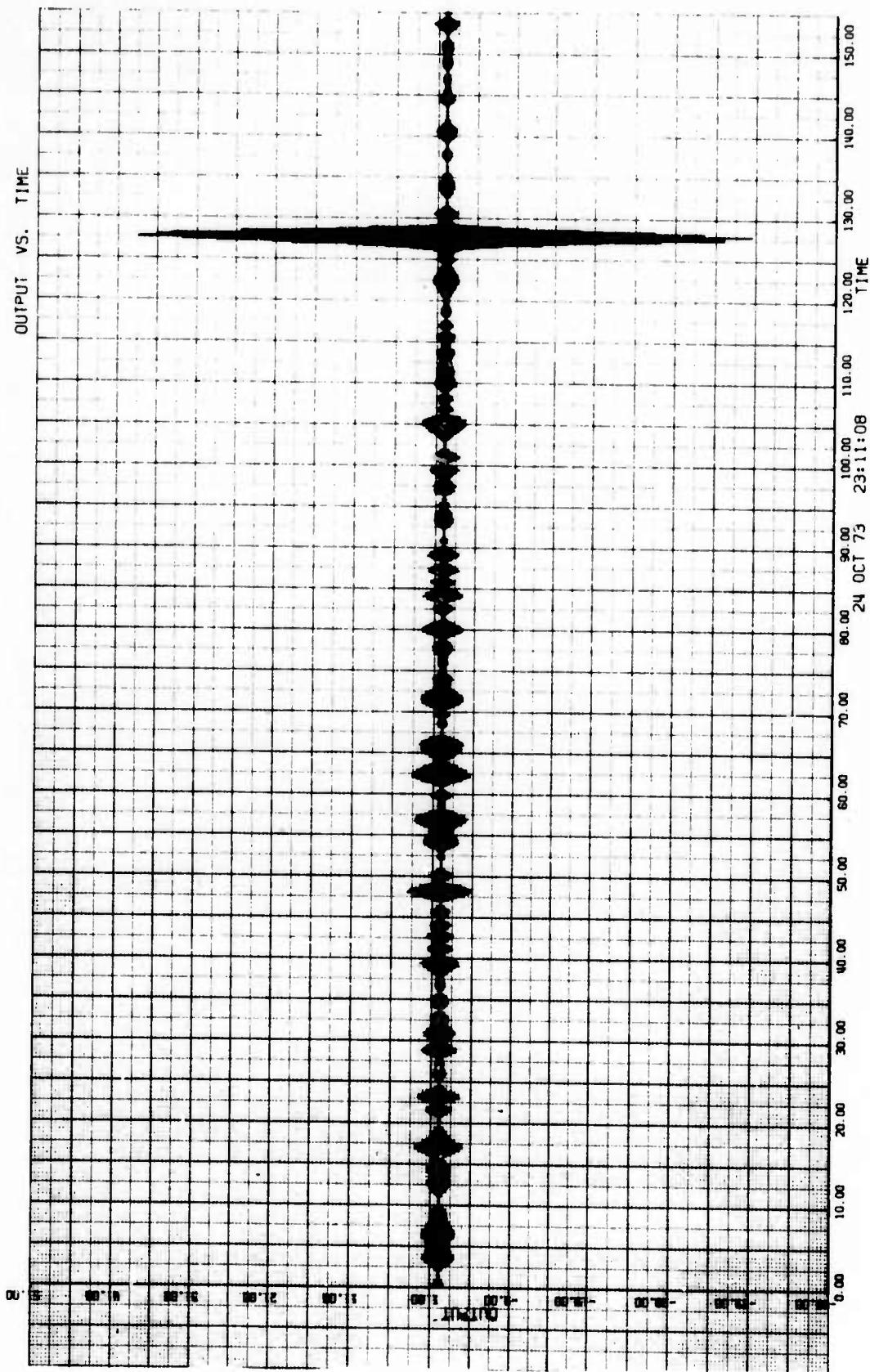


Figure 2-44. Matched Filter Response of a 127-Chip Coded Filtered Signal.

BIBLIOGRAPHY

E. A. Gerber, "State-of-the-Art - Quartz Crystal Units and Oscillators," Proc IEEE, February 1966, pp 103-115.

F. Wolf and G. Bistlino, "Quartz Crystal Life Test Data," McCoy Electronics Company, December 1966.

1972 Product Line Data, Bliley Electric Company.

E. A. Gerber and R. A. Sykes, "State-of-the-Art - Quartz Crystal Units and Oscillators," Proceedings of the IEEE, Vol. 54, No. 2, February 1966, pp 103-115.

D. T. Bell, J. D. Holmes, R. V. Ridings, "Application of Acoustic Wave Technology to Spread Spectrum Communications," Texas Instruments Technical Report, 29 November 1972; and IEEE Transactions on Microwave Theory and Techniques, Volume MTT-21, No. 4, April 1973.

W.W. Peterson, "Error Correcting Codes," The M.I. T. Press, Massachusetts Institute of Technology, Cambridge, Massachusetts, 1961.

B. Gold and C.M. Rader, "Digital Processing of Signals," McGraw-Hill Book Company, 1969.

Crystal Oscillator Stability

When defining the requirements for a crystal oscillator, the factors that must be specified are the short-term, long-term, and temperature stability rates. The short-term stability is generally a function of the drive level with greater drive giving better short-term stability, but poorer long-term stability. The long-term stability is basically a function of the cleanliness of the manufacturing process with the limiting factor being that greater cleanliness is more costly. High-stability crystals must be manufactured in cleanrooms with purity to the molecular level. In ordering a crystal oscillator, the exact parameters must be specified (for example: 1 pp 10^{10} in a period of 10 ms, 1 pp 10^8 per day and 5 pp 10^7 over a specific temperature range). For long-term stability, the per day measure is generally the standard for the industry. The frequency for maximum stability is 5 MHz. Designing to this frequency results in a crystal of optimum physical dimensions for achieving the best stability.

The specification for long-term stability such as 1 pp 10^8 per day defines the steady-state value following an initial stabilization period. This is as shown in figure 2A-1.

The length of the transient period is basically a function of the cleanliness of the crystal; therefore, the crystals with the more stringent long-term stability rates have shorter transient times. These transient times can vary from a few hours to a month. Drift rates

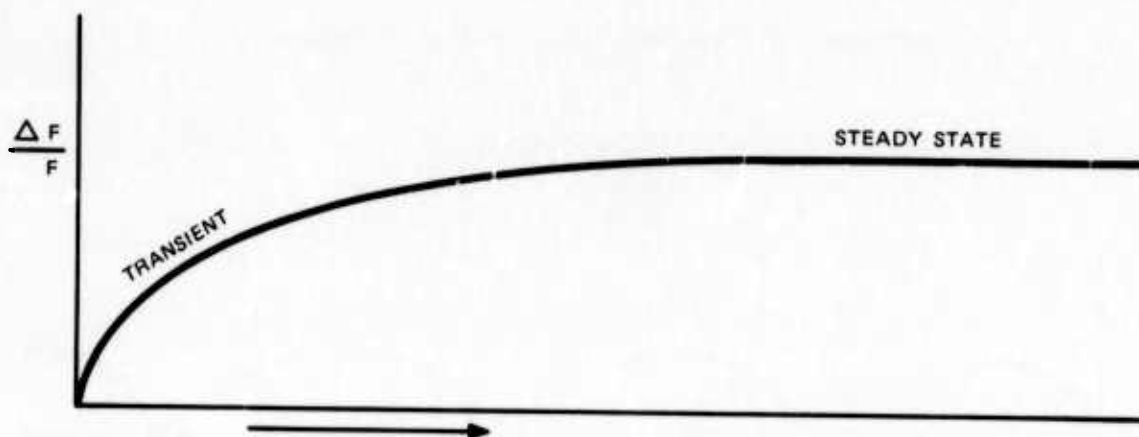


Figure 2A-1. Steady-State Value Following an Initial Stabilization Period.

crystal oscillator stability

generally are not defined for the transient period. The crystal will follow the transient curve each time it is turned on, and it does not necessarily restart at the initial frequency. Two possibilities of operation are shown in figures 2A-2 and 2A-3.

If a crystal oscillator has only a minimum margin in long-term stability, a drift problem could arise over a long period. Most crystals age in the positive direction.

For the packet radio system, the stability requirement could be primarily a short-term matter. A $1 \text{ pp } 10^8$ per day drift rate can be readily achieved and, with this, the hand-held unit could maintain a frequency rate very close to that of the repeater. The daily drift rate can be specified to the point that the long-term stability factor can be made small as compared to the drift due to temperature change. A reasonable value for frequency stability as a function of temperature change over a range of -40 to $+75^\circ\text{C}$ with temperature-compensation circuitry is $5 \text{ pp } 10^7$. A short-term stability over a period of 10 ms of a few parts in 10^{10} is possible with current technology. All of these figures pertain to crystals, operating near 5 MHz, which are reasonably priced production devices. Any of these specifications could probably be improved by one or two orders of magnitude but with an increase in cost.

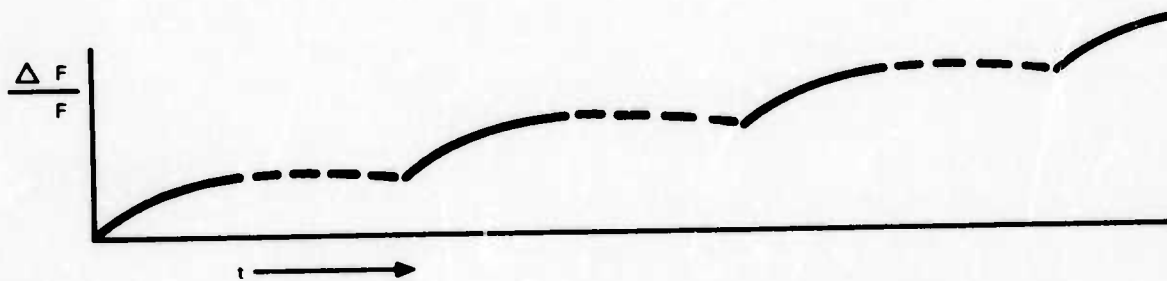


Figure 2A-2. Possibility of Operation, Example 1.

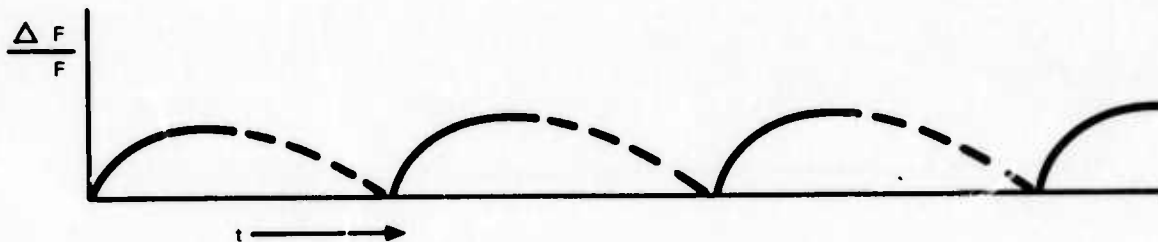


Figure 2A-3. Possibility of Operation, Example 2.

The aging history of two types of crystals over a 5000-hour period is shown in figure 2A-4. The upper curves show the aging data for a sample of 4.7755-MHz fundamental mode crystals. The lower curves show the aging data for a sample of 108.933-MHz fifth overtone crystals.

In the design of packet radio systems, the stability of both the clock and the rf carrier are important considerations.

The stability required of the rf carrier can also be a very important consideration in the design of packet radio systems because frequency uncertainty increases the time required to acquire the signal and/or affects the efficiency of the detection process. The rf stability requirements of the various detection techniques can be a significant factor affecting the choice of modulation technique. This subject was discussed previously, particularly with regard to stability required for efficient detection using surface acoustic wave correlators.

When microwave sources are to be crystal-controlled, it is convenient to operate the crystal reference oscillator at as high a frequency as possible. Fifty overtone crystal oscillators operating at a frequency near 100 MHz are typical. A typical source will employ a crystal oscillator at a suitable frequency in the region of 100 MHz, which produces a spectrum of harmonics. A cavity oscillator in the frequency range of 1 to 2 GHz is then locked to the appropriate crystal oscillator harmonic using conventional phase-lock loop techniques. Further multiplication using varactor multipliers then may be employed to achieve the desired output frequency.

Such microwave sources are not limited to use of high frequency overtone crystals; but their use does simplify considerably the frequency reference, since it minimizes the amount of frequency multiplication required and reduces the possibility of false lock on an undesired harmonic. Oscillators operating near 100 MHz may have 1 to 2 orders of magnitude poorer stability than the best crystals operating at a frequency near 5 MHz.

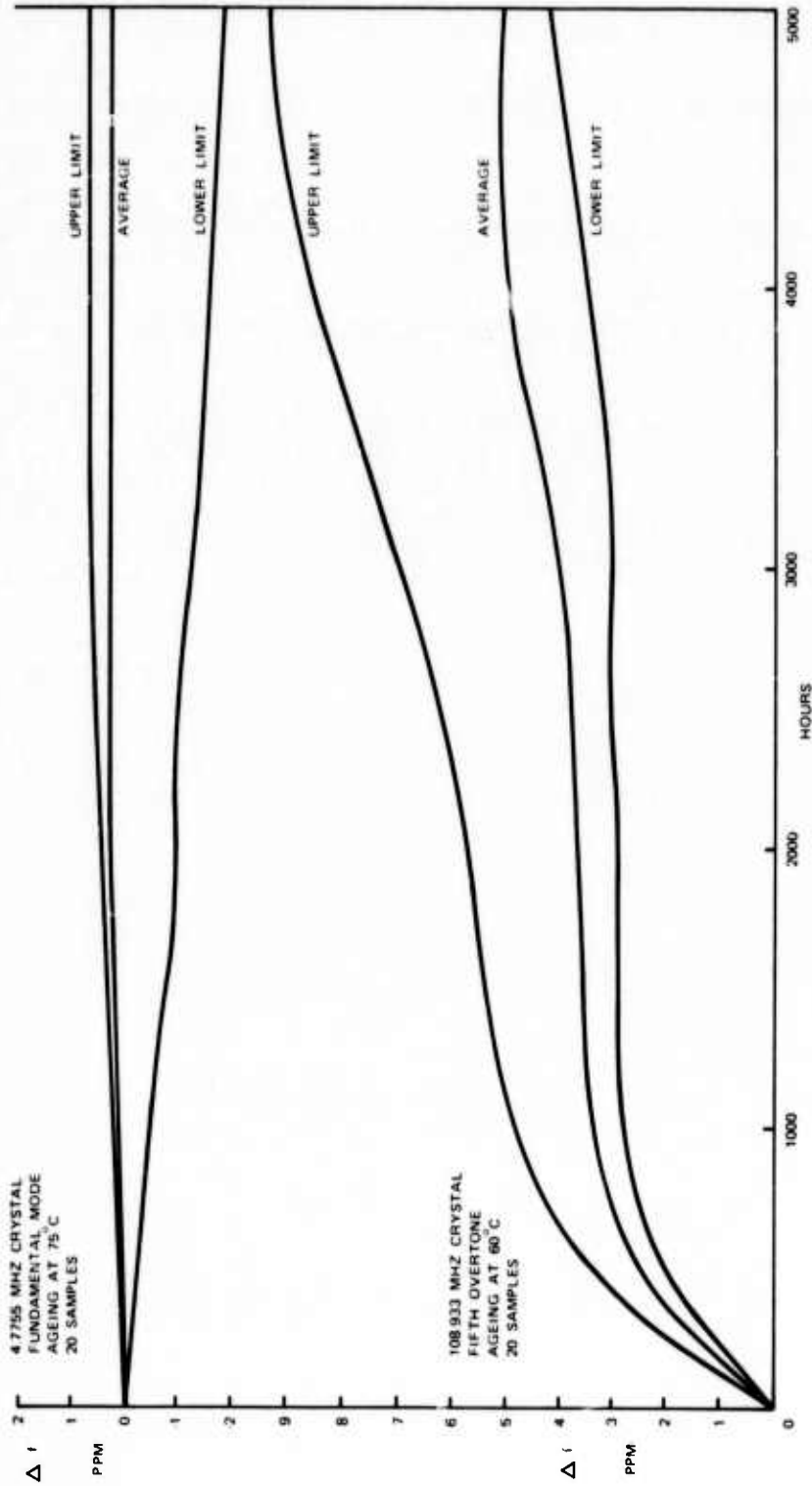


Figure 2A-4. Crystal Aging History.

Probability of Detection for Coherent Combining of Bits

This appendix gives a summary of the analysis used to derive the detection probabilities of figure 2-28. For a perfect envelope detector, the probability of detection is:

$$P_D = Q \left(\sqrt{\frac{2P_S}{\sigma^2}} \cdot \frac{T}{\sigma} \right)$$

which is the Marcum Q function where P_S is the power in the carrier sinewave at the detector input, T is the bit length and σ^2 is the noise power. The derivation of this is shown in paragraph B.1. The improvement in signal-to-noise ratio when n pulses are integrated with ideal predetection integration is n times the signal-to-noise ratio of that for a single pulse. Therefore, $10 \log n$ less signal-to-noise ratio is required in dB for n pulses combined coherently before detection.

B.1 DERIVATION OF PD FOR COHERENT COMBINING OF BITS

A model of the preamble detection circuitry is shown in figure 2B-1. The local code is crosscorrelated with the incoming signal in a SAWD. The SAWD performs the functions of a modulator and an integrator. The effective bandwidth of the SAWD is $B = 1/T_B$, where T_B is the integration time. The incoming signal itself was spread to a bandwidth $W = 1/T_c$, where T_c is the code chip duration. After the integration for time $T = NT_B$, where N is the number of bits which are coherently added, the signal is envelope-detected and applied to a threshold device for a synchronization decision.

The time required to achieve bit synchronization (i.e., for the detected output to exceed the threshold) is a function of the signal-to-noise ratio, the desired detection probability (P_D), and the false alarm probability (P_{FA}). The probability densities of the noise and the signal plus noise required to calculate these probabilities depend upon N . For $N = 1$, the probability density functions (Pdf) at the envelope detector output are Rayleigh and Rician, respectively. For $N = 8$, the probability density functions can be approximated by Gaussian densities for both noise and signal plus noise.

Consider first the case for $N = 1$. If the detector is assumed to be a perfect envelope detector the pdf of the output noise in the absence of a signal (i.e., in the absence of sync) is Rayleigh. Hence, the probability of false alarm is:

$$P_{FA} = \int_T^{\infty} \frac{V}{\sigma^2} \exp \left(-\frac{V^2}{2\sigma^2} \right) dv \quad (1)$$

$$= e^{-T^2/2\sigma^2}$$

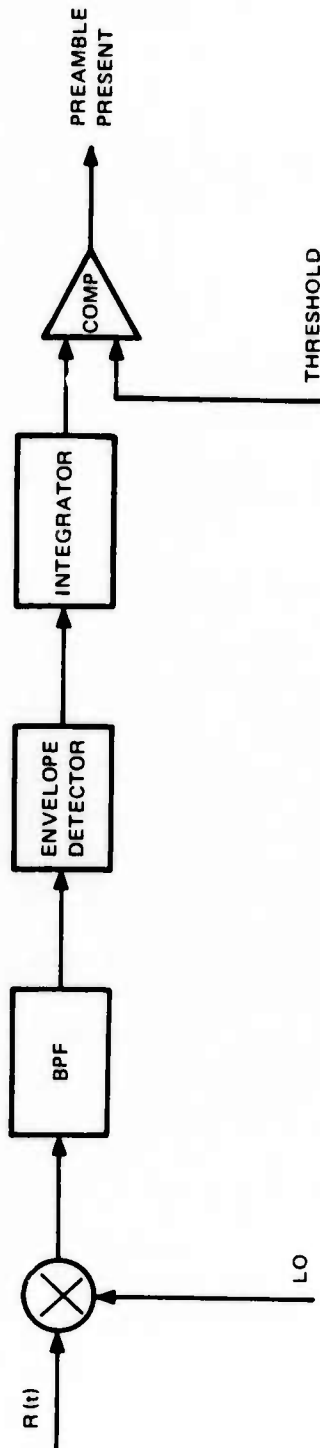


Figure 2B-1. Preamble Detection Model.

where

$$\begin{aligned} T &= \text{Threshold voltage} \\ \sigma^2 &= N_0 B = \text{Input noise power} \end{aligned}$$

and

$$\begin{aligned} P_{FA} = 10^{-6}, & \text{ we find that } T/\sigma = 5.26 \\ P_{FA} = 10^{-3}, & \text{ we find that } T/\sigma = 3.72 \end{aligned}$$

The pdf of the detector output when one is within the two chip synchronization window is Rician. Hence, the probability of detection is:

$$P_D = \int_{\frac{T}{\sigma}}^{\infty} \frac{V}{\sigma^2} \exp\left(\frac{V^2 + 2Ps}{-2\sigma^2}\right) I_0\left(\frac{V - 2Ps}{\sigma^2}\right) dv \quad (2)$$

where P_s is the power in the carrier sinewave at the detector input. This is the Marcum Q function.

$$P_D = Q\left(\sqrt{\frac{2Ps}{\sigma^2}} \cdot \frac{T}{\sigma}\right) \quad (3)$$

for $P_{FA} = 10^{-3}$ so that $T/\sigma = 3.72$, we find that $P_D = 0.999$, for $P_s/\sigma^2 = 22.5$

Hence, the predetection SNR is:

$$\text{SNR} = 13.5 \text{ dB}, P_{FA} = 10^{-3}, P_D = 0.999$$

For large BT products (i.e., for large N), we may use the central limit theorem to approximate the pdf as Gaussian, both in and out of synchronism. Consider first the out-of-sync case and assume the detector is a square law device. The envelope detector is considerably more difficult to handle analytically; however, the results are very similar. The expected value of the detector output signal is:

$$E\{n\} = 2BT N_0$$

and the variance is

$$E\{n^2\} = \sigma_r^2 = \frac{(2BT N_0)^2}{BT} = 4BT N_0^2$$

probability of detection for coherent combining of bits

The false alarm probability is therefore:

$$P_{FA} = 1/2 \left\{ 1 - \operatorname{erf} \left[\frac{T - E(n)}{\sqrt{2} \sigma_n} \right] \right\}$$

and for $P_{FA} = 10^{-3}$ we have

$$\frac{T - E(n)}{\sqrt{2} \sigma_n} = 2.19$$

If the codes are within sync (i.e., 2-chip window), the mean and variance of the detector output is:

$$E(V) = 2 BTN_o \left(1 + \frac{P_s}{BN_o} \right)$$

and

$$E(V^2) = \sigma_s^2 = (2BTN_o)^2 \left(\frac{1 + \frac{2P_s}{BN_o}}{BT} \right)$$

from which we get:

$$P_D = 1/2 \left\{ 1 + \operatorname{erf} \left[\frac{E(V) - T}{\sqrt{2} \sigma_s} \right] \right\}$$

and for $P_D = 0.999$ we have:

$$\frac{E(V) - T}{\sqrt{2} \sigma_s} = 2.19$$

Now we are interested in solving for $P_s/BN_o = \text{SNR}_i$ as a function of BT. We get:

$$BT = \left(\frac{3.1 + 3.1 \sqrt{1 + 2 \text{SNR}_i}}{\text{SNR}_i} \right)^2$$

From this expression we can plot the results as given in figure 2-29 for $P_{FA} = 10^{-3}$. A similar equation can be derived for different values of P_{FA} . The results are also plotted in figure 2-29 for $P_{FA} = 10^{-6}$.

B.2 DERIVATION OF P_D FOR M OUT OF N COMBINING

This is a summary of the analysis used to derive the preamble detection probabilities of figure 2-30. In this approach, a detection decision is made for each bit. To exceed the threshold for detecting a preamble requires M out of N bits being received correctly. If we assume that N 1's are transmitted, then M-N errors are allowed in the received sequence. Therefore, the probability of detecting the preamble is:

$$P_D = 1 - \sum_{i=1}^{M-N} \binom{N}{i} P_{eb}^i (1 - P_{eb})^{N-i}$$

where $\binom{N}{i}$ is $N! / i! (n-i)!$ and P_{eb} is the probability of a bit error. For a 7.4 dB SNR and the threshold set for a probability of a false alarm per bit ($P_{FA_b} = 0.3$ per bit), the probability of a bit error is 0.015. With an SNR = 6.5 dB and the same P_{FA_b} the probability of a bit error is 0.03. Without signal on the input, a false alarm occurs with the occurrence of M or more 1's. Therefore, the false alarm probability can be written as:

$$P_{FA} = \sum_{i=M-N}^N \binom{N}{i} P_{FA_b}^i (1 - P_{FA_b})^{N-i}$$

Utilizing these two equations, the results were plotted in figure 2-30 for $N = 26$ and various values of M.

Signal Processing Design Program Listings


```

00233 54*
00234 55*
00235 56*
00241 57*
00242 58*
00243 59*
00244 60*
00245 61*
00246 62*
00251 63*
00252 64*
00256 65*
00257 66*
00265 67*
00266 68*
00276 69*
00277 70*
00300 71*
00301 72*
00303 73*
00304 74*
00312 75*
00313 76*
00315 77*
00316 78*
00321 79*
00322 80*
00324 81*
00326 82*
00327 83*
00330 84*
00333 85*
00334 86*
00336 87*
00340 88*
00341 89*
00342 90*
00343 91*
00344 92*
00345 93*

```

```

C(I)=RETR(N)
14 CONTINUE
DO 16 I=1,NP
  THE TEST FOR EQUALITY BETWEEN NON-INTEGERS MAY NOT BE MEANINGFUL.
  IF(C(I).EQ.0.) GO TO 15
  CBAR(I)=0.
  GO TO 16
15 CBAR(I)=1.
16 CONTINUE
  JTT=JTT/2
  GO TO (1001,1002,1003),JTT
1001 WRITE(7,1005) JA,JB
1002 WRITE(7,1006) JA,JB,JC,JD
  GO TO 17
1003 WRITE(7,1007) JA,JB,JC,JD,JE,JF
  TAP NUMBERS ARE .215,///
1005 FORMAT(1H1,')
  TAP NUMBERS ARE .415,///
1006 FORMAT(1H1,')
  TAP NUMBERS ARE .615,///
1007 FORMAT(1H1,')
17 WRITE(7,1008)
  THE FOLLOWING IS THE COEF.,///
1008 FORMAT(1X,')
  C(I),I=1,NP)
20 FORMAT(20F6.0)
21 WRITE(7,21)
  LO 31 I=1,NP
  CP(I)=C(I)
31 CP(NP+I)=C(I)
  CC/C CORRELATION.,///
1009 FORMAT(1X,')
  CALL COREL
  LO 32 I=1,NP
  CP(I)=CRAM(I)
32 CP(NP+I)=C(I)
  CBAKC/C CORRELATION.,///
1010 FORMAT(1X,')
  CALL COREL
  GO TO 101
100 CONTINUE
STOP
END

```

```

000232
000240
000240
000240
000241
000242
000244
000247
000247
000252
000263
000271
000273
000303
000305
000320
000320
000320
000320
000324
000324
000344
000344
000356
000356
000357
000362
000367
000367
000371
000402
000403
000406
000413
000413
000415
000417
000417
000422

```

000017
 000017
 000017
 000034
 000041
 000041
 000044
 000047
 000051
 000051
 000056
 000056
 000056
 000074
 000074
 000074
 000077
 000077
 000102
 000105
 000107
 000107
 000114
 000114
 000114
 000125
 000125
 000130
 000145
 000152
 000152
 000155
 000160
 000162
 000162
 000167
 000167
 000167
 000200
 000204
 000220
 000220
 000225
 000225
 000230
 000233
 000236
 000241
 000244
 000245
 000270
 000270
 000275
 000306

```

1* SURROUTINE COREL
2* COMMON NP,C(200),CP(300),KR(400)
3* 101 DO 200 I=1,NP
4* SUM=0
5* DO 130 K=1,I
6* IF(C(K).EQ.CP(2*NP-I+K)) GO TO 110
7* SUM=SUM+1
8* GO TO 120
9* 110 CONTINUE
10* SUM=SUM+1
11* 120 CONTINUE
12* 130 CONTINUE
13* KR(I)=SUM
14* 200 CONTINUE
15* DO 300 I=1,NP
16* SUM=0
17* DO 230 K=1,NP
18* IF(C(K).EQ.CP(NP-I+K)) GO TO 210
19* SUM=SUM+1
20* GO TO 220
21* 210 CONTINUE
22* SUM=SUM+1
23* 220 CONTINUE
24* 230 CONTINUE
25* KR(NP+I)=SUM
26* 300 CONTINUE
27* NY=NP-1
28* DO 400 I=1,NY
29* SUM=0
30* DO 330 K=1,I
31* IF(CP(K).EQ.C(NP-I+K)) GO TO 310
32* SUM=SUM+1
33* GO TO 320
34* 310 CONTINUE
35* SUM=SUM+1
36* 320 CONTINUE
37* 330 CONTINUE
38* KR(3*NP-I)=SUM
39* 400 CONTINUE
40* NX=3*NP-1
41* WRITE(7,500) (KR(I),I=1,NX)
42* 500 FORMAT(20I6)
43* WRITE(7,501)
44* 501 FORMAT(1X,/)
45* NA=NP-1
46* NB=NP+1
47* NC=2*NP-1
48* ND=2*NP+1
49* NE=3*NP
50* SUMX=0.
51* DO 401 J=1,NA
52* SUMX=SUMX+IABS(KR(J))
53* 401 SUMY=SUMY+IABS(KR(J))**2
54* SUMA=SUMX
55*

```

```

00227 56*
00230 57*
00231 58*
00232 59*
00233 60*
00234 61*
00237 62*
00240 63*
00242 64*
00243 65*
00244 66*
00245 67*
00246 68*
00247 69*
00250 70*
00253 71*
00254 72*
00256 73*
00257 74*
00260 75*
00261 76*
00262 77*
00264 78*
00265 79*
00272 80*
00273 81*
00275 82*
00276 83*
00303 84*
00304 85*
00305 86*

```

```

XMA=SUMX/NA
XMSA=SUMY/NA
XVARA=XMSA-XMA**2
SUMX=0.
SUMY=0.
DO 402 J=NB*NC
SUMX=SUMX+IABS(KR(J))
SUMY=SUMY+IABS(KR(J))**2
402 SUMB=SUMX
XMR=SUMX/(NC-NR+1)
XMSH=SUMY/(NC-NB+1)
XVARB=XMSH-XMB**2
SUMX=0.
SUMY=0.
DO 403 J=ND*NE
SUMX=SUMX+IABS(KR(J))
SUMY=SUMY+IABS(KR(J))**2
403 SUMC=SUMX
XMC=SUMY/(NE-ND)
XMSC=SUMY/(NE-ND)
XVARC=XMSC-XMC**2
WRITE(7,504)
504 FORMAT(1X,, MEANI MEAN2 MEAN3)
505 FORMAT(3F10.2,/)
508 FORMAT(1X,, VARI VAR2 VAR3)
509 WRITE(7,509) XVARA,XVARB,XVARC
509 FORMAT(3F10.2,/)
RETURN
END

```

```

000307
000311
000313
000316
000317
000324
000324
000331
000342
000343
000345
000347
000352
000353
000360
000360
000365
000376
000377
000401
000403
000406
000413
000413
000423
000423
000430
000430
000440
000440
000475

```

AUTCOR LISTING

24 OCT 73 20:44:54. 41

W PING AUTCOR/AUTCOR
 UNIVAC 1100 FORKRA V CELL 220, 0023
 THIS COMPLETION WAS DONE ON 24 OCT 73 AT 20:44:54

MAIN PROGRAM

STORAGE USED (BLOCK, NAME, LENGTH)

0001 *CODE 001004
 0000 *DATA 022004
 0002 *BLANK 024000

EXTERNAL REFERENCES (BLOCK, NAME)

0000 CLOCK
 0004 AUTCOR
 0005 PLIOLB
 0000 PLOT
 0007 MRUS
 0010 MIU13
 0011 MIU25
 0012 MAPI3
 0013 NSIOPS

STORAGE ASSIGNMENT FOR VARIABLES (BLOCK, TYPE, RELATIVE LOCATION, NAME)

Block	Type	Relative Location	Name
0000	R	000204	11L
0001	R	000217	15L
0001	R	000732	180L
0001	R	000321	272G
0001	R	000427	336G
0001	R	000114	4L
0001	R	000655	4416
0001	R	000765	504G
0001	R	000001	A
0002	R	000203	CS
0000	R	022115	ESCL
0000	R	022122	FOLLOW
0002	I	024613	ICL
0000	I	022106	IPEPLT
0002	I	012606	M
0000	I	022100	MAILST
0000	I	022074	NCUST
0000	R	024616	PBDFAC
0000	R	022149	T
0002	R	024615	WCW
0000	R	022050	XTTL
0001	R	000207	12L
0001	R	000107	160G
0001	R	000746	190L
0001	R	000331	300G
0001	R	000447	345G
0001	R	000552	403G
0001	R	000675	450G
0001	R	000127	6L
0002	R	000002	B
0000	R	022140	DFCW
0000	R	022123	FACTOR
0000	R	022112	HCL
0002	I	024614	ICLS
0000	I	022144	IPWD
0000	I	022132	MA
0002	I	012605	N
0000	I	022074	NCUST
0000	R	022111	QCL
0000	R	022117	TESCL
0002	R	000602	WE
0002	R	000603	YI
0001	R	000212	13L
0001	R	000124	166G
0001	R	000154	204G
0001	R	000344	307G
0001	R	000467	354G
0001	R	000572	412G
0001	R	000715	457G
0001	R	000150	7L
0002	R	000004	C
0000	R	022143	DPWD
0000	R	022125	FC
0000	R	022102	I
0002	I	024617	IFIL
0000	I	022104	ISYM
0000	I	022134	MAB
0000	I	022136	NAA
0000	R	022130	PI
0000	R	022127	SAM
0000	R	022113	TOCL
0002	R	000603	XRV

```

00101 1* COMMON CHPT,A,B,P,C(127),CS(254),WC,WE,XRV(5122),N,M,DT,DUMMY,
00102 2* TIME(5122),ICL,ICLS
00103 3* 2*PNOFAC
00104 4* 2*IFIL
00105 5* DIMENSION XRA(9216),Y1(5122),
00106 6* INAME(20),XTTL(20),YTTL(20),NCUST(4),MAILST(2)
00107 7* EQUIVALENCE (XRV,Y1)
00108 8* DATA(NCUST(1),I=1,4)/4HMAN,4HT K,4H. J,4HAIN /
00109 9* DATA(MAILST(1),I=1,2)/4H124 /
00110 10* DATA(MAILST(1),I=1,3)/8*4H /
00111 11* DATA(NAME(1),I=1,13)/8*4H /
00112 12* DATA(NAME(1),I=14,20)/7*4H /
00113 13* DATA(ATT(1),I=1,20)/9*4H /
00114 14* DATA(YTTL(1),I=1,20)/9*4H /
00115 15* POINT=0.
00116 16* ISYMO
00117 17* IPAP=23
00118 18* IPGPT=0
00119 19* ISCALE=1
00120 20* ICL=127
00121 21* ICLS=254
00122 22* CLEICL=1.
00123 23* GCL=CCL/4.
00124 24* HCL=CCL/2.
00125 25* TELL=CCL*3./4.
00126 26* SCL=ICLS*1.
00127 27* OSCL=SCL/4.
00128 28* TESCL=SCL*3./8.
00129 29* READ(8,10)(C(J),J=1,ICL)
00130 30* CALL SLUCK
00131 31* 10 FORMAT(16F5.0)
00132 32* HEAD=1. INDICATES THAT THE HEADER CODE IS SAME TO WHICH THE
00133 33* SAND IS MATCHED
00134 34* FOLLOW=1. INDICATES THAT THE CODE FOLLOWING THE HEADER CODE IS
00135 35* SAME TO WHICH THE SAND IS MATCHED
00136 36* FACTOR=1. INDICATES THAT HEADER AND FOLLOW FUNC. ARE SAME
00137 37* HEAD=1.
00138 38* FOLLOW=1.
00139 39* FACTOR=1.
00140 40* *DIAGNOSTIC* THE TEST FOR EQUALITY BETWEEN NON-INTEGERS MAY NOT BE MEANINGFUL.
00141 41* IF(HEADER.EQ.1.) GO TO 4
00142 42* ICLP=ICL+1
00143 43* 3 READ(8,10)(CS(J),J=ICLP,ICLS)
00144 44* GO TO 6
00145 45* 4 DO 5 I=1,ICL
00146 46* 5 CS(ICL+1)=C(I)
00147 47* *DIAGNOSTIC* THE TEST FOR EQUALITY BETWEEN NON-INTEGERS MAY NOT BE MEANINGFUL.
00148 48* IF(FOLLOW.EQ.1.) GO TO 7
00149 49* 7 DO 8 I=1,ICL
00150 50* 8 CS(I)=C(I)
00151 51* 9 CONTINUE
00152 52* F=FFREW OF THE IMPULSE RESPONSE FUNCTION
00153 53* C F=FFREW OF THE EXCITATION FUNCTION
00154 54* C

```



```

00440 100*
00443 100*
00445 107*
00446 100*
00447 109*
00452 170*
00454 171*
00455 172*
00456 173*
00461 174*
00463 *JIANQO:11C*
00465 175*
00466 176*
00468 177*
00471 178*
00473 179*
00474 180*
00475 181*
00500 182*
00501 183*
00501 184*
00503 185*
00506 186*
00506 187*
00510 188*
00510 189*
00511 190*
00512 191*
00513 *DIAGNOSTIC*
00513 192*
00514 193*
00515 194*
00516 195*
00517 196*
00522 197*
00523 198*
00524 199*

DU 150 I=1,NA
XNA(MAA+I)=XNA(MAA+I)+XRV(I)
P=CSCL
CALL CONCOR
DU 160 I=1,NA
XNA(MAA+I)=XNA(MAA+I)+XRV(I)
P=TESL
CALL CONCOR
DU 170 I=1,NA
XNA(MAA+I)=XNA(MAA+I)+XRV(I)
P=TESL
CALL CONCOR
DU 185 I=1,MAD
XNA(MAA+I)=XNA(MAA+I)+XRA(I)
NEXT CARD IS TEMPORARY
C
190 CONTINUE
TU.
DU 300 I=1,MAD
XNA(MAA+I)=XNA(MAA+I)+XRA(I)
NEXT CARD IS TEMPORARY
C
400 XNV(I)=0.
THE ABOVE DO LOOP IS CREATED TO SET Y1(EGV. TO XRV) REG AS ZERO
CALL PLOT(TIME,XRA,MAB,I,NCUST,MAILST,NAME,XTTL,YTTL,
1POINT,ISYM,IPAP,IPGPT,ISCALE,Y1)
600 CONTINUE
GU TO 700
*DIAGNOSTIC* CONTINUL CAN NEVER REACH THE NEXT STATEMENT
FC=FC+DFCN
P=DFAC=PMUFAC+JPMW
700 CONTINUE
CALL CLOCK
2000 CONTINUE
CALL PLOT (12.,0.,999)
STOP
END

```

END OF UNIVAC 1100 FORTRAN V COMPILATION. 6 *DIAGNOSTIC* MESSAGE(S)

GN FNS,* PLTOLB,PLTOLB
UNIVAC 1100 FORTRAN V LEVEL 2206 0023
THIS COMPILATION WAS DONE ON 24 OCT 73 AT 20:44:57

END OF UNIVAC 1108 FORTRAN V COMPILATION.
PLTULB SYMBOLIC F
PLTULB CODE RELOCATABLE

24 OCT 73 20:44:57. 52
14 AUG 73 20:45:15 14 152 (DELETED)
14 AUG 73 20:45:15 1 36 1 (DELETED)
0 01500064 14 58
1 01504204 36 1
0 01504250 14 58

Q FMS CONCOR, CONCOR
SAYING 1800 FORTRAN V LEVEL 2206 0023
THIS COMPILATION WAS DONE ON 24 OCT 73 AT 20:44:58

SUBROUTINE CONCOR ENTRY POINT 001457

STORAGE USED (BLOCK, NAME, LENGTH)

0001 *CODE 001470
0000 *DATA 022533
0002 *BLANK 024620

EXTERNAL REFERENCES (BLOCK, NAME)

0003 CLOCK
0004 FFI
0005 SIN
0006 CDVS
0007 MERRJS

STORAGE ASSIGNMENT FOR VARIABLES (BLOCK, TYPE, RELATIVE LOCATION, NAME)

0001	001111	1010L	0001	001116	1020L	0001	001364	1040L	00010	1126	00042	1246		
0001	00047	1306	0001	000113	1426	0001	000234	1756	000376	2546	00567	2736		
0001	000631	3116	0001	001076	3306	0001	001140	3466	001351	3656	001372	3756		
0001	001434	4116	0001	000314	510L	0001	000320	520L	000324	530L	000330	540L		
0001	000336	800L	0001	000146	65L	0001	000176	70L	000213	71L	000213	75L		
0001	000354	960L	0001	000602	980L	0001	000607	990L	000001	A	000002	R		
0002	R 000004	C	0002	R 000000	CHIPT	0002	R 000203	CS	0000	R 020001	D	0000	R 022434	DF
0002	R 012607	DT	0002	R 012610	DUMMY	0000	R 010001	EI	0002	R 012611	ER	0000	R 022437	F
0000	R 022442	FACIAR	0000	R 022441	FBW	0000	R 000001	HI	0002	R 000604	HR	0000	I 022413	I
0000	I 022435	IA	0000	I 022436	IB	0002	I 024613	ICL	0002	I 024614	ICLS	0000	I 024617	IFIL
0000	I 022431	IFILM	0000	I 022432	IFILB	0000	I 022433	IFILC	0000	I 022505	INJPS	0000	I 022421	K
0000	I 022420	KA	0000	I 022422	KK	0000	I 022424	L	0000	I 022423	LA	0002	I 012606	M
0000	I 022417	MA	0000	I 022427	MR	0000	I 012605	N	0000	I 022425	NOISCM	0002	R 000003	P
0000	M 022426	PCHIP	0000	R 022412	PI	0002	R 024616	PWDFAC	0000	R 022440	RATIO	0000	C 022400	S
0000	R 022430	SCALL	0000	R 000000	SIGN	0000	C 022402	SL	0000	R 022414	T	0000	R 022002	TCHIP
0000	R 022419	TE	0000	C 022404	TFILA	0000	R 022445	TFILAI	0000	R 022444	TFILAR	0000	C 022406	TFILB
0000	R 022447	TFILDI	0000	R 022446	TFILDR	0000	C 022410	TFILC	0000	R 022451	TFILCI	0000	R 022450	TFILCR
0002	R 012611	TIME	0000	R 022415	TMAX	0002	R 000601	WC	0002	R 024615	MCW	0002	R 000602	WE
0000	R 022443	WS	0002	R 012610	XI	0002	R 000603	XR	0002	R 000603	XRV			

00101	1*	SUBROUTINE CONCOR
00103	2*	CUSMO, CHIPT, A, B, P, C(127), CS(254), WC, WE, XRV(5122), N, M, DT, CUMMY,
00103	3*	ITYPE(122), ICL, ICLS
00103	4*	ZPBL
00103	5*	ZPWFAC
00103	6*	ZPFI

```

00104      DIMENSION HR(4096),HI(4096),ER(4096),EI(4096),D(1025),
00105      IX(4096),XX(4096),TCHIP(254)
00106      COMPLEX SPSL,TFILA,TFILB,TFILC
00107      EQUIVALENCE (HR,XR(2)),(ER,TIME),(XR,XRV),(XI,XY)
00108      PA=3.1415926536
00109      CALL CLOCK
00110      LU 10 I=1,ICLS
00111      TCHIP(I)=I*CHIPT
00112      LET A AND H BE THE LOWER AND THE UPPER TIME LIMITS OF H FUNCTION
00113      T=A
00114      TMAX=(H-A)*2.*CHIPT
00115      NOTE P IS THE LOWER TIME LIMIT OF THE EXCITATION FUNCTION E
00116      TE=P
00117      DT=TMAX/N
00118      MA=N/4
00119      DU 90 I=1,MA
00120      HR(I)=0.
00121      DU 80 KA=1,ICL
00122      K=ICL+1-K
00123      KA=ICL+1-K
00124      IF(I,LF,TCHIP(K)) HR(I)=(-1.)*C(KK)*SIN(WC*I)
00125      HI(I)=0.
00126      WE HAVE DEFINED ABOVE THE IMPULSE RESPONSE OF THE SA#D
00127      NOTE WE ARE TAKING 2**M SAMPLES OF PERIOD TMAX
00128      ER(I)=0.
00129      -----
00130      DU 70 LA=1,ICLS
00131      LE=ICL+1-LA
00132      NUISC=0
00133      IF(NUISC*EG.1) GO TO 65
00134      IF(TE.LE.TCHIP(L)) ER(I)=CS(L)*SIN(WE*TE)
00135      GO TO 70
00136      FOLLOWING CARD FOR CW INTERFERENCE ONLY
00137      65 IF(TE.LE.TCHIP(L)) ER(I)=CS(L)*SIN(WE*TE)+SIN(WC*TE)
00138      70 CONTINUE
00139      -----
00140      GO TO 71
00141      CONTROL CAN NEVER REACH THE NEXT STATEMENT
00142      PCHIPE=DFAC*TCHIP(I)
00143      IF(TE.GT.PCHIP) GO TO 75
00144      ER(I)=1.
00145      CONTINUE
00146      71 CONTINUE
00147      75 CONTINUE
00148      -----
00149      EI(I)=0.
00150      TE=TE+.1
00151      CALL CLOCK
00152      MN=MA+1
00153      DU 93 I=MR,N
00154      HR(I)=0.
00155      HI(I)=0.
00156      ER(I)=0.
00157      EI(I)=0.
00158      93 CONTINUE
00159      LET US COMPUTE DFT OF H(T) AND E(T)
00160      C
00161
00162
00163
00164
00165
00166
00167
00168
00169
00170
00171
00172
00173
00174
00175
00176
00177
00178
00179
00180
00181
00182
00183
00184
00185
00186
00187
00188
00189
00190
00191
00192
00193
00194
00195
00196
00197
00198
00199
00200
00201
00202
00203

```

```

00205 95 SCALE=DT
00206 SIGN=-1.
00207 CALL FFT(MR*MI,M*D,SCALE,SION)
00210 CALL FFT(ER*EI,M*D,SCALE,SION)
00211 CALL CLOCK
-----
00212 IFILAR0
00213 IFILB=0
00214 IFILC=0
00215 IF(IFIL.EQ.0) 60 TO 600
00217 IF(IFIL.EQ.1) 60 TO 510
00221 IF(IFIL.EQ.2) 60 TO 520
00223 IF(IFIL.EQ.3) 60 TO 530
00225 IF(IFIL.EQ.4) 60 TO 540
00227 910 IFILAR=IFILAR+IFIL
00230 60 TO 600
00231 520 IFILB=IFILB+IFIL
00232 60 TO 600
00233 530 IFILC=IFILC+IFIL
00234 60 TO 600
00235 540 IFILA=1
00236 IFILB=2
00237 IFILC=3
00238 600 CONTINUE
00239 FOLLOWING ARE THE RATIOS OF W(308)/W(.05DB RIPPLE)
00240 RATIO =2.2685099 (2 POLE CHEB)
00241 RATIO =1.5120983 (3 POLE CHEB)
00242 RATIO =1.2783955 (4 POLE CHEB)
00243 LUN PASS CHEB FILTER RESP IS TYPICALLY NORMALIZED TO GIVE .05 DB
00244 FREQUENCY FBW. WE NEED TO NORMALIZE THIS TO PROVIDE 3 DB AT SPECIFIED
00245 REFER TO PAGE 604-606 NETWORK SYNTH. BY E.A. GUILLEMIN
00246 DF=1./TMAX
00247 IA=N/2+1
00248 ID=IA+1
00249 IF(IFILA.EQ.1) 60 TO 960
00250 60 TO 980
00251 960 F=.0001
00252 RATIO=2.2685099
00253 FBW=2.*(41./40.)
00254 FACNON=RATIO/(2.*PI*FBW)
00255 DU 970 I=1,IA
00256 WS=2.*PI*F
00257 S=CMPLX(0,WS)
00258 SL=(S+WC*WC)/S
00259 SL=SL*FACNON
00260 TFILA=1./((1.+0.62177*SL+0.2152*SL*SL)
00261 TFILAK=REAL(TFILA)
00262 TFILAI=AIMAG(TFILA)
00263 TIME(I)=ER(I)
00264 ER(I)=TIME(I)*TFILAR-EI(I)*TFILAI
00265 EI(I)=TIME(I)*TFILAI+EI(I)*TFILAR
00266 F=F+DU
00267 LU 975 I=I+N
00268 ER(I)=ER(N+2-I)
00269 EI(I)=EI(N+2-I)
00270 975 ER(I)=ER(N+2-I)
00271 EI(I)=EI(N+2-I)
00272 117*
00273 116*
00274 115*
00275 114*
00276 113*
00277 112*
00278 111*
00279 110*
00280 109*
00281 108*
00282 107*
00283 106*
00284 105*
00285 104*
00286 103*
00287 102*
00288 101*
00289 100*
00290 99*
00291 98*
00292 97*
00293 96*
00294 95*
00295 94*
00296 93*
00297 92*
00298 91*
00299 90*
00300 89*
00301 88*
00302 87*
00303 86*
00304 85*
00305 84*
00306 83*
00307 82*
00308 81*
00309 80*
00310 79*
00311 78*
00312 77*
00313 76*
00314 75*
00315 74*
00316 73*
00317 72*
00318 71*
00319 70*
00320 69*
00321 68*
00322 67*
00323 66*
00324 65*
00325 64*
00326 63*
00327 62*
00328 61*
00329 60*
00330 59*
00331 58*
00332 57*
00333 56*
00334 55*
00335 54*
00336 53*
00337 52*
00338 51*
00339 50*
00340 49*
00341 48*
00342 47*
00343 46*
00344 45*
00345 44*
00346 43*
00347 42*
00348 41*
00349 40*
00350 39*
00351 38*
00352 37*
00353 36*
00354 35*
00355 34*
00356 33*
00357 32*
00358 31*
00359 30*
00360 29*
00361 28*
00362 27*
00363 26*
00364 25*
00365 24*
00366 23*
00367 22*
00368 21*
00369 20*
00370 19*
00371 18*
00372 17*
00373 16*
00374 15*
00375 14*
00376 13*
00377 12*
00378 11*
00379 10*
00380 9*
00381 8*
00382 7*
00383 6*
00384 5*
00385 4*
00386 3*
00387 2*
00388 1*
00389 0*
00390 0*
00391 0*
00392 0*
00393 0*
00394 0*
00395 0*
00396 0*
00397 0*
00398 0*
00399 0*
00400 0*
00401 0*
00402 0*
00403 0*
00404 0*
00405 0*
00406 0*
00407 0*
00408 0*
00409 0*
00410 0*
00411 0*
00412 0*
00413 0*
00414 0*
00415 0*
00416 0*
00417 0*
00418 0*
00419 0*
00420 0*
00421 0*
00422 0*
00423 0*
00424 0*
00425 0*
00426 0*
00427 0*
00428 0*
00429 0*
00430 0*
00431 0*
00432 0*
00433 0*
00434 0*
00435 0*
00436 0*
00437 0*
00438 0*
00439 0*
00440 0*
00441 0*
00442 0*
00443 0*
00444 0*
00445 0*
00446 0*
00447 0*
00448 0*
00449 0*
00450 0*
00451 0*
00452 0*
00453 0*
00454 0*
00455 0*
00456 0*
00457 0*
00458 0*
00459 0*
00460 0*
00461 0*
00462 0*
00463 0*
00464 0*
00465 0*
00466 0*
00467 0*
00468 0*
00469 0*
00470 0*
00471 0*
00472 0*
00473 0*
00474 0*
00475 0*
00476 0*
00477 0*
00478 0*
00479 0*
00480 0*
00481 0*
00482 0*
00483 0*
00484 0*
00485 0*
00486 0*
00487 0*
00488 0*
00489 0*
00490 0*
00491 0*
00492 0*
00493 0*
00494 0*
00495 0*
00496 0*
00497 0*
00498 0*
00499 0*
00500 0*

```

```

00270 1100
00300 1190
00301 1200
00303 1210
00304 1220
00305 1230
00306 1240
00307 1250
00310 1260
00313 1270
00314 1280
00315 1290
00318 1300
00317 1310
00320 1320
00321 1330
00322 1340
00323 1350
00324 1360
00325 1370
00327 1380
00332 1390
00333 1400
00335 1410
00336 1420
00336 1430
00340 1440
00341 1450
00342 1460
00343 1470
00344 1480
00345 1490
00350 1500
00351 1510
00352 1520
00353 1530
00354 1540
00355 1550
00356 1560
00357 1570
00360 1580
00361 1590
00362 1600
00364 1610
00367 1620
00370 1630
00372 1640
00373 1650
00373 1660
00373 1670
00373 1680
00374 1690
00377 1700
00400 1710
00401 1720
00401 1730

-----
990 CONTINUE
IF (IFILC.EQ.2) GO TO 990
GO TO 1010
991 F=.0001
KAI10=1.5120983
F=.2.*(51./40.)
FUNCTION=RATIO/(2.*PI.*FBN)
DO 1000 I=1,IA
W=2.*PI.*F
S=CMPLX(0.,S)
SL=(S**3+AL**C)/S
SL=SL*FACHOK
TFILC=1./(1.+1.4360*SL+0.979*SL*SL+0.43*SL*SL*SL)
TFALC=REAL(TFILC)
TFILBI=AIMAG(TFILC)
TIME(I)=ER(I)
EN(I)=TIME(I)*TFILR-ER(I)*TFILBI
EA(I)=TIME(I)*TFILBI+ER(I)*TFILDR
1000 F=F*OF
DO 1005 I=1,IN
EN(I)=EN(N+2-I)
EA(I)=EA(N+2-I)
-----
1010 CONTINUE
IF (IFILC.EQ.3) GO TO 1020
GO TO 1040
1020 F=.0001
KAI10=1.
FBN=2.*(50./40.)
FUNCTION=RATIO/(2.*PI.*FBN)
DO 1030 I=1,IA
W=2.*PI.*F
S=CMPLX(0.,S)
SL=(S**3+AL**C)/S
SL=SL*FACHOK
TFILC=1./(1.+2.*SL+2.*SL*SL*SL+SL*SL*SL)
TFALC=REAL(TFILC)
TFILBI=AIMAG(TFILC)
TIME(I)=ER(I)
EN(I)=TIME(I)*TFILCR-ER(I)*TFILCI
EA(I)=TIME(I)*TFILCI+ER(I)*TFILCR
1030 F=F*OF
DO 1035 I=1,IN
EN(I)=EN(N+2-I)
EA(I)=EA(N+2-I)
1040 CONTINUE
CALL CLUCK
-----
C ALSO NOTE STATEMENT NO. 60, H IS DEFINED SUCH THAT THE PROCESS
C OF CONVOLUTION RESULTS INTO CORELEATION OF H AND E
C
DO 1500 I=1,N
X(I)=H(I)*ER(I)-HI(I)*EI(I)
X(I)=H(I)*EI(I)+HI(I)*ER(I)
1500 CONTINUE
C
NUM COMPUTE THE IDFT OF X(F)

```


3.1 INTRODUCTION

An important aspect of the packet radio communications development is the identification of hardware necessary to satisfy the requirements of packet radio. This identification includes the evaluation of available technology to meet packet radio needs and the assessment and direction of the future state of technology. In support of this effort, four areas of component selection and evaluation have been identified. These are surface acoustic wave devices as matched filters, broadband omnidirectional antennas, rf sources, and microprocessors. The results and state of these evaluation activities for the four selected equipment areas follow.

3.2 SURFACE ACOUSTIC WAVE DEVICES

3.2.1 Theory of Surface Acoustic Wave Devices, Signal Processing Techniques

The signal waveform of figure 3-1, or its complement, is to be used to transmit a data symbol at some bit rate $R_B = 1/T_B$ on a carrier f_0 . That is, the transmitted waveform is given by:

$$V_{\pm}(t) = \cos [2\pi f_0 t \pm \alpha_i(t)]$$

where $\alpha_i(t) = \pm \pi/2$ for each chip, depending on the code sequence being used, and the sign before α_i is determined by whether the symbol or its complement is desired.

The bandwidth is determined by the duration of the chip T_B/N_C rather than the symbol duration. Thus, the bandwidth has been increased by a factor of N_C , resulting in a spread spectrum signal.

3.2.1.1 Correlation Receiver

A conventional technique for detecting and decoding the data stream involves use of a correlation receiver in which locally generated replicas of the symbol and its complement are mixed with the arriving signal. If the locally generated signals are given by:

$$W_{\pm}(t) = \cos (2\pi f_0 t \pm \alpha_i + \gamma)$$

where γ is an arbitrary phase term, then the output of the mixers after filtering are given by:

$$\begin{aligned} X &= \cos \gamma \text{ (reference same as signal)} \\ &= \cos (2\alpha_i - \gamma) \text{ (reference complement to signal).} \end{aligned}$$

equipment considerations

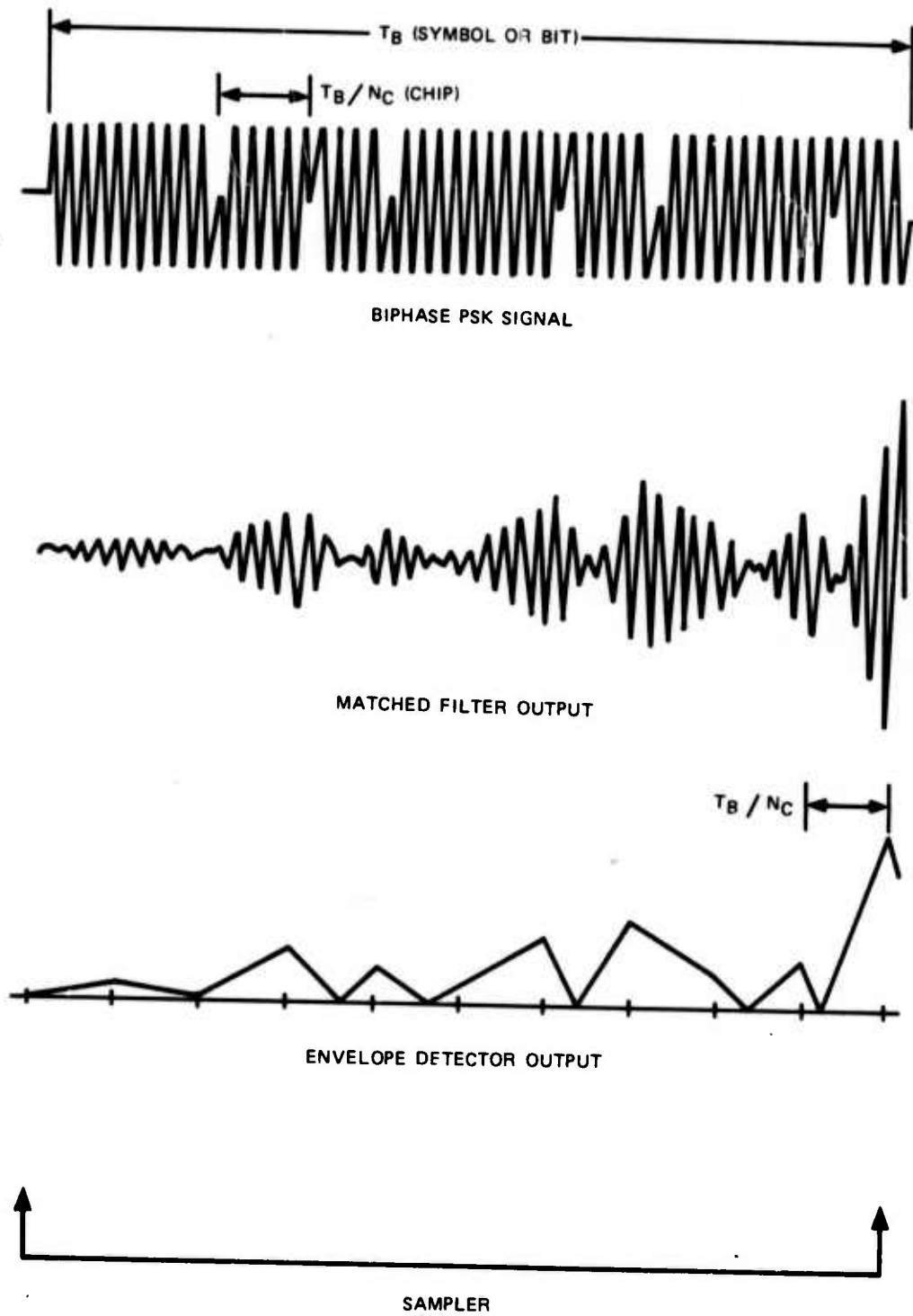


Figure 3-1. Timing Diagram for Binary Spread Spectrum System.

Provided that the local replicas are phase coherent with the incoming signal ($\gamma = 0$), then the output is +1 at the mixer that has the same reference as the received signal, and -1 otherwise. The system complexity required to achieve this coherence (i.e., synchronization) is the principal disadvantage of this technique.

3.2.1.2 Matched Filter Receiver

An alternate approach to data detection for this type of signaling format is the use of a matched filter receiver. Here, surface wave devices are especially useful as they readily permit implementation of matched filters for complex signal structures.

To illustrate the advantages of SAWD's for matched filter application, it will be helpful to briefly review the elements of matched filter theory. Let $h(t)$ be the impulse response of a linear filter. For an arbitrary input signal, $s_i(t)$, linear system theory gives the output signal, $s_o(t)$, as:

$$s_o(t) = \int_0^t s_i(\tau) h(t - \tau) d\tau.$$

For matched filter applications there is a specific relationship between the input signal and the impulse response of the filter. They are matched in the sense that:

$$h(t) = s_i(T - t),$$

where E_b is the total energy contained in the $s_i(t)$ signal

$$E_b = \int_0^{T_B} s_i^2(t) dt$$

and N_o is the noise spectral density of the additive white noise at the input to the matched filter. The maximum value of the peak signal-to-rms-noise ratio thus depends only on the signal energy E_b and the whitenoise spectral density N_o independent of signal waveform. This signal-to-noise ratio is a maximum only at time $t = T_B$, i.e., 1-bit duration after reception of the symbol. This implies that the bit samplers are synchronized to the reception time of the symbols, that is, the system has bit-synchronization. Assuming such bit sync, the quantity which determines system performance is the signal-to-noise ratio E_b/N_o .

Now, consider the effect of an average power limited noise-like jamming signal. This noise may be nonthermal noise, intentional jamming, or even a statistical representation

equipment considerations

of other users occupying the same channel. The noise spectral density in the receiver is given by:

$$N_o = N_{oR} + N_{oJ}$$

where N_{oR} and N_{oJ} are noise spectral density contributions due to receiver thermal noise and jammer, respectively. If the jammer is average power limited to J watts and adjusts its spectral occupancy to match the signal bandwidth, then:

$$N_{oJ} = \frac{J}{(N_C/T_B)} = \frac{JT_B}{N_C}$$

Since $N_{oJ}' = JT_B$ would define the jammer effect if the data signal occupied a bandwidth equal to its data rate, the effect of the bandwidth expansion has been to reduce the effect of the jammer by the factor N_C , which is also the bandwidth expansion factor.

Surface acoustic wave devices (SAWD's) have the potential to revolutionize spread spectrum systems. The necessary matched filtering can be performed at high rates with a simple microelectronic device of small size. For example, a signal waveform 50 chips long with 5-MHz chip rate would require a digital processor capable of handling 250 analog multiplications and additions per microsecond to perform real time matched filtering. Equivalent signal processing can be performed by a SAWD with dimensions of approximately 1.5 x 0.3 x 0.1 inches. A signal with the same number of chips and a 50-MHz chip rate would require an even more complex digital processor, while the corresponding SAWD matched filter is even smaller than the 5-MHz device.

The principles of the SAWD matched filter for phase-coded waveforms are illustrated in figure 3-2. An incoming phase-coded waveform, in this case a 7-bit Barker phase code, is fed into the input interdigital transducer (IDT), which converts it into a traveling surface acoustic wave in the piezoelectric substrate. The electric field associated with the acoustic wave in piezoelectric materials allows the signal to be sampled (tapped) at multiple points in the delay path by other IDT's (taps). The taps in figure 3-2 are placed at precise identical time intervals equal to the chip period of the incoming waveform.

The physical spacing between taps depends on the surface wave velocity (v_s) of the substrate materials and the chip rate of the incoming waveform. For a 10-MHz chip rate on temperature stable ST cut quartz ($v_s = 3.157 \times 10^5$ cm/s) the tap spacing is 12.49 mils with a normal accuracy of placement of ≤ 10 microinches.

The taps are phase-coded so that when the waveform is completely loaded into the TDL all tap outputs add in phase, giving the correct correlation function. Figure 3-2 shows an external phase shift network to produce 180-degree phase shifts prior to summation. Other techniques of tap phase-coding are illustrated in figure 3-3, where 3-3a and 3-3b are fixed coding techniques. Figure 3-3c represents a switchable tap approach. For the configuration of figure 3-3a, the tap coding is built into a photomask used to fabricate the SAWD and normally would only be used for large production runs of identical coded lines. Figure 3-3b shows a technique whereby SAWD's can be fabricated with both sides of the tap connected to both sum lines and the phase-coding achieved by opening two lines per tap, as indicated in

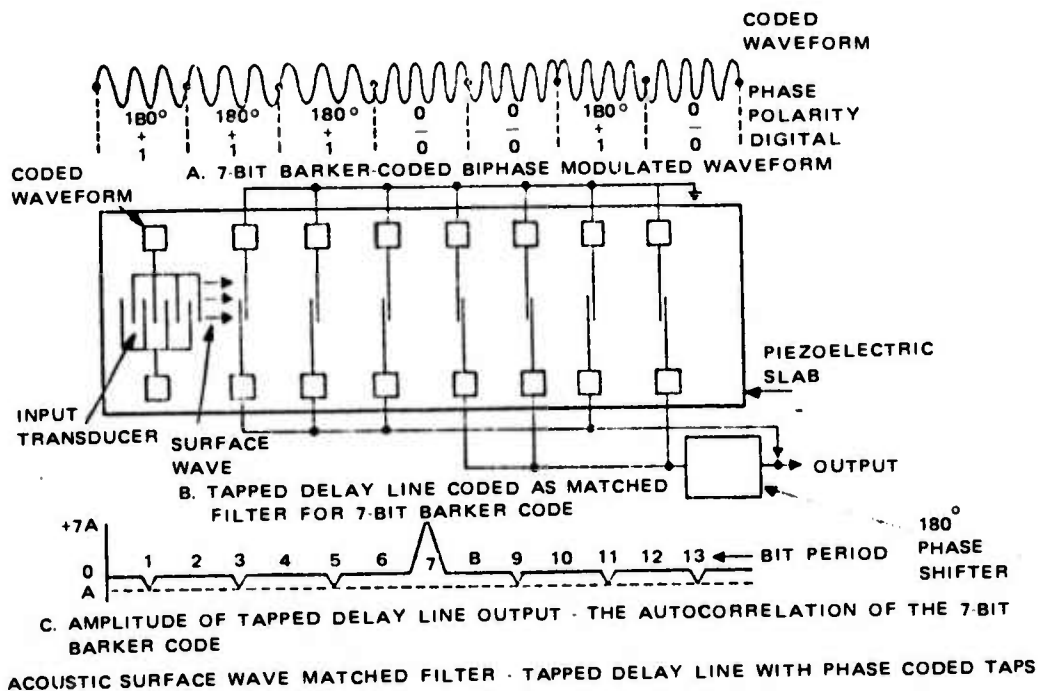


Figure 3-2. Principles of the SAWD Matched Filter for Phase-Coded Waveforms.

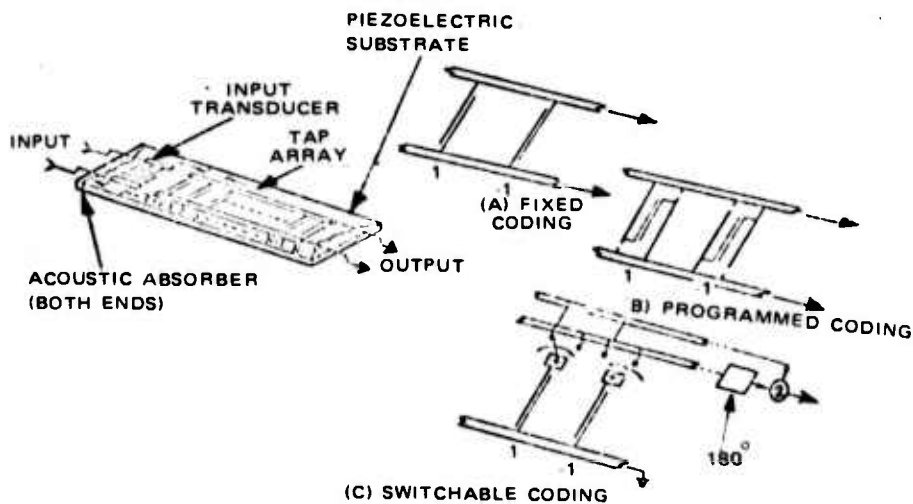


Figure 3-3. Tap Phase-Coding Techniques.

equipment considerations

the schematic. This approach allows large numbers of devices to be fabricated with identical structure and the individual line coding to be carried out quickly and conveniently by techniques such as laser beam burnout on a tape programmed XY table.

The transfer function of the surface wave device will exhibit the response required to be a matched filter for each chip of a square modulated waveform. The response of the taps is relatively wideband, and so, does not distort the waveform. To first order, this function is the ideal triangular shape expected for a square chip, although some slight rounding is usually observed at the peak.

3.2.2 Design and Operation of Coded Surface Acoustic Wave Devices

The matched filter operation described in the previous paragraph is one of a class of filters called transversal filters that may be described as tapped delay lines. While a great many techniques have been proposed for generating and detecting surface waves, the interdigital transducer has proven to be the most practical, especially in application to spread spectrum and communications systems.

A typical coded SAWD (as in figure 3-4) consists of n-pair interdigital transducers at each end of a multiple-tapped center transducer. A voltage applied between the pads results in a strong field between alternate fingers of the pattern. Since the substrate is piezoelectric, this field produces a periodically varying stress in the material. The resultant wave propagates on the surface away from the electrodes in both directions, in a manner similar to radiation from an end-fire antenna. Conversely, as the wave passes under other electrodes, it produces an autocorrelation voltage that may be detected by external circuitry.

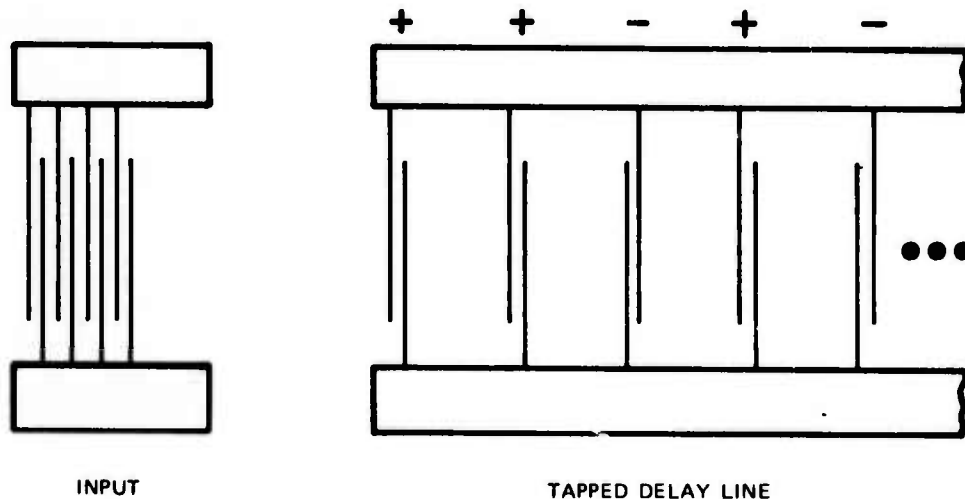


Figure 3-4. Tapped Delay Line Finger Placement.

In a spread spectrum communication system, the generated signal is normally clipped, gated, and transmitted from a Class C amplifier. In the receiver, the signal will be applied (usually after some signal conditioning) to a second device with the time-inversed code. When the signal matches the coded device, a strong response results. The operation of the system then depends on detecting the existence and timing of the main correlation peak.

The accessibility of the wave to tapping is the key to very flexible code generation and transversal filtering. To first order, there is a one-to-one relation between the location of a tap on the substrate and the signal generated by the transducer (i. e., its impulse response). By proper design of the electrode placement and overlap, it is possible to generate signals of prescribed amplitude, phase, and frequency versus time, including all the standard weighted and unweighted biphasic and polyphasic codes. Most work to date has been done with codes of fixed center frequency, equal chip length, and fixed chip sequence, but even these restrictions are not necessary.

Thus, the design of a device consists of two steps: specify the desired impulse response, then choose substrate material and finger geometry to realize this impulse response in a practical device. Specification of the desired impulse response (code sequence, frequency, etc.) is primarily the responsibility of the communication system designer, who must be aware that some practical limitations exist due to fabrication techniques and choice of material. As will be discussed in the next section, these limitations affect the total time length, carrier frequency, fractional bandwidth, and allowable temperature variation.

Realization of a specified impulse response starts with a first order design based only on the required impulse response, and results in approximate numbers for overall device size, beamwidths, finger placement, impedance, insertion loss, etc. As more and more chips are added to the code sequence at higher frequencies, smaller and smaller levels of distortion become significant, while the distortive effects become stronger. The early surface equivalent circuit models can be used to analyze the effect of electrical loading of the taps, but must be extended to include the effects of acoustic reflections at each electrode edge. While the details of the design can be complicated, the result is that it is possible to realize in practice almost any desired impulse response within the size and frequency limits that can be fabricated.

3.2.3 Surface Acoustic Wave Device Characteristics

3.2.3.1 Insertion Loss

The sources of insertion loss in surface wave devices are:

- a. Bidirectionality loss
- b. Electrical mismatch loss
- c. Parasitic resistance in the transducer pattern
- d. Losses in the matching networks
- e. Propagation losses in the substrate

equipment considerations

- f. Losses due to beam spreading
- g. Apodization losses.

As discussed in the following paragraphs, the first two are the dominant losses for most filters of interest. The remaining ones are usually small if proper care is exercised in design and fabrication.

The normal filter transducer configuration has a bidirectionality loss of 6 dB, half of which occurs because the input transducer radiates only half of the power toward the output transducer. The remaining 3 dB occurs at the output transducer, by reciprocity, it can only reconvert half of the acoustic power incident on it into electrical output. Under perfect electrical matching condition, the other half of the power is reradiated as regenerated acoustic waves giving rise to the triple-transit reflections.

Half this bidirectionality loss can be removed by placing a second output transducer on the substrate on the opposite side of the input transducer. The resulting three-transducer configuration has a basic 3-dB loss due to bidirectionality. This configuration also has inherent tripletransit suppression if the center transducer is properly matched. Unfortunately, this three-transducer configuration cannot be used for dispersive transducers, which limits its usefulness.

It is possible to eliminate the bidirectionality loss completely by using multiphase unidirectional transducers. The multiphase drive removes the bidirectional symmetry and permits complete conversion from electrical signals to acoustic signals traveling in one direction. Thus, this structure has no inherent bidirectionality losses. This structure also suppresses triple-transit effects because the output transducer can absorb all the incident acoustic power. The limitations on this transducer are due to added fabrication complexity of the multilayer electrode geometry.

Electrical mismatch is often another major source of loss for two reasons. First, filters are often mismatched as previously prescribed to minimize triple transit due to regeneration. Second, transducers are sometimes mismatched to lower the electrical Q of the input so that the matching network does not introduce unwanted bandnarrowing.

The minimum insertion loss that can be achieved at a given fraction bandwidth can be calculated by using the approximate expression for the electrical Q of a transducer. As long as the Q is less than the reciprocal of the fractional bandwidth, one can easily match the device across the entire bandwidth.

Figure 3-5 shows minimum insertion loss as a function of fractional bandwidth for several substrates of interest. In this figure ST-cut quartz indicates the zero temperature coefficient cut and HC-cut quartz is the designation for the highest coupling coefficient cut available on quartz. The 6-dB minimum loss that is indicated accounts for bidirectionality. Use of the three-transducer configuration or the unidirectional transducers would uniformly reduce the curves by 3 and 6 dB, respectively. In practice, these curves provide a good estimate of loss expected for typical bandpass filter designs, although some error must be expected for filters with bandwidth over 30 percent due to the uncertainties created by parasitic elements. For moderate bandwidth filters, parasitic elements and propagation losses are normally negligible below 100 MHz. Finally, losses due to beam spreading and apodization typically never exceed 2 dB for most devices.

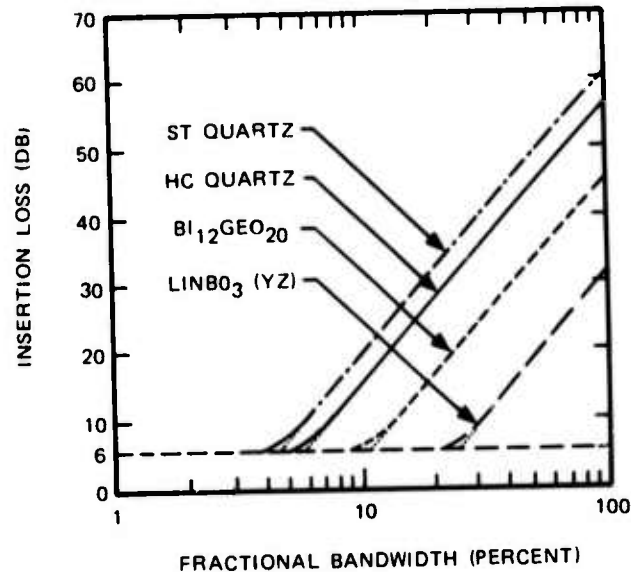


Figure 3-5. Minimum Achievable Insertion Loss for Two Transducers on Various Substrates.

3.2.3.2 Frequency Uncertainty

A major factor that can contribute to loss of processing gain is frequency offset of the coded waveform. Figure 3-6 is a curve illustrating the loss in processing gain versus frequency error. A null frequency (providing infinite loss) occurs at a frequency offset equal to the reciprocal of the time delay of the matched filter. As an example, a line 64 μ s long would lose 3 dB in processing gain if the frequency offset were $0.45 \times 1/64 \mu$ s, or about 7 kHz.

Three sources of frequency error are the transmitter LO, receiver LO, and the matched filter (SAWD) used for sync detection. Doppler must also be considered. Worst-case frequency errors for a 1-GHz radio system with sources stabilized to 10 ppm and 0.1 ppm are given in table 3-1.

One means of avoiding the loss effect due to frequency mismatch is to provide several delay lines in series, each operating coherently on a short segment of a sync sequence. Each filter output is detected and then noncoherently summed. As long as the number of lines is small, the loss in overall processing gain is reduced. Thus, if four delay lines (each having a line length of 25 μ s) were connected in series, a 6-kHz frequency error would result in approximately a 0.2-dB loss in processing gain for each line. This would result in an overall loss of processing gain of 0.8 dB, plus a loss due to the noncoherent addition of each of the lines.

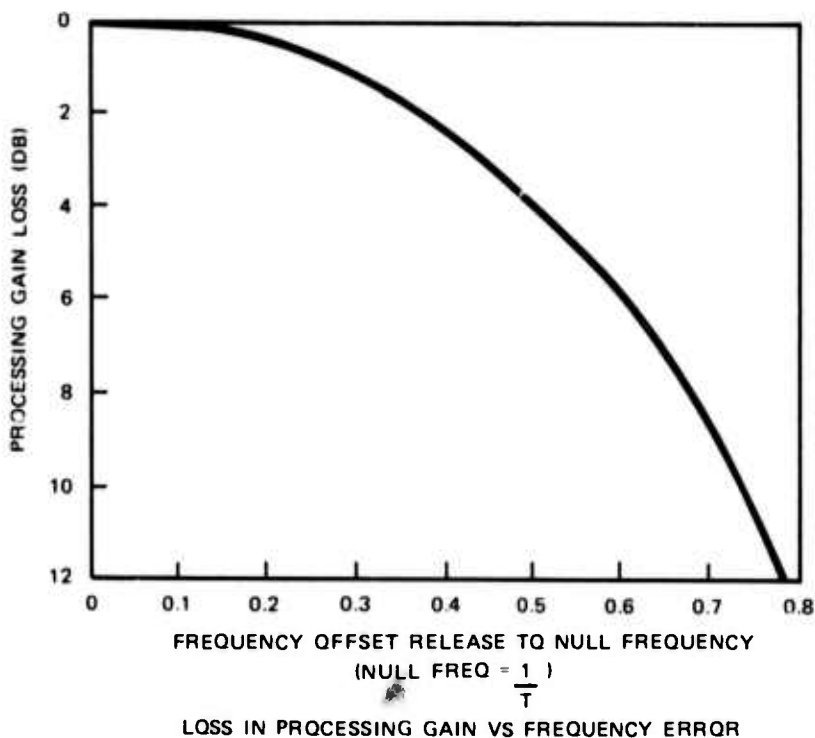


Figure 3-6. Loss in Processing Gain Versus Frequency Error.

Table 3-1. Worst-Case Frequency Errors.

LO SOURCE STABILITY	-50°C to +65°C		0° to +50°C	
	± 10 ppm	± 0.1 ppm	± 10 ppm	± 0.1 ppm
Transmit LO (1 GHz)	1.0	0.1	1.0	0.1
Receive LO (1 GHz)	1.0	0.1	1.0	0.1
SAWD*	6.0	6.0	2.4	2.4
Doppler (Mach 1)	0.44	0.44	0.44	0.44
Worst Case Error	8.44 kHz	6.63 kHz	4.84 kHz	3.04 kHz

*SAWD error based on 50 ppm, fo = 120 MHz for -50°C to +65°C and 20 ppm for 0°C to +50°C.

3.2.4 Test Set SAWD Experience

This paragraph discusses results of our experience with the test set Surface Acoustic Wave Device's (SAWD's) and indicates how this information may be used in the ARPA experimental equipment design. The SAWD's for the propagation test set were 127 chips/bit coded biphasic (psk) modulation. Two SAWD's were used, one at 20 megachips per second (mcps), and the second at 10 mcps, resulting in bit rates of 157.48 kHz and 78.74 kHz, respectively (6.35- μ s and 12.7- μ s bit code period, respectively). The resulting carrier rate to chip rate results in an integer number of carrier cycles in a chip period. Texas Instruments Incorporated later manufactured two devices with the ratio not an integer. These devices are discussed in a subsequent paragraph.

The 127 maximal length chip code was selected from one of 18 possible codes for higher correlation peak to sidelobe ratio. These SAWD's were purchased from Texas Instruments Incorporated. The actual material used was quartz. The SAWD's were mounted on a slab of aluminum with covers installed. In the assembly, 50-ohm matching networks were included for each port. Each port was brought out on an SMA connector. The assembly size was 1 x 1-3/16 x 3 inches excluding connectors.

The actual size of the 10-mcps SAWD was 1/16 X 3/8 X 2.5 inches. As is evident from the dimensions, a tremendous amount of volume in the assembly was wasted to include terminal, matching networks, and connectors.

3.2.4.1 Test Results

Since the correlation peak-to-sidelobe ratios for continuous code are ideally 42 dB and these SAWD's were in the 25-dB range, there was some concern that the matching networks were degrading SAWD performance. A 10-mcps SAWD was selected for test, and SAWD performance was examined with and without matching networks. The block diagram of the test setup is depicted in figure 3-7. Table 3-2 and accompanying figures 3-8 through 3-14 illustrate the results of these tests.

The optimum carrier and chip rate frequency was derived by monitoring the correlation peak on the scope and adjusting frequency for maximum level, or best waveform. Peak-to-sidelobe measurements were made by monitoring the worst-case sidelobe level on the scope and then using the step attenuator to set the correlation peak at the same level. The comparative insertion loss measurements are taken with respect to the matched network case. Absolute insertion loss for the matched network case was not accounted for.

The test results indicate that carrier frequency is rather immune (± 2.5 kHz) to matching networks, although frequency is 15 kHz below desired carrier of 140 MHz. All SAWD's of this batch were from 0 to 40 kHz low, with mean of about 20 kHz low. However, changing carrier frequency ± 20 kHz from optimum carrier on any SAWD completely obliterates the correlation peak.

The optimum chip frequency seems to vary up to ± 100 kHz, depending on which matching networks are removed or which shape is desired; however, the peak-to-sidelobe ratio did not change ± 1 dB over the noted ranges of chip rates.

Insertion loss is predominant with matching networks. This is to be expected since the function of these networks is to match 50 ohms to the high impedance of the SAWD's. Note that the loss of the tapped output port is less than the transducer input. This is probably due to lower resistive values of the summed taps.

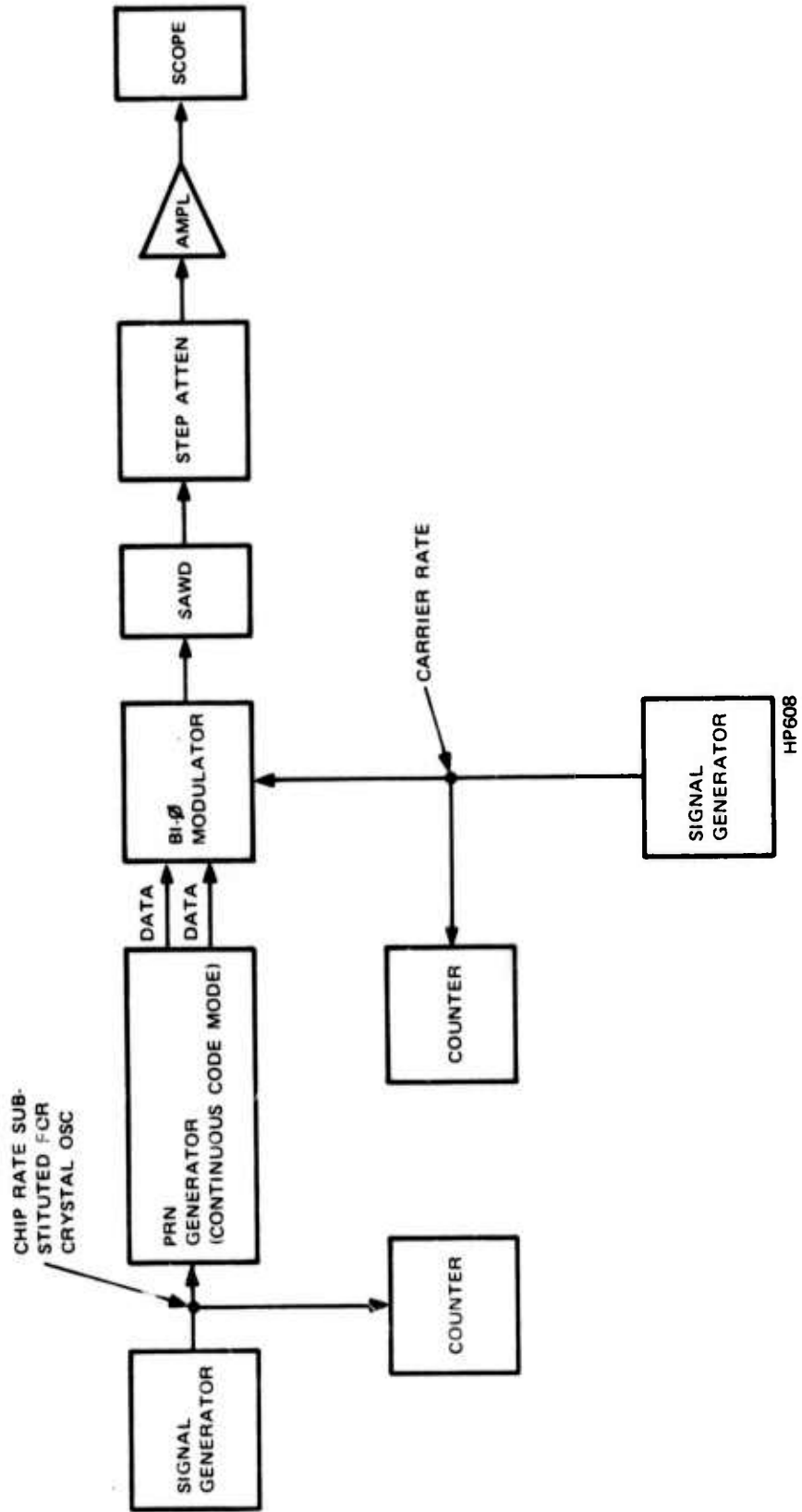


Figure 3-7. SAWD Test Setup.

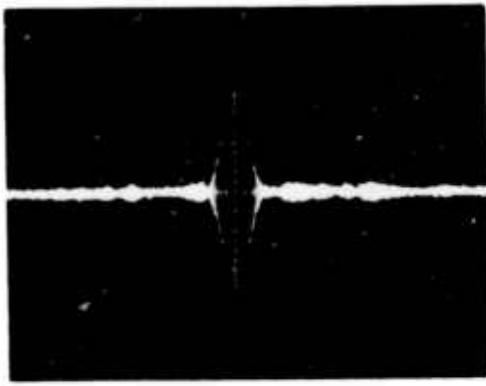


Figure 3-8. Test Result A.

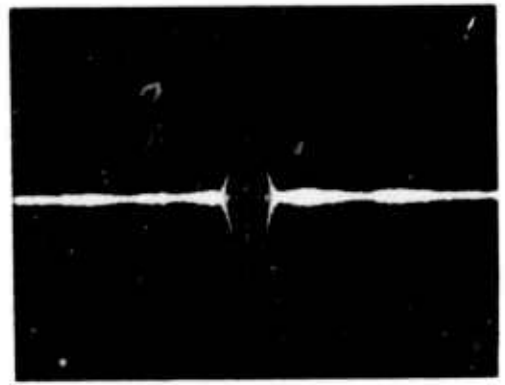


Figure 3-9. Test Result B.

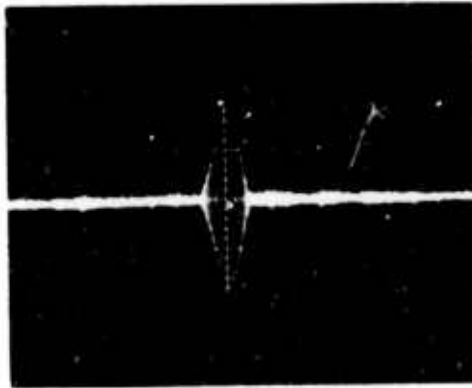


Figure 3-10. Test Result C.

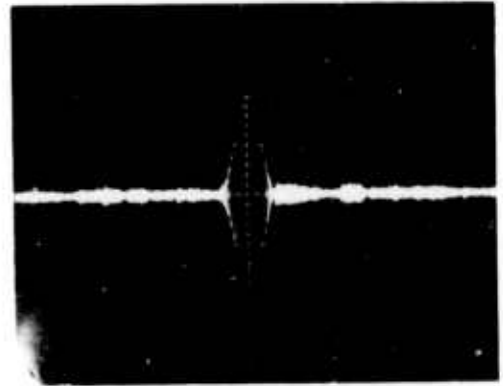


Figure 3-11. Test Result D.



Figure 3-12. Test Result E.

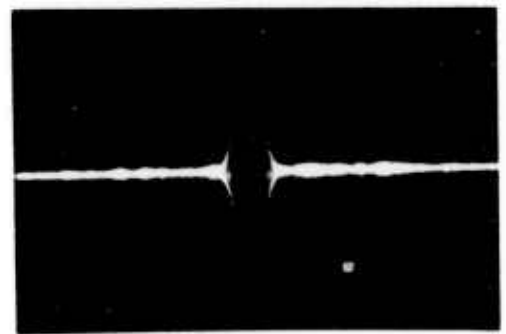


Figure 3-13. Test Result F.

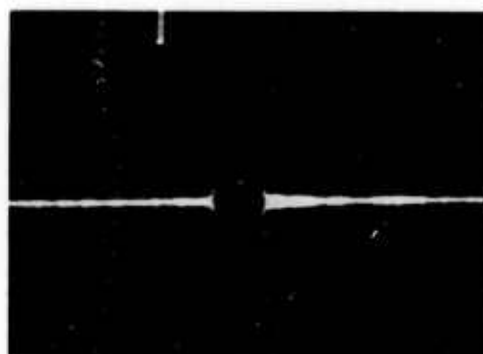


Figure 3-14. Test Result G.

Table 3-2. Test Results.

TEST SET SAWD NO 5	OPTIMUM CARRIER FREQUENCY (MHz)	OPTIMUM CHIP FREQUENCY (MHz)	WORST-CASE PEAK/SIDE- LOBE (dB)	COMPARATIVE INSERTION LOSS (dB)	FIGURE
With input and output match- ing network	139.985	19.999	+23	0	3-8
Input matching network removed	139.987	20.101 *	+23	-8	3-9
	139.987	19.951	+23	-8	3-10
Output matching network removed	139.984	20.074 *	+23	-4	3-11
	139.984	19.987	+23	-4	3-12
Both input and output matching network removed	139.989	19.901 *	+23	-14	3-13
	139.989	19.992	+23	-14	3-14

*Chip rate adjusted for ideal shape..

The only performance effect other than insertion loss of the SAWD matching networks is that the correlation peaks a little sharper at the epoch without the matching networks. This should be expected since a bandwidth limiting of the matching networks is excluded; however, these sharper peaks did not improve the peak-to-sidelobe ratio.

Note that the peak-to-sidelobe ratio of 23 dB for continuous code is much worse than 42 dB for the ideal case. Earlier tests for these sets of SAWD's were in the 25- to 26-dB range. The difference between the two tests could be the result of different views, since these are waveform comparisons off the screen of an oscilloscope. Regardless, 15- to 20-dB degradation is seen in the test set SAWD's.

Degradation is due to transmission line type of acoustic reflections on the substrate between taps.

For biphase psk, since taps are spaced 180 degrees, reflections from tap back to the previous tap and reflections forward again produce 360-degree round trip: hence, reflections add together arithmetically. However, for 4-phase psk (or ± 90 -degree phase increments systems such as msk), round trip reflections are 180 degrees; hence, reflections tend to cancel for some polarity taps and add for opposite polarity taps. Hence, degradation would be less for 4-phase psk or msk modulation schemes, or about 6 dB better or ≈ 30 dB.

3.2.4.2 20-mcps Code into 10-mcps SAWD

A peculiar phenomenon has been observed with the test SAWD's. This occurs whenever a 20-mcps code is applied to a 10-mcps SAWD, which results in correlation peaks occurring at a 20-mcps rate with insertion loss and correlation peak-to-sidelobe performance nearly as good as operation with 10-mcps code rate. This phenomenon also occurs at a 40-mcps rate, but does not occur with 30-mcps rate or rates which are submultiples of 10 mcps, such as 5 mcps and 2.5 mcps.

This can be explained by the following example. Consider a 7-bit continuous code (1110010) that is alternately sampled at half rate. This results in two 10 mcps codes as shown below.

Original Code (20 mcps): 1 1 1 0 0 1 0 1 1 1 0 0 1 0 1 1 1 0 0 1 0

Half-Rate Code (20 mcps): 1 1 0 0 1 0 1 1 1 0 0

Half-Rate Code, Delayed
1 Chip (20 mcps) 1 0 1 1 1 0 1 1 0 1

Autocorrelation of
Half Rate

Autocorrelation of Half
Rate, Delayed



Thus, two 10-mcps channels are created, but separated by half bit intervals. When the two outputs are summed, a 20-mcps bit rate correlation results.

3.2.4.3 Noninteger SAWD's

Texas Instruments recently developed a new set of SAWD's. These are non-integer type of SAWD's; i.e., the ratio of carrier-frequency-to-chip-rate is not an integer. TI implemented this by spacing the taps on the substrate at the nearest zero crossings to evenly space sine wave 180-degree increments, not evenly spaced 180-degree increments as in previous SAWD's.

Table 3-3 shows the performance of these SAWD's. These SAWD's did not have any matching networks, so insertion loss measurements were not taken. These SAWD's were subsequently returned to TI.

Table 3-3. SAWD Performance.

TEST SET	OPTIMUM CARRIER FREQUENCY (MHz)	OPTIMUM CHIP FREQUENCY (MHz)	WORST-CASE PEAK-TO-SIDELOBE (dB)
SAWD No. 1	139.960	10.120	17
SAWD No. 2	139.960	10.155	23

The peak-to-sidelobe ratio is somewhat worse with this type of SAWD, therefore, new designs should not use non-integer SAWD's if possible.

3.2.4.4 Conclusions and Recommendations

The primary conclusion is that the matching network on the input and output ports have no effect on SAWD performance. Matching networks appear to do their intended function of impedance matching to improve insertion loss of the device. Therefore, SAWD imperfections must account for 23-dB peak-to-sidelobe performance (continuous code) where an ideal SAWD would be 42 dB.

Non-integer SAWD's should be avoided because of the degradation in peak-to-sidelobe ratio.

From the results of the test set SAWD's, a peak-to-sidelobe ratio of 30 dB maximum seems to be the limit. Allowing processing gain to be 10 dB better so that degradation is solely SAWD limited, spread factors of no more than 100 is warranted for continuous code and code/code inverted types of modulation.

With dual data rate packet radio concepts, the same codes or truncated codes should be avoided between the two code rates.

3.2.5 State of Technology in SAWD

Texas Instruments has published a graph (figure 3-15) summarizing their fabrication limitations; it is indicative of the present SAWD technology and is included for reference. A quote from TI relating to the attached graph is as follows:

"A 25-percent bandwidth has been assumed for practical reasons (insertion loss, spurious responses from device and electronics, etc.). Devices within the center shaded region are readily obtainable in large quantities. Devices in the lightly shaded region are also readily available but require more custom work. The outer shaded region contains those devices that are technically feasible and potentially producible in quantity but still in the development stage. Extrapolations outside this region entail considerable technical as well as economic risk. The top and right-hand boundary determine the maximum bandwidth and time lengths which may be obtained using the given level of technology. The product is the maximum chip length obtainable and is shown in the figure for each of the three regions."

The curves developed by TI provide a good indication of the spread factors we should consider for spread spectrum equipment implemented using surface wave devices. We should think in terms of 100 chips per bit or less initially. Devices in the 100-chip to 1000-chip area are possible, but are still in the developmental stage.

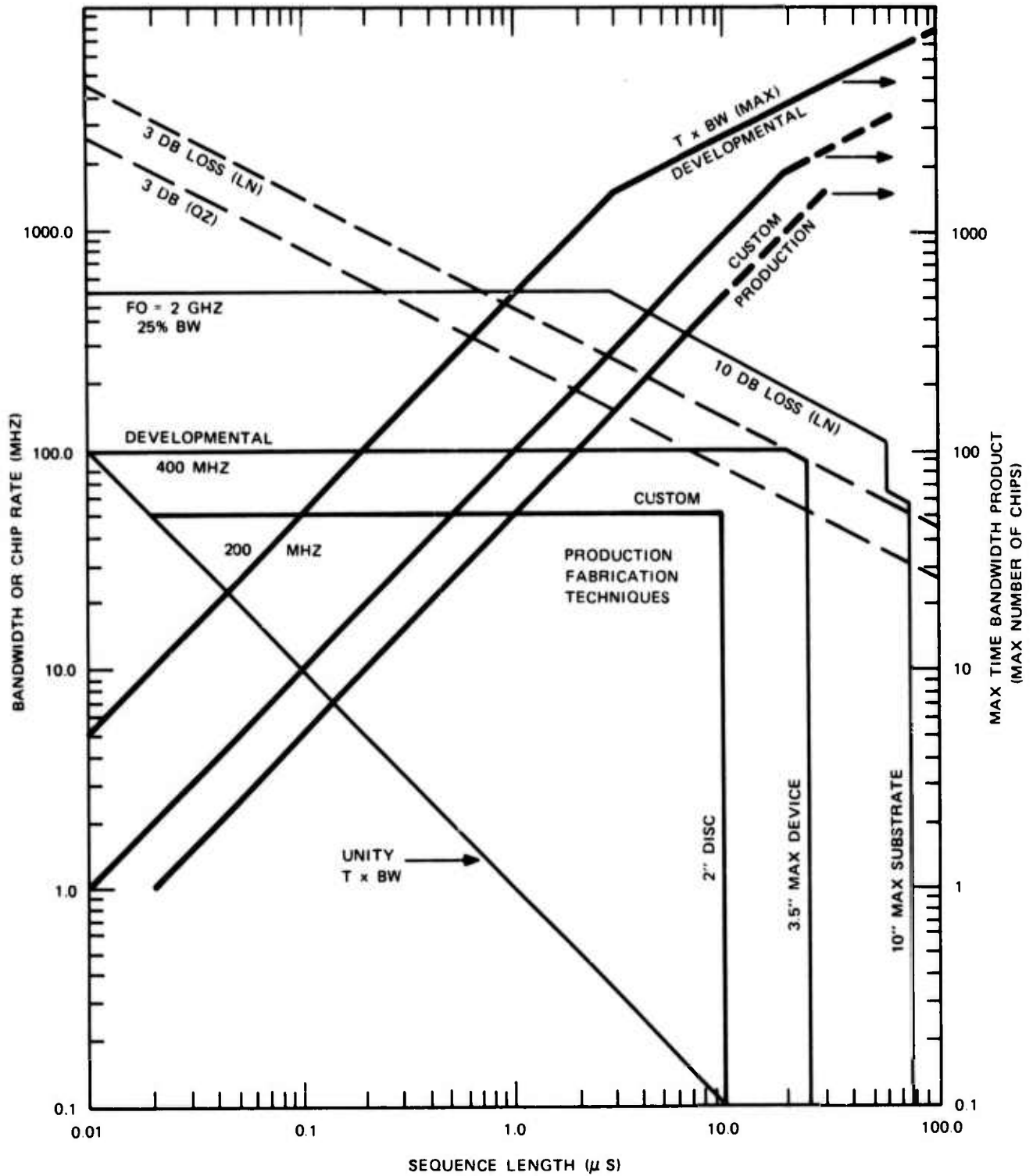


Figure 3-15. Current Fabrication Capabilities for Coded Devices.

3.2.6 Performance Limitations

The performance of SAWD's has been improving at a rapid rate for several years as device designers become more familiar with the photolithographic techniques developed for integrated circuits. Progress is expected to continue at a rapid rate because the microelectronics industry is itself on the threshold of a revolution in circuit lithography as electron beam and ion etching techniques become practical. In perspective, it should be remembered that we are discussing applications in communication systems. Since large numbers of users are usually involved, the choice of technique becomes price sensitive as well as technology sensitive. With this in mind, let us look first at what can be done within the constraints of current mass production techniques.

The most highly automated production lines in the world for photolithography are those used for making integrated circuits. Both quartz and lithium niobate are readily available on a 2-inch quartz slice using such equipment. The codes shown are 10 μ s on ST-quartz. Longer codes (up to 13 μ s) can be accommodated by deleting one of the end transducers and scraping more material at the top and bottom of the slice. While it is desirable to operate below 200 MHz, acceptable results can still be obtained at 300 MHz on ST-quartz or 400 MHz on 41.5 degree Z-cut X-propagating lithium niobate. For those production lines using 3-inch slices, an additional 8 to 10 μ s is available, but at slightly lower resolution.

Size restrictions are removed by going to custom fabrication, although increases above about 4 inches involve some premium from materials suppliers and increasing difficulty in handling and fabrication. For example, a single code pattern longer than 3.5 inches requires special equipment to generate and use. Maximum possible code length is a somewhat nebulous quantity usually not of practical interest in multiple-user communication systems because of the expense involved. Quartz may be obtained longer than 10 inches and lithium niobate in lengths approaching 10 inches. The corresponding delay times can be increased even more by such techniques as the wraparound delay line with separate devices being driven from each delay line tap, or by printing parts of the code on each side of the substrate.

Resolution restrictions can be eased by use of narrow field of view projection printing. Resolution of 1 micrometer (0.7 to 1.0 GHz fundamental) is paid for by a maximum field of 0.25 inch from a given reticle. Larger patterns require joining several segments with placement errors of a fraction of a line-width.

Further improvement in resolution can be obtained by using electron beam techniques for producing photomasks and/or devices. The very best resolution (0.14 micrometer) has been obtained using scanning electron microscopes but over extremely limited fields of view. Machines designed especially for mask generation are capable of larger fields at somewhat worse resolution (e.g., 0.5 micrometer over 50 mils, for 2500 lines, and similar numbers of lines for larger fields).

Several pattern generation and reproduction machines are compared in table 3-4 in terms of field of view, resolution, and maximum number of line pairs (i.e., cycles of carrier signal) that can be produced without realignment.

For frequencies above 300 MHz and code sequences longer than 1 μ s, intrinsic surface wave attenuation can become important. Small losses can usually be ignored and larger losses can be compensated by weighting the taps. Weighting is less desirable, since the same device cannot be used for both code generation and correlation, thereby making fabrication tolerances more stringent. A reasonable loss allowance for practical devices is 3 dB. Assuming that surface preparation has been properly done, then attenuation increases quadratically with frequency, with one dB/ μ s at 0.6 and 1.05 GHz for quartz and lithium niobate, respectively.

Table 3-4. Typical Lithography Limitations.

TECHNIQUE	TYPICAL EQUIPMENT	FULL FIELD CAPABILITIES		
		FIELD SIZE (In.)	LINE WIDTH (μm)	LINE PAIRS
Large-scale photoplotting	Gerber Photoplotter	30 x 40	50	10,000
Contact printing	Conventional Production Equipment, 3-inch Mask	3.5 (diagonal)	4	12,000
High resolution projection printing	Mann Projection printer	0.25 x 0.25	1	3,100
Electron beam	Production Oriented	0.300	2.5	1,500
		0.050	2.5	1,250
Electron beam	Scanning Electron Microscope	0.004	0.1	500

3.2.7 SAWD Technology Summary

The present state-of-the-art technology of SAWD's as applied to the ARPA packet radio concept (spread spectrum) may best be summarized by table 3-5.

Devices in the first two columns are readily available in large quantities. Custom manufactured SAWD's are also readily available, but take more time and are more expensive. Developmental SAWD's are technically feasible, are potentially producible in quantity, but are still in developmental stage. Extrapolations outside this region entail considerable technical and economic risk.

Materials used are usually either quartz or lithium niobate (LiNbO_3). Which material is used, transducer type, and configuration of SAWD's are determined by the device manufacturer to best match to performance parameters specified.

3.2.8 Summary of Definitions

$$T_b = \frac{1}{R_b} = \frac{1}{\text{bit rate}} = \text{bit interval}$$

$$T_c = \frac{1}{R_c} = \frac{1}{\text{chip rate}} = \text{chip interval}$$

$$R_b = \text{bit rate}$$

$$R_c = \text{chip rate}$$

Table 3-5. SAWD State-of-the-Art Technology.

CONFIGURATION	PREFERRED PRODUCTION SAWD'S	PRODUCTION SAWD'S	CUSTOM SAWD'S	DEVELOPMENTAL SAWD'S
Carrier Frequency	10 to 50 MHz	10 to 200 MHz	2 to 600 MHz	2 to 1000+ MHz
Percentage Bandwidth	5 to 20%	5 to 20%	5 to 25%	—
Bit Period (total delay)	0.1 to 10 μ s	0.1 to 10 μ s	0.1 to 25 μ s	0.01 to 75 μ s
Spread Factor (10- to 20- μ s delay)	1 to 500	1 to 500	1 to 1000	1 to 10,000
Insertion Loss	15 to 35 dB	15 to 35 dB	—	—
Temperature Variations	\pm 50 ppm	\pm 20 ppm 0° to 50°C	\pm 50 ppm -50°C to +65°C	—

E_b = energy per bit

E_c = energy per chip

E_p = energy of preamble

S = E/T = signal power

N_o = Gaussian noise (per Hz bandwidth)

N = $N_o B$ = total integrated noise over bandwidth B

N_c = number of chips per bit (spread factor)

3.3 EVALUATION OF ANTENNA FOR PACKET RADIO

The objective of the following is to outline omnidirectional antenna concepts and considerations with emphasis on those best suited to the hand-held terminals. The treatment is given from an antenna point of view and conclusions drawn herein may be obviated when the antennas are included as part of a complete link performance model. Issues such as bandwidth, tuning, and matching are not addressed in this brief investigation of antennas.

Implementation of the packet communications system will require the use of several types of antennas; however, the difference in technology represented by the change from conventional communications to packet communications does not create any new demands on the antenna

design not previously encountered. The basic parameters to be analyzed for the various terminals that make up the complete system are:

- a. Directivity, or area of radiation covered by each specific antenna
- b. Polarization of the radiated signal
- c. Efficiency of the antenna
- d. Frequency
- e. The size of the antenna that is primarily a function of the other four parameters.

The proper choice of these parameters is a major factor in effectively and efficiently completing the path that links the source of a message with its final destination.

3.3.1 Terminal Antenna

In order to be practical, the antenna for the hand-held personal terminal must be small and simple. The size of an efficient antenna is largely a function of frequency; hence, from a physical point of view, the higher frequencies are desirable. However, as indicated in section 2, this convenience is bought with higher transmit power. In considering the frequency band likely to be available for packet radio service, any frequency likely available will not result in objectionably large antennas.

The simplest and most common type now in use on most hand-held transceivers is the quarter-wave or near quarter-wave monopole shown in figure 3-16. At 300 MHz this is a

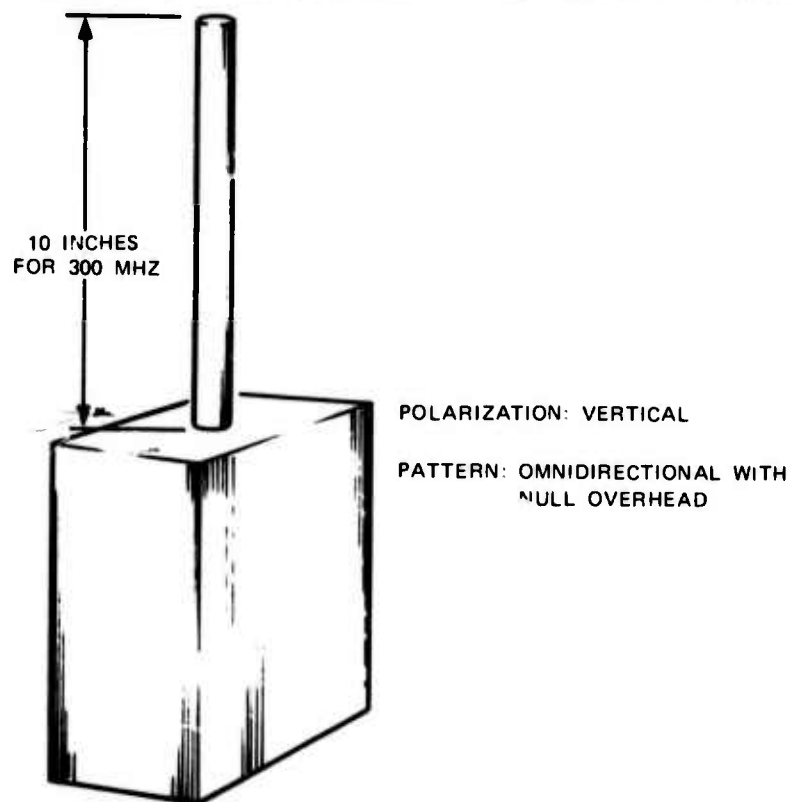


Figure 3-16. Quarter-Wave Monopole.

equipment considerations

10-inch whip, or at 3000 MHz a 1-inch post mounted on top of the transceiver. Under ideal conditions, the radiation pattern is omnidirectional with the maximum signal at an elevation angle of 20 to 40 degrees above the horizon and a null directly overhead. The polarization is vertical. Under these ideal conditions, the radiation pattern characteristics are also ideal; however, when in actual use, these conditions do not always exist. At 300 MHz, the position of the radio with respect to the operator will affect the antenna impedance, its efficiency, and its radiation pattern.

As the frequency is increased, the impedance and efficiency are less dependent on operator proximity. Also, the radiation pattern in the near field becomes more stable; but at the same time, the reflections from nearby objects, including the operator's body, are more pronounced and partial fading of the signal results from the cancellation effect when the direct and reflected signal arrives out of phase. An example of this is seen in the portable uhf television receiver. Reception can vary from perfect to unsatisfactory by simply moving its location 2 or 3 feet with respect to nearby reflecting objects. Overcoming this multipath effect is one of the most difficult problems associated with the hand-held personal terminal.

The antenna radiation characteristics can be made less dependent on operator proximity at the lower frequencies by using a balanced antenna such as a dipole, as shown in figure 3-17, rather than a monopole, and choking off the rf current that ordinarily flows down and is radiated from the radio housing. This increases the size of the antenna and complicates its design, but would improve the signal level significantly at 300 MHz. The crossover point above which a dipole would no longer provide improved operation over a monopole is the frequency at which the top of the transceiver becomes approximately one-half wavelength across its surface. This would probably occur somewhere near 1500 to 2000 MHz.

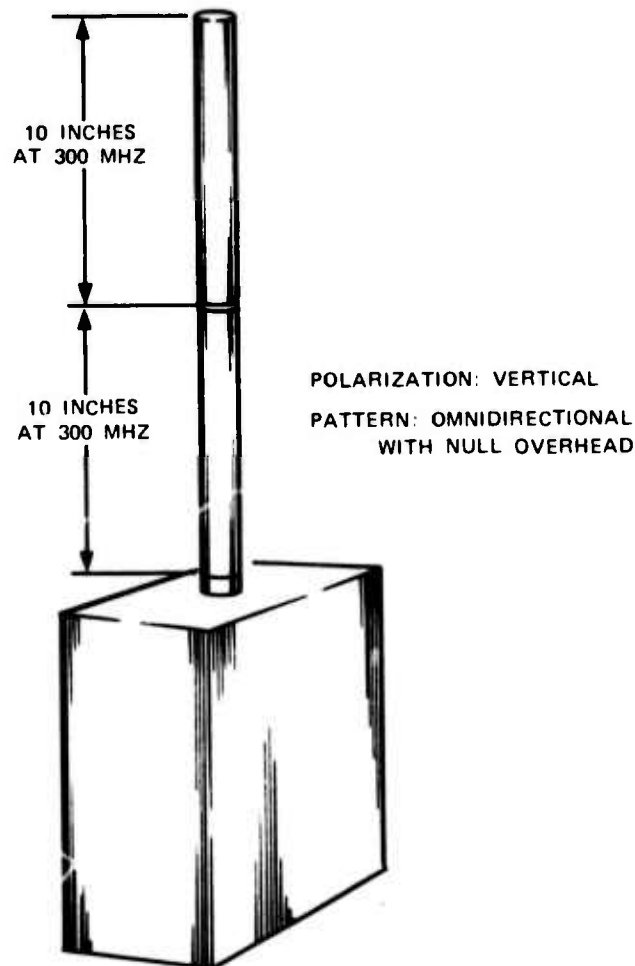


Figure 3-17. Half-Wave Dipole.

With antennas it is necessary to consider the nature of the polarization of the signal they receive or radiate. This rf polarization, which is a measurement or indication of the direction of the electrical field vector, can be linear, elliptical, or circular. A pictorial representation of this is shown in figure 3-18a., b., and c. Linear polarization can be oriented in any direction such as vertical, horizontal, or diagonal, and circular can have either a right- or left-hand sense of rotation. Vertically polarized antennas will receive either a vertically polarized field or a circularly polarized field; however, a 50-percent power reduction or loss results if the antenna is linear and the field is circular. Likewise, the horizontal antenna will receive either horizontal or circularly polarized energy with a 3-dB loss for circular. A right-hand circularly polarized antenna will theoretically receive no signal from a left-hand field, provided both the antenna and the field are purely circular.

One of the major problems associated with portable hand-held antennas is multipath fading causing a strong reflected signal arriving at the antenna 180 degrees out of phase with the direct signal. For linear polarization this can cause almost complete cancellation of the direct signal; however, with circular polarization the reflected signal is of the reverse sense and the cancellation is less severe.

The polarization of both the monopole and the dipole is linear, and in order to radiate omnidirectionally, both must be vertically oriented. Since this is the most normal attitude for a hand-held transceiver, maintaining vertical polarization should present no problem. Horizontal polarization that is omnidirectional can be obtained through the use of a horizontally oriented tri-dipole antenna, shown in figure 3-19. If horizontal polarization had any operational advantages over the vertical, it would be considered; however, it has no advantage and will not be further considered.

Circular polarization, however, will have three limited advantages. It will not have the overhead null that is characteristic of the monopole or dipole. Also, the requirement for maintaining vertical orientation of the transceiver will not be as critical. The third and most significant advantage is the phenomenon mentioned previously whereby the signals bouncing off reflective surfaces tend to be of the opposite sense or circular polarization, thus minimizing the fading due to multipath cancellation. It was primarily for this reason that circular polarization was chosen for uhf satellite communication. The improvement is in the order of 6 to 10 dB.

The only disadvantage of circular polarization is that it complicates the design of the antenna. This is true for the other antennas in the system as well as the hand-held units, since all antennas in the system should have the same type polarization.

There are several antenna configurations that can be used for obtaining omnidirectional circular polarization such as: 1. the conical spiral, 2. four diagonal dipoles, or 3. the slot excited biconical horn, as shown in figures 3-20, 3-21, and 3-22. Of these, the conical spiral is probably the least expensive. The diameter of the base of the conical spiral is approximately one-half wavelength at the lowest usable frequency; therefore, this antenna could be considered impractical for frequencies below 1500 MHz. The base diameter for this frequency would be 4 inches. It is difficult to envision an antenna of larger dimensions as being practical for a hand-held radio.

It is then concluded that a vertical monopole or a center-fed dipole is best suited for the hand-held unit if the frequency chosen is below 1500 MHz. A circular polarized antenna might provide 6-dB improvement in circuit margin due to reduced multipath and would be practical above 1500 MHz.

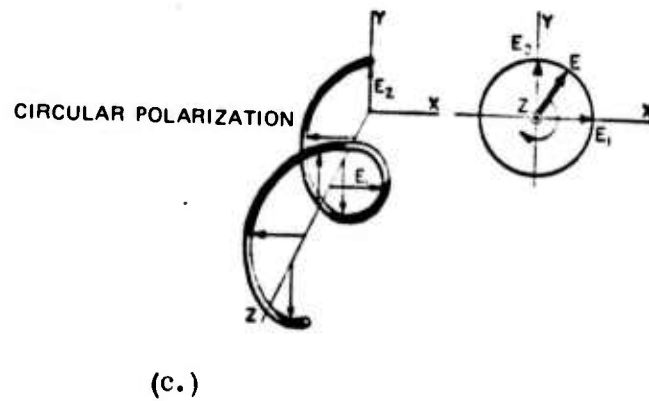
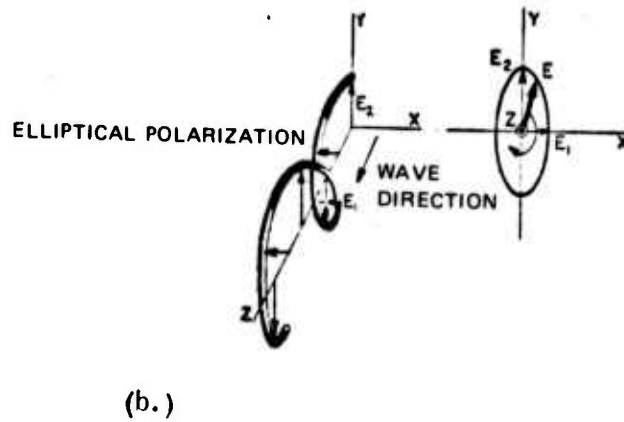
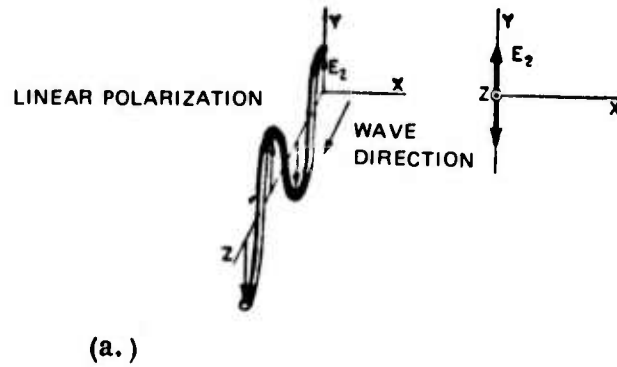


Figure 3-18. Pictorial Representation of Linear, Elliptical, and Circular Polarization.

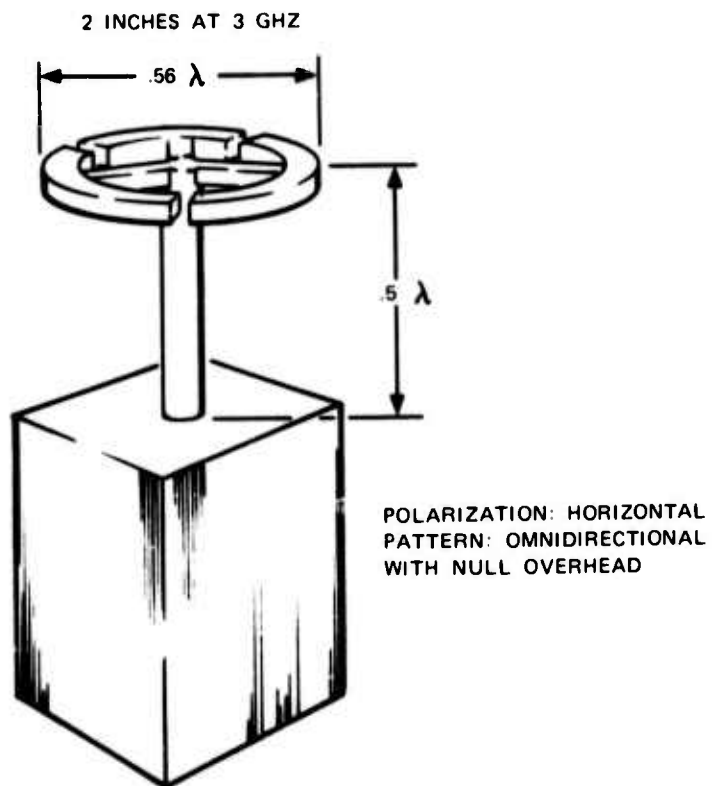


Figure 3-19. Tri-Dipole Loop Antenna.

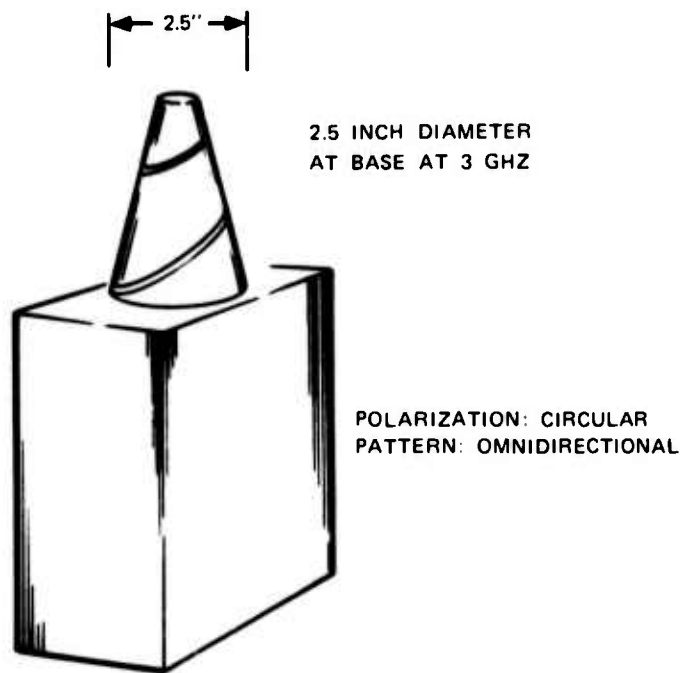


Figure 3-20. Conical Spiral.

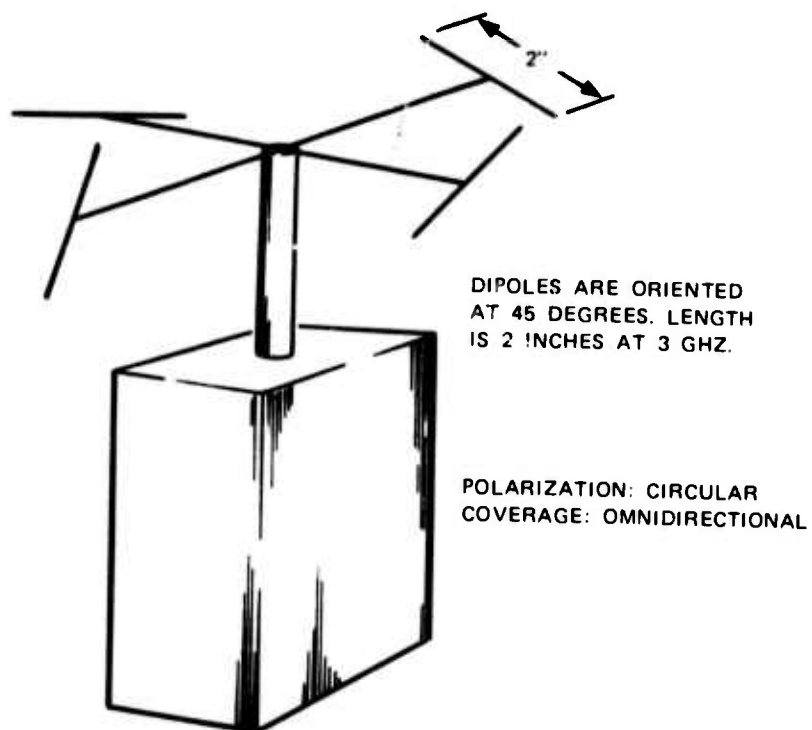


Figure 3-21. Diagonal Dipoles.

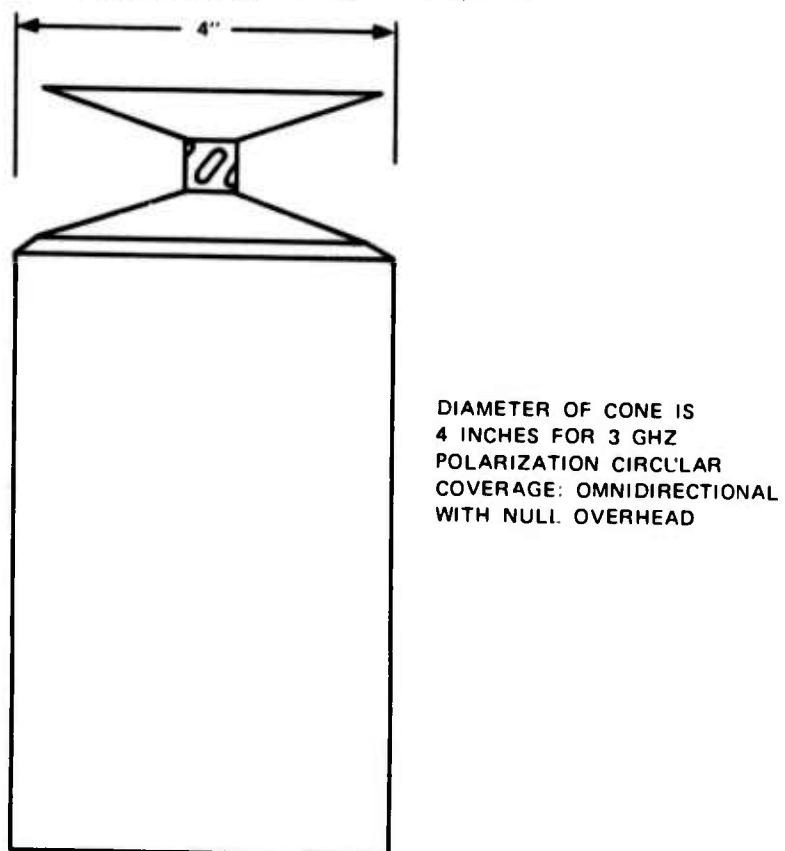


Figure 3-22. Slot-Fed Bicone.

3.3.2 Repeater Antenna

Many of the problems associated with the hand-held units such as the proximity effect of the operator, tilting of the antenna, and size limitations are not applicable to the repeater/station antennas. Since the antenna is fixed, higher gain in the form of directivity is more practical as well as desirable. Two types of antennas are required. One type is needed to provide communications with the individual portable personal transceivers. The other is needed to communicate with the central control station. The antenna that is used for receiving and transmitting to the portable units must have a radiation pattern that is omnidirectional in the azimuth plane with gain accomplished by reducing the vertical plane beamwidth.

Since the antenna that is used to transmit to and receive from the portable units must have broad azimuth coverage (somewhere between 180 and 360 degrees) a gain of 8 to 10 dB is considered practical. A vertically stacked array of four radiating elements will provide this amount of gain. To achieve 3-dB more gain theoretically requires twice as many radiating elements; however, the added complexity of the antenna feed system increases the losses and a gain in the order of only 2 dB in all that is actually achieved. A four-element array will have a vertical plane beamwidth of approximately 20 degrees.

What has been said for the hand-held units regarding size polarization and cost is also true for the fixed site omnidirectional antennas. For the lower frequencies, collinearly stacked, vertically polarized dipoles are practical. At 300 MHz one dipole is 20 inches long and a four-element array with optimum spacing between elements is 100 inches long. At the lower uhf frequencies, circular polarization can be obtained with diagonal or inclined dipoles as shown in figure 3-21. At higher frequencies this technique becomes less practical. At 3 GHz, an array consisting of slots on a vertical cylinder are more appropriate and easier to manufacture.

The repeater/station antenna that is used to transmit to and receive information from a single central station is not limited to 8- or 10-dB gain since it is not required to have broad azimuth coverage. A gain of 29 dB can be obtained at 3 GHz with a 4-foot diameter parabolic reflector type antenna. A 2-foot diameter reflector will have 23-dB gain at the same frequency. The reflector type antenna is probably the most practical for this application at frequencies below 3 GHz. Above 3 GHz a horn may be less expensive.

The polarization for this antenna is not as important as it is for the hand-held units since reflections and multipath do not present a serious problem. For reasons of simplicity, linear polarization is more appropriate.

3.4 RF SOURCES FOR PACKET RADIO

3.4.1 Introduction

The state-of-the-art of solid-state rf sources in terms of power output and cost for several frequency bands from 225 MHz to 36 GHz is presented herein. It is emphasized that the cost of current devices is influenced by many factors, including production quantities, frequency stability, noise characteristics, tuning requirements, and power output. These factors and their relation to current design and future needs for packet are also presented.

equipment considerations

3.4.2 General Considerations in RF Source Design and Economics

3.4.2.1 Cost Factors

The power output requirement is an obvious cost factor; however, it is not as obvious as is the frequency stability and noise requirements that strongly influence the source design. For example, a 6-GHz low power microwave source that sells in quantity for less than \$500 may appear a poor economic choice compared to the reflex klystron it replaced, which could be purchased for about \$50. However, when one considers the power supply and automatic frequency control requirements needed for the klystron, the solid-state source typically is more economical. The power supply requirements are typically 24 volts dc, which is often obtained directly from float charged batteries, and the frequency control is contained within the solid-state source by means of a phase-locked loop that synchronizes the microwave oscillator to the harmonic of a lower frequency crystal oscillator.

For the system being considered, simplification may be possible. In particular, digital modulation systems can tolerate considerably higher level or phase noise than most analog systems for which most current rf sources are designed. This could lead to simpler and more economical devices. Further, it should be recognized that avalanche transit time and transferred electron device technology is yet quite young and, hence, considerable improvement in the cost versus power output relationship can be expected.

The cost is almost certain to remain closely related to the power output requirement. Quite low powers can provide reliable high data rate transmission over long line-of-sight paths, if directional antennas are used; however, power output requirements will be moderate for omnidirectional systems, and this has influenced the status of current technology. As will be noted below, rf sources with output capability in the 10- to 100-watt range exist for P-band (225 to 400 MHz). This is achieved by techniques of combining the outputs of two or more amplifiers through hybrids. Such sources are typically used in various mobile applications that employ omniantennas, and often suffer severe obstruction loss.

Power combining techniques are also applicable to microwave sources, but are generally not applied because the resulting complexity would make the device both costly and unreliable compared to alternative devices such as twt amplifiers for the 1- to 100-watt power range and multicavity klystrons for higher powers. Both these devices, have high power gains (30 to 50 dB); hence, where power requirements exceed 1 or 2 watts at frequencies above 2 GHz, such electron devices typically are still applied.

3.4.2.2 Peak Power Capabilities

Most solid-state microwave devices have relatively low thermal time constants and very definite peak voltage limitations. Therefore, the devices are peak power limited; hence, peak power cannot be substantially increased by lowering the duty cycle. This is likely of little importance in designing repeaters and high capacity stations, since they must be designed to be transmitting a substantial period of the time; however, for low-capacity portable terminals, it would be desirable to employ devices that operate efficiently with high peak power and low duty cycle. If rf power devices are employed that are peak power limited, it is desirable that the devices may be turned off and on rapidly to minimize power consumption of the portable terminal.

3.4.3 Characteristics of Available RF Sources

Cost and performance characteristics of available uhf and microwave rf sources for several microwave frequency bands from 225 MHz through 36 GHz are summarized below. The

characteristics listed are believed to represent the state-of-the-art for sources that are currently production devices for commercial and military systems.

3.4.3.1 Sources for P-Band (225 to 400 MHz)

Transistors are exclusively used to generate up to 150 watts of cw power in this frequency band. The power train takes the form of a low-level oscillator followed with series amplifier stages up to 50 watts, then parallel power stages to reach the 100- to 150-watt level. The parallel output stages use hybrid power combiners to sum the individual stage powers. These power sources are widely used in military systems, and commonly, the amplifiers operate over the entire 225- to 400-MHz band with no tuning. Transmitters are common at 1-watt, 10-watt, and 100-watt outputs, depending upon the application.

Modulation is usually applied at the low-level source input; typical modulations used are am., fm, pm, and multitone. The limiting characteristic of transmitters using such power trains is amplifier distortion and thermal properties. At the higher power levels (50 watts and above) a forced cooling system is required to keep transistor junction temperatures within acceptable reliability range.

Typical available sources in this band have the following characteristics:

Frequency:	225 to 400 MHz, broadband
Power Output:	Up to 100 W
Efficiency:	30 percent
Volume:	10 W — 6 in. ³ 100 W — 20 in. ³ (not including cooling hardware)
Weight:	10 W — 6 oz. 100 W — 20 oz.
Cost:	10 W — \$600 100 W — \$2100

Future trends are toward higher power transistors designed for improved impedance matching, lower distortion, and lower thermal resistance. This will result in lower hardware costs by reducing the number of parallel stages required to obtain 100-watt levels. Packaging trends are toward hybrid construction, providing low volume and weight.

3.4.3.2 L-Band Sources (400 to 1700 MHz)

Microwave transistors are widely used in this band. Power output varies from a few milliwatts to 20 watts. The best available power transistor sources are capable of about 15 watts cw at L-band, or 100-watt pulse power. Efficiencies reach 60 percent at 1 GHz (50 percent at 2 GHz). Input voltage requirement is normally 28 volts dc. Size and weight vary with output power. Typical available source in this band has the following characteristics:

(A) High Power		(B) Low Power	
Frequency:	1 GHz	Frequency:	1 GHz
Power Output:	2 W	Power Output:	50 MW

equipment considerations

(A) High Power

Efficiency:	20 percent
Volume:	15 in. ³
Weight:	25 oz.
Price:	< \$1500
Tuning:	Voltage tuning

(B) Low Power

Efficiency:	1.5 percent
Volume:	2 in. ³
Weight:	2 oz.
Price:	\$300
Tuning:	Voltage tuning

3.4.3.3 S-Band Sources (1.7 to 3.7 GHz)

Several solid-state microwave devices are used in this band: namely, microwave transistors, transistor driven varactor harmonic-generator chains, bulk effect devices in LSA modes, and avalanche devices in both TRAPATT and IMPATT modes. Power output, efficiency, size, and price vary depending on the device used. Maximum attainable power in this band is 10 watts cw using microwave transistors and 20 watts using a transistor multiplier chain. The following are typically available characteristics in the S-band.

(A) High Power

Frequency:	2 GHz
Power Output:	2 W
Efficiency:	15 percent
Size:	170 in. ³
Weight:	—
Price:	< \$12,000
Tuning:	Both electrical and mechanical

(B) Low Power

Frequency:	2.0 GHz
Power Output:	40 MW
Efficiency:	2 percent
Size:	2 in. ³
Weight:	3 oz.
Price:	\$ \$350
Tuning:	Voltage tuning

3.4.3.4 C-Band Sources (3.7 to 6.4 GHz)

In this band, there are wide selections of microwave sources ranging in power from a few milliwatts to a maximum of 4 watts cw at the high end of the band. Various devices are used in this band, depending on frequency, power output, and size. Microwave transistors are used at the low end, transistor multiplier chain is used at mid and high end of the band, and bulk and avalanche devices are used at the high end of the band. A typical source in this band has the following characteristics:

(A) High Power

Frequency:	6 GHz
Power Output:	1.5 W
Efficiency:	10 percent
Size:	125 cu. in.
Weight:	—
Price:	< \$12,000
Tuning:	Voltage

(B) Low Power

Frequency:	5.5 GHz
Power Output:	100 MW
Efficiency:	4 percent
Size:	1 in. ³
Weight:	1.5 oz.
Price:	< \$500
Tuning:	Mechanical

3.4.3.5 X-Band Sources (6.4 to 10.9 GHz)

Sources using both bulk and avalanche devices are used in this band. Maximum power attainable is 4 watts in the low end of the band and 2 watts at the high end of the band; however, higher power is becoming available with new circuit techniques. A typical source in this band has the following characteristics:

<u>(A) High Power</u>		<u>(B) Low Power</u>	
Frequency:	10.9 GHz	Frequency:	8.0 GHz
Power Output:	1 W	Power Output:	50 MW
Efficiency:	8 percent	Efficiency:	1 percent
Size:	25 in. ³	Size:	< 2 in. ³
Weight:	20 oz.	Weight:	4.0 oz.
Price:	<\$2000	Price:	<\$500
Tuning:	Varactor tuning	Tuning:	Mechanical

3.4.3.6 K-Band Sources (10.9 to 36 GHz)

Maximum attainable power in this band is 2 watts at the low end and a few hundreds of milliwatts at the high end of the band. Tunnel diodes and both bulk and avalanche devices are used in this band. Sources with higher power are currently being built in the laboratory; however, they are not commercially available but may be practical in the next year or two. A typical source has the following characteristics:

Frequency:	26 GHz
Power Output:	100 MW
Efficiency:	0.5 percent
Volume:	9 in. ³
Weight:	8 oz.
Price:	<\$700
Tuning:	Mechanical

3.4.4. Summary

An evaluation of rf solid-state sources from 225 MHz to 36 GHz has been presented. This survey has included power output capability, efficiency, volume, and cost information. A detailed bibliography is included at the end of this section.

3.5 MICROPROCESSOR EVALUATION FOR PACKET RADIO

The packet radio network will require the use of a microprocessor in the network elements. This will allow a substantial and flexible information decision and handling capability. The use of programmable logic will allow network and device operating characteristics to be postulated, tested, and optimized via software changes in the system operating softwares.

equipment considerations

This will allow the experimental system to seek an optimum solution relatively rapidly under operating conditions, without requiring hardware modification with the inherent delays and difficulties.

Requirements of the microprocessor for the packet radio network are fast operating speed, to minimize node processing delay; low power requirements, for battery operation; and current availability, so the hardware can be implemented. These and other considerations are discussed in this report.

The purpose of this investigation was to characterize the technology of microprocessor components, memories, and structures. The study is heavily weighted in favor of components that are available now. The many designs that are being planned or that are on-going at the various semiconductor houses are not considered in this evaluation. It is felt that there is not enough assurance that these devices will be available for equipment delivery in 1974.

3.5.1 Evaluation Factors

Refer to table 3-6 for a list of the microprocessor sets available. Also included are lists of random access memories and programmable read only memories.

Table 3-6. List of Available Microprocessor Sets.

COMPANIES WITH MICROPROCESSOR SETS

1. Intel: 4-bit, 4004; 8-bit, 8008; both are single chip cpu's.
2. National Semiconductor: Multichip cpu, can choose word width.
3. Rockwell-Microelectronics: 4-bit single chip cpu.
4. Fairchild: PPS 25, decimal-oriented set.

COMPANIES WITH PLANS FOR MICROPROCESSOR SETS

1. INTEL: 8-bit N-channel cpu, 8080, December 1973.
2. Motorola: 8-bit N-channel cpu, first quarter 1974,
3. Rockwell-Microelectronics: 8-bit cpu.
4. Western Digital Corp.: 8-bit N-channel cpu, before 1974.
5. Signetics: No information.
6. Hughes Aircraft Co.: No information.
7. AMI: 16-bit general-purpose set.

A listing of the several factors considered in evaluating the various component sets is included in the following tables:

- a. Table 3-7. MOS Random Access Memories. This table gives a comparison of several of the available semiconductor RAM's. The parameters used for comparison are listed in the table.
- b. Table 3-8. MOS Programmable Read Only Memories. This table gives the parameters of two available PROM's for comparison.
- c. Table 3-9. CPU Parameters Used in Evaluation.
- d. Table 3-10. RAM Parameters Used in Evaluation. Tables 3-9 and 3-10 define the parameters that were considered in evaluating the various systems.
- e. Table 3-11. Comparison of Microprocessor Sets. This table gives a comparison of the INTEL 8008-1, and the National Semiconductor IMP-16 and IMP-8 Microprocessors.

3.5.2 Conclusions

Based on the investigation, the following selections have been made:

- a. The National General-Purpose Controller/Processor appears the most promising for the packet radio repeater requirements.
- b. Complementary MOS (C-MOS) for random access memories.
- c. Programmable (electrically erasable) read only memories will be used.

Table 3-7. MOS Random Access Memories.

PARAMETER	INTEL			MOSTEK	NATIONAL		EA	RCA AMS (256 bit)		
	1103-1	2102	2102-1		2105-1	4260		5260	1502	6002
Maximum Power Dissipation (mW)	475	300	300	500	4006-6	575	575	165	275	80
Typical Power Dissipation (mW)	375	150	150	325	400	400	400	100	180	5
Standby Power (mW)	75	150	150	65	50	100	100	30	2	25 μ W
Access Time (ns)	150	700	350	80	400	450	375	150	150	290
Cycle Times: Read (ns)	300	1000	500	180	400	600	500	290	250	490
Write (ns)	340	1000	500	180	650	750	625	450	250	500
Type of Input	MOS ¹	TTL ²	TTL ²	MOS-TTL ³	TTL ²	MOS-TTL ³	MOS-TTL ³	MOS-TTL ³	MOS ¹	TTL ²
Type of Output	Current Sense	TTL	TTL	Current Sense	Current Sense	TTL	TTL	TTL	Current Sense	TTL
Refresh Interval=No. of Refresh Cycles	2 ms 32 cycles	Static	Static	10 μ s 1 cycle	2 ms 32 cycles	32 cycles	32 cycles	2 ms 1 cycle	2 ms 32 cycles	Static
Operating Temperature	0°C to 70°C	0°C to 70°C	0°C to 70°C	0°C to 70°C	0°C to 70°C	-55°C to 125°C	-25°C to 70°C	0°C to 70°C	0°C to 70°C	-55°C to 125°C
Power Supplies (volts)	+19, +22	+5	+5	+12, -5	+5, -12	+5, -12	+5, -12	\pm 12	+7, +20 +22, 5	Variable +3 to +15
Number of Pins	18	18	18	18	16	16	16	18	22	16
Prices (1 to 24 quantities)	\$13.50	\$24.00	\$44.50	\$60.00	\$16.75	\$47.80	\$18.00	\$41.20	\$25.00	\$12.00
Number of Level Shifters and Sense Amps (024x8 bit)	29	0	0	10	8	2	2	2	29	0
Type of MOS	P	N	N	N	P	P	P	N	P	Both

1. MOS: 15- to 20-volt swings are needed.

2. TTL: 5-volt logic levels

3. MOS-TTL: Part of the inputs require MOS voltages and part can be driven by TTL levels.

Table 3-8. MOS Programmable Read Only Memories.

PARAMETER	INTEL 1702A	NATIONAL MM4203
1. Power dissipation	700 mW	700 mW
2. Cycle time	700 ns	700 ns
3. Chip enable logic	Single line	3-bit control
4. TTL compatible	Yes	Yes
5. Power supplies	+5, -9	+5, -12
6. Number of pins	24	24
7. Operating temperature	0°C to 70°C	-55°C to 85°C
8. Required clocks	None	None

Table 3-9. CPU Parameters Used in Evaluation
(Refer to table 3-11.).

1. Power Requirements	Includes cpu, supporting circuitry, and one input/output port. Does not include any memory.
2. Supporting Circuitry Required	The number of integrated circuits required to make the cpu a workable system. Does not include memory or tty interface.
3. Program Storage Efficiency	The number of memory locations necessary to store a benchmark program.
4. Power Supplies	
a. Number required.	
b. Voltages required are the voltages of common usage.	
5. Input/Output Interfacing	
a. Ease of design — What is available to aid hardware design.	
b. Number of input and output ports.	
c. Software — What is available under software control.	
6. Printed Circuit Board Partitioning Ease	— Breaking up components on two or three boards, how many pin-outs are necessary.

Table 3-9. CPU Parameters Used in Evaluation
(Refer to table 3-11.) (Cont).

7. Clock Requirements
 - a. Frequency — Is it easy to derive;
 - b. Number of phases.
 - c. TTL or MOS level.
8. Allowable Voltage Fluctuations or Ripple
9. Cost
 - a. CPU chip(s).
 - b. Supporting circuitry.
 - c. Printed circuit boards.
 - d. Prototype kit.
10. Memory Addressing
 - a. Direct.
 - b. Indirect.
 - c. Indexed.
 - d. Literal.
11. Instruction Set Utility
 - a. Number of instructions.
 - b. Number of different instruction types.
 - c. Unusual instructions.
12. Number of Registers
 - a. Accumulator.
 - b. Index.
 - c. Scratch pad.
13. Stack Capabilities
 - a. Size of stack.
 - b. Is it accessible through software?
14. Largest memory capacity addressable
15. Capability for customer microprogramming

equipment considerations

Table 3-10. RAM Parameters Used in Evaluation (Refer to table 3-11.).

1. Cost per Bit. Interface and control circuitry included. (Refresh circuitry included if necessary).
 - a. 1024 word x 8-bit system
 - b. 1024 word x 16-bit system
2. Power Dissipation per bit Interface and control circuitry. (Refresh circuitry included if necessary).
3. Cycle Times
 - a. Access — Time from chip select until data available.
 - b. Read — Access time plus deselect time.
 - c. Write/refresh.
4. Refresh Requirements
 - a. Number of address changes required for complete memory refresh.
 - b. Minimum time between refreshed.
5. TTL Compatibility
6. Operating Temperature If not specified over the military range, will the memory function at high temperatures?
7. Power supplies
 - a. Number required.
 - b. Voltages required — Are the voltages of common usage?
8. Availability
 - a. Can the part be had in large quantities?
 - b. Second sourced.
 - c. State-of-the-art Is it the current design?
9. Packaging Efficiency Using 16,192 bits as a standard, how many interface code's are necessary to produce a memory system with interface, control, and refresh circuitry included.

Table 3-11. Comparison of Microprocessor Sets.

	INTEL 8008-1	NATIONAL SEMICONDUCTOR IMP-16	NATIONAL SEMICONDUCTOR IMP-8
1. Power Requirements (Watts)	With TTL — 7 W With CMOS — 1 W	With TTL — 14 W With CMOS — 3 W	With TTL — 8 W With CMOS — 2 W
2. Supporting Circuitry Required	37 interface codes	40 interface codes	34 interface codes
3. Program Storage Efficiency	124 words x 8 bits	49 words x 16 bits	
4. Power Supplies	+5 V, -9 V	+5 V, -12 V	+5 V, -12 V
5. Input/Output Interfacing	8 possible input/output ports No input lines for communicating with epu except control panel interrupt	6 general-purpose flags 4 general-purpose jump condition inputs 1 general interrupt input	Same as IMP-16
6. Printed Circuit Board Partitioning	An 8-bit bidirectional bus is used for data input/output and addressing. This allows for fewer pinouts from board.	16-bit bidirectional bus is used for input/output and addressing. The wider word and greater number of epu lines makes for more pinouts.	8-bit bidirectional bus is used for input/output and addressing.
7. Clock Requirements	TTL level clocks 2-phase	-12 V to +5 V swing 4-phase	-12 V to +5 V 4-phase
8. Allowable Voltage Fluctuations	±5%	±5 percent	±5 percent
9. Cost	CPU chip — \$180 SIM 8-01 — \$900 INTELLEC — 8 \$3650	CPU chips — \$430 IMP — 16C — \$950 IMP — 16P — \$3850	CPU chips — \$270 IMP — 8C — \$800 IMP — 8P — \$3750
10. Memory Addressing	Indexed only	Direct, indirect, indexed, literal rel Relative type	Direct, indirect, indexed, literal Paged type
11. Instruction Set Utility	48 instructions	43 instructions Software control of stack and external flags External jump condition inputs	38 instructions Software control of stack and external flags External jump condition inputs
12. Number of Registers	1 8-bit accumulator 6 general registers 2 of the 6 can be used for indexing.	Four 16-bit accumulators	Four 16-bit accumulators
13. Stack Capabilities	7 14-bit registers for program counter storage only.	Sixteen 16-bit registers accessible through software	Sixteen 8-bit registers accessible through software
14. Largest Memory Addressable	16K word x 8 bit	65K word x 16-bit	65K word x 8-bit
15. Capability for Microprogramming	None	Instruction sets can be developed	Same as IMP-16

BIBLIOGRAPHY

R. Gold, "Optimal Binary Sequences for Spread Spectrum Multiplexing," IEEE Transactions on Information Theory, October 1967, pp 619-621.

M.I. Skolnik, Introduction to Radar Systems, McGraw-Hill Book Company, 1962, pp 31-35.

P. Swerling, "Parameter Estimation for Waveforms in Additive Gaussian Noise," J. Soc. Indust. Appl. Math., Vol. 7, No. 2, June 1959, pp 152-166.

M.I. Skolnik, "Theoretical Accuracy of Radar Measurements," PGANE Trans., Vol. ANE-7, December 1960, pp 123-129.

Bell, Holmes, and Ridings, "Application of Surface Wave Technology to Spread Spectrum Communications," Combined Issue of IEEE Transactions on Microwave Theory and Techniques: Sonics and Ultrasonics, April 1973.

"Proceedings of the 1973 Symposium on Spread Spectrum Communications," Naval Electronic Systems Command, Naval Electronics Laboratory Center.

IEEE Transactions (combined) of MTT and Sonics and Ultrasonics, April 1973.

Solid-State Source References

NBS Technical Note 597, Tabulation of Data on Semiconductor Amplifiers and Oscillators at Microwave Frequencies; US Dept. of Commerce Publication.

Roger J. Becker, "Late Diode Entries Enliven Solid-State Source Race," Microwaves, June 1972.

Malcolm McColl, State-of-the-Art Study of Solid-State Microwave Generators, Aerospace Corp., El Segundo, California, Distributed by Clearinghouse, AD 691 234, 31 Jan 1969.

"FET's Step Up to Low-Noise Microwave Applications," Richard T. Davis Managing Editor, Microwaves, April 1972.

Proceedings 1971 European Microwave Conference, Volume I, The Royal Swedish Academy of Engineering Sciences (IVA), Stockholm, Sweden.

Hans-Jorg Thaler, Gerhard Ulrich, and Gerhard Weidmann, "Noise in IMPATT Diode Amplifiers and Oscillators," IEEE Transactions on Microwave Theory and Techniques, Vol. MTT-19, No. 8, August 1971.

H.J. Kuno, D.L. English, P.S. Pusateri, Millimeter-Wave Solid-State Exciter-Modulator-Amplifier Module for Gigabit Data-Rate, Hughes Research Laboratories, Torrance, California 90509.

"A 22-Percent C.W. Efficiency Solid-State Microwave Oscillator," 1972 IEEE-GMTT International Microwave Symposium, Digest of Technical Papers, 22-24 May 1972, pp 187-189.

Kenneth M. Johnson, "Wide-Bandwidth IMPATT and Gunn Voltage Tuned Oscillators," Omni Spectra, Inc., Tempe, Arizona; 1972 IEEE-GMTT International Microwave Symposium, Digest of Technical Papers, 22-24 May 1972, pp 185, 186.

"K-Band High Power Single-Tuned IMPATT Oscillator Stabilized by Hybrid-Coupled Cavities," 1972 IEEE-GMTT International Microwave Symposium, Digest of Technical Papers, 22-24 May 1972, pp 176-178.

"Microwave Transistors, Bipolar and Field Effect — Today and Tomorrow, 1972 IEEE-GMTT International Microwave Symposium, Digest of Technical Papers, 22-24 May 1972, pp 170-172.

"High-Power, Low-Noise Avalanche Diode Oscillators," 1971 IEEE-GMTT International Microwave Symposium, 16-19 May 1971, pp 86, 87.

T. T. Fong, and David L. English, H.J. Kuno, "Characterization of IMPATT Diodes at Millimeter-Wave Frequencies," IEEE Transactions on Electron Devices, Vol. Ed-19, No. 6, June 1972.

A. Kondo and T. Ishii, Performance of Read Diodes at K-band, Authors are with the Central Research Laboratory, Mitsubishi Electric Corporation, Itami Hyogo, Japan.

A.A. Sweet, "Waveguide Cavity Gunn Amplifiers," The Microwave Journal, February 1972.

One-Watt Gunn Diode Sources; Litton Industries Electron Tube Division, San Carlos, California.

Simon Stopek, "Frontier Microwave Products—Solid State," The Microwave Journal, February 1972.

J. A. Turner and S. Arnold, "Schottky-Barrier FET's—New Low-Noise Designs," Microwaves, April 1972.

P. A. Levine, H. C. Huang and H. Johnson, "IMPATTs Shoot for Gunn Noise Levels.

George W. Fitzsimmons, Sr., "Heat Sinking CW TRAPATT Oscillators," Microwaves, January 1972.

Lyman J. Hardeman, "A 1971 Guide to Microwave Diodes," Microwaves, February 1971.

"You Can Rely on LSA Diodes," Microwaves, December 1973.

"K-Band High-Power Single-Tuned IMPATT Oscillator Stabilized by Hybrid-Coupled Cavities," IEEE Transactions on Microwave Theory and Techniques, Vol. MTT-20, No. 12, December 1972.

"Multilayer Vapor-Phase Epitaxial Silicon Millimeter-Wave IMPATT Diodes," IEEE Transactions on Electron Devices, Vol. Ed-19, No. 7, July 1972.

"A Highly Stabilized K_a -Band Gunn Oscillator," IEEE Transactions on Microwave Theory and Techniques, February 1972.

1971 Wescon Technical Papers presented at the Western Electronic Show and Convention, 24-27 Aug 1971; Session 26, Microwave Solid-State Devices; IMPATT Diodes; Technology and Applications Review of Gunn Effect Devices, Transistors for the Era of Microwave Communication, Microwave Acoustic Devices for High Data Rate Processing.

equipment considerations

1972 Wescon Technical Papers presented at the Western Electronic Show and Convention, 19-22 September 1972, Session 25, Advances in Electronic Tuned and Wideband Solid State Microwave Sources; Recent Advances in Low Noise Microwave Transistor Development, Wideband Varactor-Tuned Gunn Effect Oscillators, Some Theoretical and Practical Considerations in the Design of Wideband Varactor Tuned Gunn Oscillators, Advances in Yig-Tuned Gunn Effect Oscillators.

Bernard E. Sigmon, "Designing Circuits for Pulsed IMPATT Oscillators," Microwaves, June 1972.

"Intermodulation Characteristics of X-Band IMPATT Amplifiers," IEEE Transactions on Microwave Theory and Techniques, Vol. MTT-20, No. 12, December 1972.

Motoharu Ohtomo, "Experimental Evaluation of Noise Parameters in Gunn and Avalanche Oscillators," IEEE Transactions on Microwave Theory and Techniques, Vol. MTT-20, No. 7, July 1972.

K.N. Kawakami, "Optimize Gunn Circuits for Wideband Varactor Tuning," Microwaves, December 1972.

Robert T. Oyafuso, Robert E. Brown, "Think Young with Agile YIG and Varactor Tuning," Microwaves, December 1972.

Dr. Max J. Lazarus, "Have a High-Quality V-Band Link and Low Costs, Too," Microwaves, November 1972.

Alexander J. Kelly, "Design Front Ends for Low Noise Operation," Microwaves, April 1971.

"New Products" Microwaves, January 1972.

Berin Fank, "Bulk-Effect Oscillators Give Low-Cost Microwaves," Microwaves, February 1971.

R.J. Clark, Jr., and D.B. Swartz, "Take a Fresh Look at YIG-Tuned Sources," Microwaves, February 1972.

N.G. Bechtel, W.W. Hooper, and D. Mock, X-Band GaAs Fet, Fairchild Microwave and Optoelectronics Division, Palo Alto, Calif.

Ian Thompson, "DC Temperature and Field Profiles in TRAPATT Diode Structures," IEEE Transactions on Electron Devices, Vol. Ed-19, No. 6, June 1972.

"Noise in IMPATT Diodes: Intrinsic Properties," IEEE Transactions on Electron Devices, Vol. Ed-19, No. 2, February 1972.

Gordon S. Kino, Correction to "High-Efficiency Operation of a Gunn Oscillator in the Domain Mode" IEEE Transactions on Electron Devices, February 1972.

"D-MOS Transistor for Microwave Applications," IEEE Transactions on Electron Devices, Vol. Ed-19, No. 1, January 1972.

M. Takeuchi, A. Higashisaka, and K. Sekido, GaAs Planar Gunn Diodes for DC-Biased Operation, with the Central Research Laboratories, Nippon Electric Company, Ltd., Kawasaki, Japan.

V.S. Andreyev and V.A. Borisov, "The Gunn Effect and Its Applications in Microwave Engineering," Radio Engineering, Vol. 25, No. 5, 1969.

"An Integrated, X-Band, Image and Sum Frequency Enhanced Mixer with 1 GHz IF," 1971 IEEE-GMTT International Microwave Symposium 16-19 May 1971, pp 16-17.

"Integrated Mixer for 18 and 26 GHz," 1971 IEEE-GMTT International Microwave Symposium, 16-19 May 1971, pp 18, 19.

"High-Power Microwave Amplifier Using Anti-Parallel Avalanche-Diode Pair," 1971 IEEE-GMTT International Microwave Symposium, 16-19 May 1971.

"Second Harmonic Tuning Effects on IMPATT Diode Oscillator Noise Characteristics," 1971 IEEE-GMTT International Microwave Symposium, 16-19 May 1971, pp 92-93.

"Reduction of FM Noise in Microwave Diode Oscillators by Cavity and Injection Stabilization," 1971 IEEE-GMTT International Microwave Symposium, 16-19 May 1971, pp 94-95.

"Multi-Parallel Operation of Gunn Diodes for High RF Power," 1971 IEEE-GMTT International Microwave Symposium, 16-19 May 1971, pp 156-157.

"Improved Injection Locking of Microwave FM-Oscillators," 1972 IEEE-GMTT International Microwave Symposium, Digest of Technical Papers, 22-24 May 1972, pp 173-175.

"A C-Band All Ferrite Integrated Wideband High Power GaAs Avalanche Diode Amplifier," 1972 IEEE-GMTT International Microwave Symposium, 22-24 May 1972, pp 179-181.

"Intermodulation Characteristics of X-Band IMPATT Amplifiers," 1972 IEEE-GMTT International Microwave Symposium, 22-24 May 1972, pp 182-184.

"Single and Dual Gate GaAs FET Integrated Amplifiers in C-Band," 1972 IEEE-GMTT International Microwave Symposium, 22-24 May 1972, pp 233-234.

"Development of an FM Pulsed Gunn Oscillator at X Band," IEEE Transactions on Electron Devices, July 1971.

"The Performance of Planar Gunn Oscillators in X Band," IEEE Transactions on Electron Devices, Vol. Ed-18, No. 10, October 1971.

"Linear Wide Band Amplifiers Using Transferred Electron Devices," 1972 IEEE Intercon, Synopses of Papers Presented at the 1972 IEEE International Convention, 20-23 March 1972, Paper 7B.1.

"Tunable Locked Avalanche Diode Oscillator," 1972 IEEE Intercon Digest, Paper 7B.3.

"High Power CW Gunn Oscillator for Communication Applications," 1972 IEEE Intercon Digest, Paper 7CJ.1.